NASA CR-54449
GE R66FPD259

ANALYSIS OF OVERALL AND INTERNAL PERFORMANCE OF VARIABLE-GEOMETRY ONE- AND TWO-STAGE AXIAL-FLOW TURBINES

by

E. E. Flagg

prepared for

NATIONAL AERONAUTICS AND SPACE ADMINISTRATION

April 30, 1966

CONTRACT NAS3 -7262

Technical Management
NASA Lewis Research Center
Cleveland, Ohio
Lewis Project Manager: E. L. Warren
Lewis Research Advisor: A. J. Glassman

GENERAL ELECTRIC COMPANY
Cincinnati, Ohio 45215

(BLANK)

CONTENTS

ILLUSTRATIONS

ANALYSIS OF OVERALL AND INTERNAL PERFORMANCE OF VARIABLE-GEOMETRY ONE- AND TWO-STAGE AXIAL FLOW TURBINES

by E. E. Flagg
General Electric Company

1.0 SUMMARY

The method of analyzing the off-design performance, of multi-stage axial-flow turbines, with both fixed and variable turbines developed under Task I and Task II (Reference 1) was used to study performance variation for a single stage and a two-stage turbine. The off-design loss definition parameters calculated for the NASA Lewis Research Center turbine in Task II were used in determining the performance maps. Performance maps are presented in the form of equivalent work versus equivalent weight-flow-speed parameter with contours of total pressure ratio as well as mean section incidence angle, rotor-hub Mach Number and rotor-hub reaction versus equivalent work are also presented.

1.1 Single Stage Turbine. - The single stage turbine specified by the NASA Project Manager was evaluated by computing three performance maps: a.) stator at design point position; b.) stator at open position; c.) stator at closed position. Peak turbine efficiency was .901, .866, and .910 for the three maps respectively.

1.2 Two-Stage Turbine. - The two-stage turbine specified by the NASA Project Manager was evaluated by computing nine performance maps with the first and second stage stators at design point position, open position and closed position. The pitchline effective areas associated with the stator positions were 130% open and 70% closed on both stators for a net area change of 186% over minimum. Representative points are evaluated in detail.

2.0 INTRODUCTION

Advanced air breathing propulsion engines will have to operate over a broad range of conditions during subsonic and supersonic flight operations. Consequently, a wide range of requirements will be imposed on the propulsion system and turbine stator area variation appears to offer very good potential to obtain the desired cycle flexibility through variation in cycle pressure ratio, air flow and/or turbine inlet temperature to approach more optimum conditions. The achievement of optimum aero-thermodynamic design of the turbine for variable stator operation will depend upon a knowledge of the change in overall and interstage turbine performance as a function of the requirement variations.

3.0 TASK III - ANALYSES OF SELECTED GEOMETRIES

3.1 Objective. - The aerodynamic design and off-design analyses of a multistage variable stator area turbine require a lengthy series of trials, rejections, and retrials relative to both the overall design and to smaller details within the design. The aero-thermodynamic design must be closely integrated with the mechanical design, cooling system design and cycle and mission analyses in order to arrive at an optimum machine. There are many variables and sub-variables interwoven in a design, so that a true optimum is difficult to achieve and is directly related to the coordination of the aero-thermodynamic design, cooling system design and cycle and systems analysis.

In order to achieve wide modulation over the range of subsonic and supersonic flight conditions, propulsion systems with variable turbine stator area appear to offer very good potential to obtain the desired cycle flexibility. The degree of performance payoff, however, depends upon the particular mission and cycle being considered, and trade-offs between supersonic and subsonic flight conditions must be made in order to arrive at an optimum turbine stator area variation. The turbine off-design performance analysis for a variable turbine stator machine, is many times more involved and time-consuming than previous turbine practice.

The specific objectives of Task III were to use the digital computer program prepared in Task II to study interstage and overall performance variation for two example cases. The two example turbines were a single stage and a two-stage turbine specified by the NASA Project Manager. There were a total of twelve sets of performance maps for specified speed and stator position settings. In performing the computations to obtain the performance maps, the speed of the turbine was varied from 60 percent to 120 percent of design speed, and the work output varied from 0 to the maximum work condition, limited by discharge annulus choking which is beyond the first blade row choke and the last rotor choke operating point. The following performance maps were computed by the General Electric Company:

A.) Single stage turbine (3 maps)

1.) Stator at design position

2.) Stator at open position

3.) Stator at closed position

B.) Two stage turbine (9 maps)

1.) First and second stage stators at design position

2.) First stage stator at open position with second stage stator at design position.

3.) First stage stator at closed position with second stage stator at design position

4.) First stage stator at design position with second stage stator at open position

5.) First and second stage stators at open position

6.) First stage stator at closed positionwith second stage stator at open position

7.) First stage stator at design position with second stage stator at closed position

8.) First stage stator at open position with second stage stator at closed position

9.) First and second stage stators at closed position.

3.2 Assumptions. - At the beginning of Task III, the NASA Project Manager specified the example turbines selected for analysis, i.e., a single stage and a two-stage turbine. The turbine geometrics as provided by Lewis Research Center are shown in the following table. A flowpath elevation is shown in Figure 1.

SINGLE-STAGE TURBINE FOR TASK III

Total Efficiency = 0.885

P_T, in/P_T, out = 1.797

P_T, in/P_S, out = 2.004

Design Flow = 39.90 lb/sec

T_T, in = 518.7°R

N = 4407.4 rpm

P_T, in = 1 atm

STG = 1

SECT = 5

RG = 53.3

PCNH = .2, .2, .2, .2, .2

STAGE 1

GAMG1 = 1.4, 1.4, 1.4, 1.4, 1.4,

DR1 = 22., 22., 22., 22., 22.,

DT1 = 30., 30., 30., 30., 30.,

RWG1 = 1., 1., 1., 1., 1.,

SDIA1 = 0.0, 0.0, 0.0, 0.0, 0.0,

SDEA1 = 69.58, 68.28, 67.00, 65.75, 64.51

SESTH1 = 1.00

RDIA1 = 51.70, 44.74, 36.38, 26.60, 15.62

RDEA1 = 56.35, 57.30, 58.26, 59.20, 60.13

RERTH1 = 1.00

Open setting:

ΔSDIA1, SDEA1 = -7.53°

Closed setting:

ΔSDIA1, SDEA1 = 7.13°

TWO-STAGE TURBINE FOR TASK III

Total Efficiency = 0.88

P_T, in/P_T, out = 3.438

Overall

P_T, in/P_S, out = 4.018

Design Flow, 1st stage P/P, T_T, in, N, P_T, in, SECT, RG, PCNH are same as for single-stage turbine.

All Stage 1 input are same as for single-stage turbine.

Stage 2

GAMG2 = 1.4, 1.4, 1.4, 1.4, 1.4

DR2 = 22.000, 20.658, 20.658, 20.091, 20.091

DT2 = 30.000, 31.341, 31.341, 31.908, 31.908

RWG2 = 1.0, 1.0, 1.0, 1.0, 1.0,

SDIA2 = 20.07, 18.85, 17.77, 16.79, 15.92

SDEA2 = 66.05, 63.99, 62.00, 60.09, 58.24

SESTH2 = 1.00

RDIA2 = 49.34, 40.57, 30.16, 17.97, 5.82

RDEA2 = 48.88, 50.83, 52.70, 54.50, 56.18

RERTH2 = 1.00

Open Setting: ΔSDIA2, SDEA2 = -9.62°

Closed Setting: ΔSDIA2, SDEA2 = 8.81°

3.2.1 Loss Definition. - A parametric variation of loss definition parameters at design speed and design stator setting for the Task III single stage turbine was completed to produce 88.5% total-total efficiency at a total-total pressure ratio of 1.797. Shown in Figures 2 through 4 are the interaction of inlet recovery factor, stator efficiency, rotor efficiency and test factor to produce 88.5% total-total efficiency at design point total-total pressure ratio. Much lower levels of efficiency and/or test factor must be used when compared with the level required for the NASA Two Stage Turbine evaluated in Task II (see Reference 1). The efficiency characteristic with total pressure ratio along the 100% design speed line is shown in Figures 5 through 11 demonstrating the trade-off between stator and rotor efficiency and test factor for constant radial profiles, loss profiles and test factor profiles.

If constant radial profiles of stator efficiency η_S, rotor efficiency η_R, and test factor RTF, are utilized with a rotor recovery factor η_{RR} = 1.0, to establish the design point condition, then Figure 2 may be used to select values of stator and rotor efficiency and test factor to produce 88.5% total-total efficiency at a total-total pressure ratio of 1.797 at the design point as shown in the following table:

RTF	.95		1.0	
	η_S	η_R	η_S	η_R
	.98	.92	.98	.856
	.96	.938	.96	.870
	.94	.96	.94	.886

The efficiency characteristic with total pressure ratio along the 100% design speed line is shown in Figures 5 and 6. It can be seen that with high stator efficiency and low rotor efficiency the maximum efficiency was higher, occurs at a lower pressure ratio, and the decrease in efficiency with pressure ratio was greater than with low stator efficiency and high rotor efficiency. It is also shown that with a high rotor test factor and low rotor efficiency that the maximum efficiency was higher and the decrease in efficiency with pressure ratio was greater than with a low rotor test factor and high rotor efficiency.

Two methods to produce radial variation in stagnation condition are presented as a loss profile method and a test factor profile method. In the loss profile method, the radial variation in stator efficiency and rotor efficiency were selected as:

$$\eta_S \text{ and } \eta_R = 1\text{-}2x,\ 1\text{-}x,\ 1\text{-}x,\ 1\text{-}x,\ 1\text{-}2x$$

where 1-x in the three center sectors was selected the same as Figure 5 for comparison purposes. Shown in Figure 7 is the efficiency characteristic with total pressure ratio along the 100% design speed line. It is shown that the trade-off between stator and rotor efficiency was similar to Figure 5, however, the efficiency level was approximately 2% higher. Therefore lower values of stator efficiency and/or rotor efficiency must be used with the loss profile method to produce 88.5% total-total efficiency at the design point.

In the test factor profile method, the radial variation in rotor test factor was selected as:

$$TF = .875,\ 1.0,\ 1.0,\ 1.0,\ .875$$

to produce a sector height average test factor of .95 for comparison purposes. The results shown in Figure 8 are identical to Figure 5.

The constant radial profile, loss profile, and test factor profile methods are compared in Figures 9 through 11 along the 100% design speed line. It is shown that high stator efficiency with low rotor efficiency produces a higher maximum efficiency along the 100% speed line and the decrease in efficiency with pressure ratio was greater than with low stator efficiency and high rotor efficiency. With a high rotor test factor and low rotor efficiency, the maximum efficiency along the 100% speed line was higher and the decrease in efficiency with pressure ratio was greater than with a low rotor test factor and high rotor efficiency. With the loss profile method, the efficiency was approximately 2% higher, therefore lower values of stator efficiency and/or rotor efficiency must be used to produce the same efficiency. The test factor profile method produced overall results which were the same as the constant test factor method for the same average test factor. Discussion of the Task III selected geometrics with the NASA Project Manager and the NASA Research Advisor resulted in the following selected loss parameter input:

a) TF = 1.0

b) η_S = .94, .97, .97, .97, .94

c) η_R = 1-2x, 1-x, 1-x, 1-x, 1-2x,

where x was selected as .093 on stage one and .108 on stage two to match design data.

3.2.2 Optimum Incidence. - The optimum incidence angle and off-design incidence angle relationship calculated for the NASA Lewis Research Center turbine in Task II were used in determining the performance maps. The optimum incidence angle was assumed to occur at -8° from the design condition and the inlet recovery factor for off-design incidence was assumed to vary as $\cos^{3.}$ for positive incidence angle and negative incidence angle.

3.3 - Results. - The results are presented as performance maps in the form of equivalent work versus equivalent weight-flow-speed parameter with contours of total pressure ratio, equivalent speed and efficiency. Equivalent weight-flow versus total pressure ratio as well as mean section incidence angle, rotor-hub Mach Number and rotor-hub reaction versus equivalent work are also presented.

3.3.1 Single Stage Turbine. - Shown in Figures 12 through 29 are the performance maps and additional graphs showing rotor incidence angle, stage exit angle, rotor hub relative inlet Mach Number and hub reaction versus equivalent work in the speed range of 60% to 120% of design for three stator positions. The variation of significant parameters along the peak efficiency ridge is given in the three following tables for the three stator schedules.

SINGLE STAGE

STATOR SCHEDULE 0.0

$\%N/\sqrt{\theta_{CR}}$	60	70	80	90	100	110	120
$W\sqrt{\theta_{cr}}\,\epsilon/\delta$	26.20	30.18	33.07	35.64	37.54	39.15	39.70
$WN\epsilon/60\delta$	1154.6	1551.5	1943.6	2356.7	2757.2	3163.7	3499.4
$\Delta h/\theta_{cr}$	4.27	6.10	7.94	10.14	12.43	15.32	17.09
P_{To}/P_{T2}	1.145	1.216	1.294	1.395	1.513	1.682	1.802
η_{TT}	.901	.900	.899	.898	.895	.892	.886
I_R	-.27	1.22	.31	-.34	-2.03	-5.45	-8.99
R_{XR}	.106	.117	.136	.161	.194	.289	.288
α_2	-7.03	-3.37	-2.37	-.31	1.28	5.01	4.21
M_f	.158	.193	.225	.261	.299	.334	.381

STATOR SCHEDULE -7.53

$\%N/\sqrt{\theta_{CR}}$	60	70	80	90	100	110	120
$W\sqrt{\theta_{cr}}\,\epsilon/\delta$	37.38	40.08	42.33	44.22	44.79	45.06	44.96
$WN\epsilon/60\delta$	1647.2	2060.7	2487.4	2923.9	3290.2	3641.1	3962.8
$\Delta h/\theta_{cr}$	6.29	7.94	9.76	11.95	13.37	14.77	15.59
P_{To}/P_{T2}	1.234	1.308	1.400	1.523	1.618	1.726	1.807
η_{TT}	.866	.863	.857	.848	.837	.822	.805
I_R	-4.50	-8.70	-7.53	-17.51	-25.18	-33.62	-43.03
R_{XR}	.357	.391	.431	.485	.526	.571	.602
α_2	26.35	24.68	23.82	24.41	22.45	20.98	18.11
M_f	.248	.283	.322	.371	.402	.436	.457

STATOR SCHEDULE 7.13

$\%N/\sqrt{\theta_{cr}}$	60	70	80	90	100	110	120
$W\sqrt{\theta_{cr}}\,C/S$	18.07	20.34	22.09	23.78	25.30	26.60	27.84
$WNC/60S$	796.3	1045.7	1298.0	1572.2	1858.7	2149.2	2454.1
$\Delta h/\theta_{cr}$	3.41	4.56	5.66	6.97	8.48	10.18	12.52
P_{To}/P_{T2}	1.113	1.155	1.196	1.249	1.313	1.390	1.507
η_{TT}	.907	.908	.909	.910	.910	.910	.909
I_R	14.07	13.18	10.82	9.43	8.50	7.69	8.61
R_{XR}	-.117	-.111	-.101	-.093	-.086	-.078	-.072
α_2	-43.61	-43.94	-45.41	-45.85	-45.77	-45.42	-43.43
M_f	.106	.124	.140	.158	.177	.197	.224

The single stage turbine evaluated with: a.) stator at design point position; b.) stator at open position; and, c.) stator at closed position; had a peak turbine total-total efficiency of .901, .866, and .910 for the three maps respectively. At design speed, as the stator was opened to 130% design area the equivalent flow parameter increased to 119% design and as the stator was closed to 70% design area the equivalent flow parameter decreased to 67% design. As the the stator was opened, due to the restriction of the rotor area, the weight flow did not increase as fast as the stator area was increased; however, as the stator was closed it was the controlling restriction and the weight flow decreased nearly proportional to the area schedule. At design schedule the stator pressure ratio was 1.330 at peak turbine efficiency; and as the stator was opened, the stator pressure ratio decreased to 1.240; and when closed, the stator pressure ratio was 1.30. The rotor pressure ratio was 1.275, 1.535, and 1.090 for the three stator positions respectively. Of significant importance is the swing in rotor incidence angle and leaving exit angle with the stator position. As the stator was opened, the rotor incidence changed -23.15° and the leaving swirl changed +21.17°. As the stator was closed, the rotor incidence changed +10.53° and the leaving swirl changed -47.05°. For a net area change of 186% over minimum, the equivalent flow changed 177% over minimum, the rotor incidence angle changed 33.68° and the leaving angle changed 68.22°.

3.3.2 Two Stage Turbine. - Shown in Figures 30 through 119 are the performance maps and additional graphs showing rotor incidence angle, stator exit angle, turbine exit angle, rotor hub relative inlet Mach Number and hub reaction versus equivalent work in the speed range of 60% to 120% of design for three stator positions on each of the two stators. The variation of significant parameters along the peak efficiency ridge is given in the nine following tables for the nine stator schedules.

TWO STAGE

STATOR SCHEDULE 0.0, 0.0

$\%N/\sqrt{\theta_{cr}}$	60	70	80	90	100	110	120
$W\sqrt{\theta cr}$ C/S	33.56	34.02	36.66	38.30	39.34	39.70	39.70
WNC/60S	1478.9	1749.3	1254.5	2532.1	2890.1	3207.6	3499.4
$\Delta h/\theta cr$	10.73	11.68	15.73	20.01	25.14	29.80	35.58
P_{To}/P_{T_2}	1.443	1.485	1.718	2.016	2.465	3.005	4.169
η_{TT}	.867	.878	.882	.886	.889	.888	.878
$I_{R,1}$	15.39	9.51	8.51	6.14	2.80	-2.95	-10.99
RXR, 1	.091	.112	.143	.181	.224	.261	289
$Is_{,2}$	11.91	3.12	4.19	3.87	3.25	-.06	-5.60
$I_{R,2}$	-5.11	-15.98	-12.05	-9.22	-5.38	-4.18	-5.37
$R_{XR,2}$	-.035	.005	.005	.016	.044	.106	.310
$\alpha_{2,2}$	-20.22	-29.88	-24.97	-20.15	-12.46	-5.08	9.93
$M_{f,2}$	.168	.175	.217	.264	.331	.411	.584

STATOR SCHEDULE -7.53, 0.0

$\%N/\sqrt{\theta_{cr}}$	60	70	80	90	100	110	120
$W\sqrt{\theta cr}$ C/S	35.26	38.34	40.87	42.99	43.69	43.81	43.63
WNC/60S	1553.7	1971.2	2402.0	2842.6	3209.1	3539.7	3845.6
$\Delta h/\theta cr$	8.92	11.77	15.24	20.15	24.07	27.50	31.65
P_{To}/P_{T_2}	1.352	1.498	1.706	2.067	2.437	2.850	3.556
η_{TT}	.867	.867	.865	.864	.860	.854	.839
$Ir_{,1}$	-11.08	-14.77	-18.77	-22.94	-30.63	-39.86	-49.59
$RXR_{,1}$	.351	.381	.417	.462	.496	.519	.534
$Is_{,2}$	11.63	10.38	9.66	9.98	7.10	2.42	-3.96
$Ir_{,2}$	-4.99	-4.93	-3.45	0.76	1.16	-0.30	-4.26
$R_{XR,2}$	-.036	-.026	-.014	.007	.053	.126	.314
$\alpha_{2,2}$	-20.17	-18.96	-15.69	-7.68	-3.10	1.17	11.14
$M_{f,2}$	.167	.200	.242	.308	.371	.441	.582

TWO STAGE

STATOR SCHEDULE 7.13, 0.0

$\%N/\sqrt{\theta cr}$	60	70	80	90	100	110	120
$W\sqrt{\theta cr}\,\epsilon/S$	24.67	26.96	28.80	29.67	29.88	29.88	29.88
$WN\epsilon/60S$	1087.1	1386.0	1692.2	1961.5	2194.6	2414.0	2633.5
$\Delta h/\theta cr$	8.122	11.22	15.74	21.49	34.13	37.03	41.37
P_{T0}/P_{T2}	1.346	1.514	1.804	2.271	3.929	4.388	5.415
η_{TT}	.800	.806	.815	.827	.847	.863	.868
$I_{r,1}$	29.91	29.77	30.17	30.35	30.72	28.32	25.42
$R_{XR,1}$	-.184	-.175	-.163	-.143	-.078	-.059	-.042
$I_{s,2}$	-13.32	-12.41	-8.58	-4.72	5.26	-1.43	-8.97
$I_{r,2}$	-40.13	-37.74	-31.02	-22.89	-.43	-4.86	-9.95
$R_{XR,2}$	.082	.079	.063	.050	.076	.139	.313
$\alpha_{2,2}$	-47.44	-45.46	-40.30	-32.85	-3.17	-3.02	6.554
$M_{f,2}$	.116	.142	.179	.228	.391	.440	.570

STATOR SCHEDULE 0.0, -9.62

$\%N/\sqrt{\theta cr}$	60	70	80	90	100	110	120
$W\sqrt{\theta cr}\,\epsilon/S$	33.56	36.66	38.75	40.31	40.70	40.59	40.41
$WN\epsilon/60S$	1478.9	1885.0	2277.0	2665.3	2989.7	3279.6	3561.9
$\Delta h/\theta cr$	9.22	12.73	16.70	22.59	27.68	29.56	30.98
P_{To}/P_{T2}	1.389	1.582	1.843	2.337	2.912	3.198	3.500
η_{TT}	.828	.832	.837	.843	.845	.840	.827
$I_{r,1}$	15.39	14.63	13.20	11.76	7.65	1.11	-6.99
$R_{XR,1}$	.091	.124	.169	.246	.317	.338	.351
$I_{s,2}$	2.29	3.16	3.78	6.54	6.22	1.30	-4.94
$I_{r,2}$	-40.55	-38.83	-37.25	-32.08	-31.17	-36.96	-43.28
$R_{XR,2}$	.276	.285	.302	.335	.407	.465	.526
$\alpha_{2,2}$	-22.56	-19.05	-14.94	-4.74	3.20	2.80	3.31
$M_{f,2}$	.162	.201	.246	.323	.412	.457	.508

TWO STAGE

STATOR SCHEDULE -7.53, -9.62

$\%N/\sqrt{\theta_{cr}}$	60	70	80	90	100	110	120
$W\sqrt{\theta_{cr}}\ \epsilon/S$	40.08	42.33	44.79	45.33	45.43	45.22	44.85
$WN\epsilon/60S$	1766.2	2176.3	2632.2	2997.0	3337.3	3654.0	3953.1
$\Delta H/\theta_{cr}$	10.53	13.27	17.91	20.97	24.11	26.82	27.04
P_{To}/P_{T2}	1.453	1.614	1.944	2.220	2.572	2.967	3.105
η_{TT}	.835	.834	.832	.827	.819	.807	.785
$Ir,_1$	-1.61	-6.06	-9.38	-16.57	-25.21	-35.09	-45.40
$R_{XR,1}$	.373	.413	.479	.524	.565	.589	.591
$Is,_2$	12.28	10.53	11.70	9.70	7.35	3.57	-2.94
$Ir,_2$	-24.46	-26.95	-24.06	-26.60	-29.32	-33.78	-41.14
$R_{XR,2}$	.238	.264	.295	.341	.404	.490	.527
$\alpha_{2,2}$	-4.33	-5.24	1.26	2.23	4.84	8.13	5.31
$Mf,_2$	.203	.238	.303	.352	.414	.488	.513

STATOR SCHEDULE 7.13, -9.62

$\%N/\sqrt{\theta_{cr}}$	60	70	80	90	100	110	120
$W\sqrt{\theta_{cr}}\ \epsilon/S$	25.86	28.11	29.48	29.88	29.88	29.88	29.88
$WN\epsilon/60S$	1139.6	1445.5	1732.3	1975.5	2194.9	2414.3	2633.9
$\Delta h/\theta_{cr}$	8.32	11.79	16.48	31.81	37.77	37.58	38.89
P_{To}/P_{T2}	1.390	1.603	1.953	3.939	5.175	4.984	5.343
η_{TT}	.745β	.751	.761	.789	.810	.820	.822
$Ir,_1$	31.61	31.75	32.04	33.23	31.34	29.06	26.33
$R_{XR},1$	-.192	-.181	-.163	-.013	.034	.026	.023
$Is,_2$	-15.34	-12.93	-9.02	10.46	7.52	.34	-7.82
$Ir,_2$	-59.42	-57.01	-52.90	-25.46	-28.83	-38.08	-46.31
$R_{XR},2$	.317	.320	.324	.377	.557	.532	.590
$\alpha_{2,2}$	-42.41	-39.01	-33.12	6.69	17.78	8.34	7.61
$Mf,2$	.125	.156	.197	.398	.561	.521	.571

TWO STAGE

STATOR SCHEDULE 0.0, 8.81

$\%N/\sqrt{\theta cr}$	60	70	80	90	100	110	120
$W\sqrt{\theta cr}\ \epsilon/S$	26.20	29.12	31.73	33.32	34.46	34.79	34.79
$WN\epsilon/60S$	1154.6	1497.2	1864.7	2203.1	2531.3	2811.4	3067.1
$\Delta h/\theta cr$	7.23	9.81	13.13	16.20	19.74	22.13	23.84
P_{To}/P_{T2}	1.265	1.382	1.564	1.743	2.009	2.235	2.443
η_{TT}	.895	.894	.891	.886	.878	.866	.850
$Ir,_1$	-2.27	-4.47	-6.53	-11.49	-17.75	-27.84	-39.80
$R_{XR,1}$	.106	.122	.140	.163	.188	.214	.239
$Is,_2$	-8.02	-9.21	-9.73	-13.13	-17.11	-23.97	-31.41
$Ir,_2$	12.65	14.06	16.94	18.01	19.94	19.49	18.18
$R_{XR,2}$	-.249	-.252	-.261	-.261	-.261	-.249	-.233
$\alpha_{2,2}$	-46.54	-45.02	-41.81	-39.90	-36.41	-35.64	-35.78
$Mf,_2$	.117	.142	.173	.203	.241	.271	.299

STATOR SCHEDULE -7.53, 8.81

$\%N/\sqrt{\theta cr}$	60	70	80	90	100	110	120
$W\sqrt{\theta cr}\ \epsilon/S$	28.26	34.08	34.08	36.04	36.67	37.38	37.18
$WN\epsilon/60S$	1245.1	1752.2	2002.6	2382.5	2694.7	3020.3	3277.5
$\Delta h/\theta cr$	6.85	11.96	12.25	15.66	17.63	22.40	23.10
P_{To}/P_{T2}	1.261	1.528	1.540	1.764	1.926	2.394	2.514
η_{TT}	.858	.848	.848	.840	.830	.815	.801
$Ir,_1$	-32.67	-26.90	-40.19	-45.52	-54.26	-61.41	-69.97
$R_{XR,1}$	.357	.373	.396	.417	.436	.452	.463
$Is,_2$	-2.16	6.19	-5.26	-8.00	-14.87	-20.39	-28.95
$Ir,_2$	18.17	27.08	21.18	23.21	22.10	25.67	23.11
$R_{XR,2}$	-.274	-.311	-.281	-.284	-.271	-.268	-.247
$\alpha_{2,2}$	-41.65	-27.75	-36.88	-32.87	-33.47	-24.48	-27.72
$Mf,_2$	.126	.180	.184	.222	.248	.312	.330

TWO STAGE

STATOR SCHEDULE 7.13, 8.81

$\%N/\sqrt{\theta cr}$	60	70	80	90	100	110	120
$W\sqrt{\theta cr}\ G/S$	22.39	24.67	26.63	28.01	28.74	29.15	29.19
WNG/60S	986.6	1268.4	1564.7	1851.8	2110.0	2355.6	2573.0
$\Delta h/\theta cr$	7.58	10.31	13.86	18.07	22.08	27.15	29.51
P_{To}/P_{T_2}	1.294	1.423	1.617	1.889	2.200	2.704	2.995
η_{TT}	.859	.863	.868	.874	.879	.882	.881
$Ir,_1$	25.78	25.18	24.88	24.24	22.45	20.05	14.93
$R_{XR,1}$	-.165	-.157	-.148	-.137	-.121	-.103	-.081
$Is,_2$	-19.30	-19.95	-19.43	-19.51	-22.32	-25.77	-33.17
$Ir,_2$	-1.14	0.78	5.09	9.78	12.47	17.18	16.08
$R_{XR,2}$	-.187	-.192	-.206	-.221	-.226	-.233	-.216
$\alpha_{2,2}$	-54.17	-53.04	-50.47	-46.97	-44.07	-37.95	-37.52
$Mf,_2$	.103	.125	.152	.185	.219	.270	.301

The two stage turbine evaluated with both stators set at a.) design position; b.) open position; and c.) closed position; for a total of nine schedules had a range of peak turbine total-total efficiency as shown in the following table:

η_{TT}

	S2 @ design	S2 @ open	S2 @ closed
S1 @ design	.889	.845	.895
S1 @ open	.867	.835	.858
S1 @ closed	.868	.822	.882

The peak turbine total-total efficiency occurred at different corrected speeds with stator schedule. The first stage stator schedule was the primary influence on the corrected speed at which peak efficiency occurred. When the first stage stator was open, peak efficiency occurred at the low corrected speed end and when the first stage stator was closed, peak efficiency occurred at the high corrected speed end. Closing the second stage stator moved peak efficiency to lower corrected speeds, however not as effective as the first stage stator.

At maximum efficiency on the 100% design speed line, the equivalent flow parameter was influenced by the stator schedule as shown in the following table:

$W \sqrt{\theta_{cr}}\, \epsilon/S$

	S2 @ design	S2 @ open	S2 @ closed
S1 @ design	39.34	40.70	34.46
S1 @ open	43.69	45.43	36.67
S1 @ closed	29.88	29.88	28.74

At design speed with the second stage stator at design position, as the first stator was opened to 130% design area the equivalent flow parameter increased to 111% design and as the 1st stator was closed to 70% design area the equivalent flow parameter decreased to 76% design. With the first stage stator at design position, as the second stator was opened to 130% design area the equivalent flow parameter increased to 1.03% design and as the 2nd stator was closed to 70% design area the equivalent flow parameter decreased to 87% design. With both stators open to 130% design area, the equivalent flow parameter only increased to 115% design; however, with both stators closed to 70% design area, the equivalent flow parameter decreased to 73% design. Due to the restriction of the rotor areas, as the stators were opened the weight flow did not increase as fast as the stator area was increased. As the stators were closed the 1st stage stator was the primary controlling restriction and the weight flow decreased nearly proportional to the area schedule. The second stage stator was approximately half as effective.

Of significant importance is the swing in blade row incidence angle with stator schedule. The first rotor incidence angle was primarily a function of the first stator position. With stator 1 open the first rotor incidence was negative with a minimum value of -55.26° when the stator 2 was closed. With stator 1 closed the 1st rotor incidence was positive with a maximum value of 31.34 when the stator 2 was open. The second stator incidence angle was primarily a function of its own position. With stator 2 open the second stator incidence was positive with a maximum value of 7.52° when the stator 1 was closed. With stator 2 closed the second stator incidence was negative with a minimum value of -22.32° when stator 1 was closed. The second rotor incidence angle was primarily a function of the second stator position. With stator 2 open the second rotor incidence was negative with a minimum value of -31.17° when the stator 1 was design. With stator 2 closed the second rotor incidence was positive with a maximum value of 22.10° when the stator 1 was open. The leaving swirl at design speed maximum efficiency was primarily a function of the second stator position. With stator 2 open the leaving swirl was positive with a maximum value of 17.78° when the first stator was closed. With stator 2 closed, the leaving swirl was negative with a minimum value of -44.07° when the first stator was closed. For a net area change of 186% over minimum for both stators, the first rotor incidence angle changed 86.60°, the second stator incidence angle changed 29.84°, the second rotor incidence angle changed 53.27° and the leaving swirl angle changed 61.85°.

4.0 REFERENCES

Flagg, E. E. "Analytical Procedure and Computer Program for Determining Performance of Axial Flow Turbines".

SYMBOL LIST

h	total enthalpy, (Btu/lb.)
I	incidence angle (°)
M	Mach Number
Mf	axial Mach Number
N	rotational speed (rpm)
P	pressure (psi)
Rx	reaction
TF	test factor
W	weight flow (lb/sec)
$N/\sqrt{\theta cr}$	equivalent speed parameter
$W\sqrt{\theta cr}\ \epsilon/\delta$	equivalent weight-flow parameter
$WN\epsilon/60\delta$	equivalent weight flow-speed parameter
$\Delta h/\theta cr$	equivalent work parameter
α	gas flow angle (°)
δ	ratio of total pressure to standard pressure
ϵ	function of ratio of specific heats
θ	ratio of total temperature to standard temperature
η	efficiency

SUBSCRIPTS

cr	critical
R	rotor
R	root
RR	rotor recovery
RT	root
S	stator
T	total
TT	total-total
0,1,1A,2,2A	station designation
1,2	stage number

Figure 1.
NASA - TASK III
Turbine Flowpath

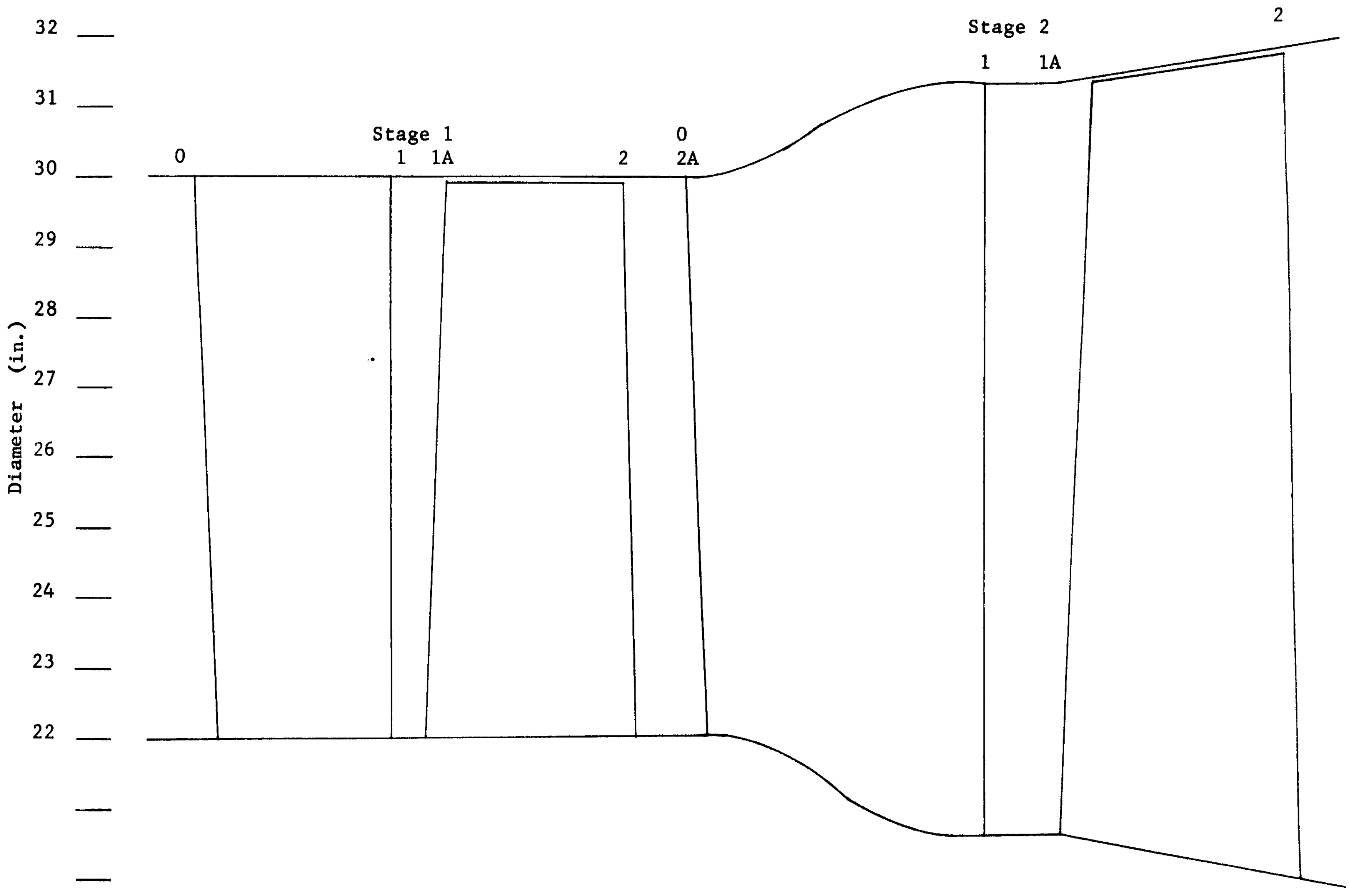

Figure 2

NASA - TASK III

Single Stage Parametric

RTF vs. η_R & η_S

η_{TT} = .885 at Design Point

η_{RR} = 1.00

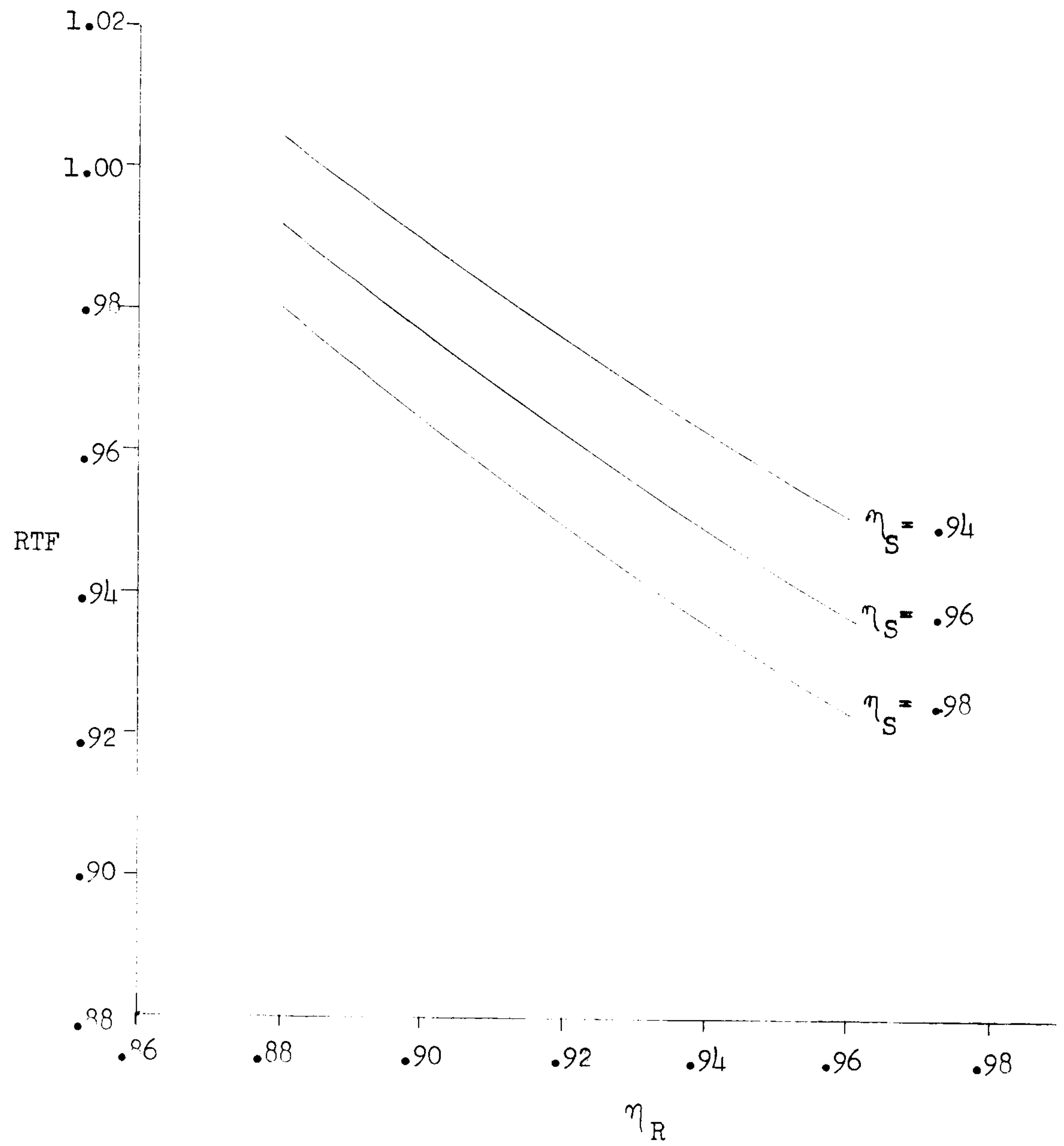

Figure 3

NASA - TASK III

Single Stage Parametric

RTF vs. η_R & η_S

η_{TT} = .885 at Design Point

η_{RR} = .95

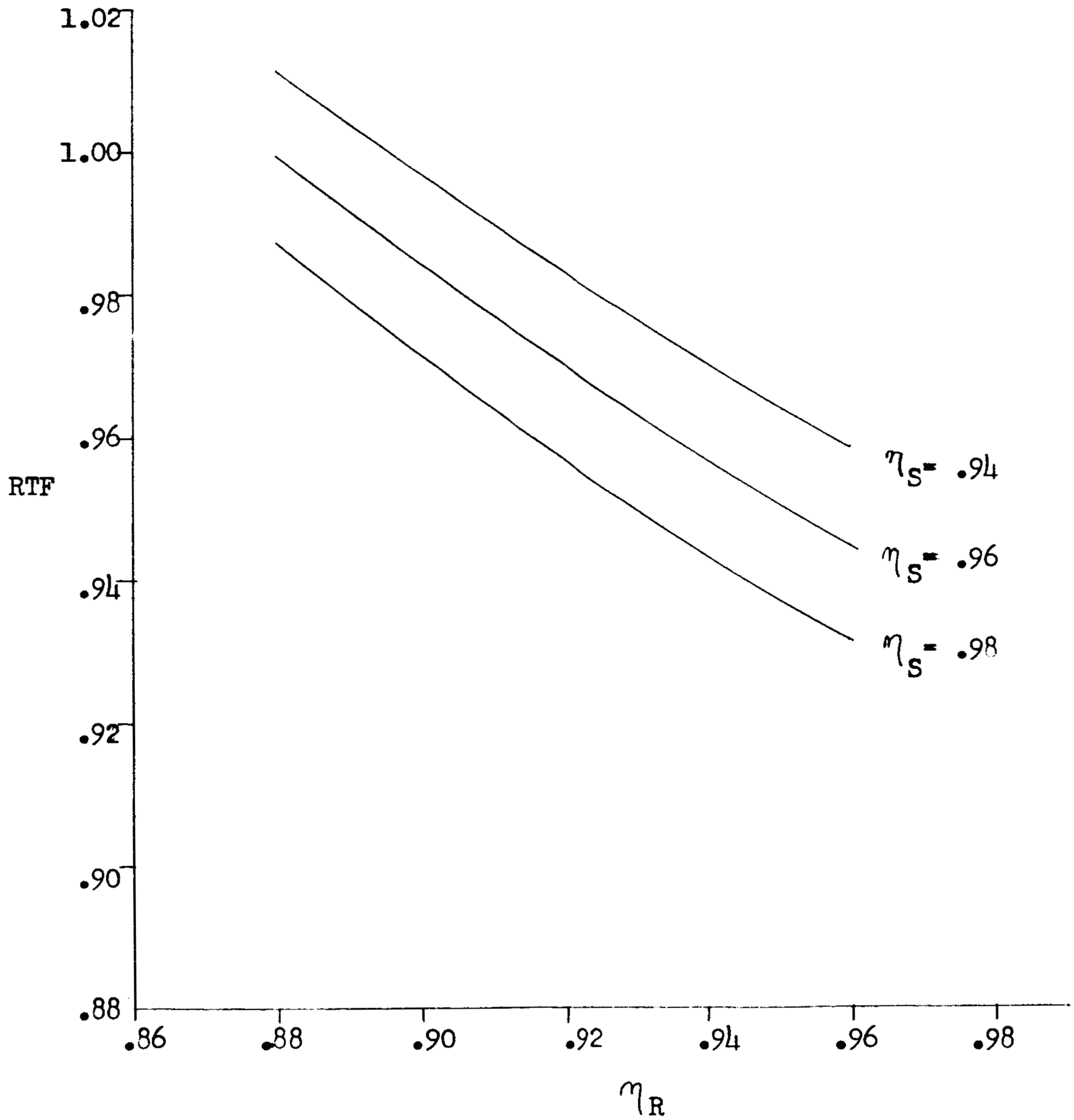

Figure 4

NASA - TASK III

Single Stage Parametric

RTF vs. η_R & η_S

η_{TT} = .885 at Design Point

η_{RR} = .90

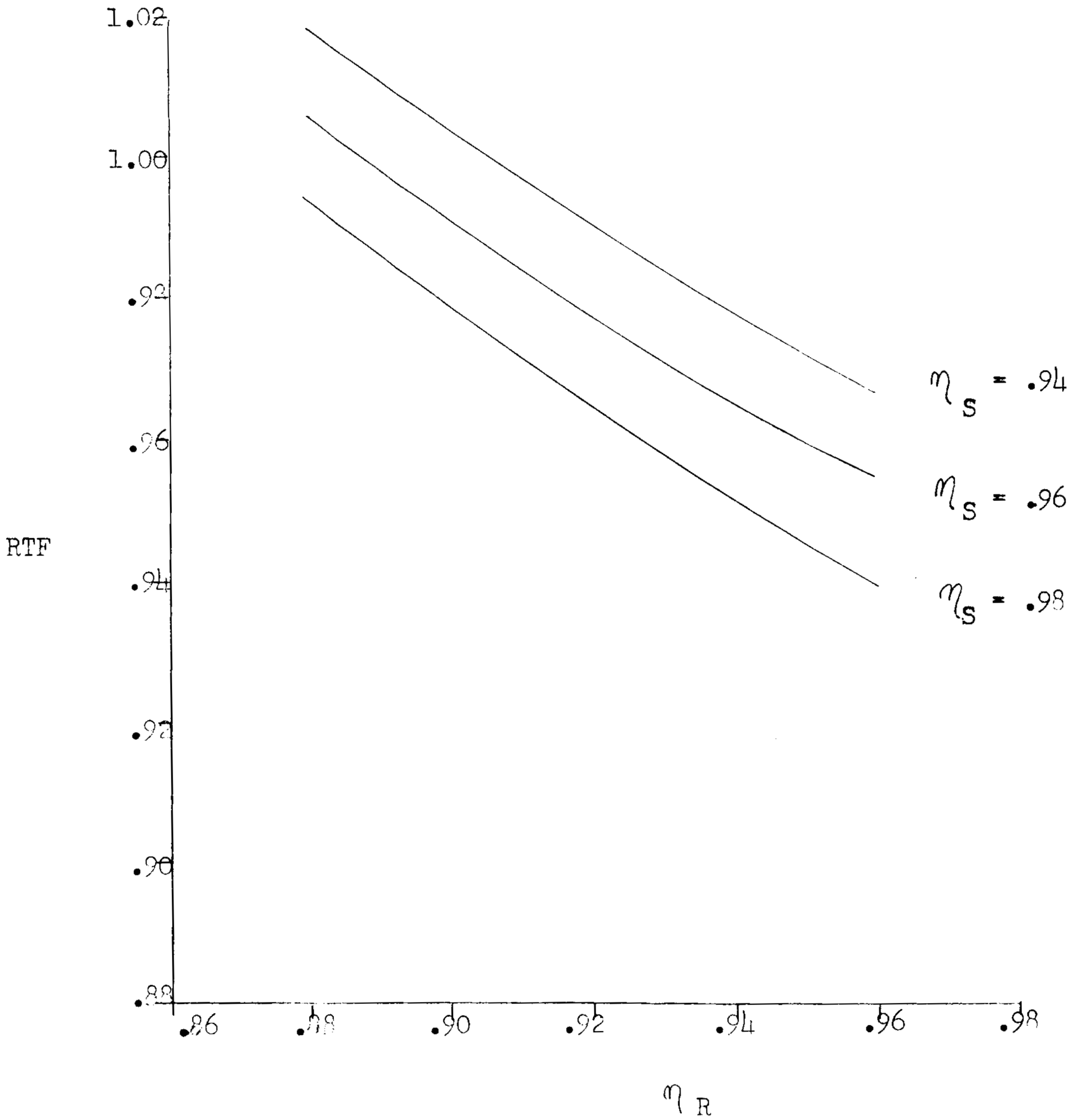

Figure 5

NASA - TASK III

Single Stage Parametric

Efficiency vs. Pressure Ratio

RTF = .95

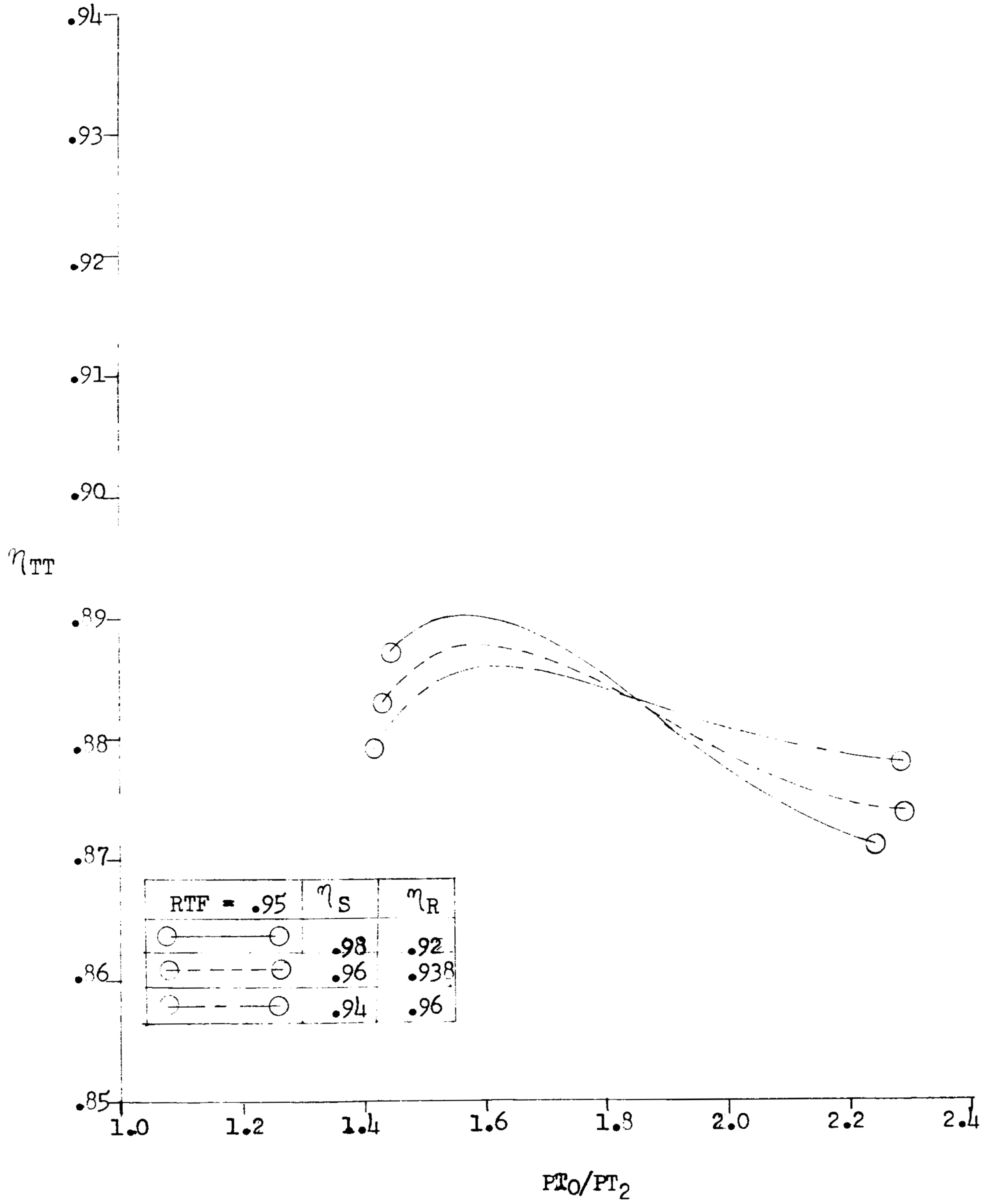

Figure 6

NASA - TASK III

Single Stage Parametric

Efficiency vs. Pressure Ratio

RTF = 1.0

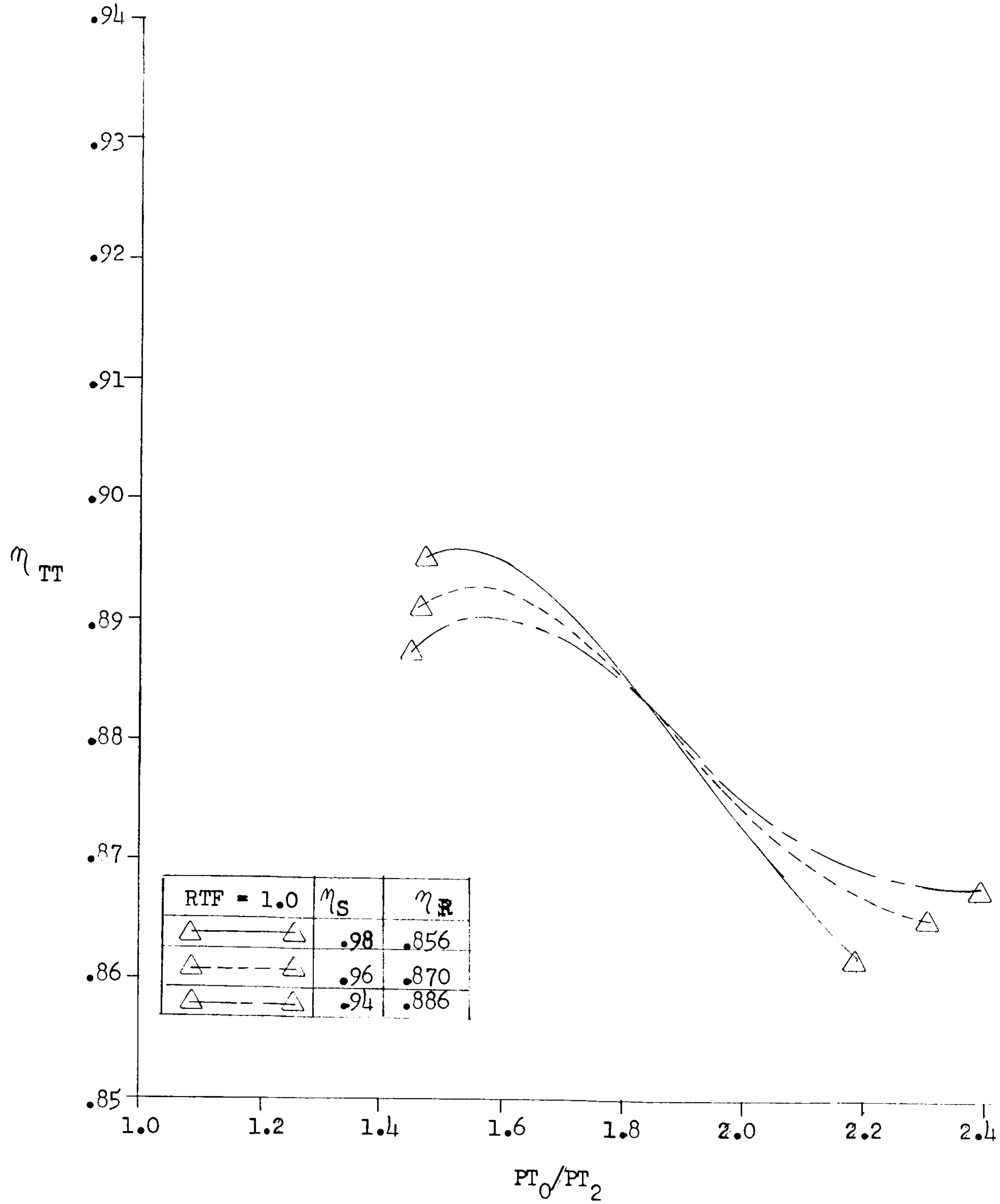

Figure 7

NASA - TASK III

Single Stage Parametric

Efficiency vs. Pressure Ratio

LOSS PROFILE

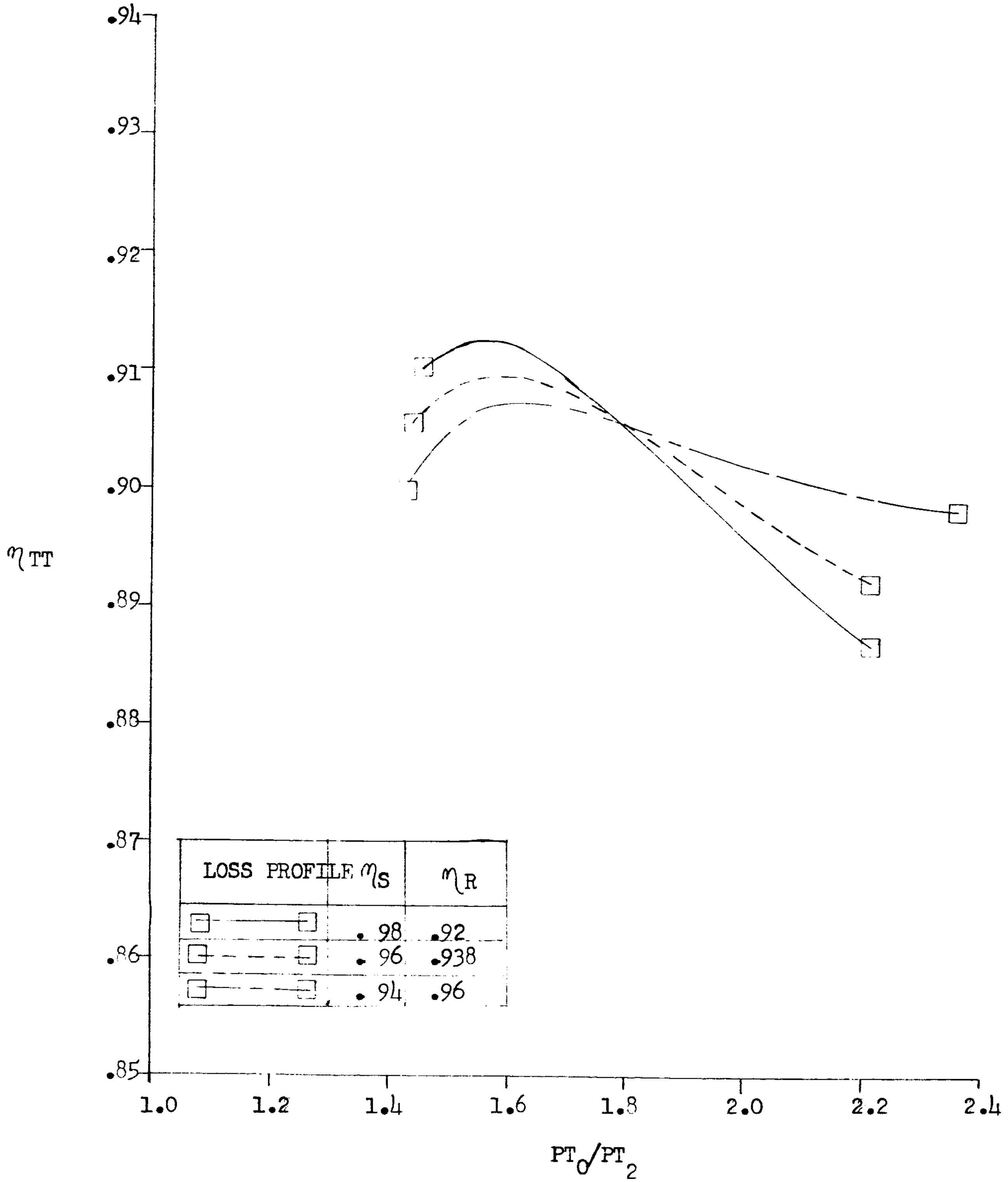

Figure 8

NASA - TASK III

Single Stage Parametric

Efficiency vs. Pressure Ratio

RTF PROFILE

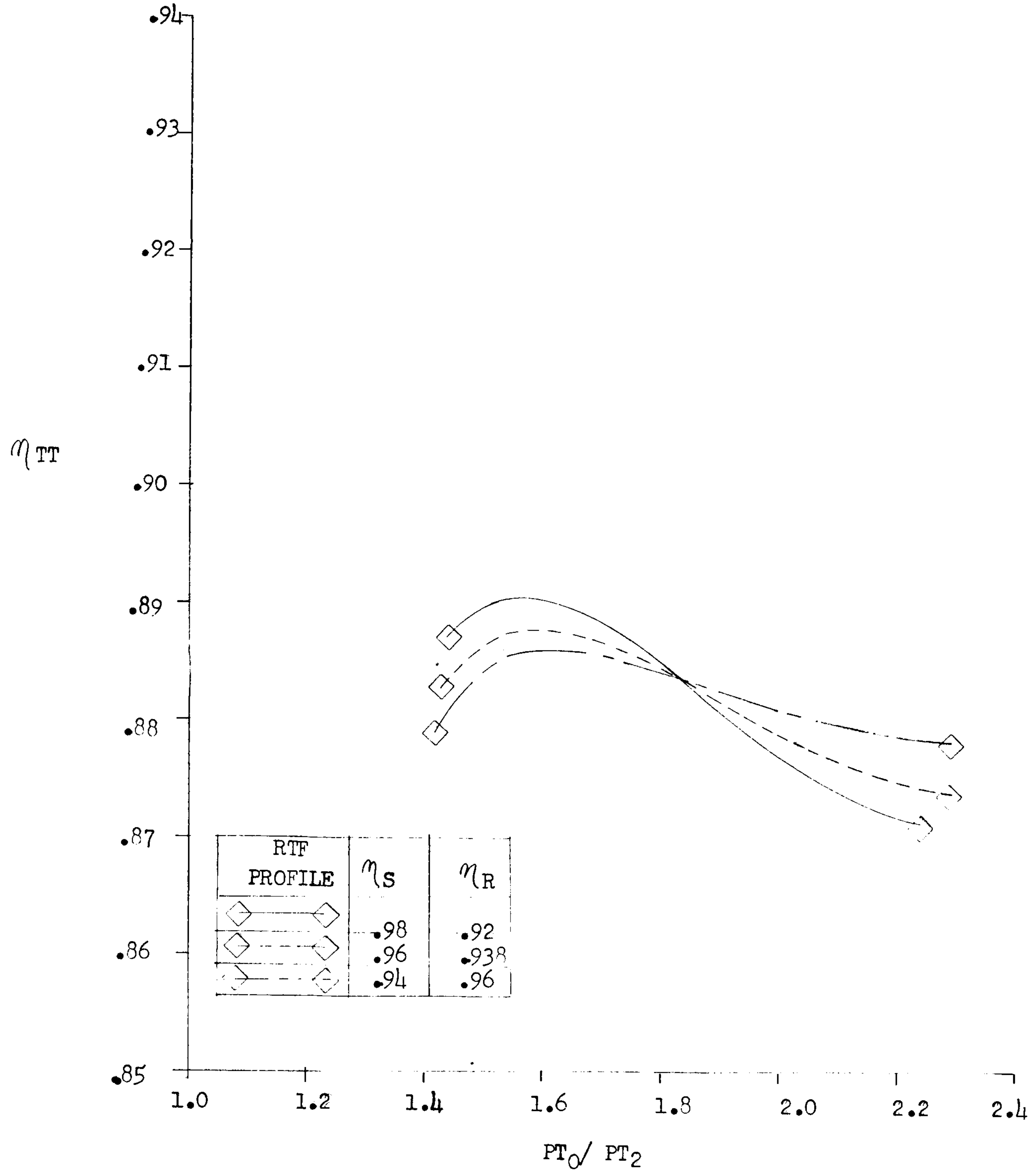

Figure 9

NASA - TASK III

Single Stage Parametric

Efficiency vs. Pressure Ratio

METHOD COMPARISON

$\eta_S = .98$

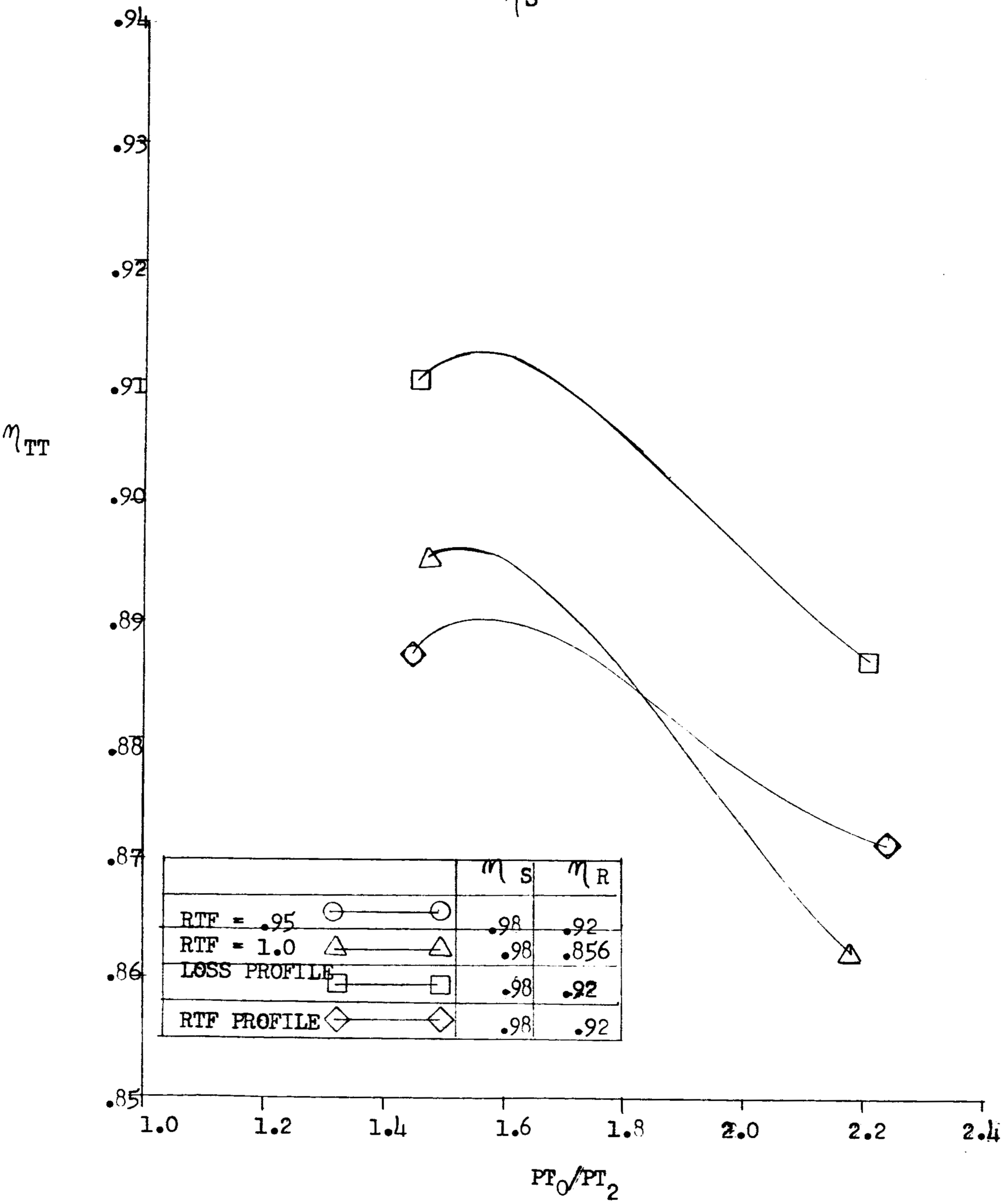

Figure 10

NASA - TASK III

Single Stage Parametric

Efficiency vs. Pressure Ratio

METHOD COMPARISON

$\eta_S = .96$

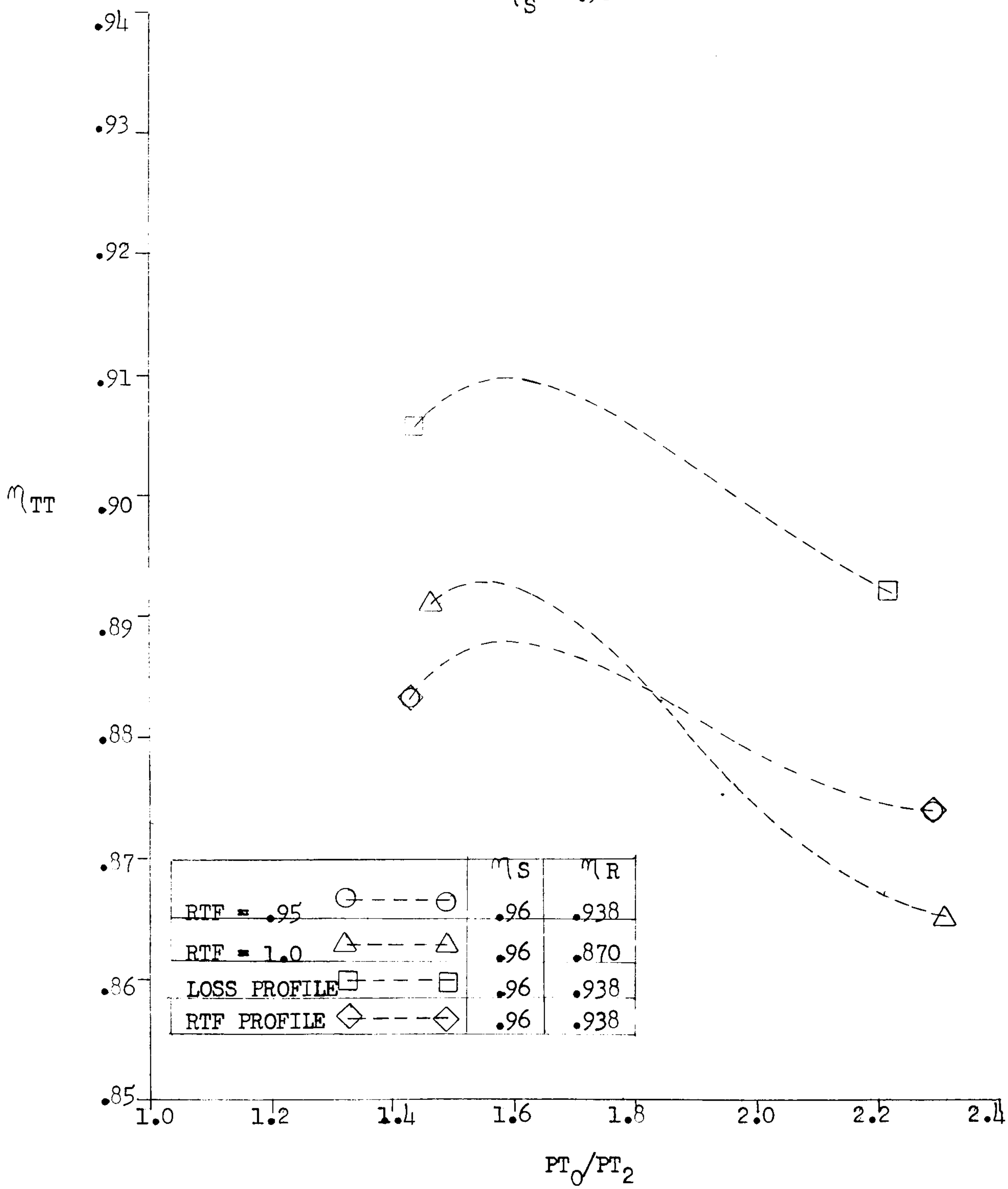

Figure 11

NASA - TASK III

Single Stage Parametric

Efficiency vs. Pressure Ratio

METHOD COMPARISON

$\eta_S = .94$

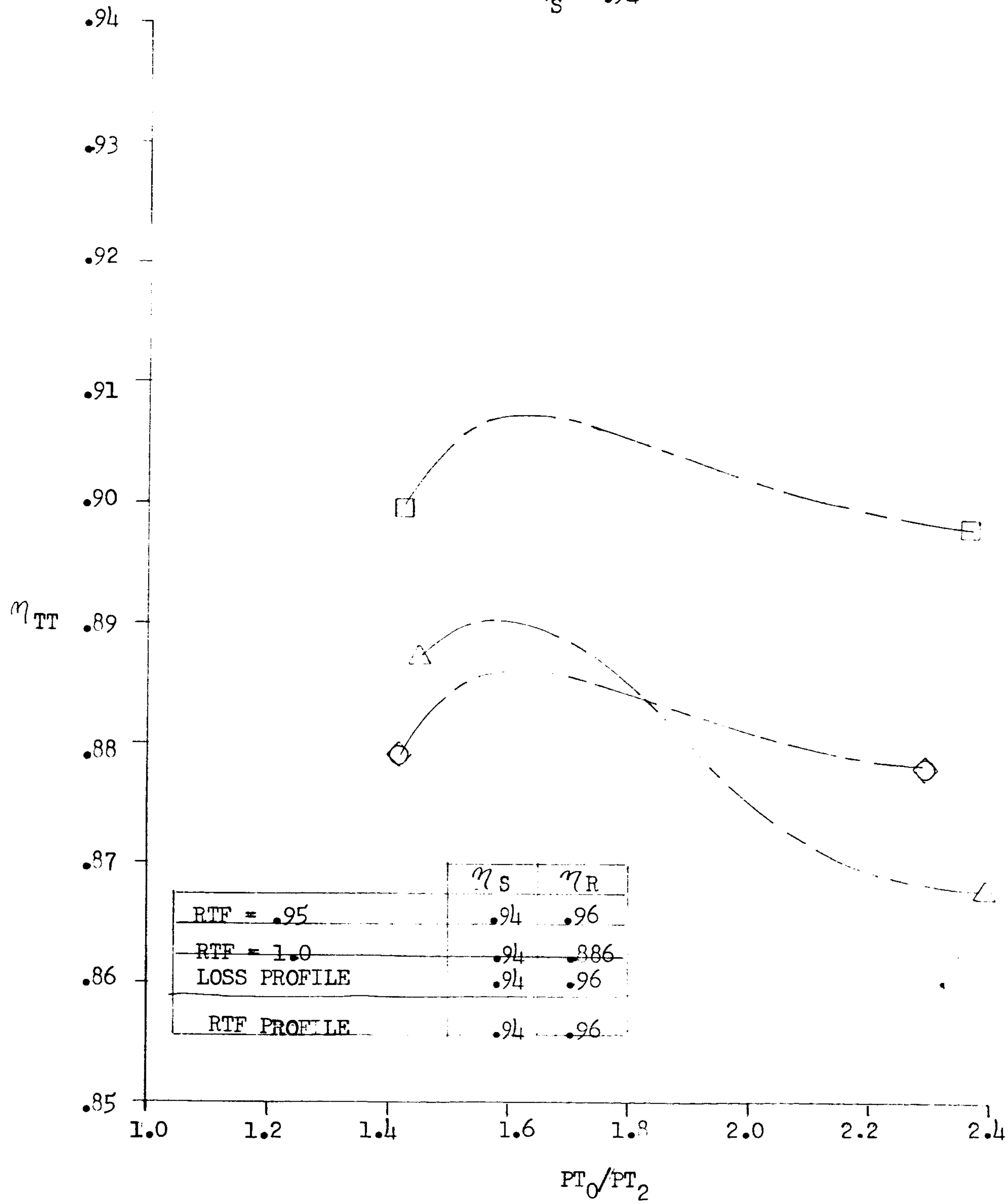

Figure 12

NASA - TASK III

Single Stage - Schedule 0.0

Performance Map

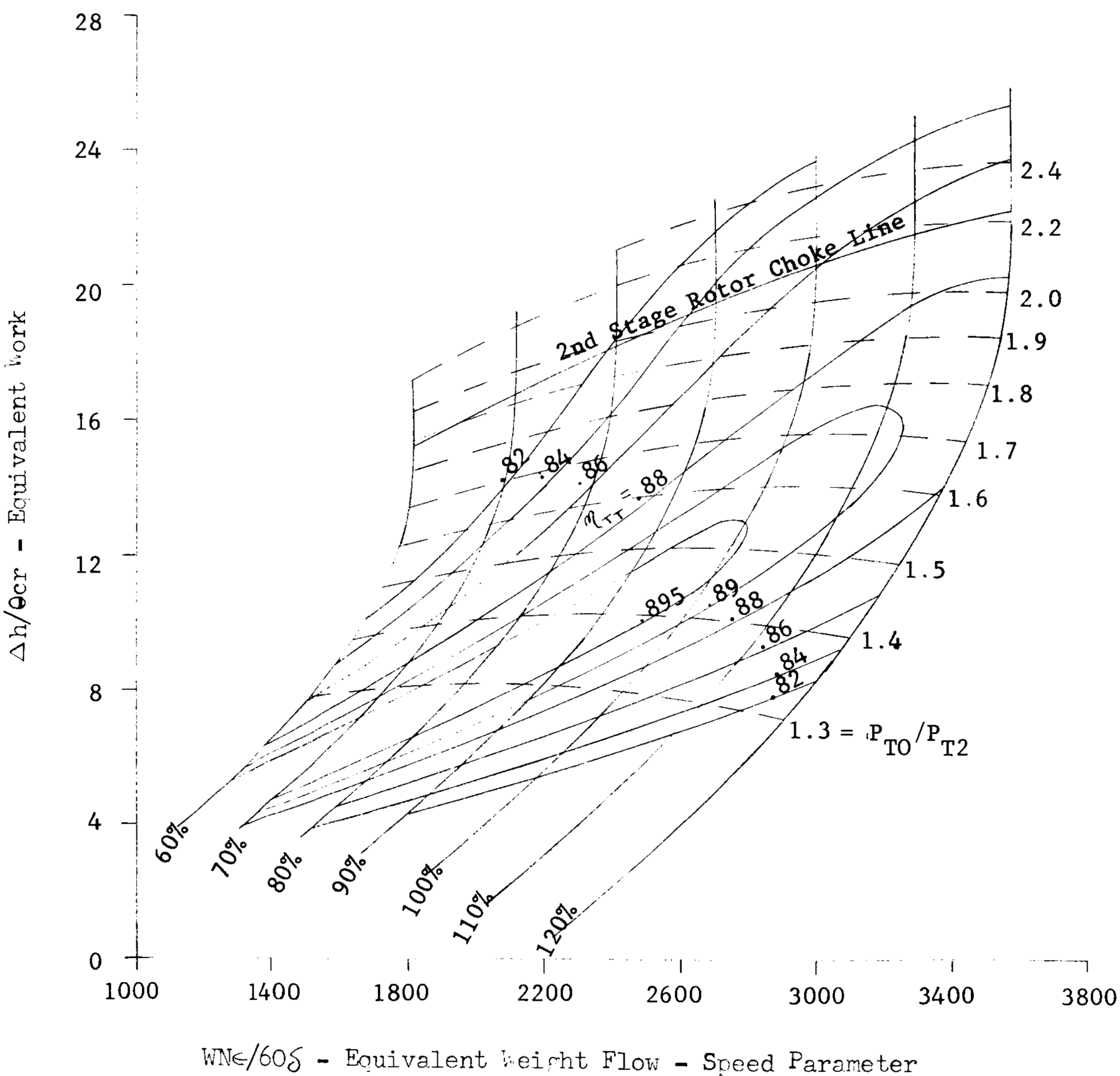

Figure 13

NASA - TASK III

Single-Stage Schedule 0.0

Equivalent Flow vs. Pressure Ratio

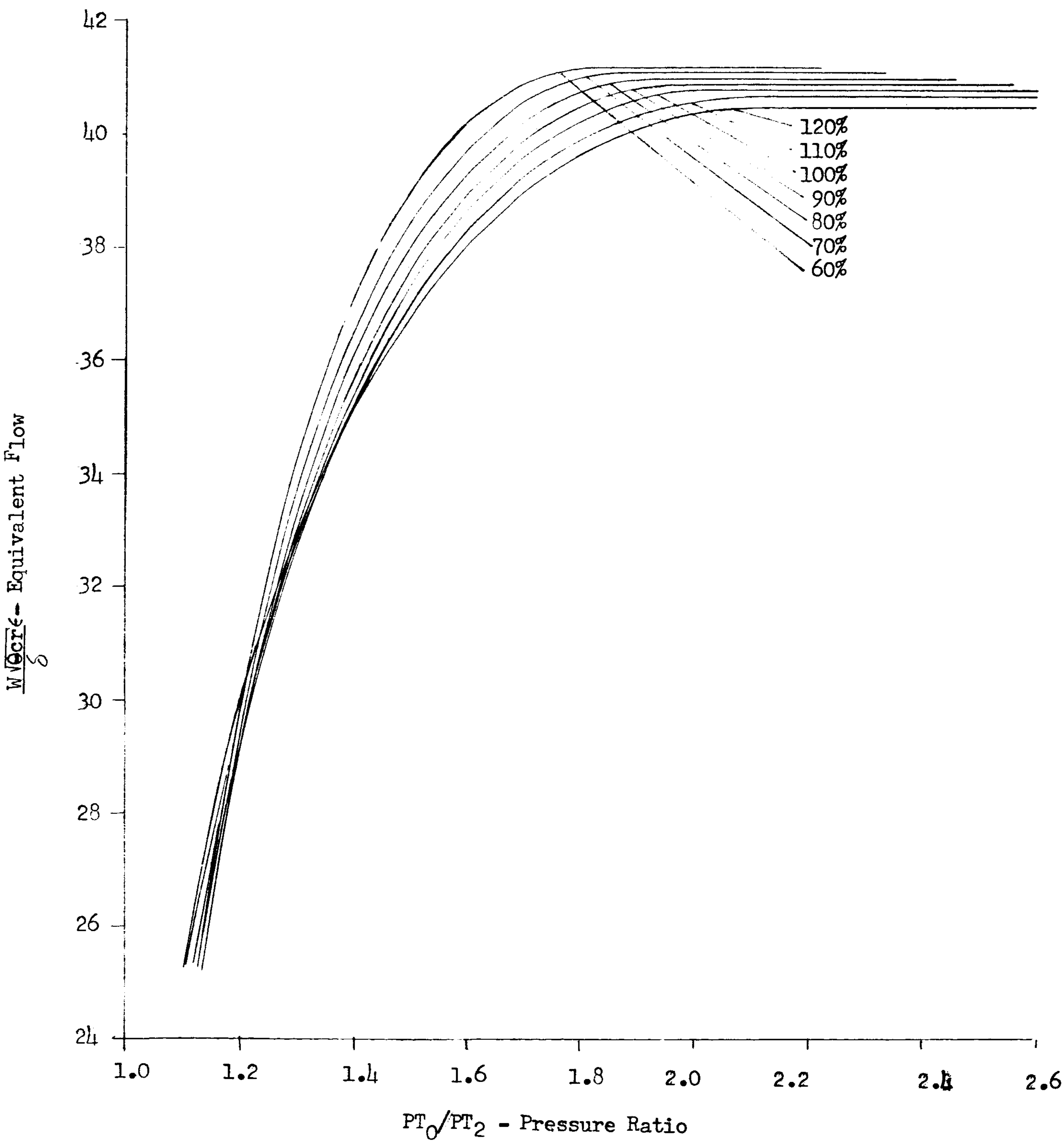

Figure 14

NASA - TASK III

Single Stage - Schedule 0.0

Rotor Incidence vs. Equivalent Work

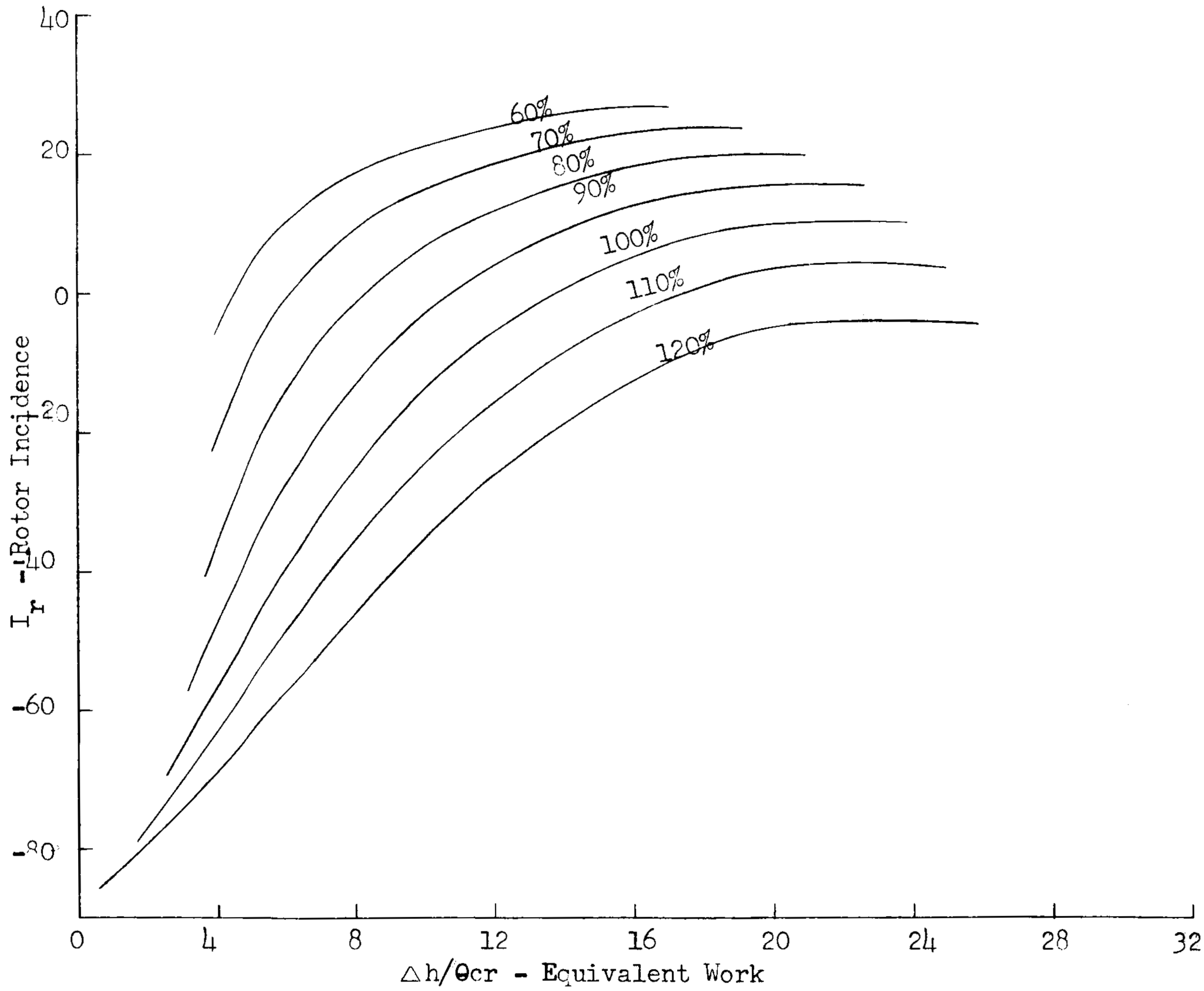

Figure 15

NASA - TASK III

Single Stage - Schedule 0.0

Exit Angle vs. Equivalent Work

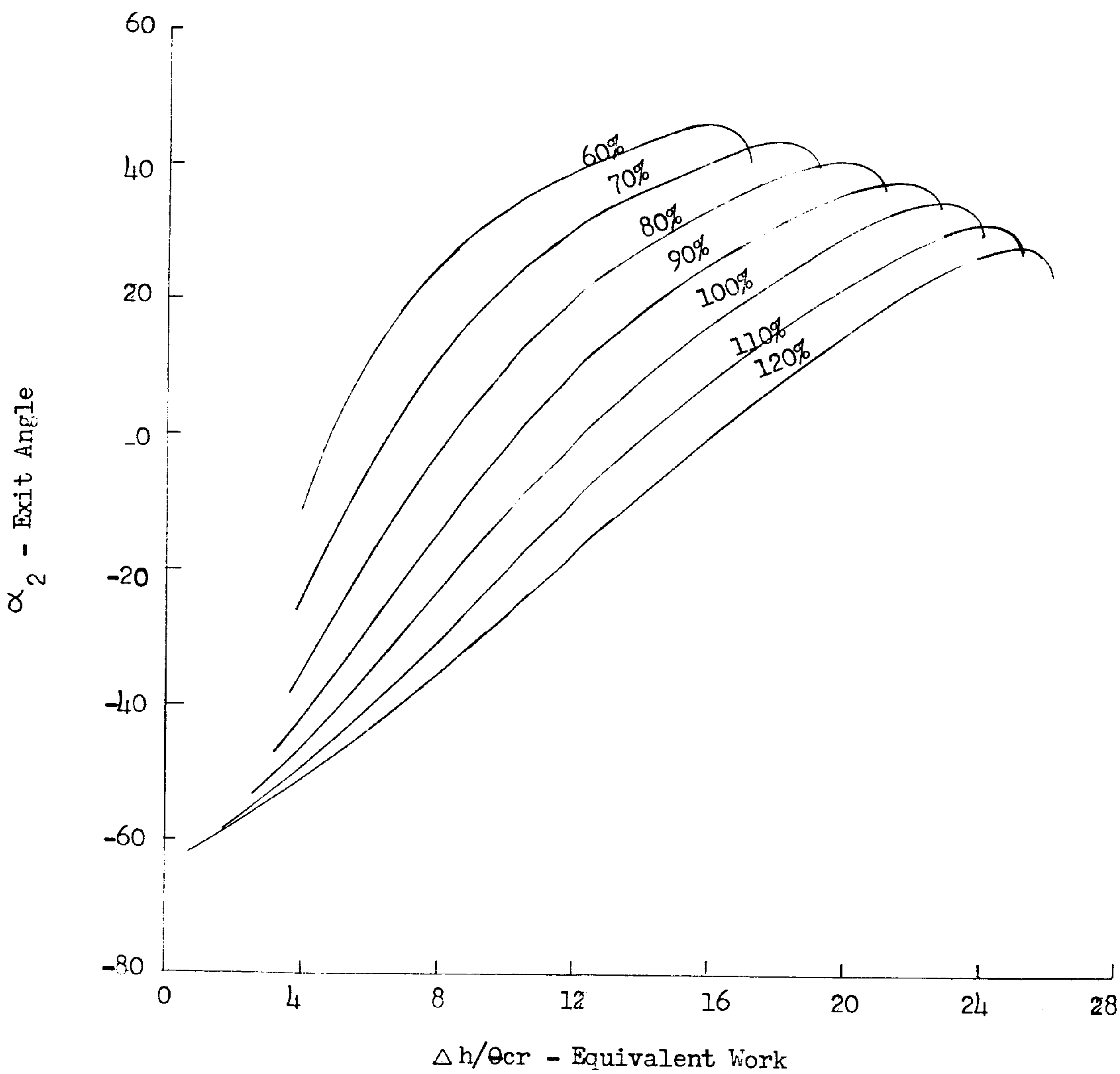

Figure 16

NASA - TASK III

Single Stage - Schedule 0.0

Hub Mach Number
vs.
Equivalent Work

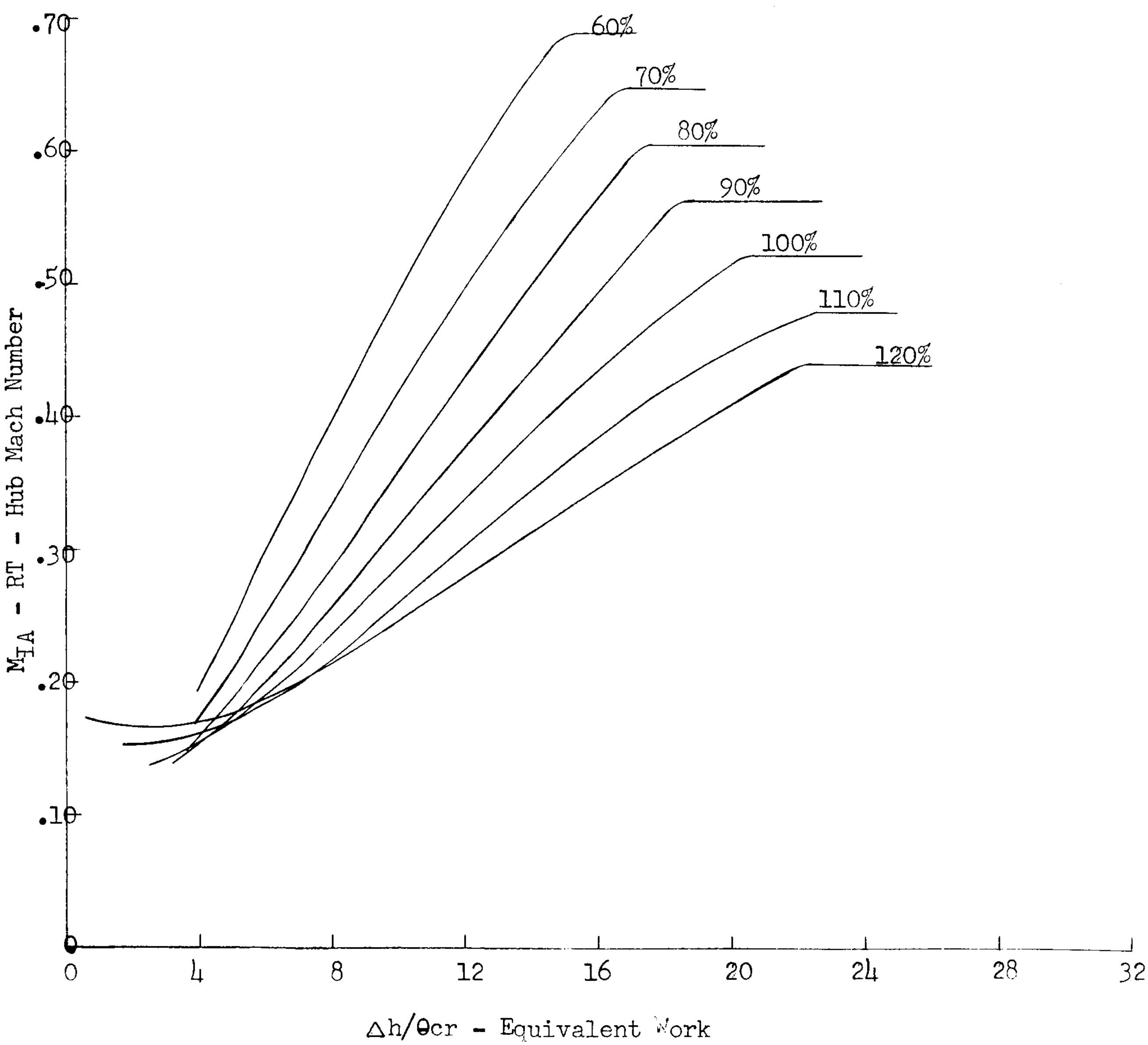

Figure 17

NASA - TASK III

Single Stage - Schedule 0.0

Hub Reaction
vs.
Equivalent Work

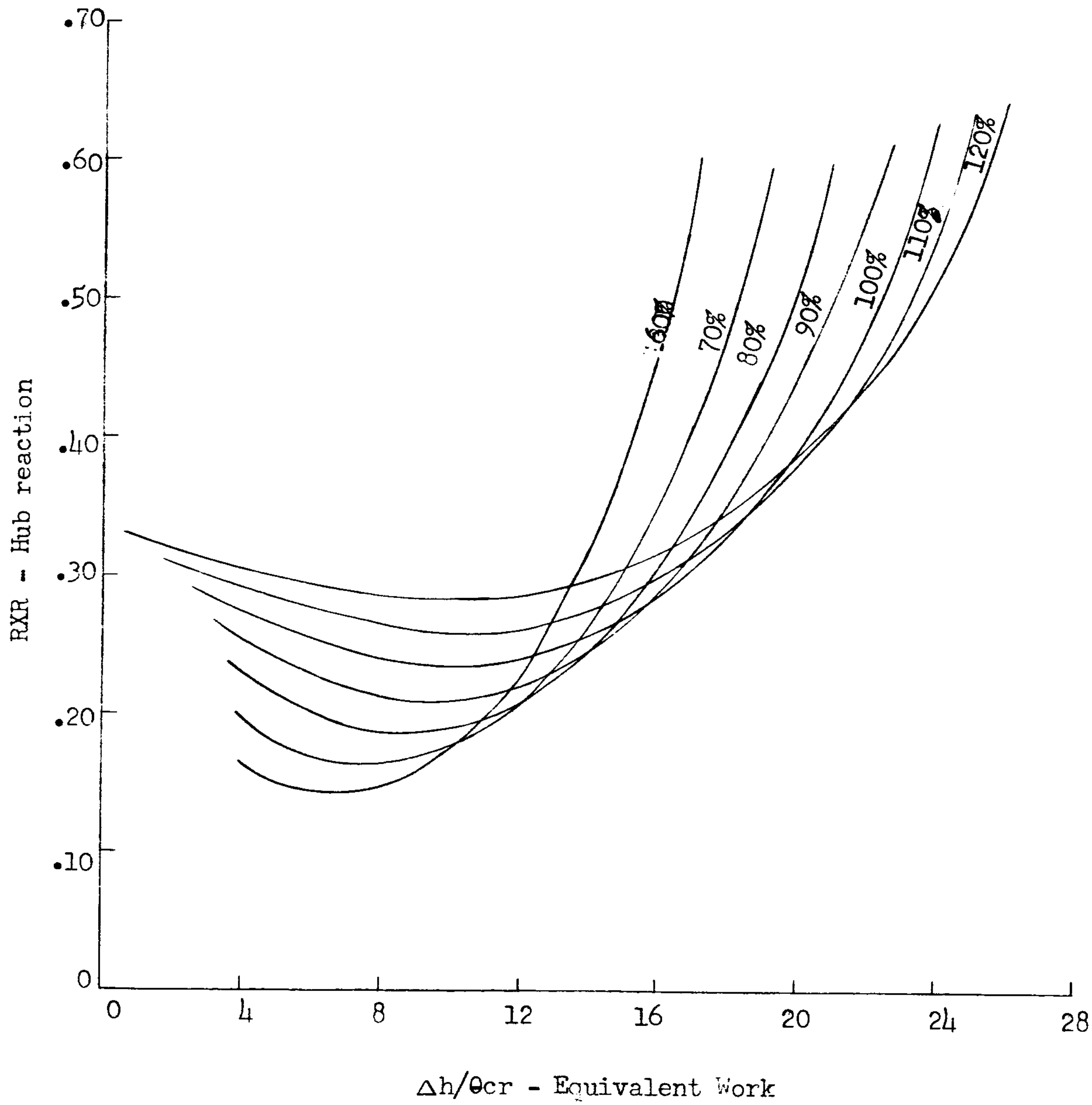

Figure 18

NASA - TASK III

Single Stage - Schedule -7.53

Performance Map

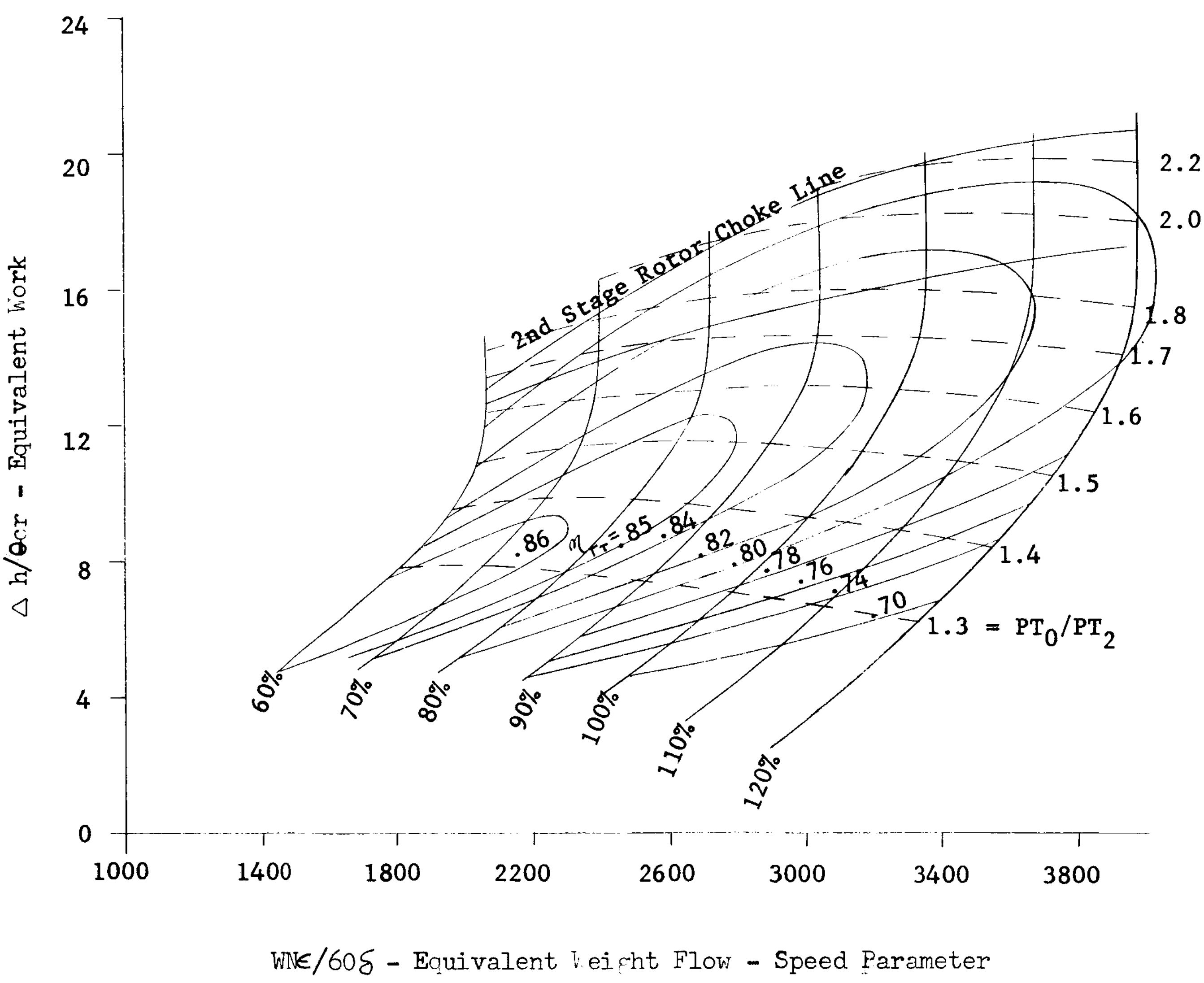

Figure 19

NASA - TASK III

Single Stage - Schedule -7.53

Equivalent Flow vs. Pressure Ratio

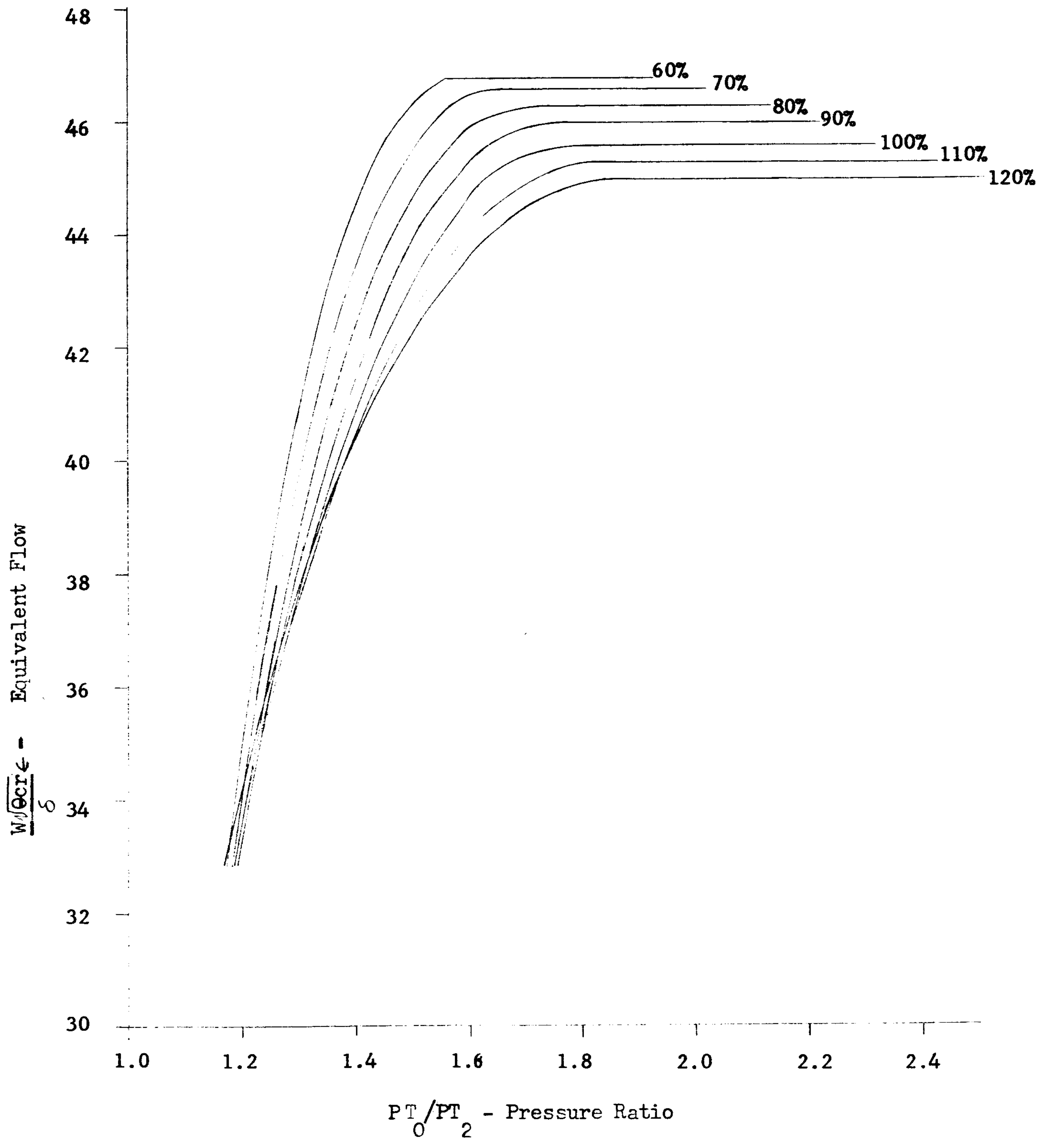

Figure 20

NASA - TASK III

Single Stage - Schedule -7.53

Rotor Incidence vs. Equivalent Work

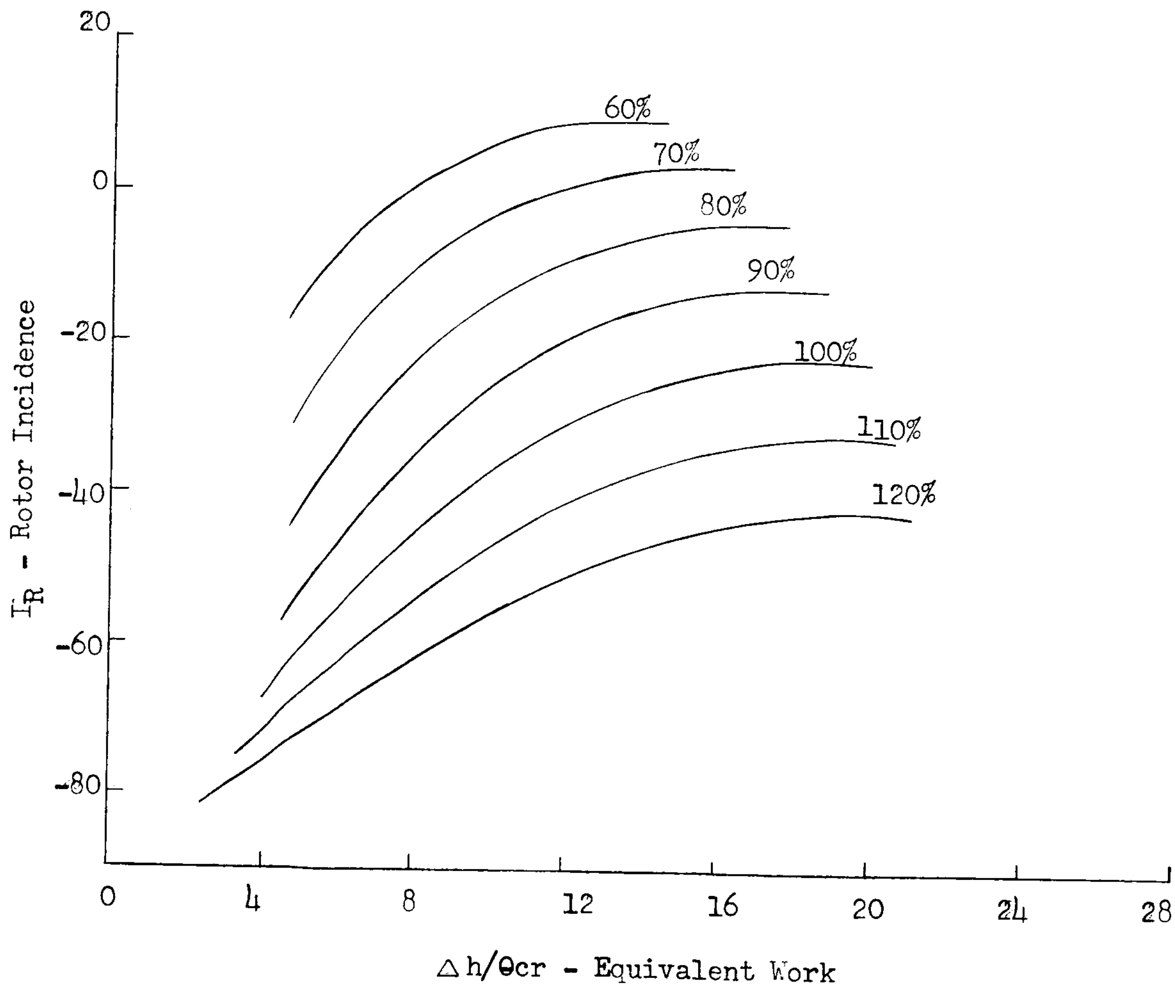

Figure 21

NASA - TASK III

Single Stage - Schedule -7.53

Exit Angle vs. Equivalent Work

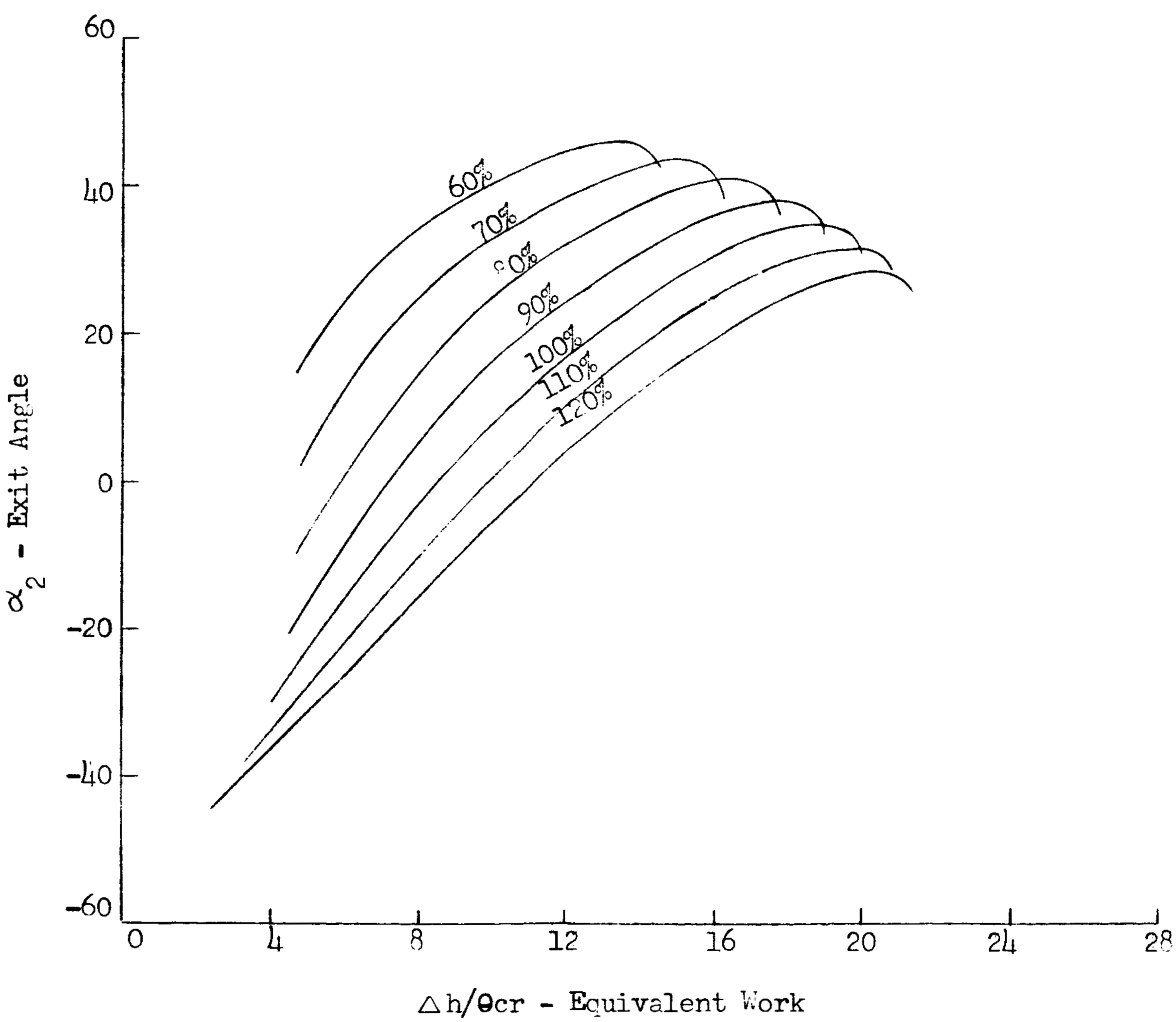

Figure 22

NASA - TASK III

Single Stage - Schedule -7.53

Hub Mach Number

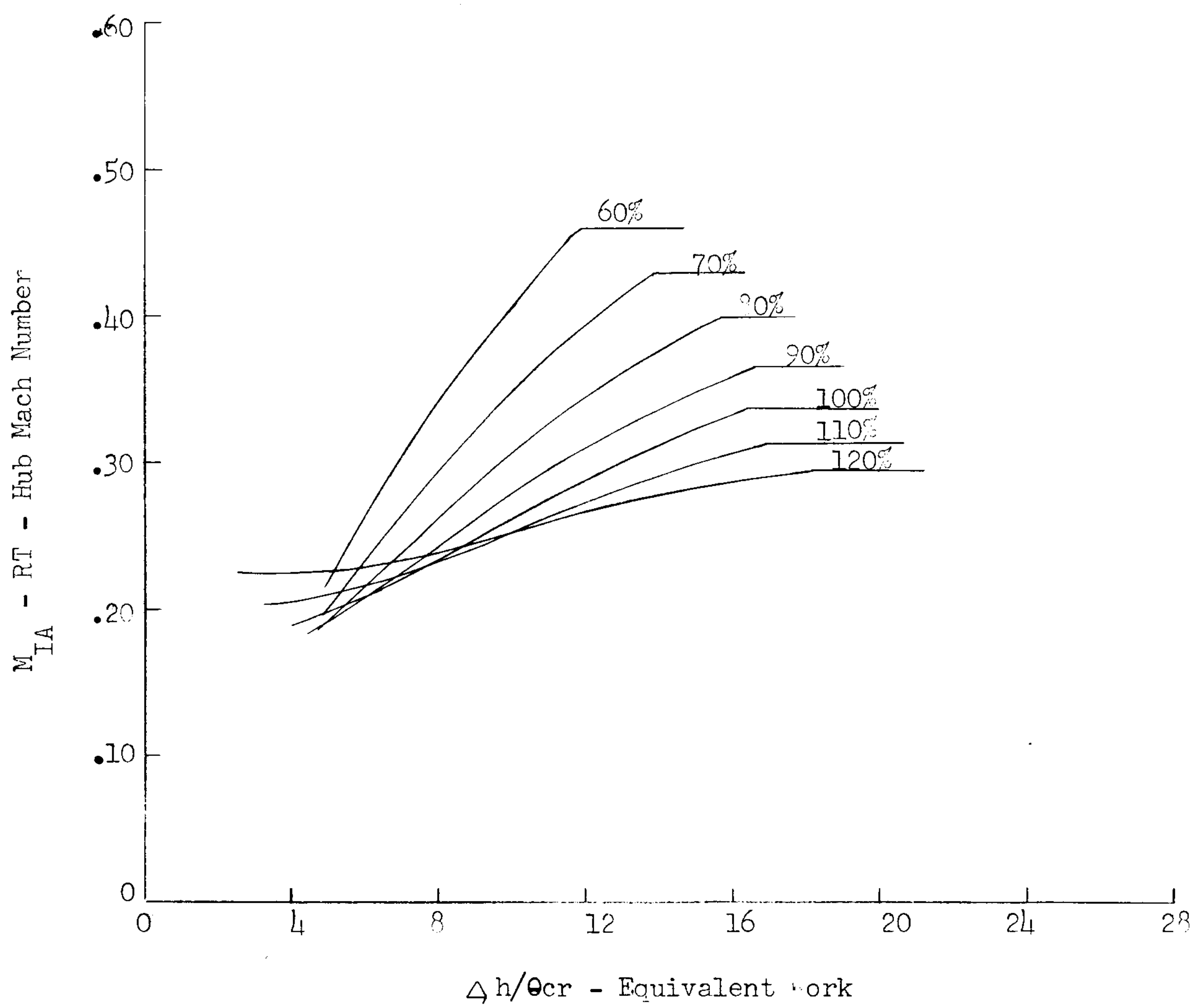

Figure 23

NASA - TASK III

Single Stage - Schedule -7.53

Hub Reaction
vs.
Equivalent Work

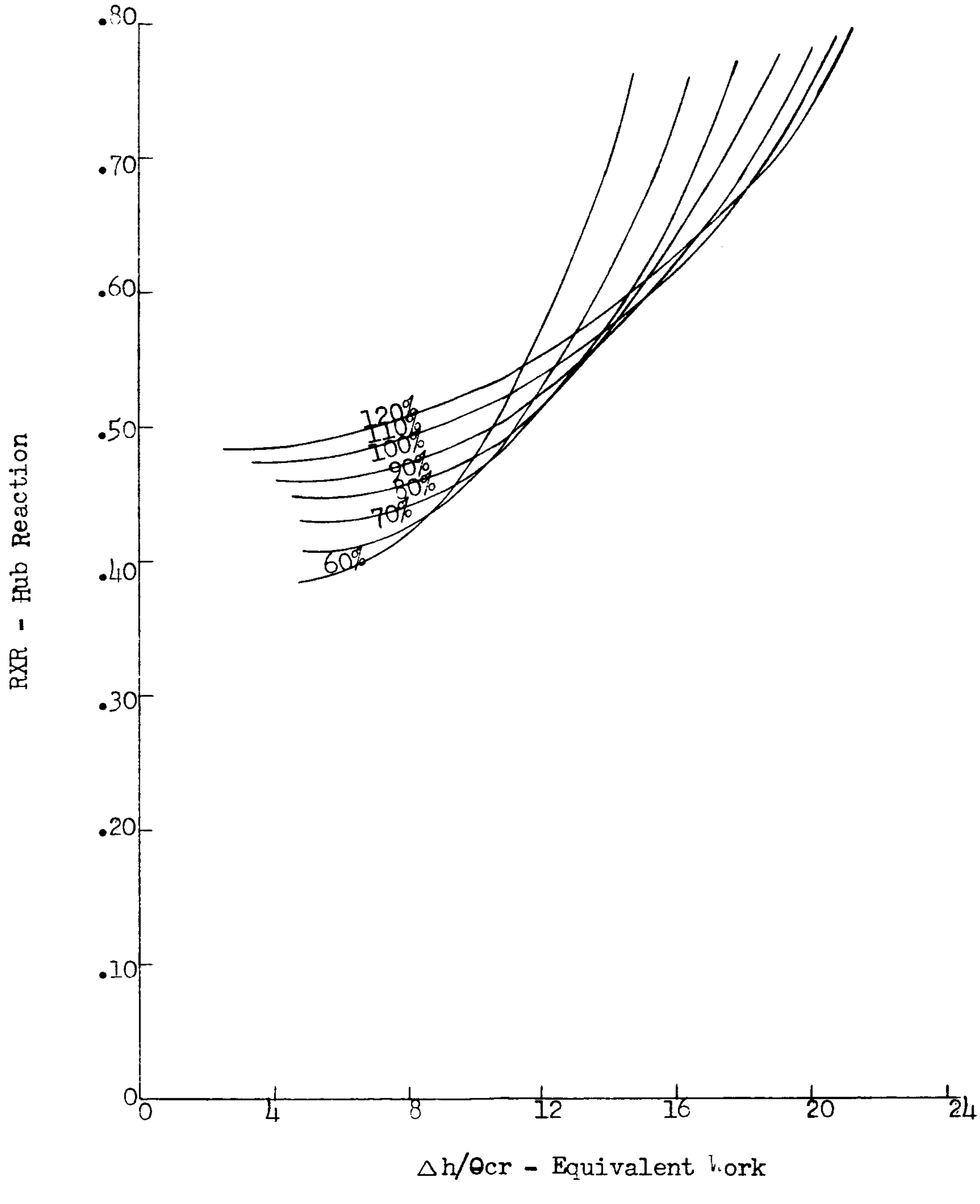

Figure 24

NASA - TASK III

Single Stage - Schedule 7.13

Performance Map

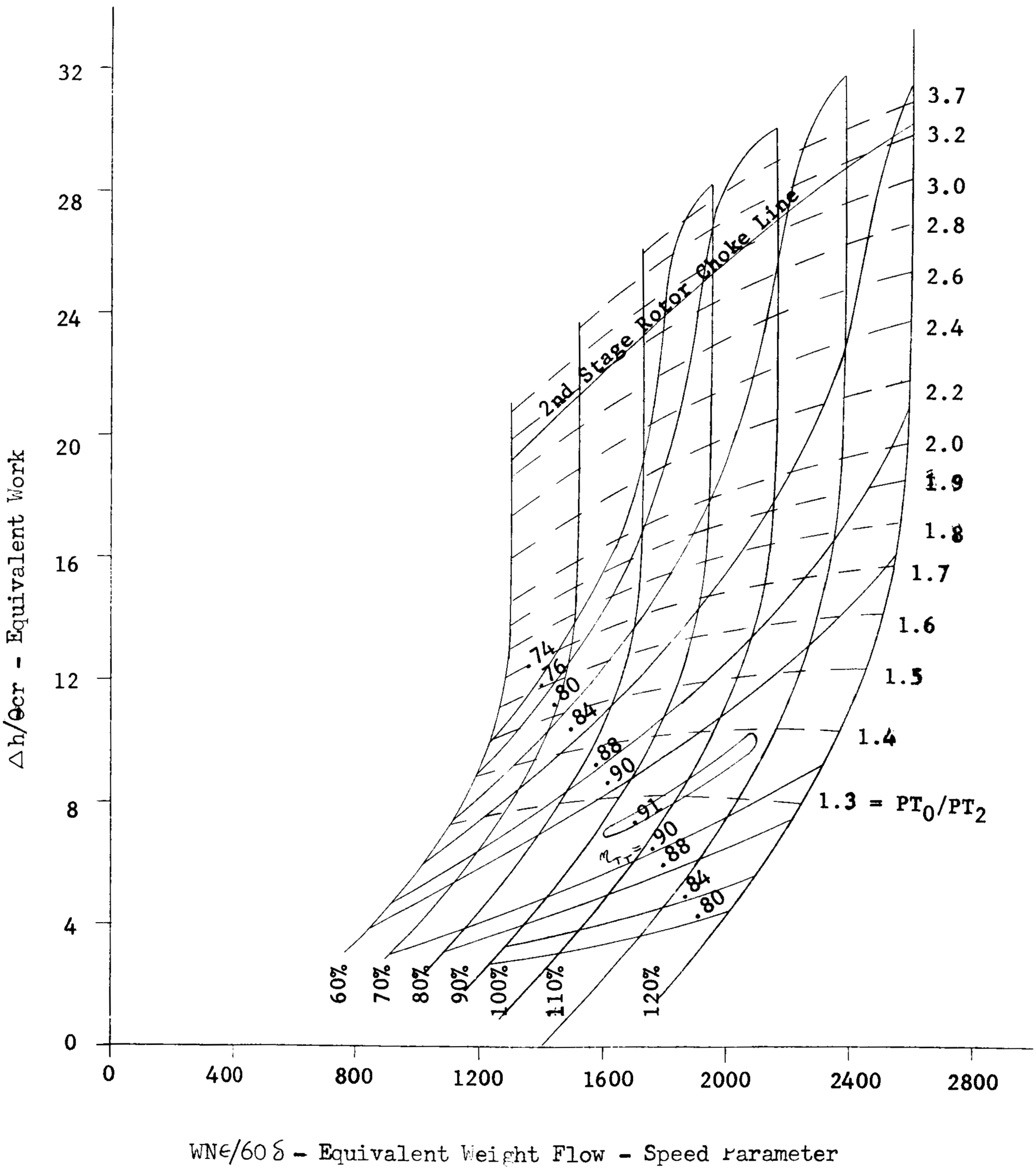

Figure 25

NASA - TASK III

Single Stage - Schedule 7.13

Equivalent Flow vs. Pressure Ratio

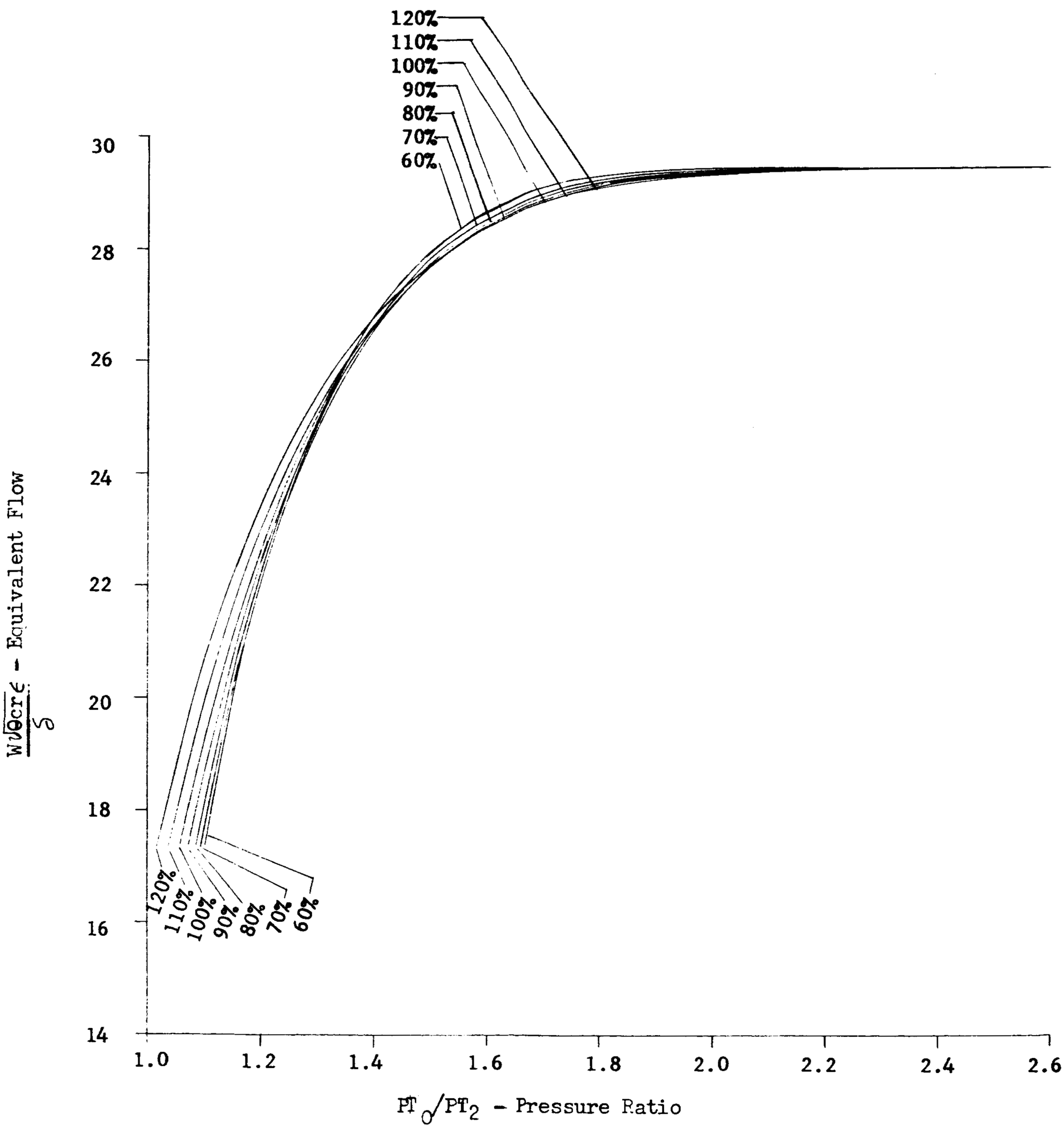

Figure 26

NASA - TASK III

Single Stage - Schedule 7.13

Rotor Incidence vs. Equivalent Work

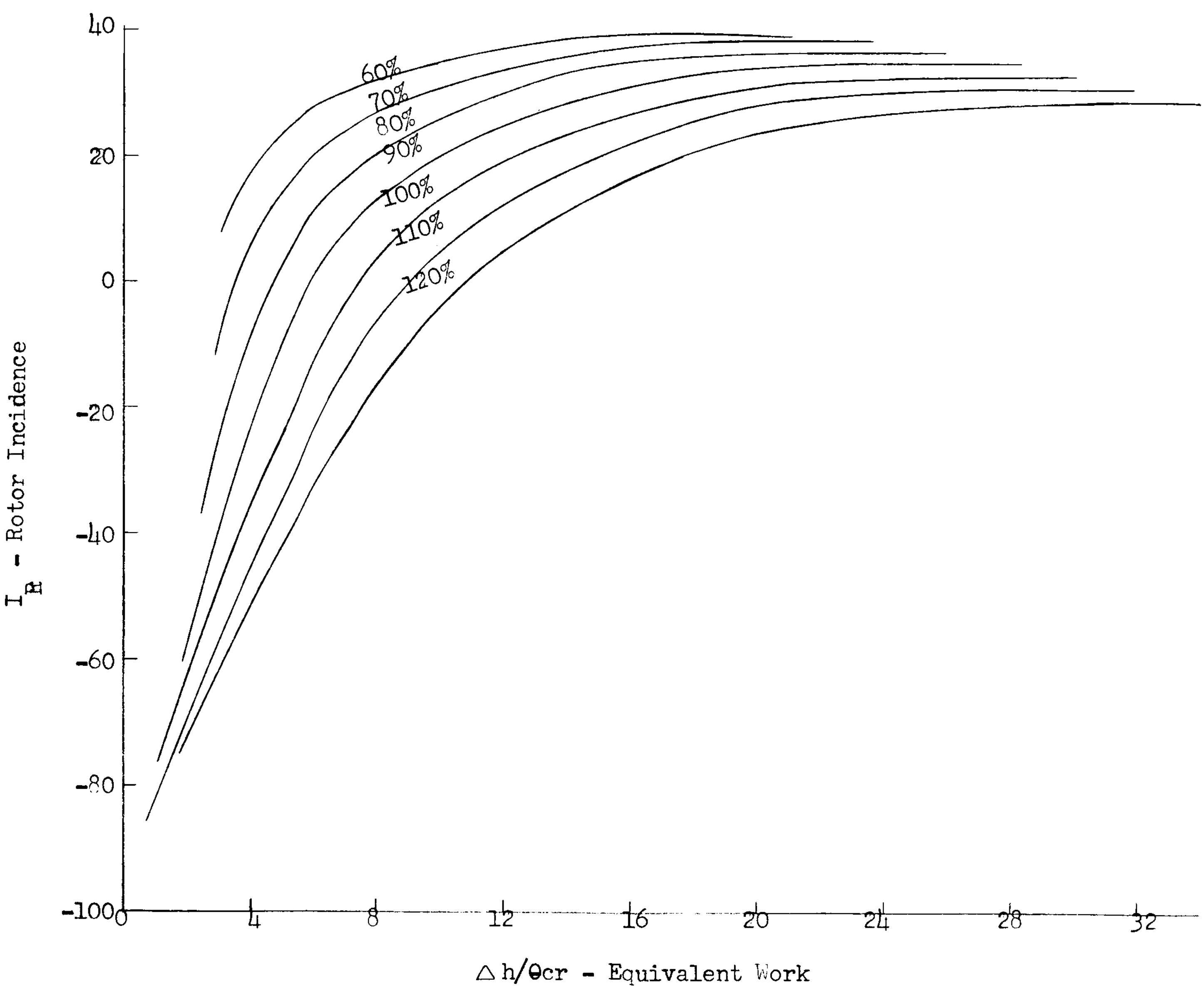

Figure 27

NASA - TASK III

Single Stage - Schedule 7.13

Exit Angle vs. Equivalent Work

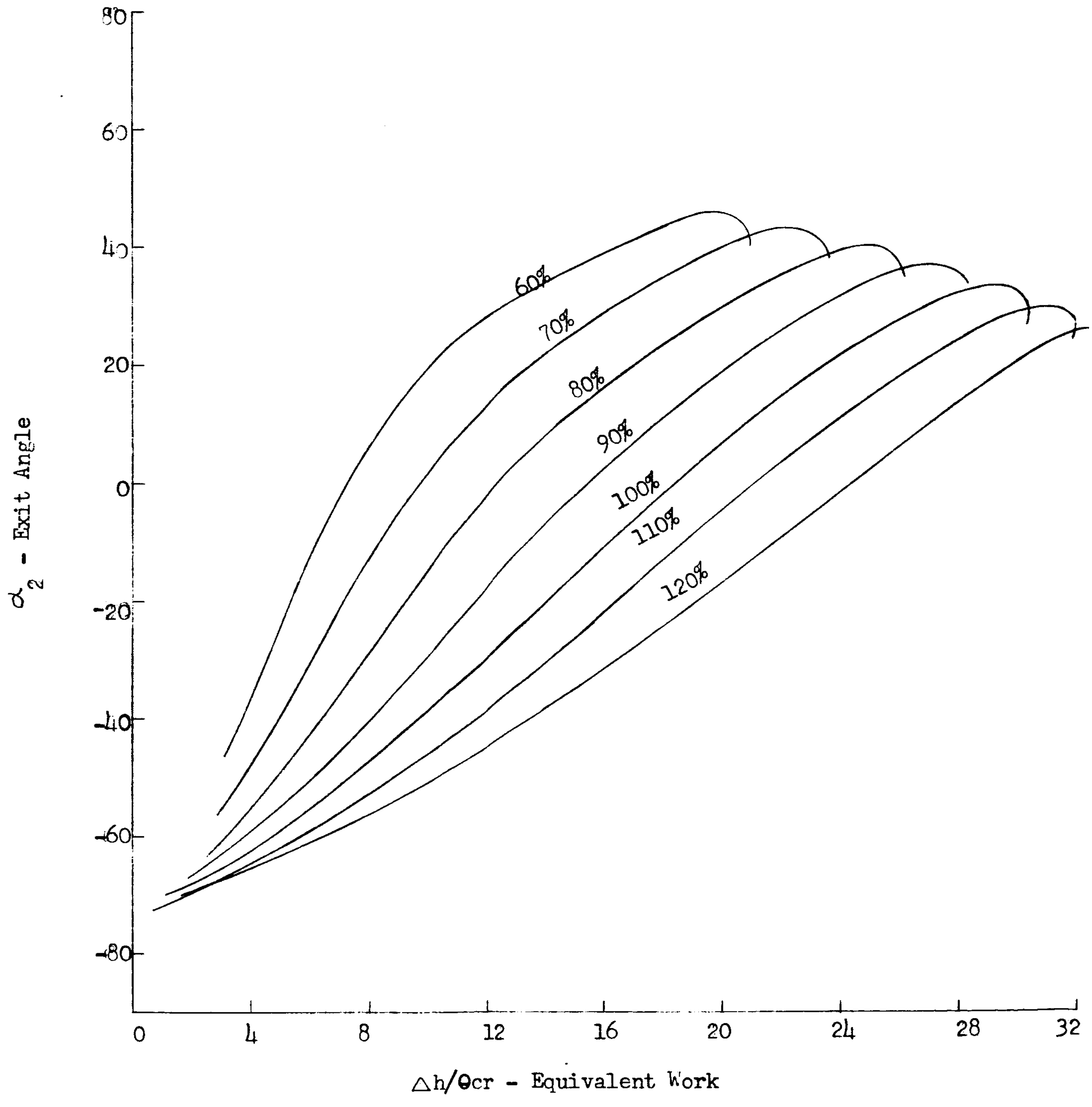

Figure 28

NASA - TASK III

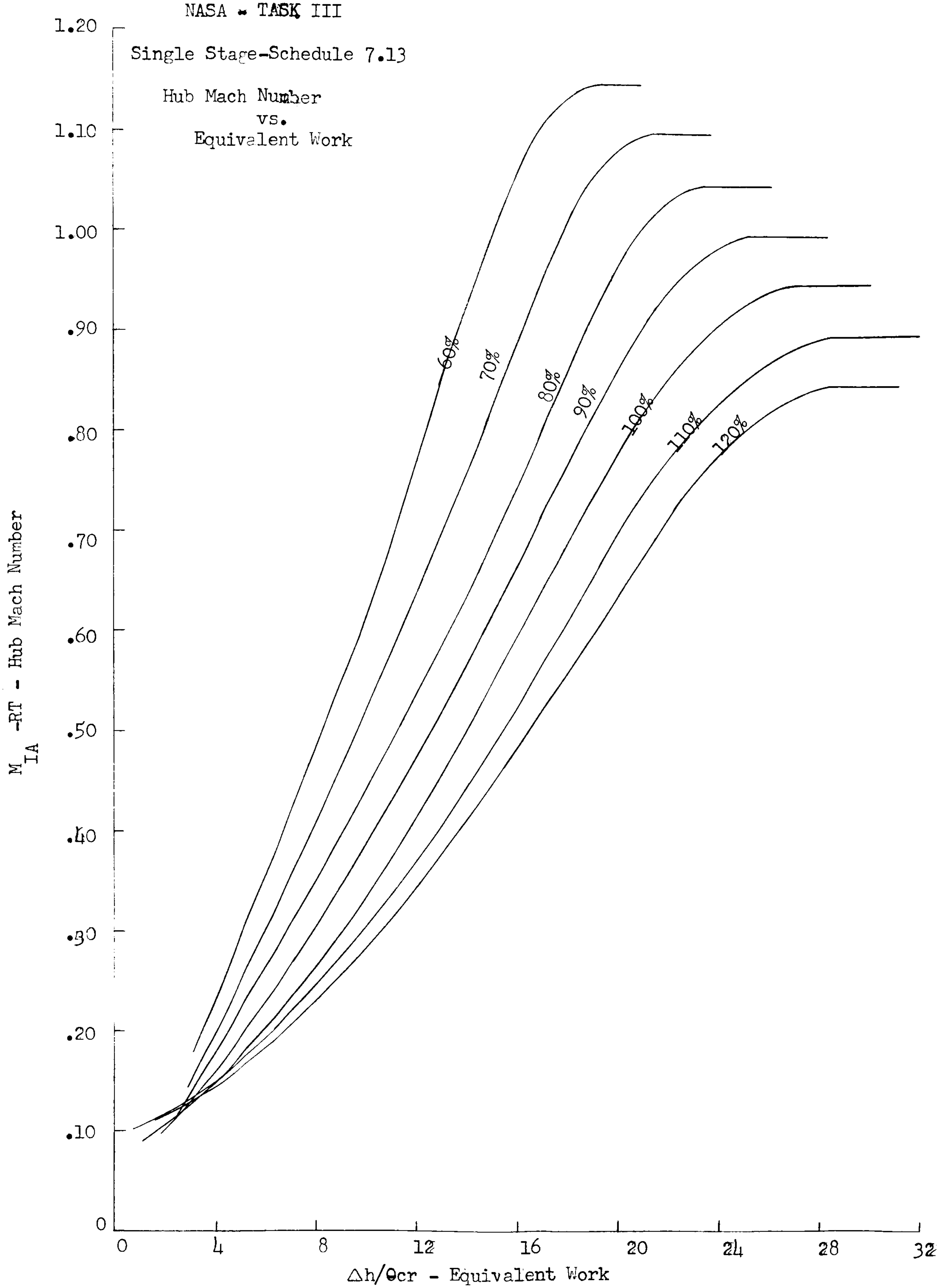

Figure 29

NASA - TASK III

Single Stage - Schedule 7.13

Hub Reaction
vs.
Equivalent Work

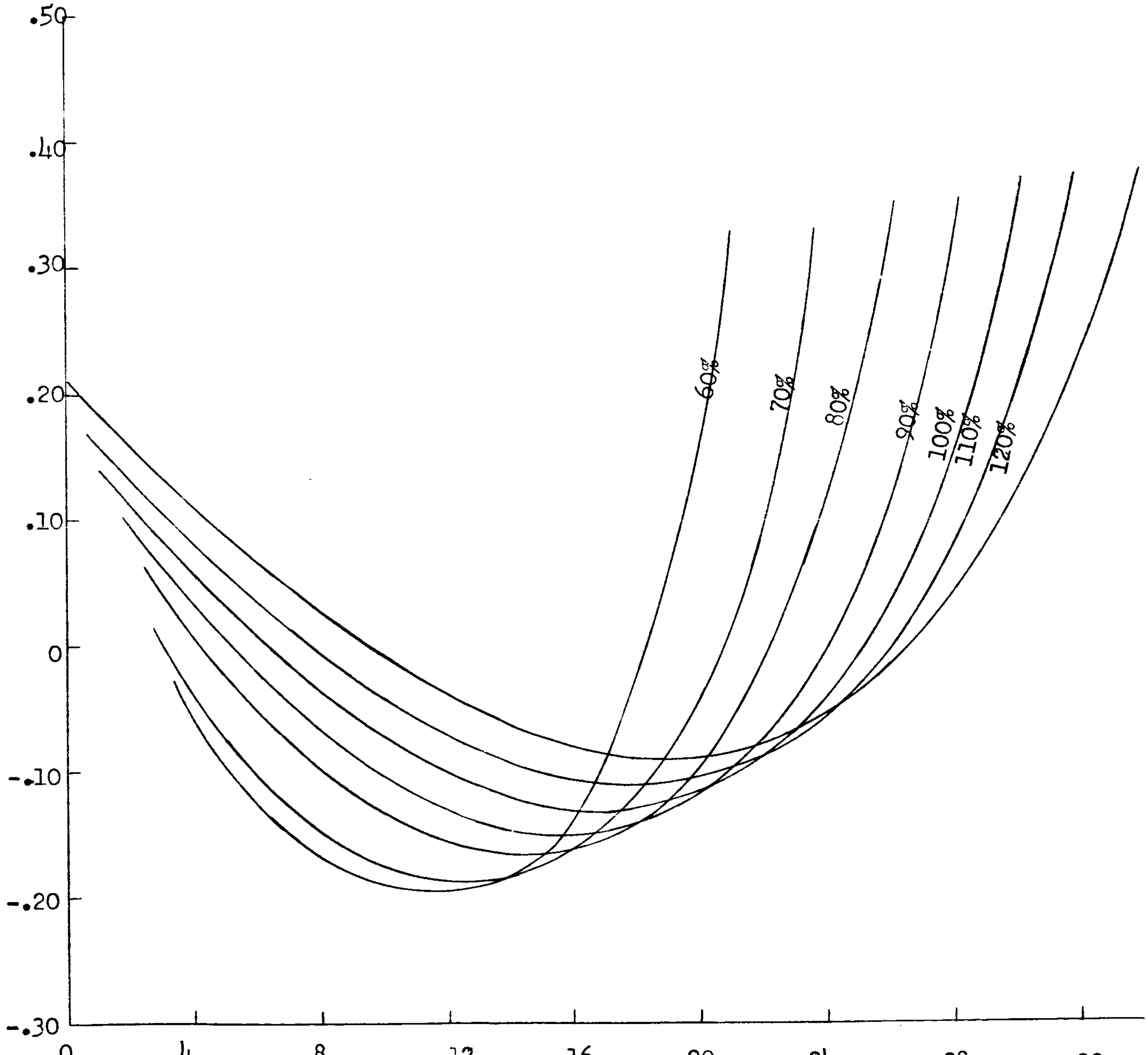

Figure 30

NASA - TASK III

Two Stage-Schedule 0.0, 0.0

Performance Map

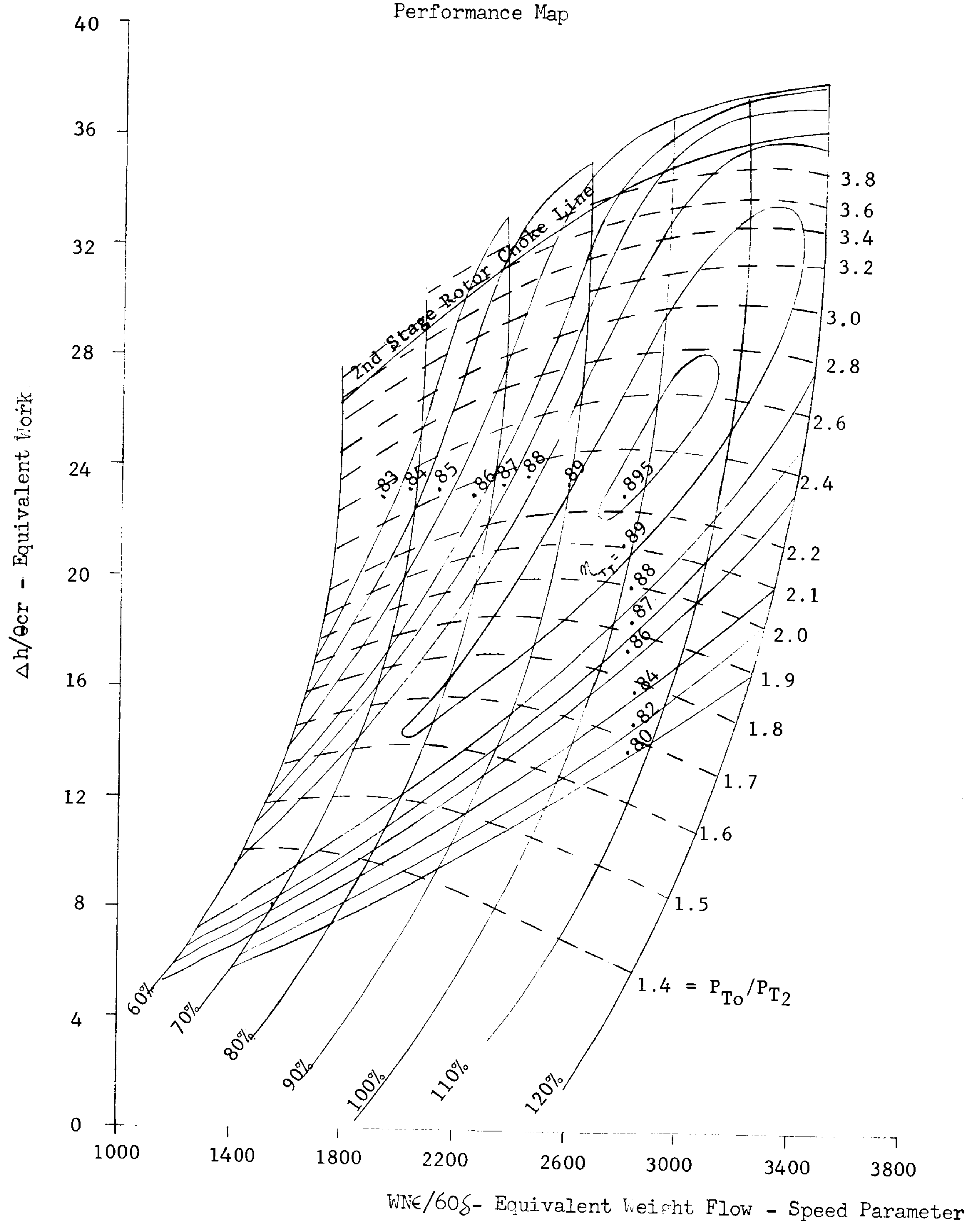

Figure 31

NASA - TASK III

Two Stage-Schedule 0.0, 0.0

Equivalent Flow vs. Pressure Ratio

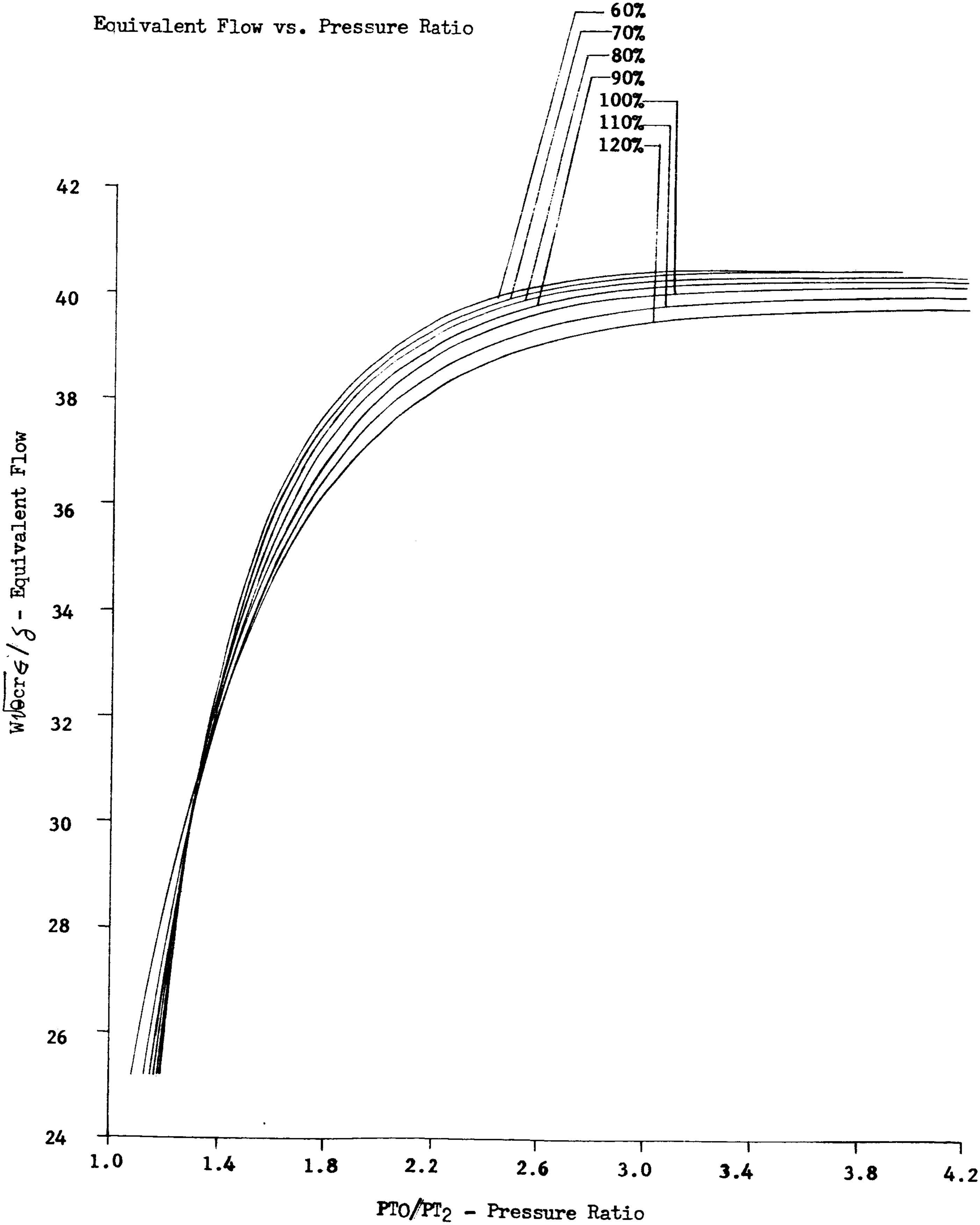

Figure 32

NASA - TASK III

Two Stage-Schedule 0.0, 0.0

Rotor 1 Incidence vs. Equivalent Work

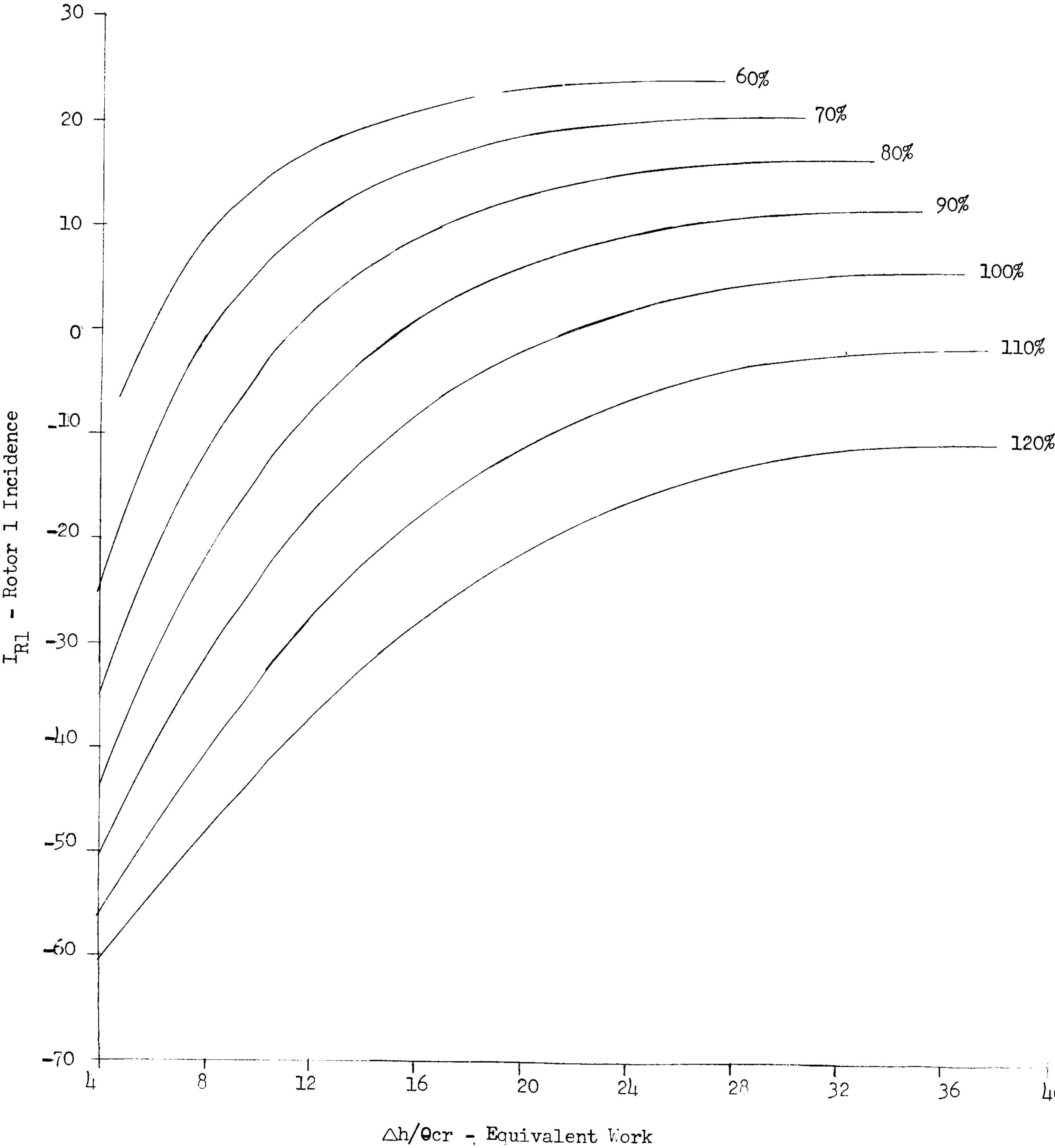

Figure 33

NASA - TASK III

Two Stage-schedule 0.0, 0.0

Stator 2 Incidence vs. Equivalent Work

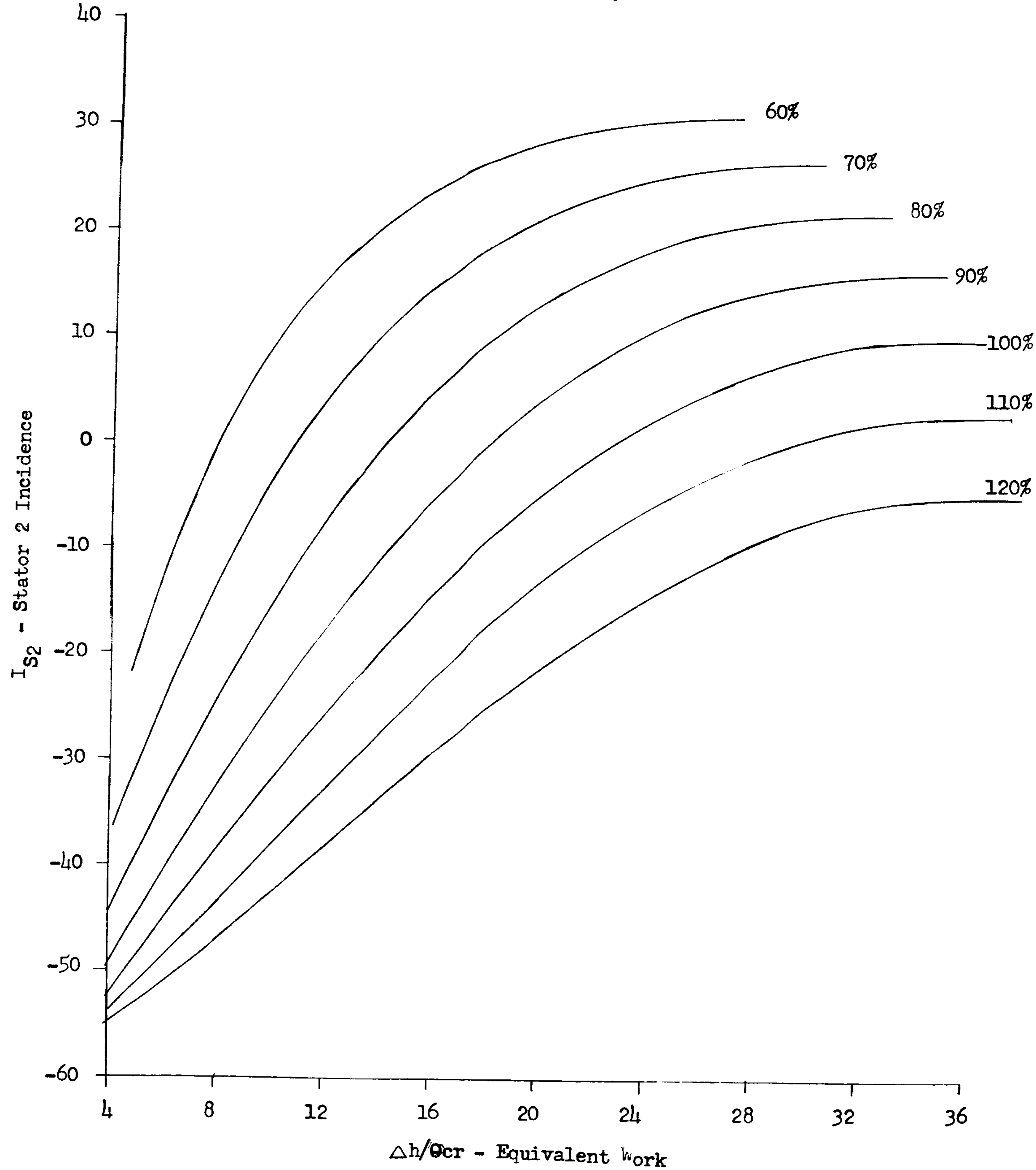

Figure 34

NASA - TASK III

Two Stage-Schedule 0.0, 0.0

Rotor 2 Incidence vs. Equivalent Work

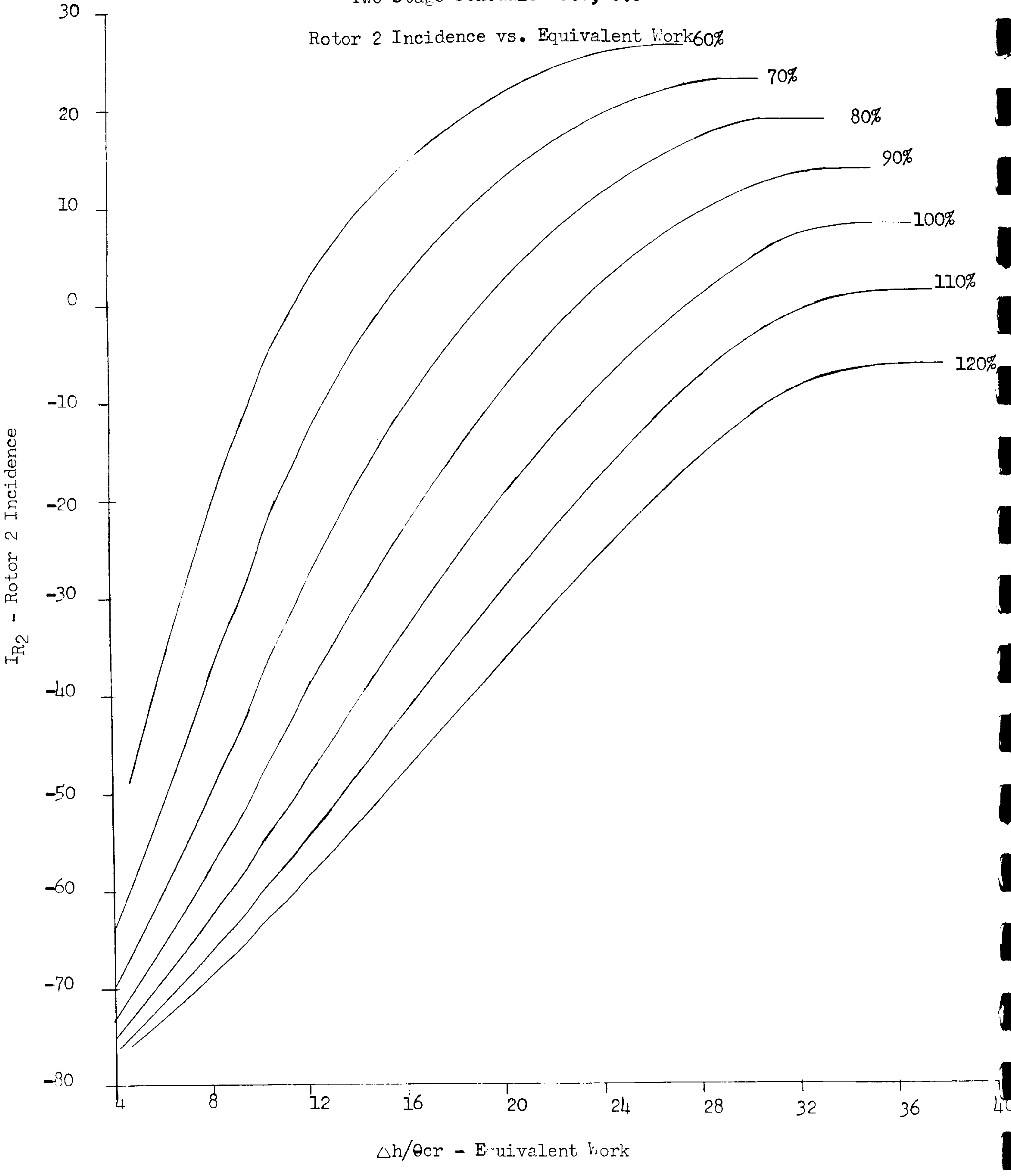

Figure 35

NASA - TASK III

Two Stage-Schedule 0.0, 0.0

Exit Angle vs. Equivalent Work

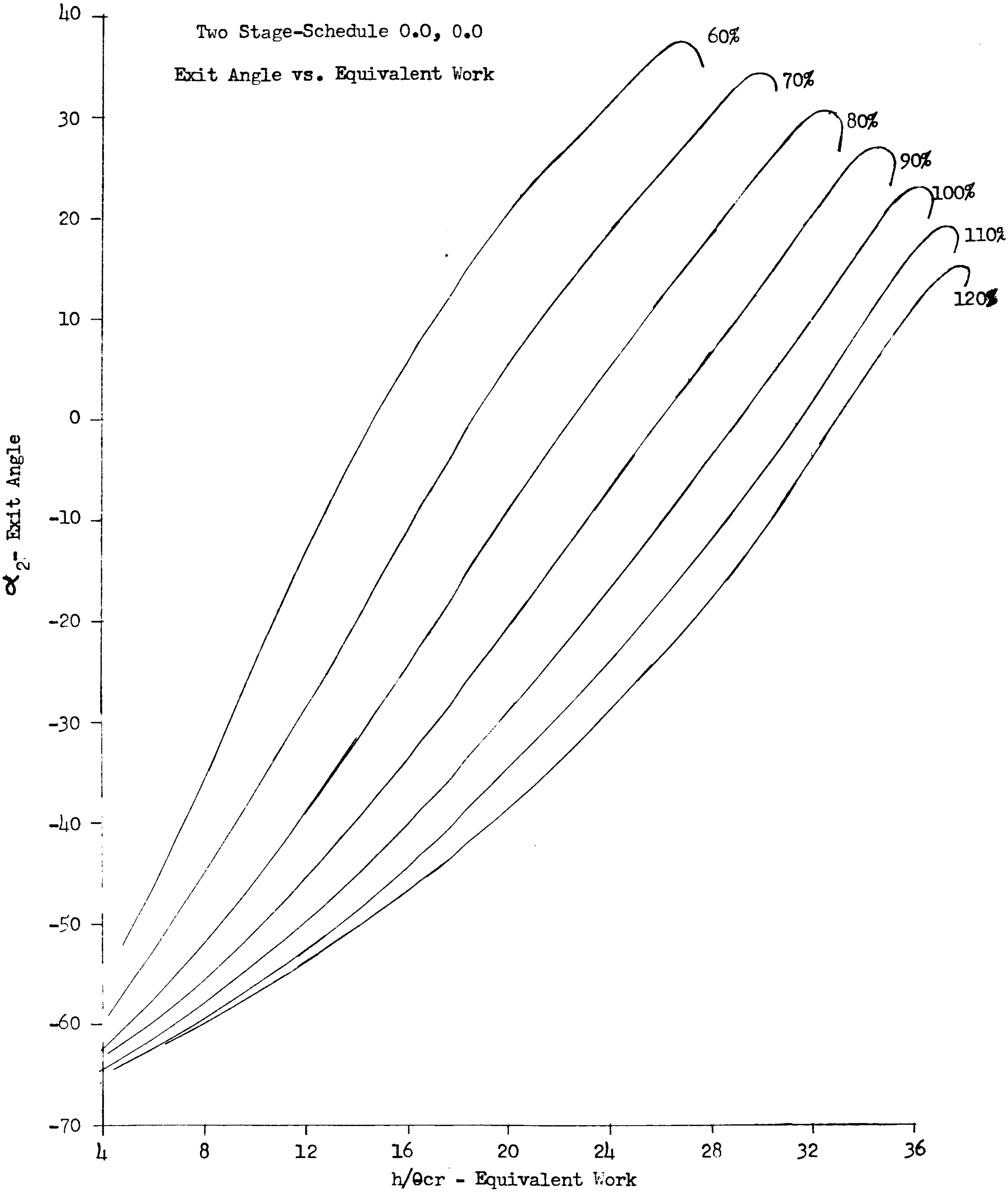

Figure 36

NASA - TASK III

Two Stage-Schedule 0.0, 0.0

Rotor Hub Mach Number
vs.
Equivalent Work

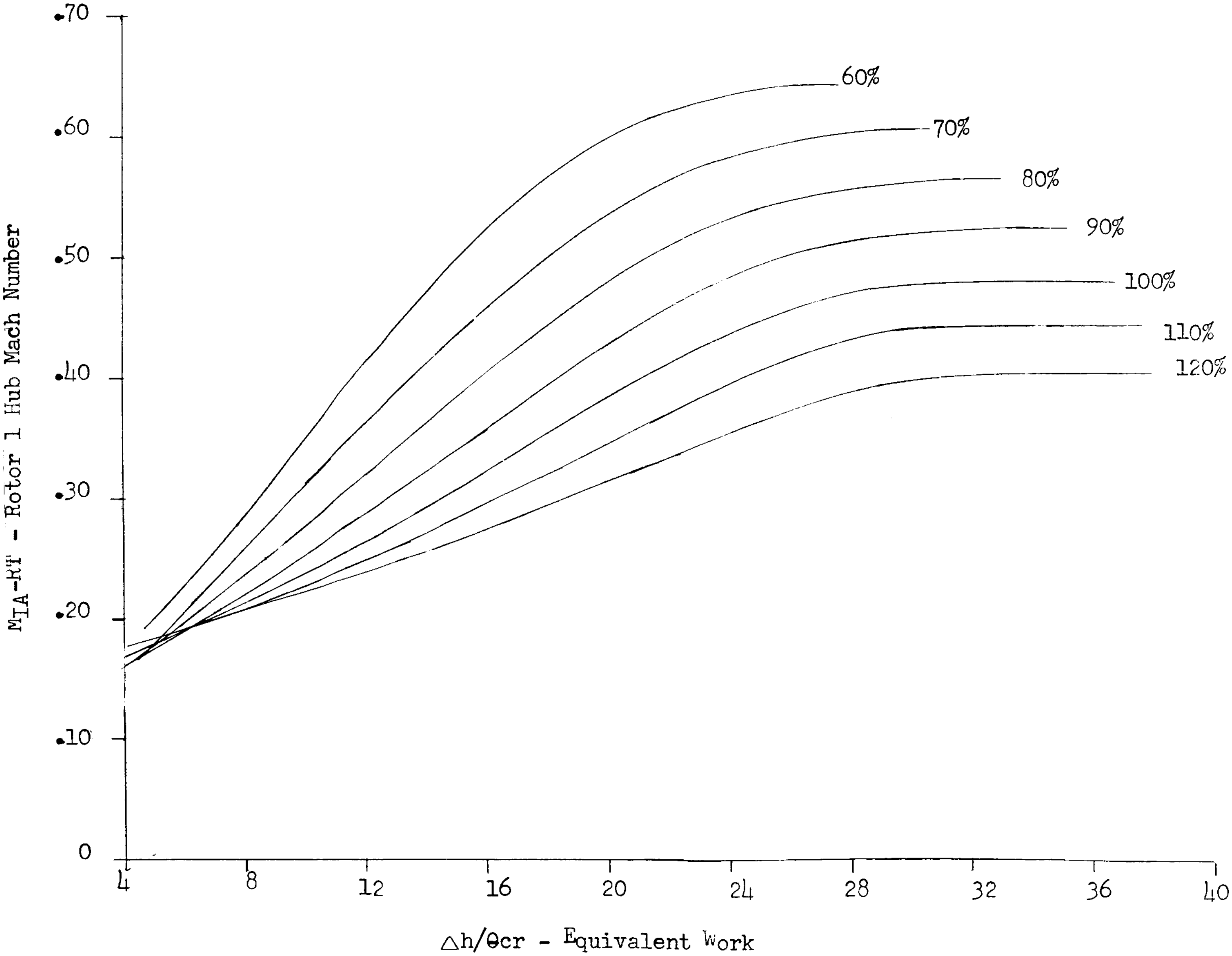

Figure 37

NASA - TASK III

Two Stage-Schedule 0.0, 0.0

Rotor 2 Hub Mach Number vs. Equivalent Work

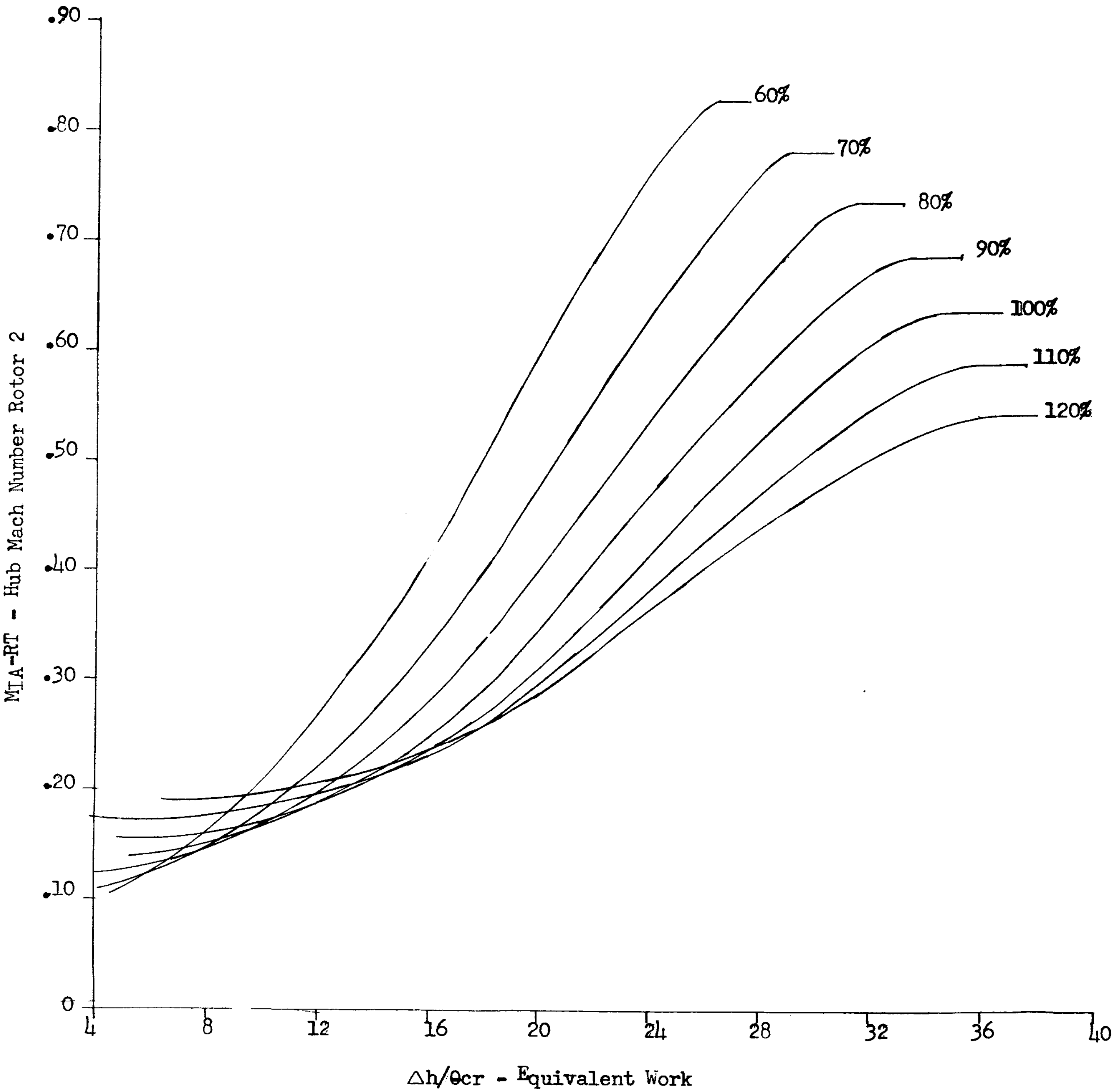

Figure 38

NASA - TASK III

Two Stage-Schedule 0.0, 0.0

Stage 1 Hub Reaction
vs.
Equivalent Work

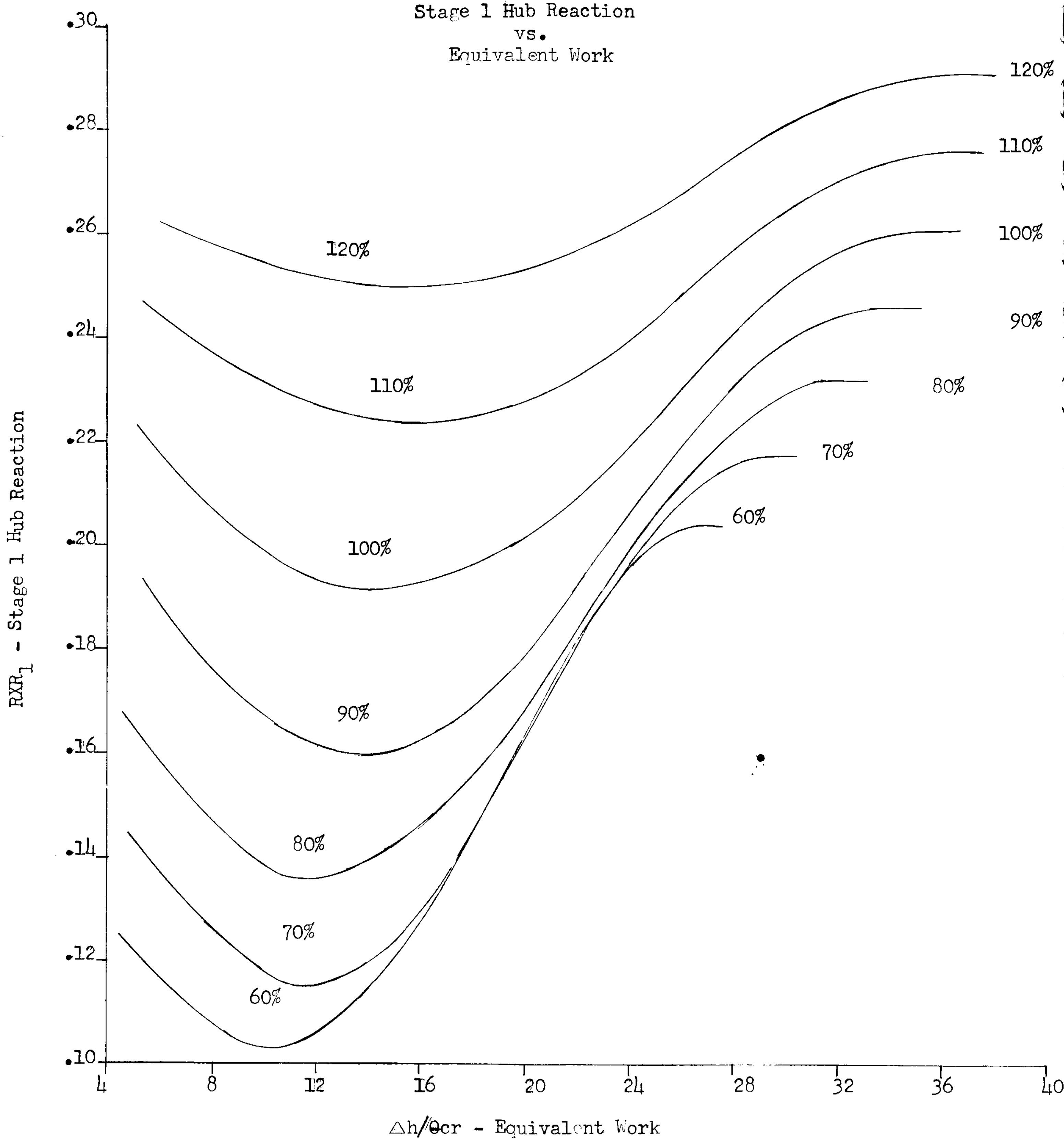

Figure 39

NASA - TASK III

Two Stage-Schedule 0.0, 0.0

Stage 2 Hub Reaction
vs.
Equivalent Work

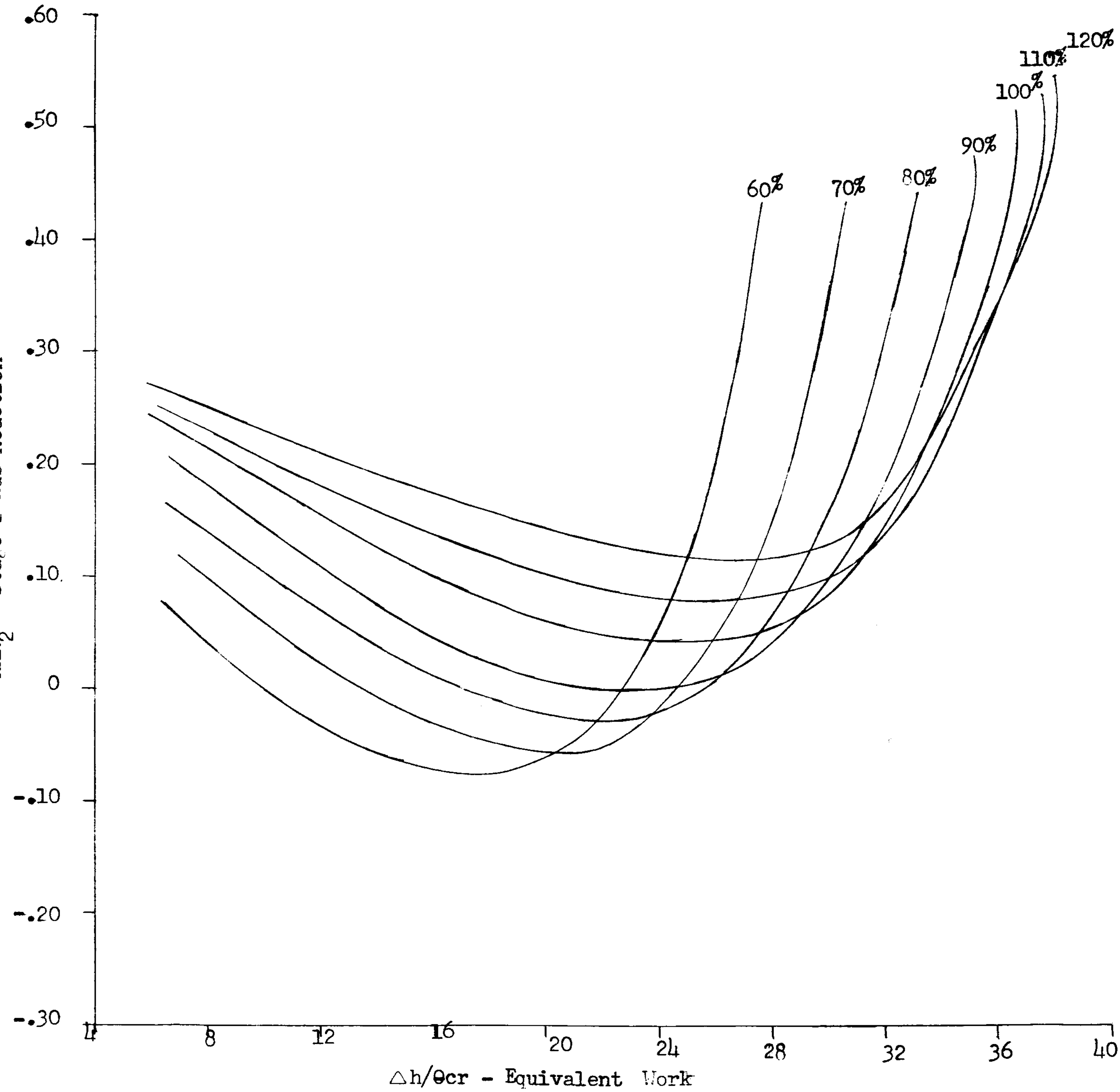

Figure 40

NASA - TASK III

Two Stage - Schedule -7.53, 0.0

Performance Map

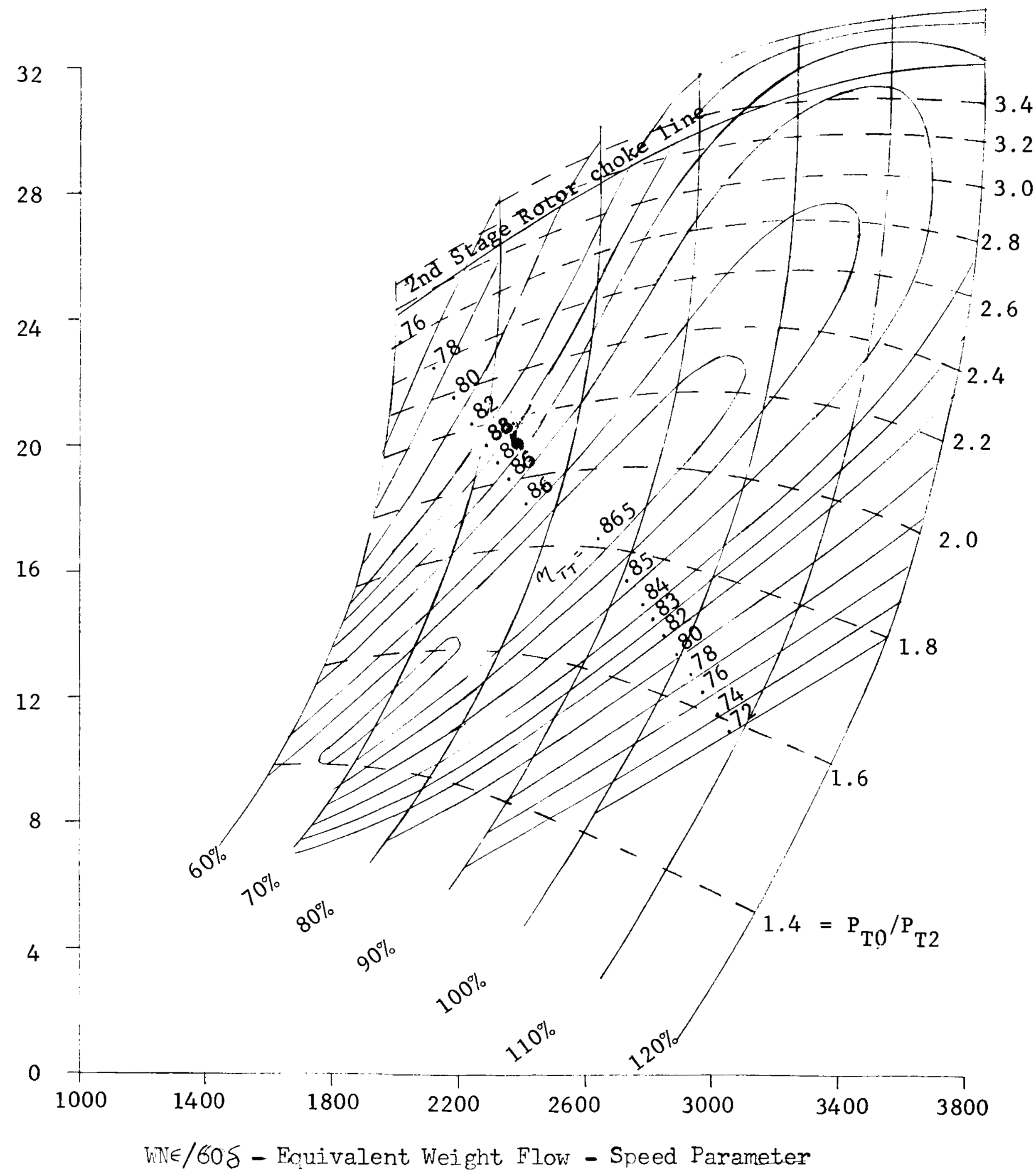

Figure 41

NASA - TASK III

Two Stage-Schedule -7.53, 0.0

Equivalent Flow vs. Pressure Ratio

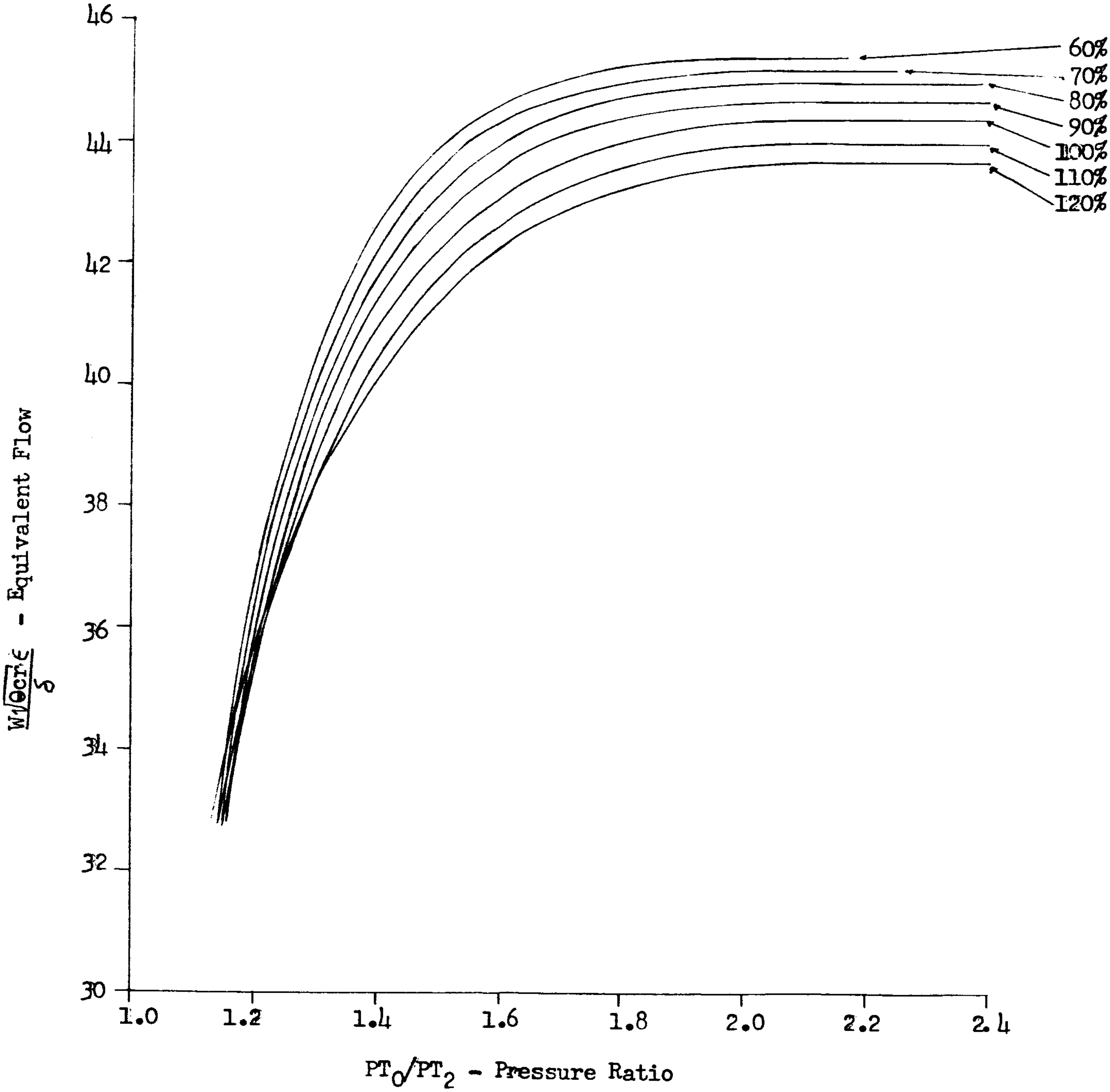

Figure 42

NASA - TASK III

Two Stage-Schedule -7.53, 0.0

Rotor 1 Incidence vs. Equivalent Work

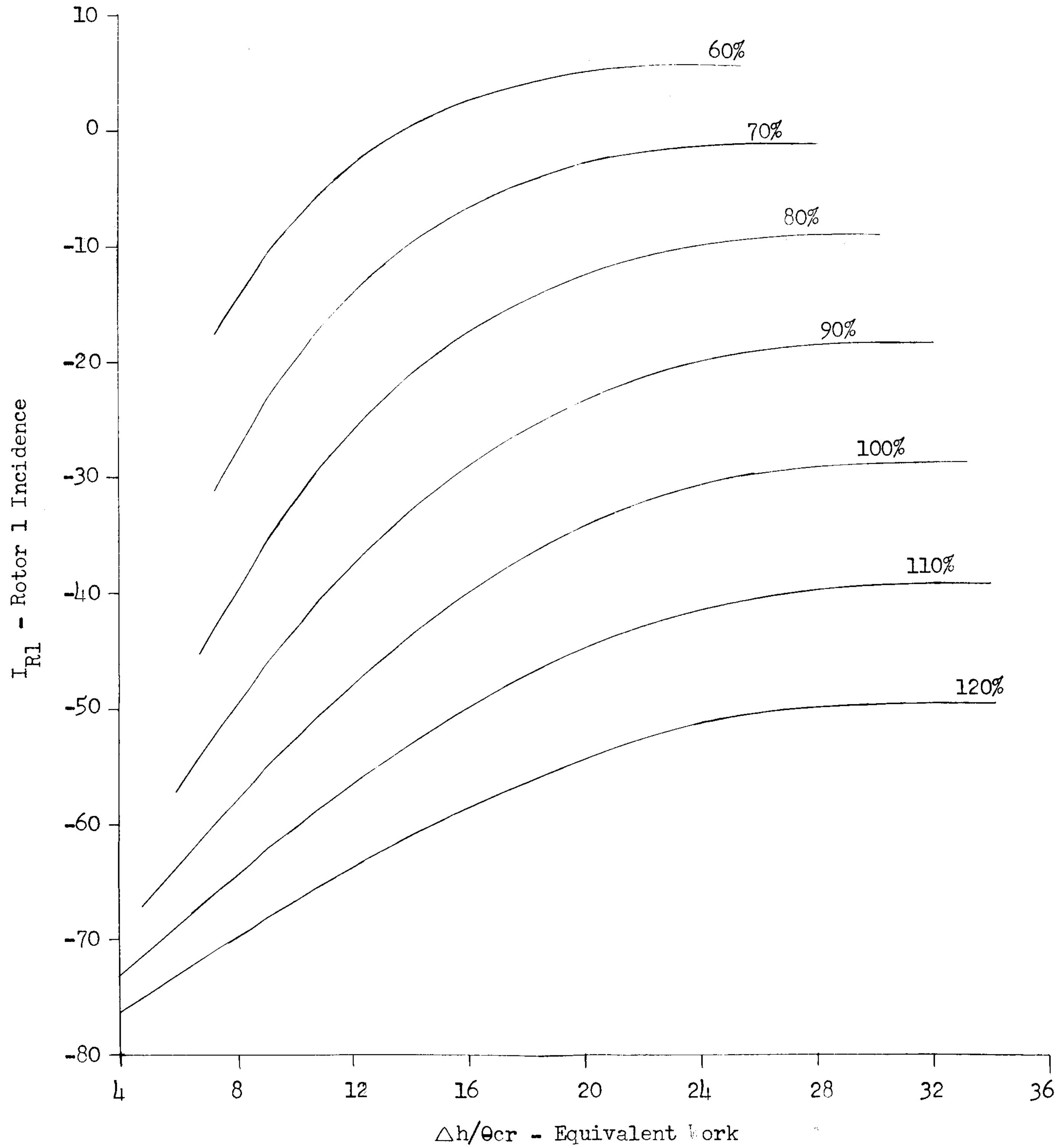

Figure 43

NASA - TASK III

Two Stage-Schedule -7.53, 0.0

Stator 2 Incidence vs. Equivalent Work

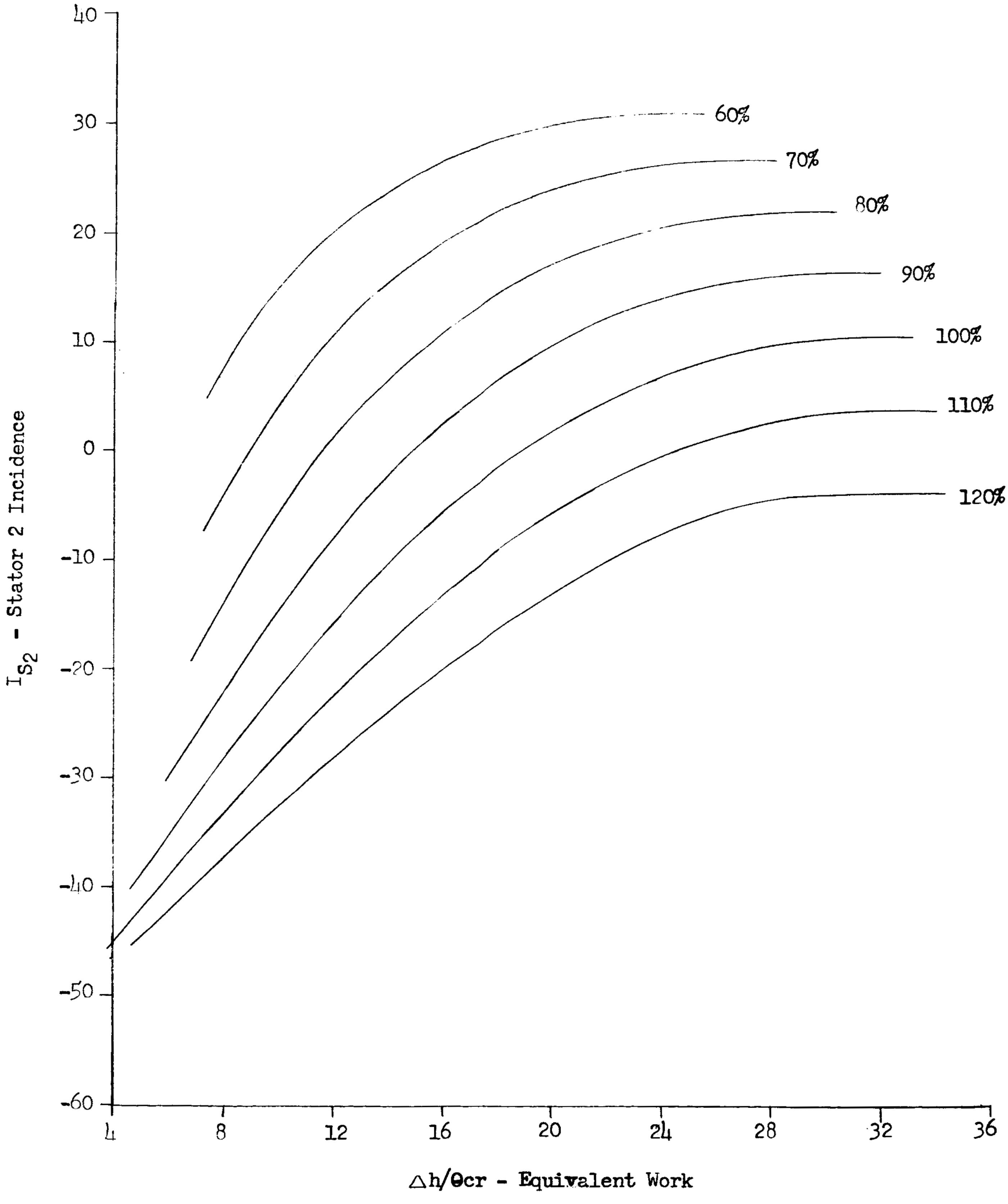

Figure 44

NASA - TASK III

Two Stage-Schedule -7.53, 0.0

Rotor 2 Incidence vs. Equivalent Work

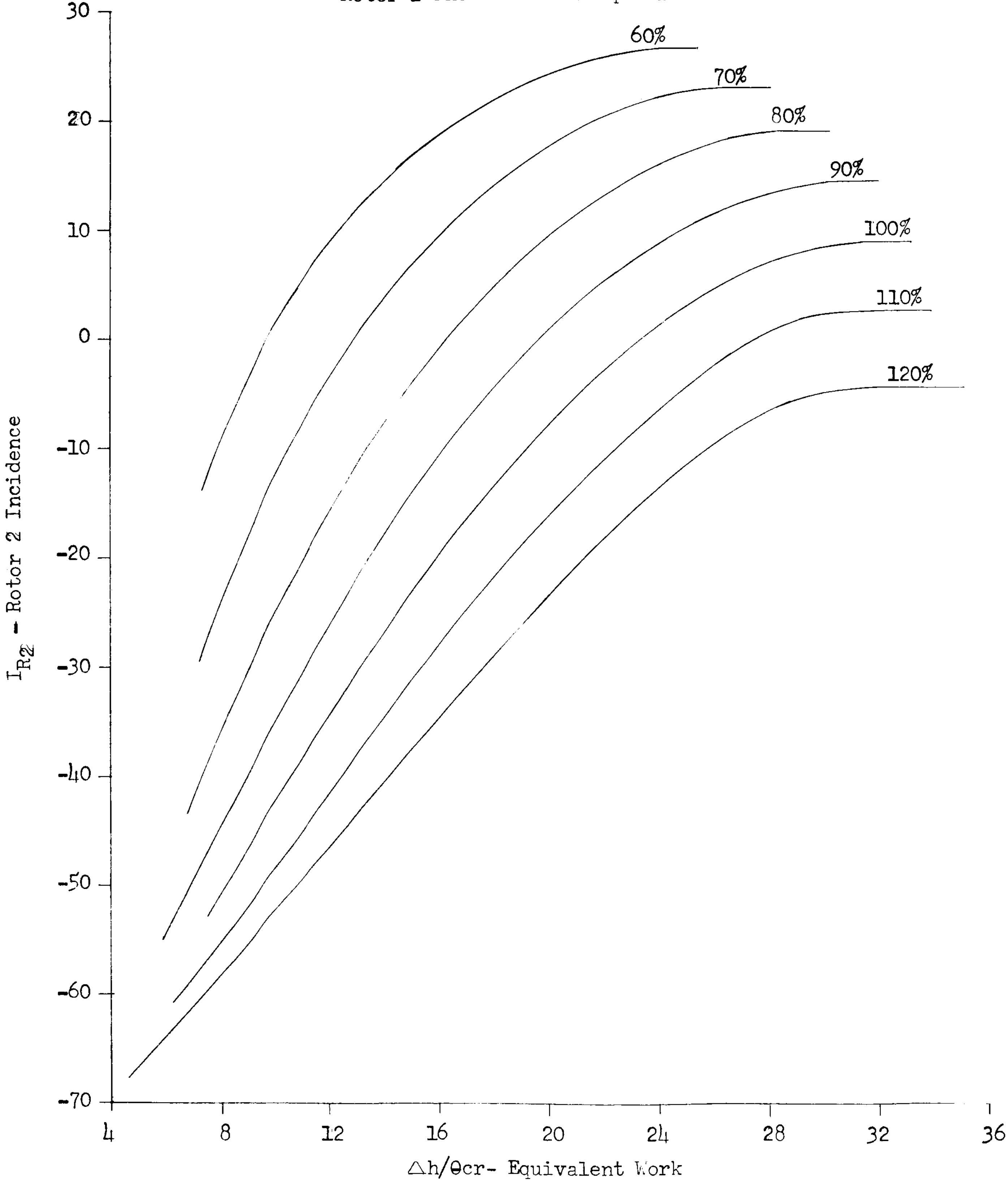

Figure 45

NASA - TASK III

Two Stage-Schedule -7.53, 0.0

Exit Angle vs. Equivalent Work

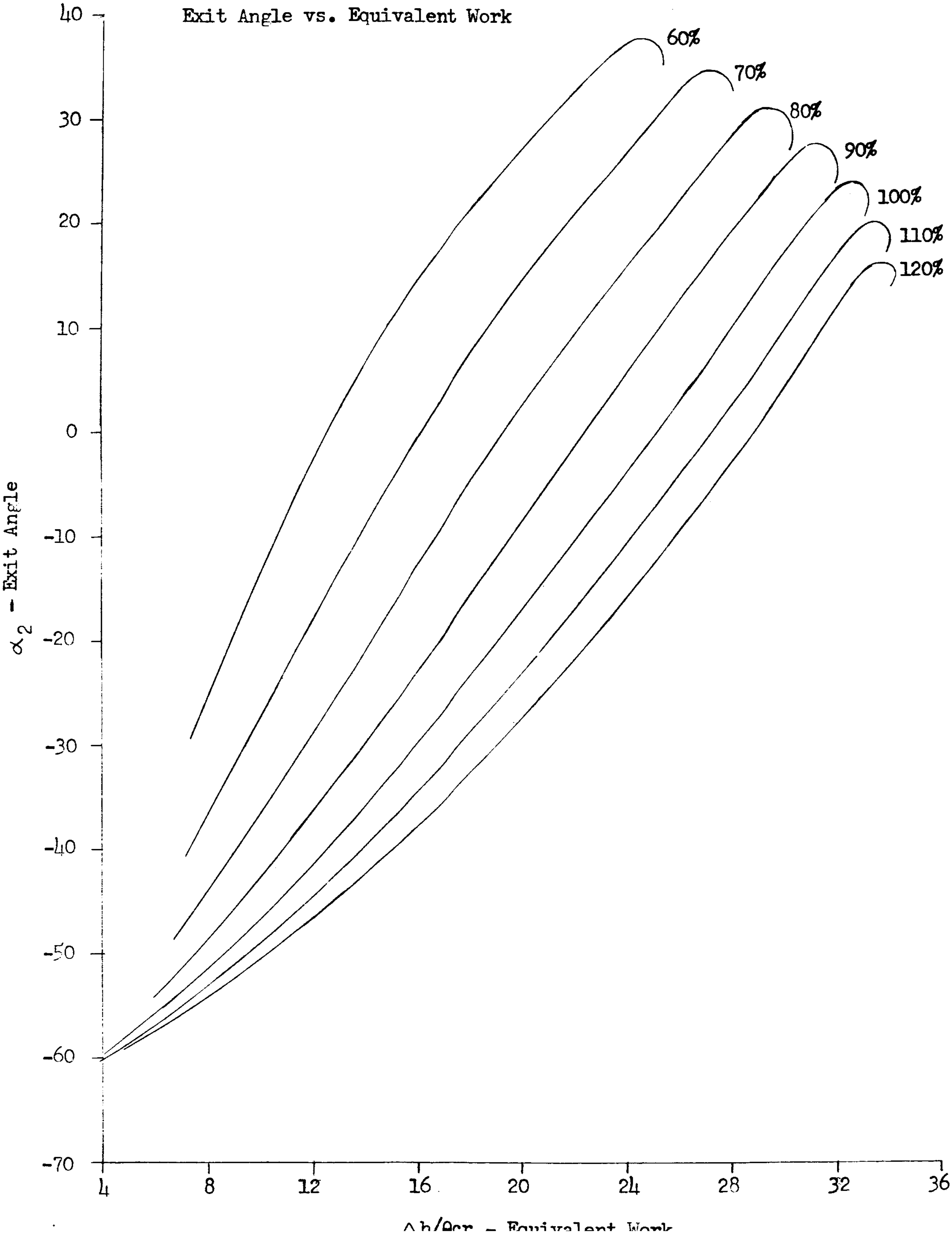

Figure 46

NASA - TASK III

Two Stage-Schedule -7.53, 0.0

Rotor 1 Hub Mach Number
vs.
Equivalent Work

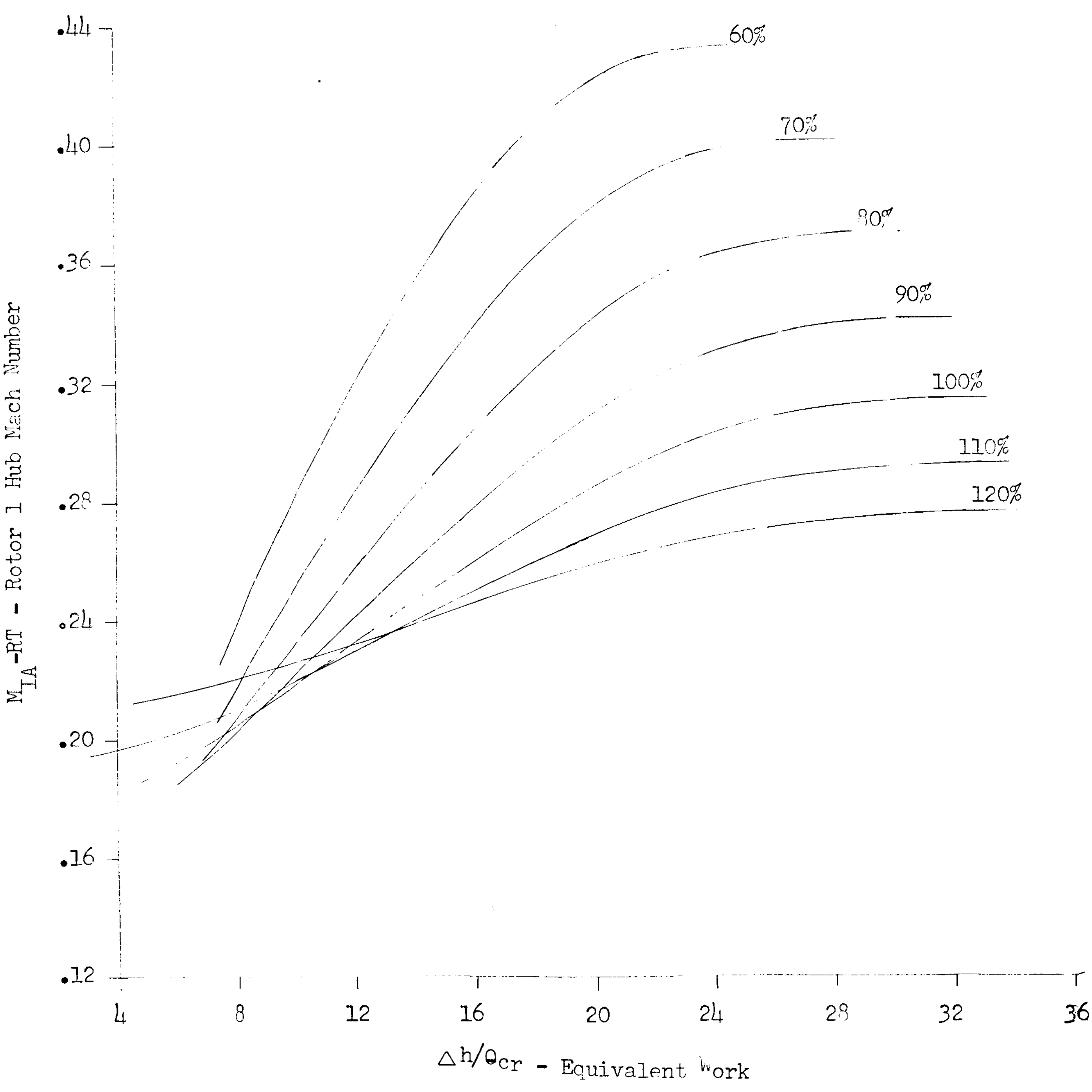

Figure 47

NASA - TASK III

Two Stage-Schedule -7.53, 0.0

Rotor 2 Hub Mach Number
vs.
Equivalent Work

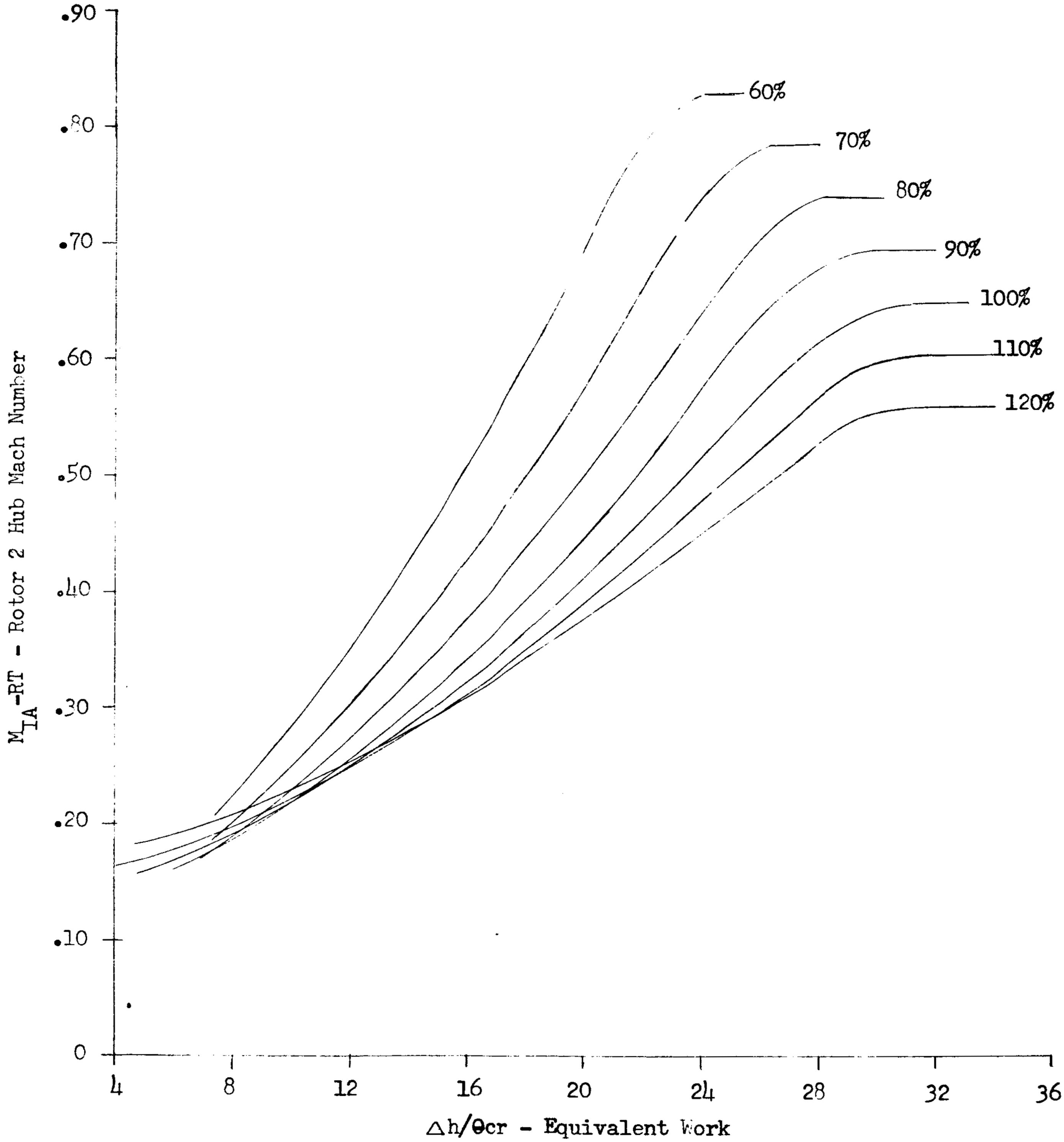

Figure 48

NASA - TASK III

Two Stage-Schedule -7.53, 0.0

Stage 1 Hub Reaction vs. Equivalent Work

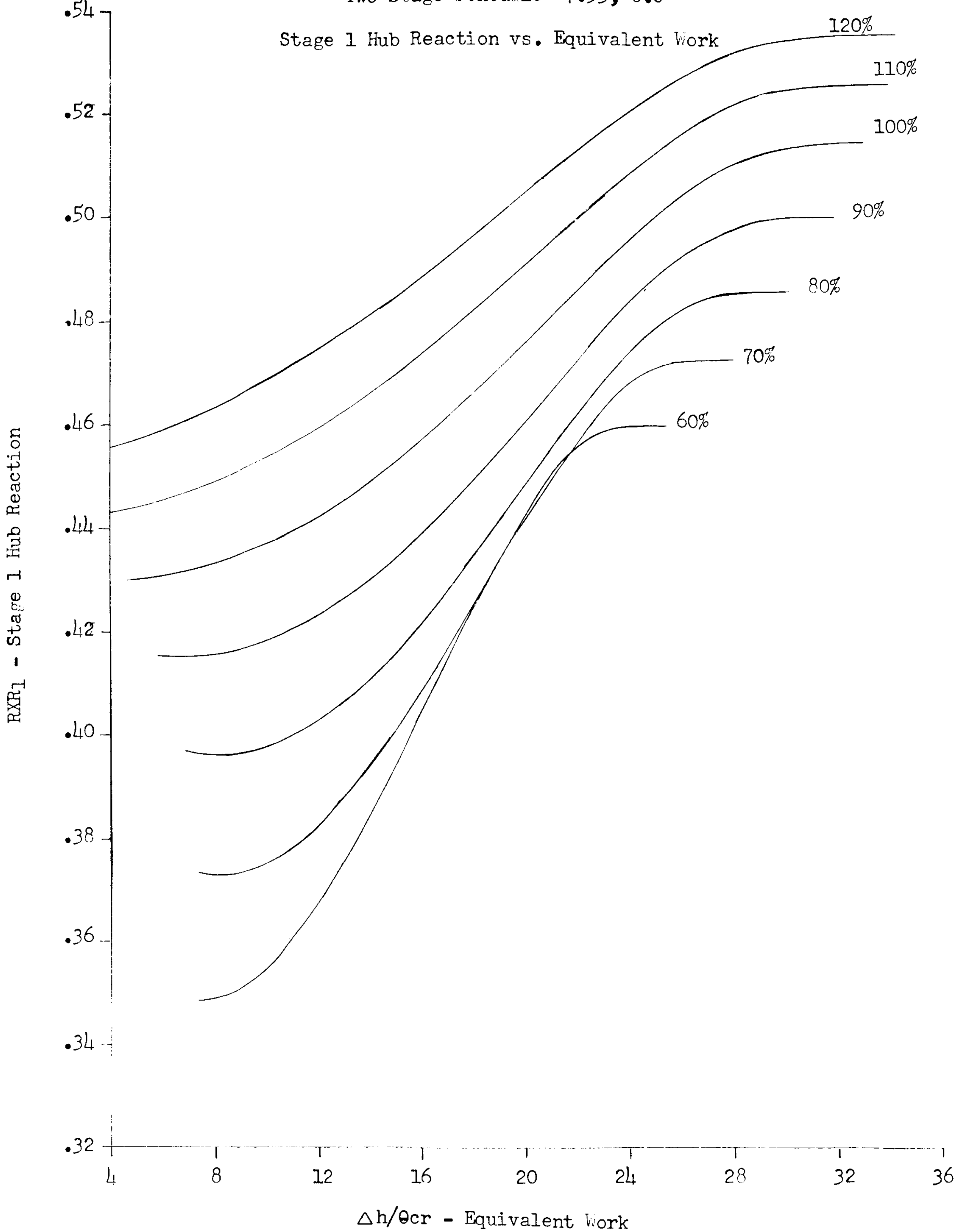

Figure 49

NASA - TASK III

Two Stage-Schedule -7.53, 0.0

Stage 2 Hub Reaction vs. Equivalent Work

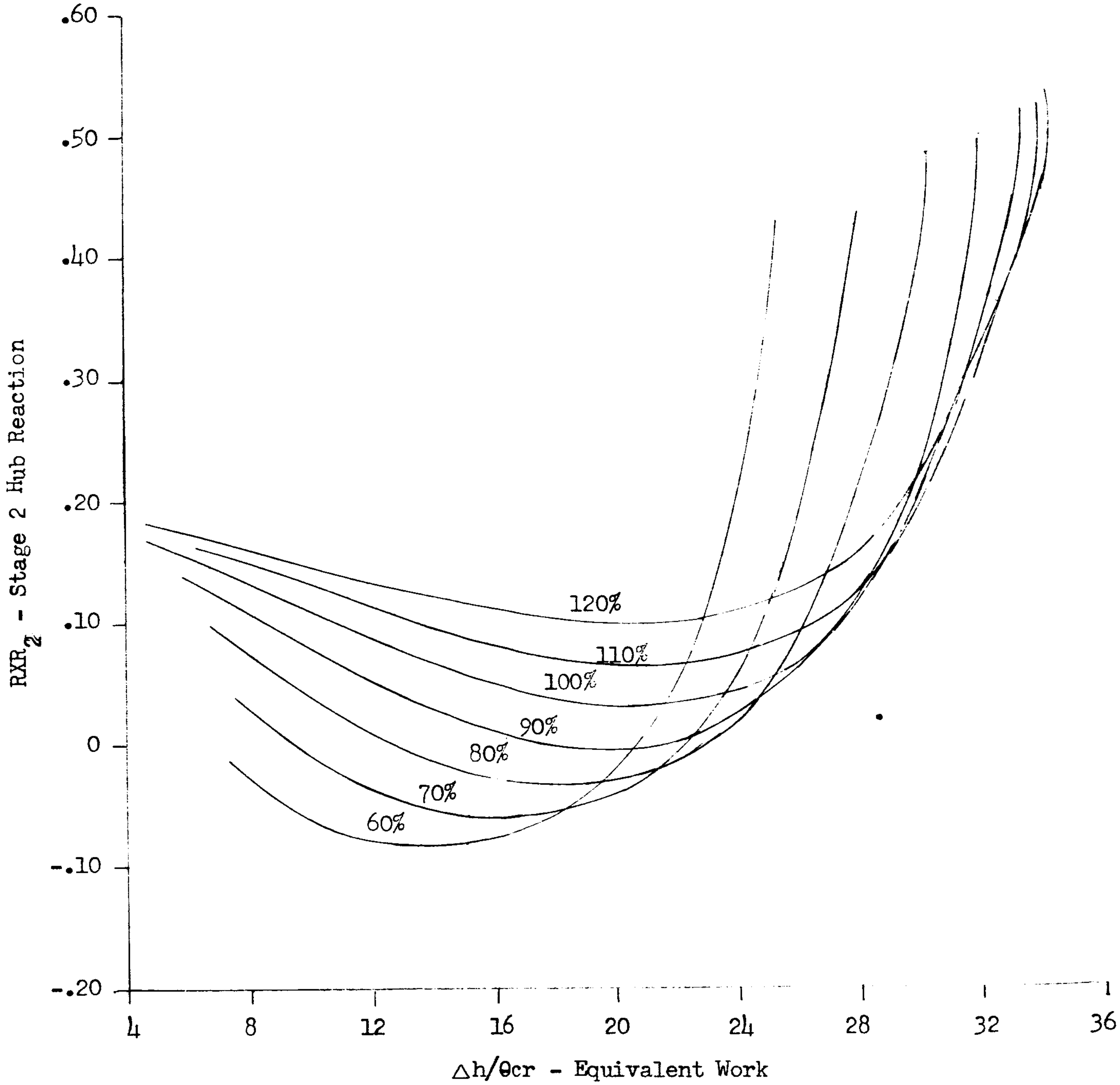

Figure 50

NASA - TASK III

Two Stage Schedule 7.13, 0.0
Performance Map

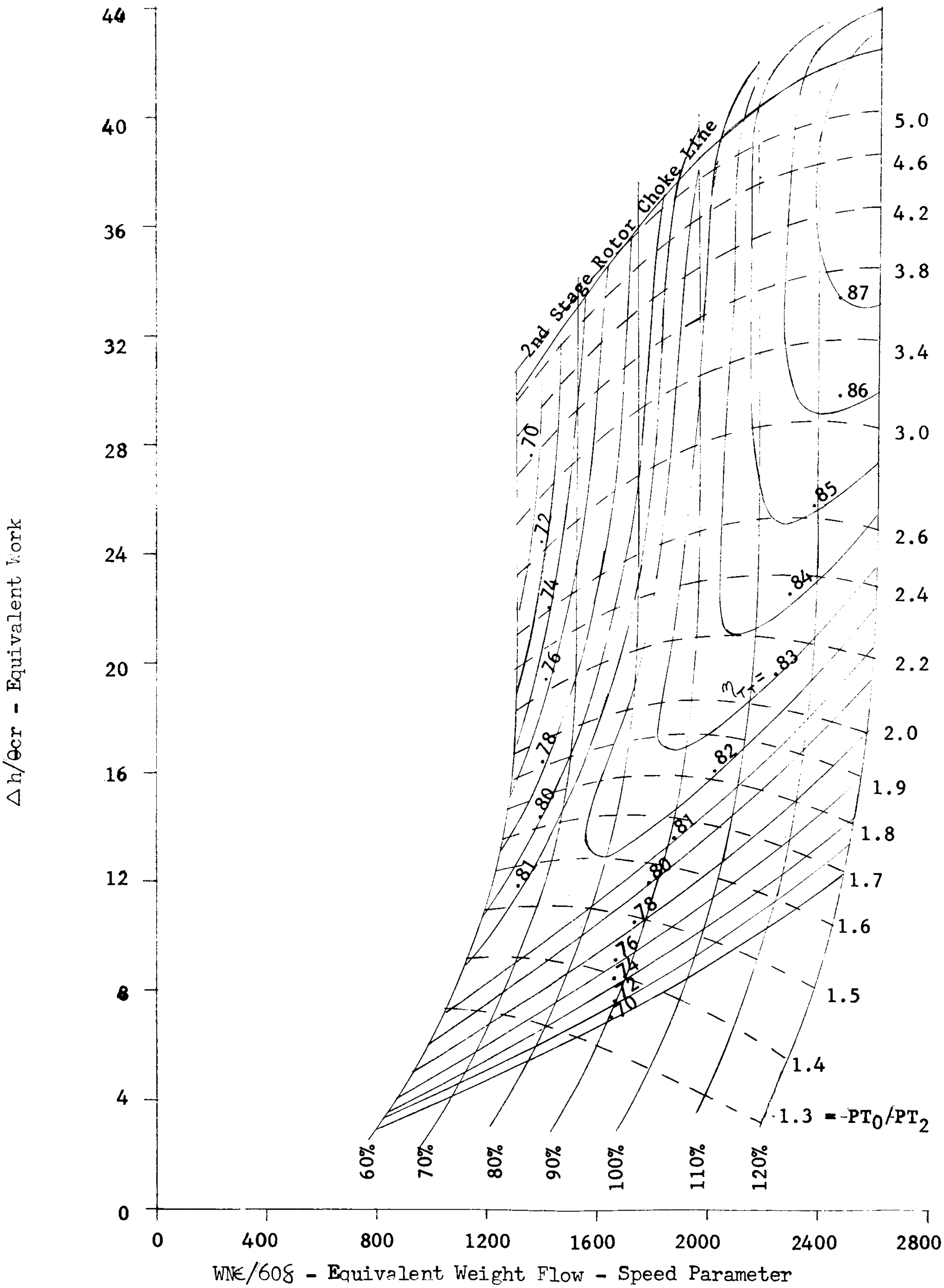

Figure 51

NASA - TASK III

Two Stage Schedule 7.13, 0.0

Equivalent Flow vs. Pressure Ratio

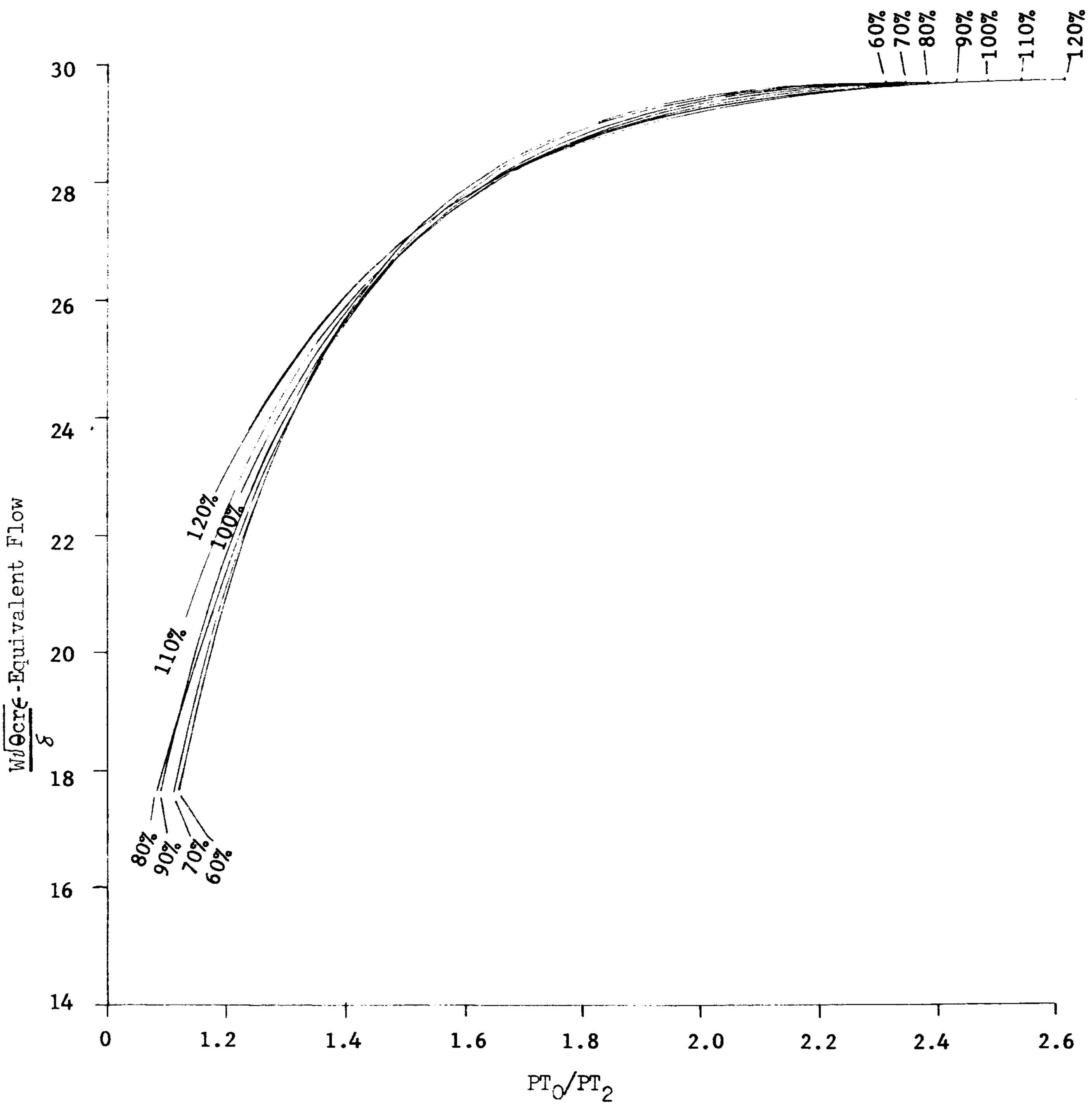

Figure 52

NASA - TASK III

Two Stage-Schedule 7.13, 0.0

Rotor 1 Incidence vs. Equivalent Work

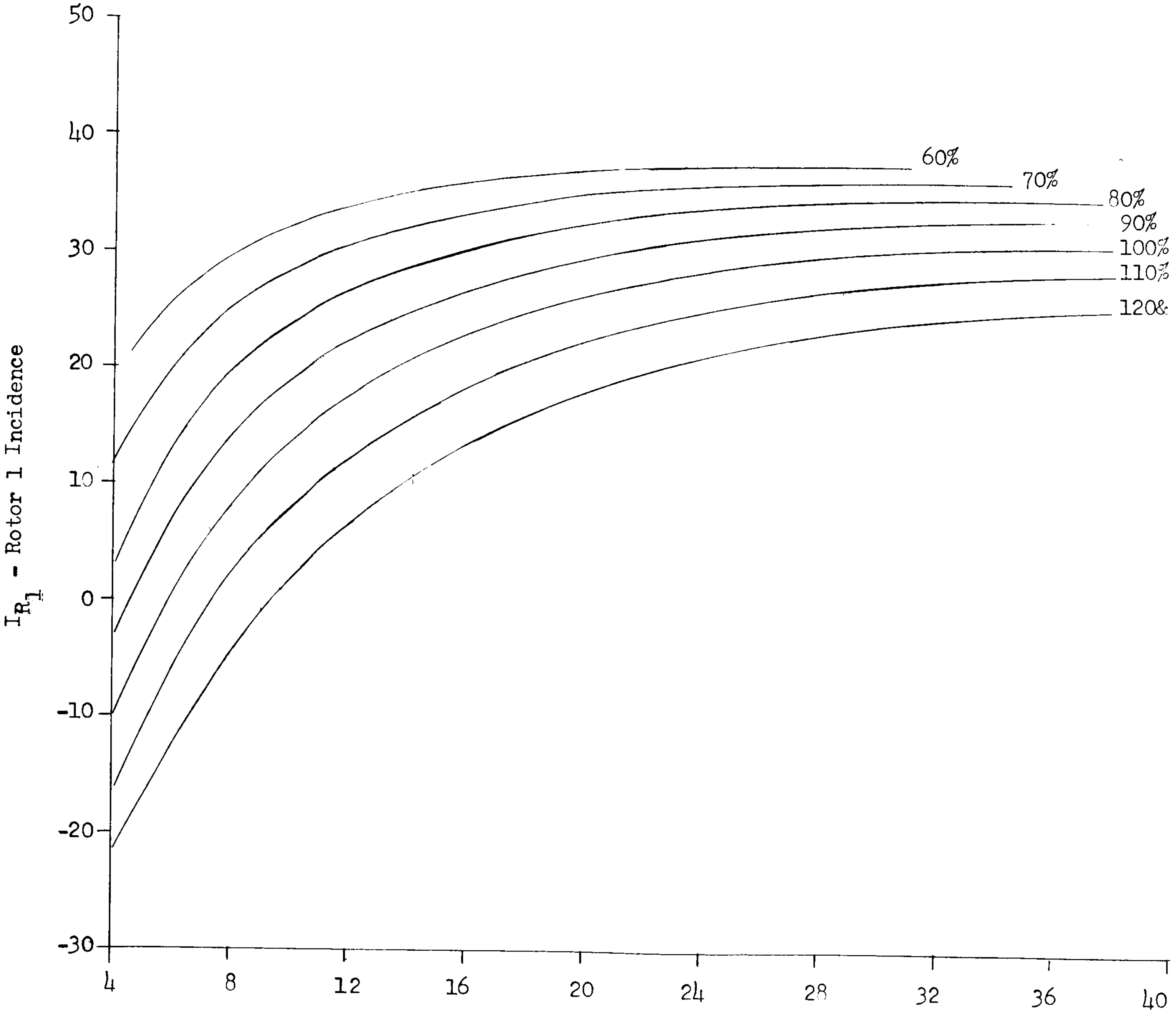

Figure 53

NASA - TASK III

Two Stage Schedule 7.13, 0.0

Stator 2 Incidence vs. Equivalent Work

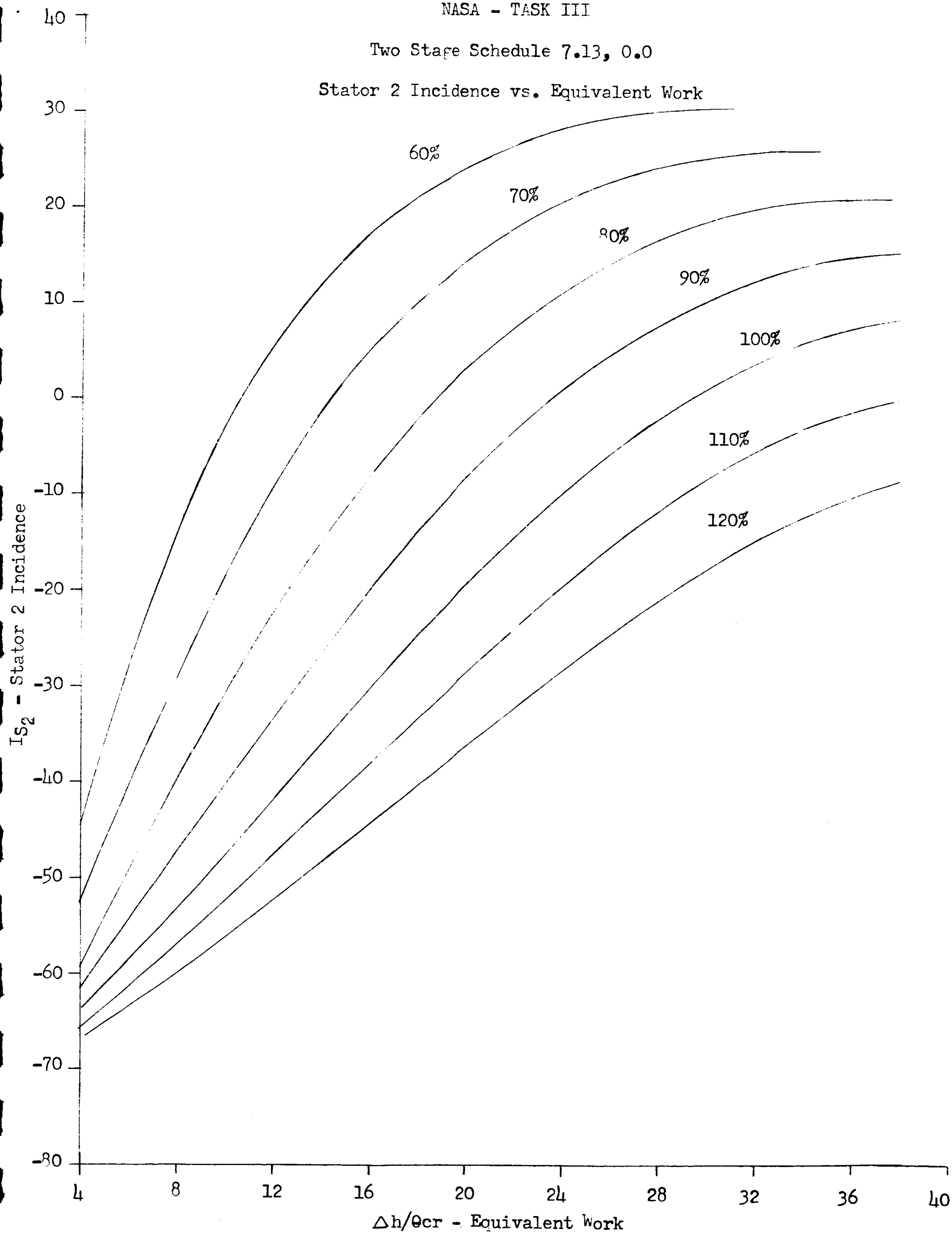

Figure 54

NASA-TASK III

Two Stage-Schedule 7.13, 0.0

Rotor 1 Incidence vs. Equivalent Work

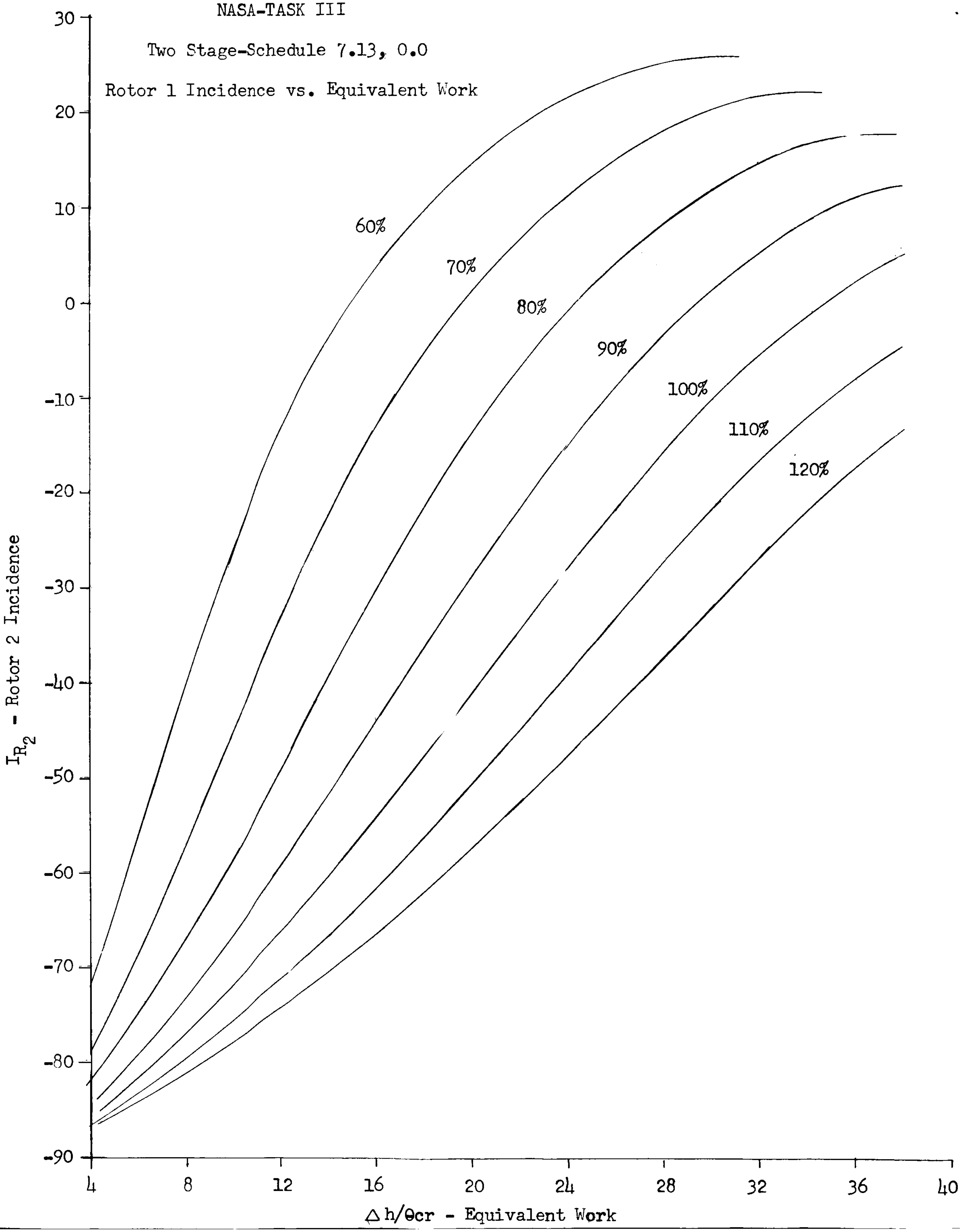

Figure 55

NASA - TASK III

Two Stage -Schedule 7.13, 0.0

Exit Angle vs. Equivalent Work

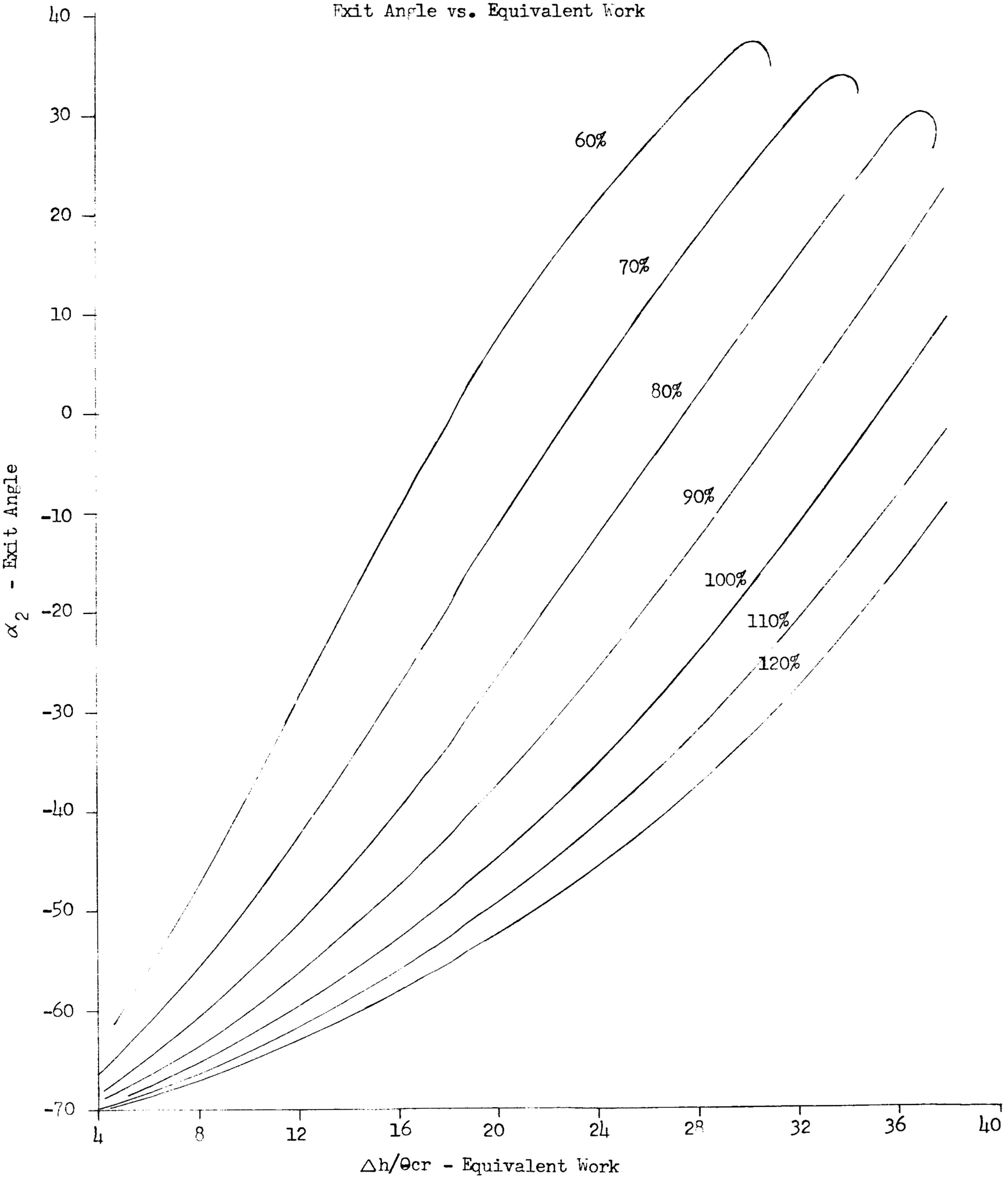

Figure 56

NASA - TASK III

Two Stage-Schedule 7.13, 0.0

Rotor 1 Hub Mach Number vs. Equivalent Work

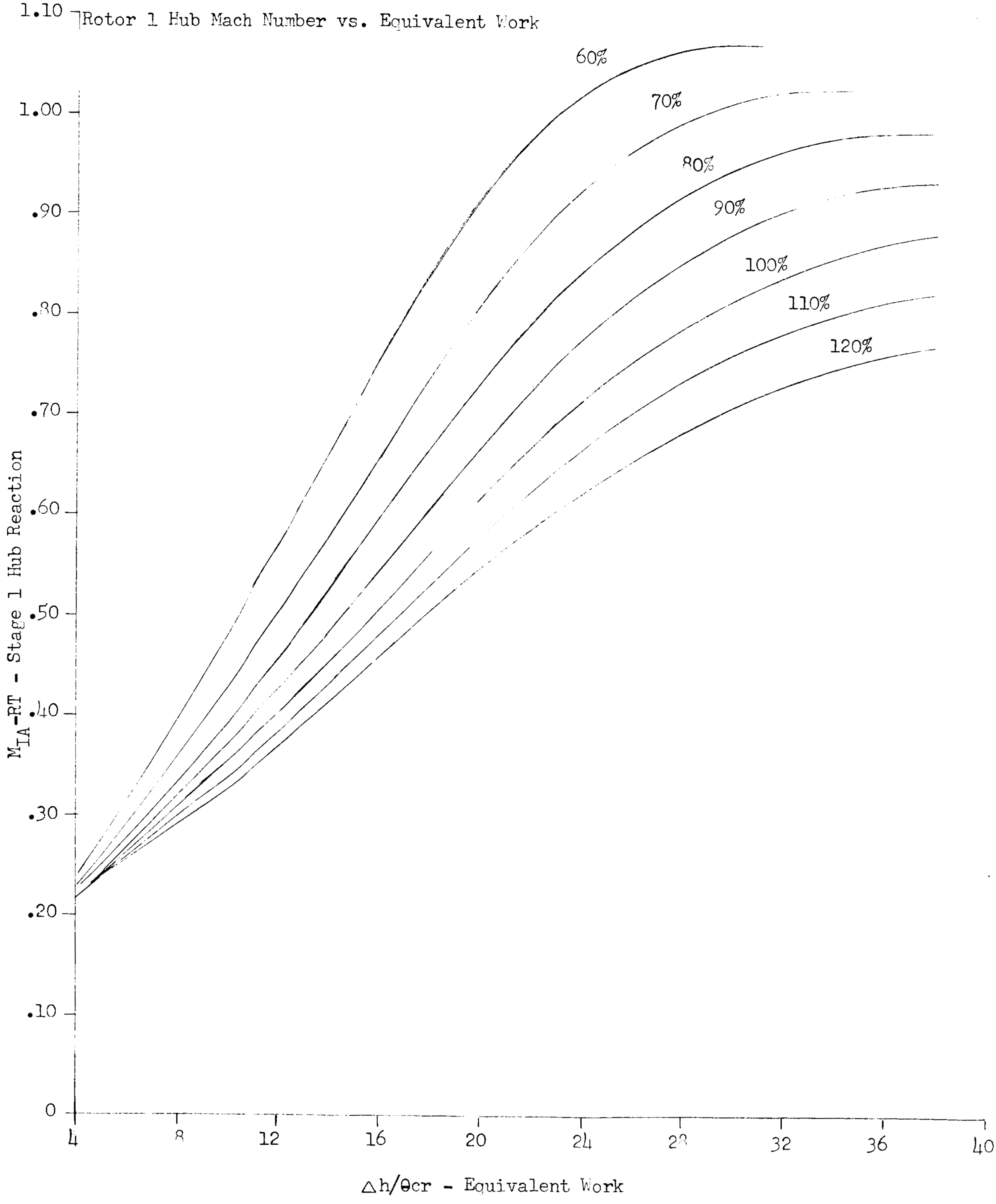

Figure 57

NASA - TASK III

Two Stage-Schedule 7.13, 0.0

Rotor 2 Hub Mach Number vs. Equivalent Work

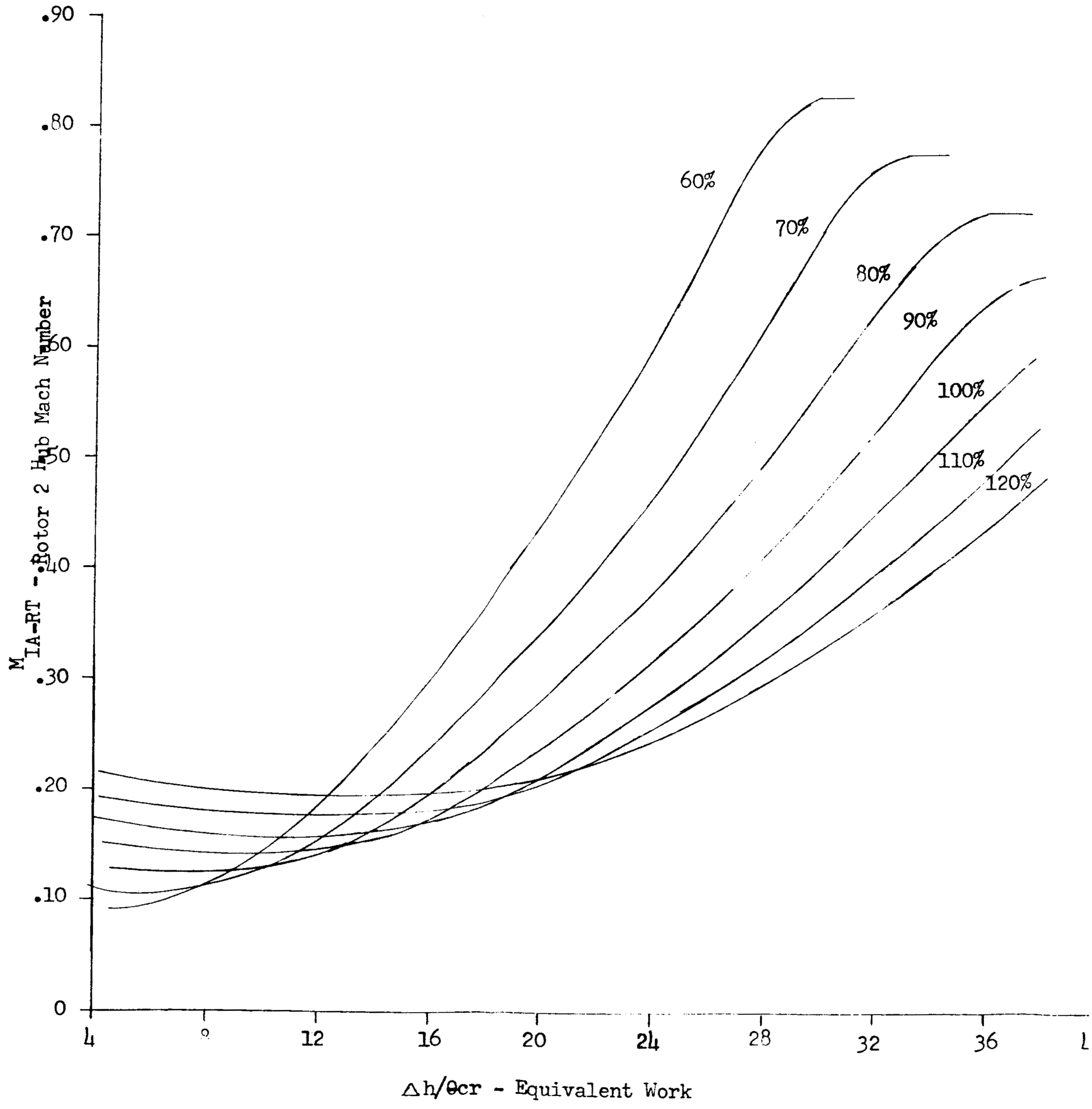

Figure 58

NASA - TASK III

Two Stage-Schedule 7.13, 0.0

Stage 1 Hub Reaction vs. Equivalent Work

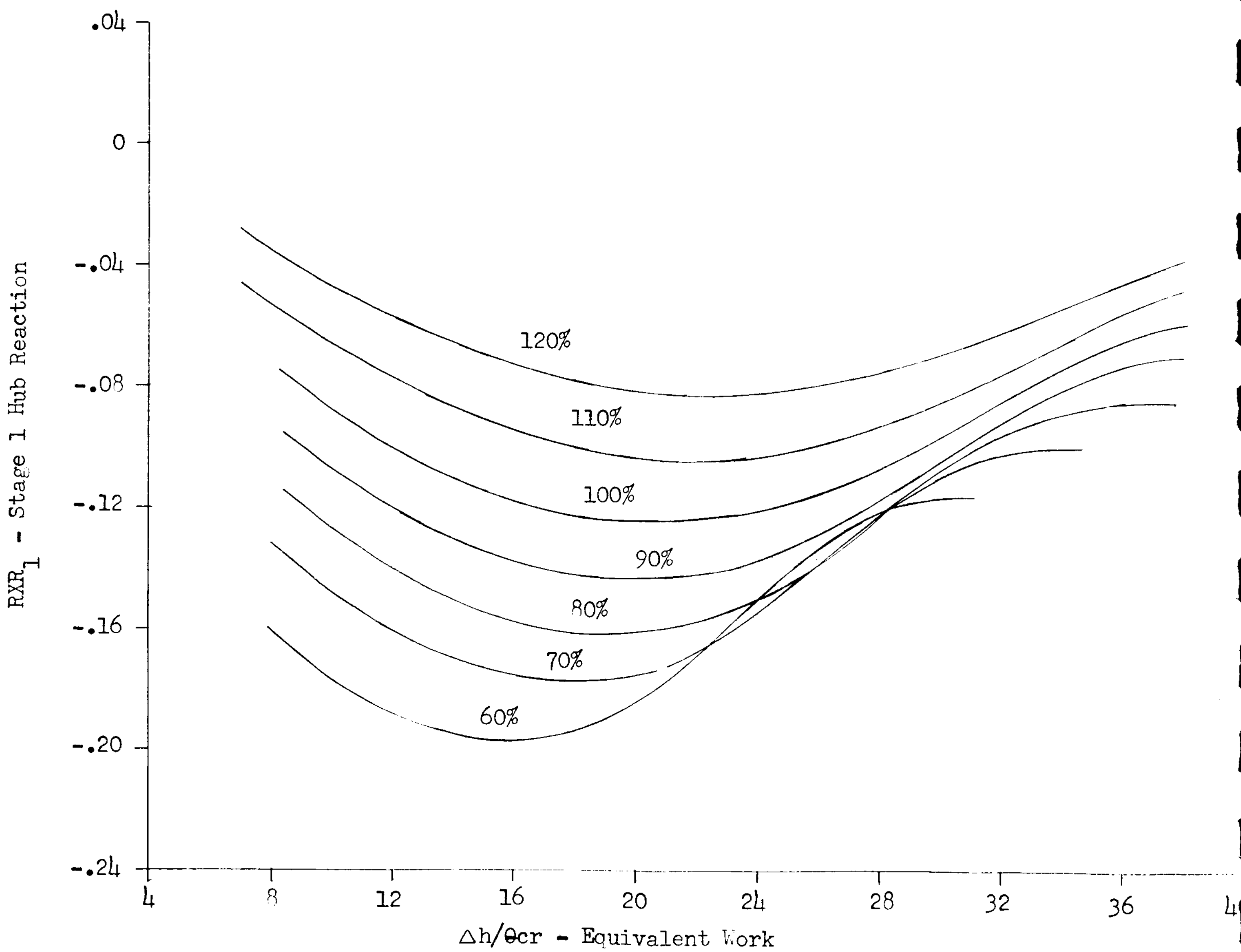

Figure 59

NASA - TASK III

Two Stage Schedule 7.13, 0.0

Stage 2 Hub Reaction vs. Equivalent Work

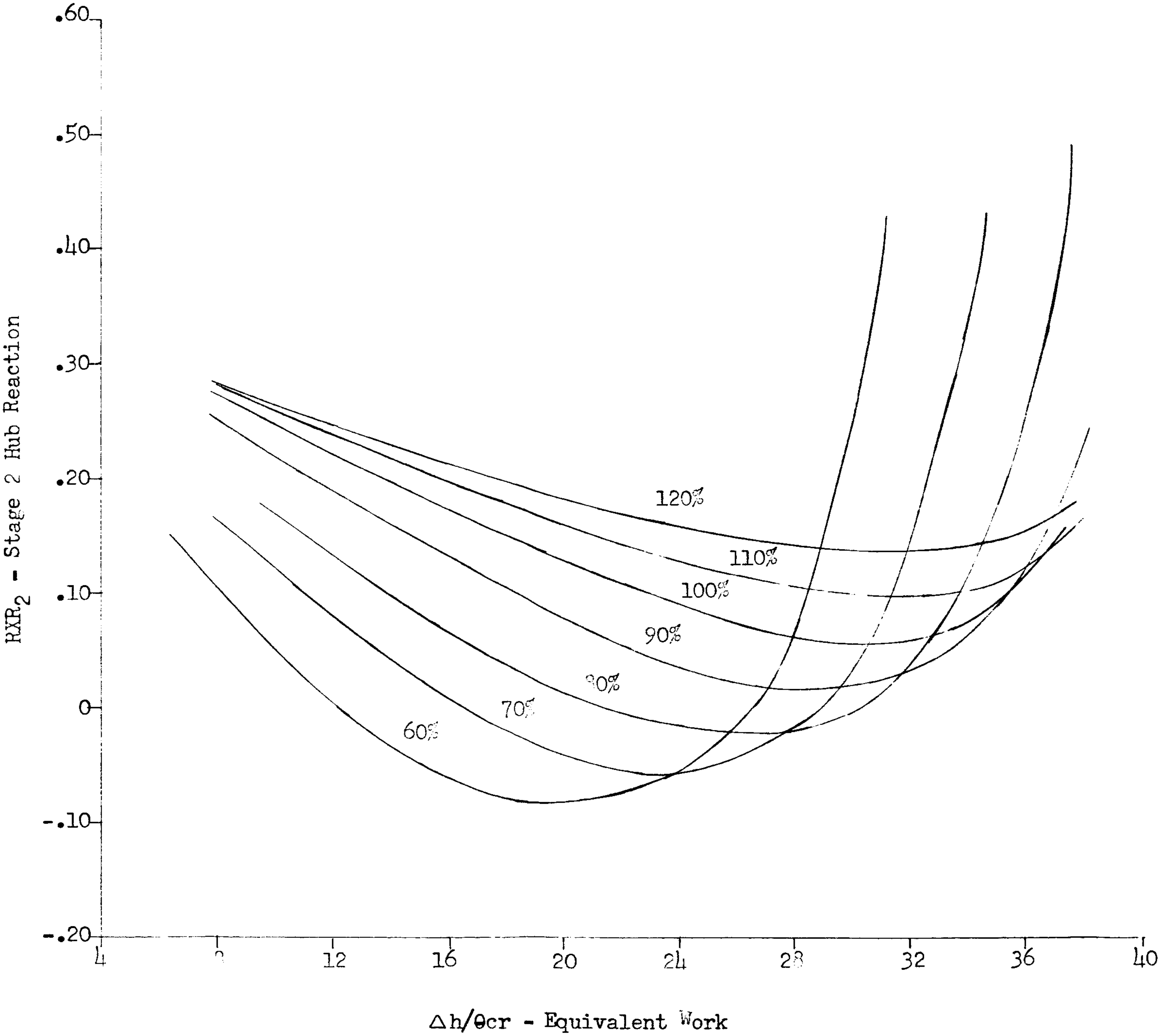

Figure 60

NASA - TASK III

Two Stage-Schedule 0.0, -9.62

Performance Map

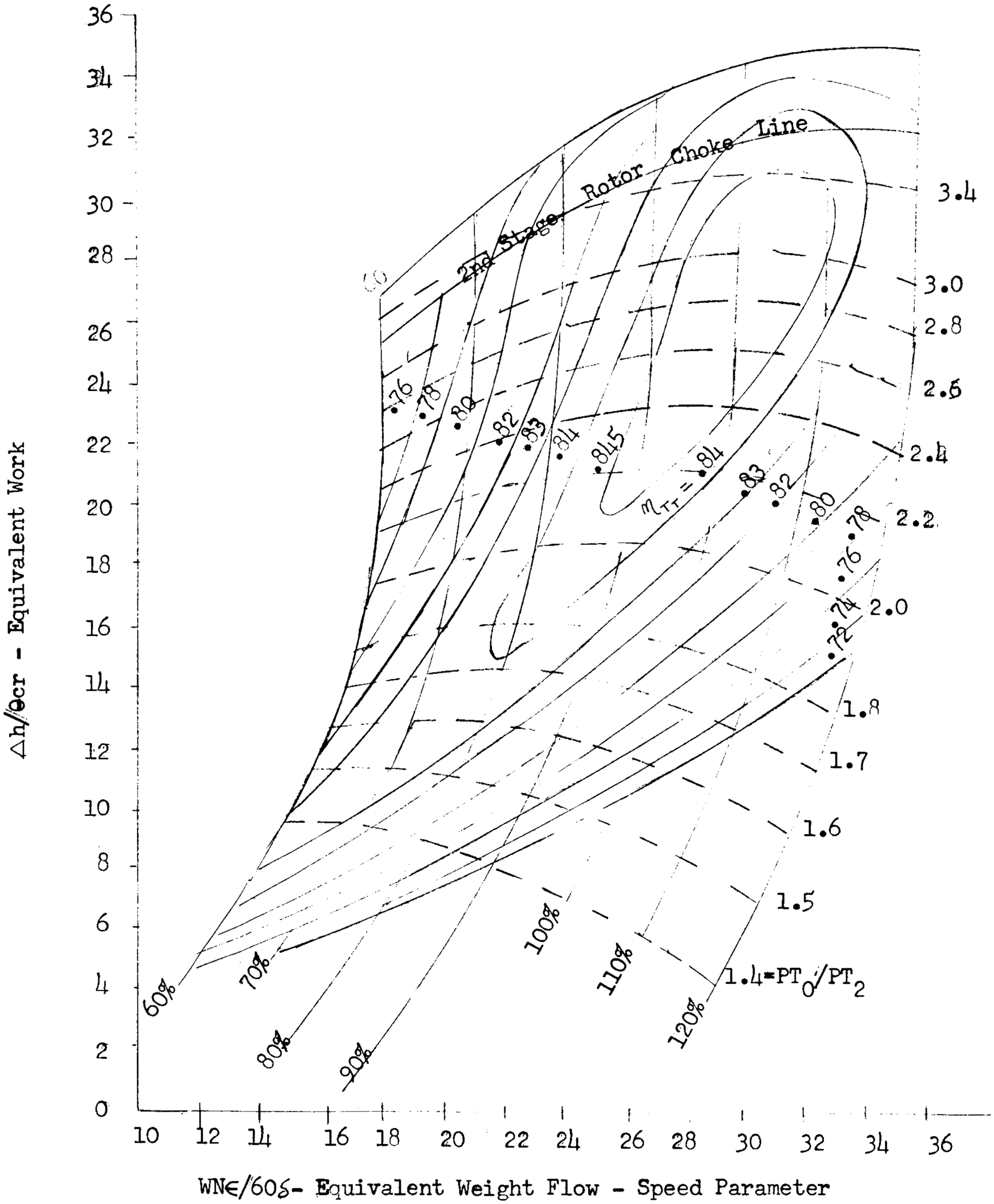

Figure 61

NASA - TASK III

Two Stage-Schedule 0.0, -9.62

Equivalent Flow vs. Pressure Ratio

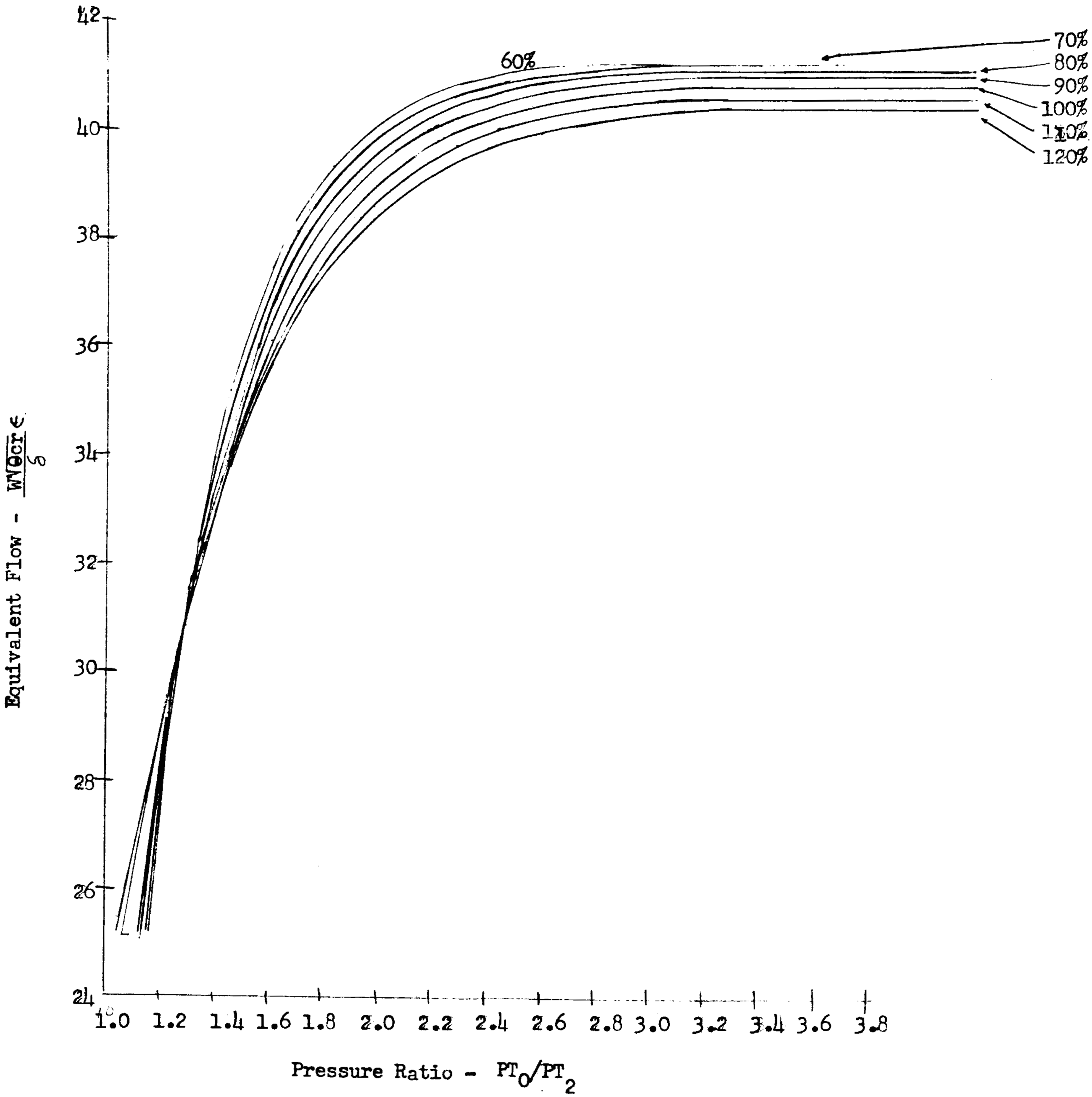

Figure 62

NASA - TASK III

Two Stage-Schedule 0.0, -9,62

Rotor 1 Incidence vs. Equivalent Work

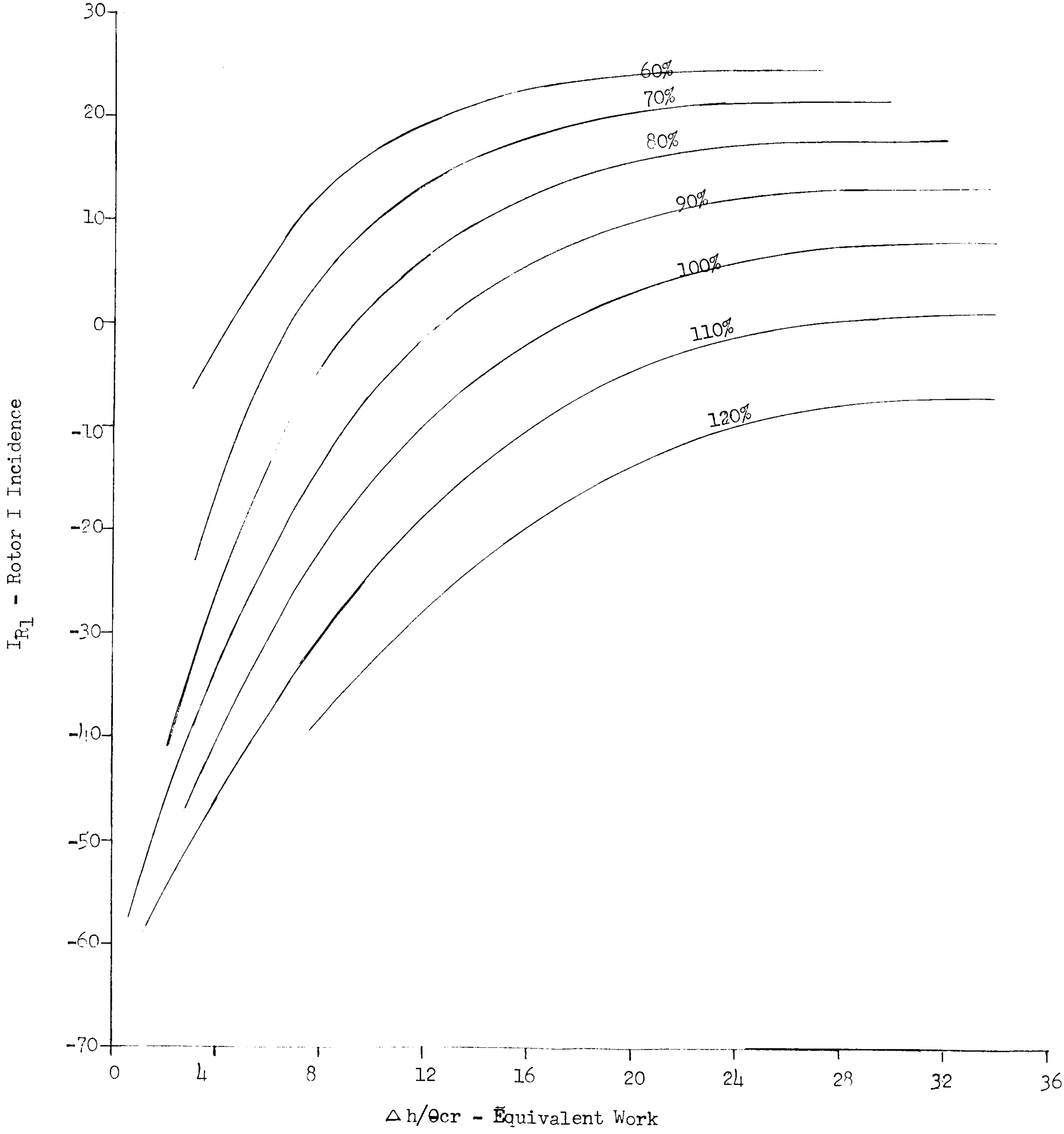

Figure 63

NASA - TASK III

Two Stage-Schedule 0.0, -9.62

Stator 2 Incidence vs. Equivalent Work

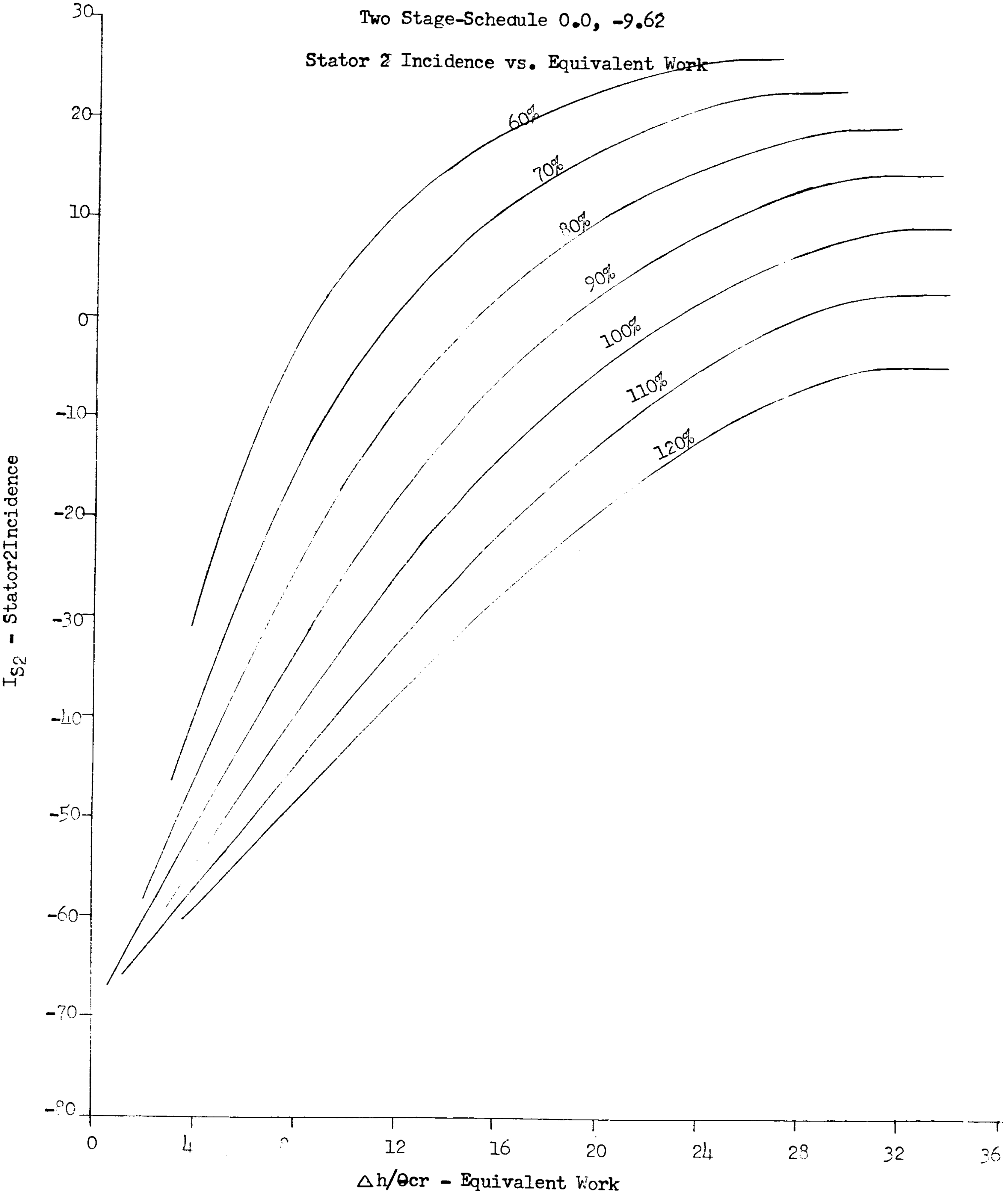

Figure 64

NASA - TASK III

Two Stage-Schedule 0.0, -9.62

Rotor 2 Incidence vs. Equivalent Work

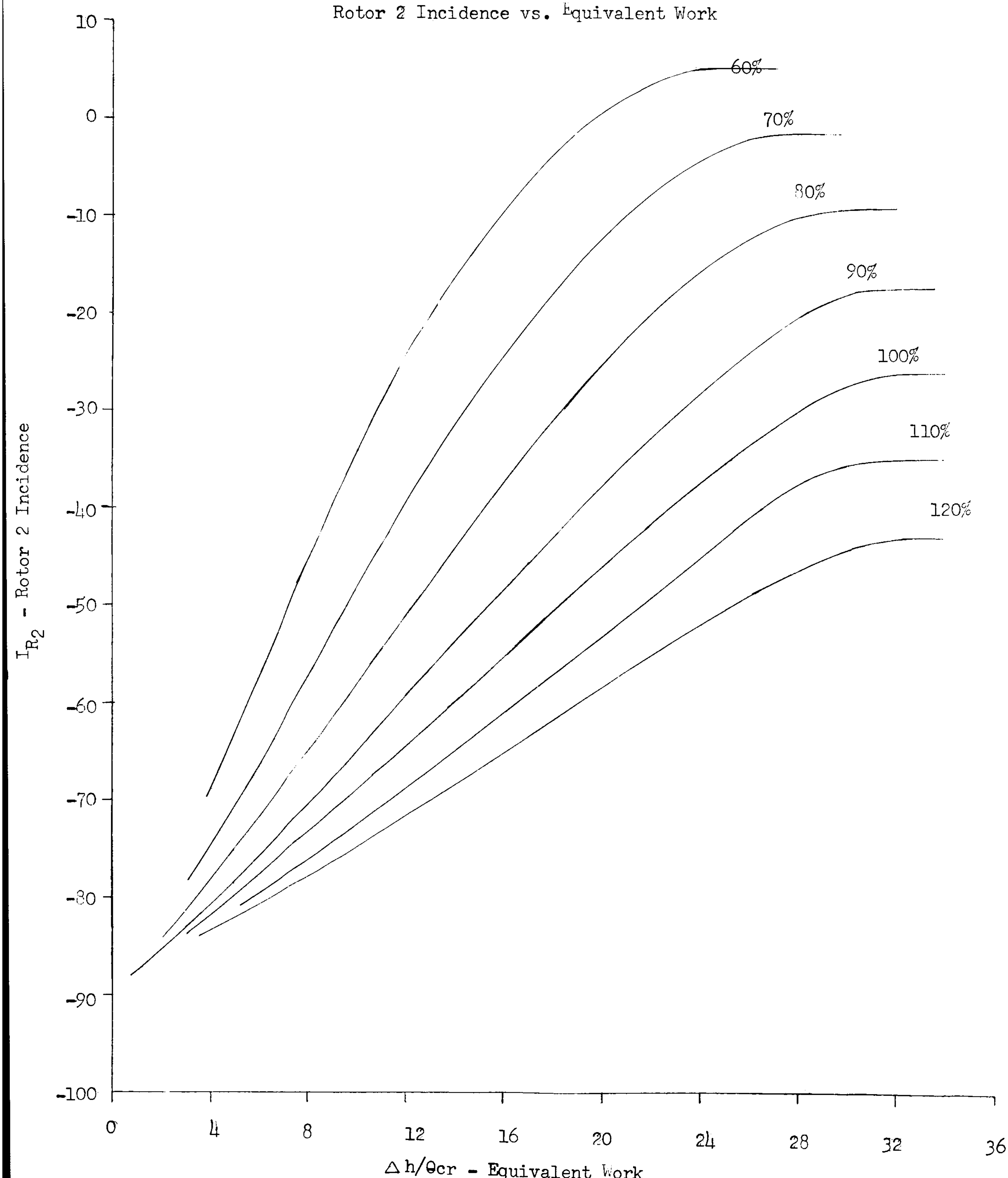

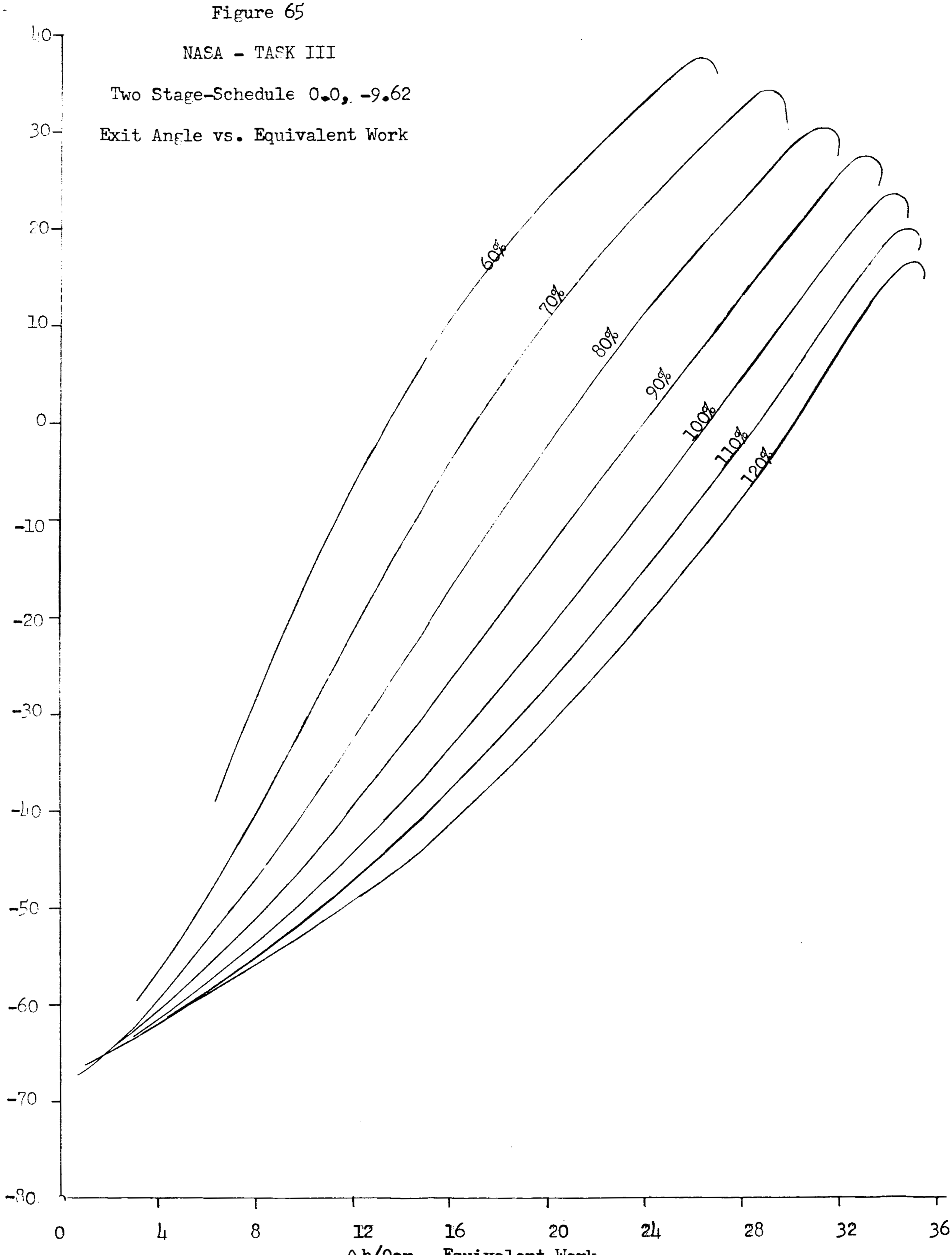
Figure 65
NASA - TASK III
Two Stage-Schedule 0.0, -9.62
Exit Angle vs. Equivalent Work
60%
70%
80%
90%
100%
110%
120%
40
30
20
10
0
-10
-20
-30
-40
-50
-60
-70
-80
0
4
8
12
16
20
24
28
32
36
α_2 - Exit Angle
$\Delta h/\theta cr$ - Equivalent Work

Figure 66

NASA - TASK III

Two Stage-Schedule 0.0, -9.62

Rotor 1 Hub Mach Number vs. Equivalent Work

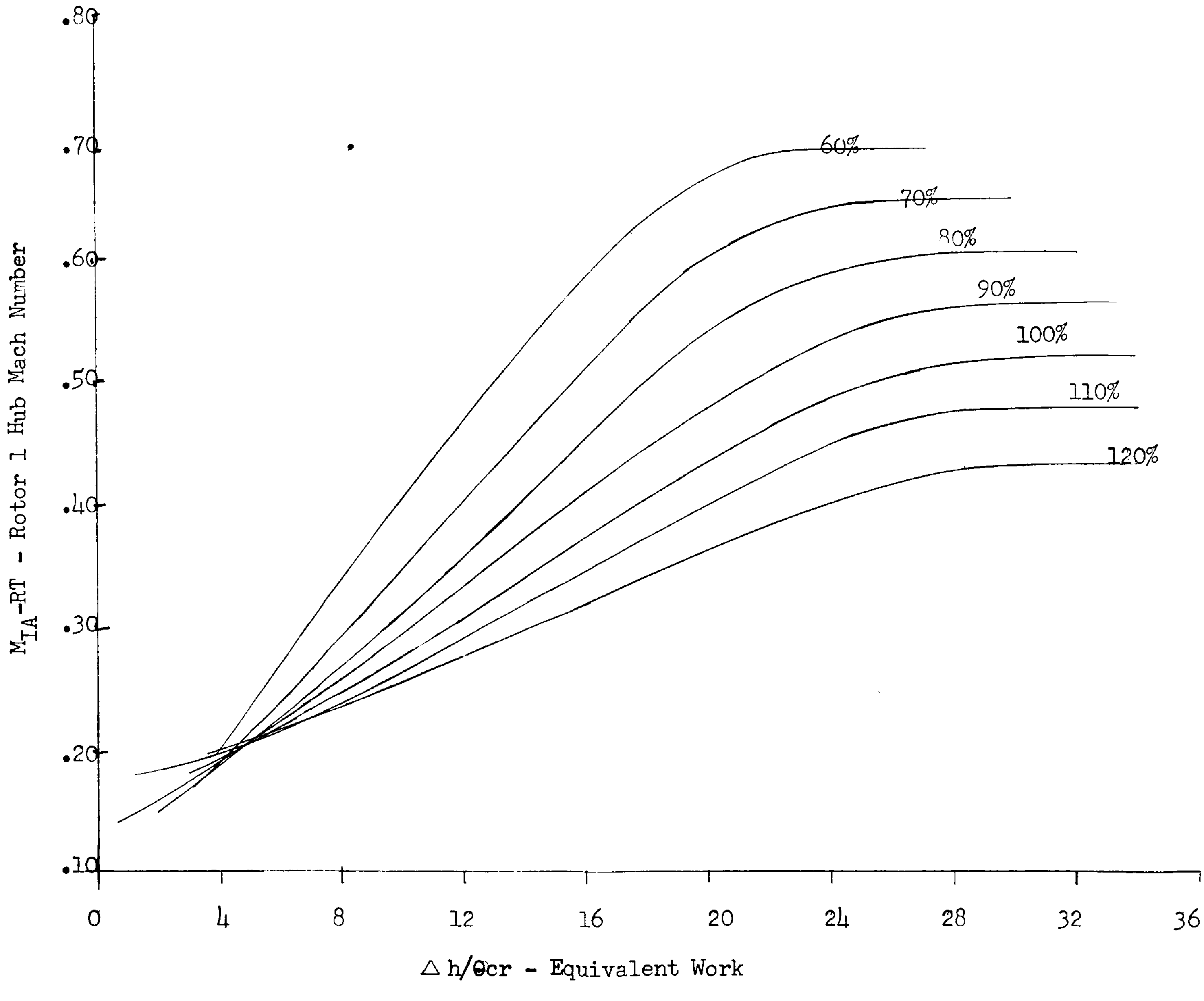

Figure 67

NASA - TASK III

Two Stage-Schedule 0.0, -9.62

Rotor Hub Mach Number vs. Equivalent Work

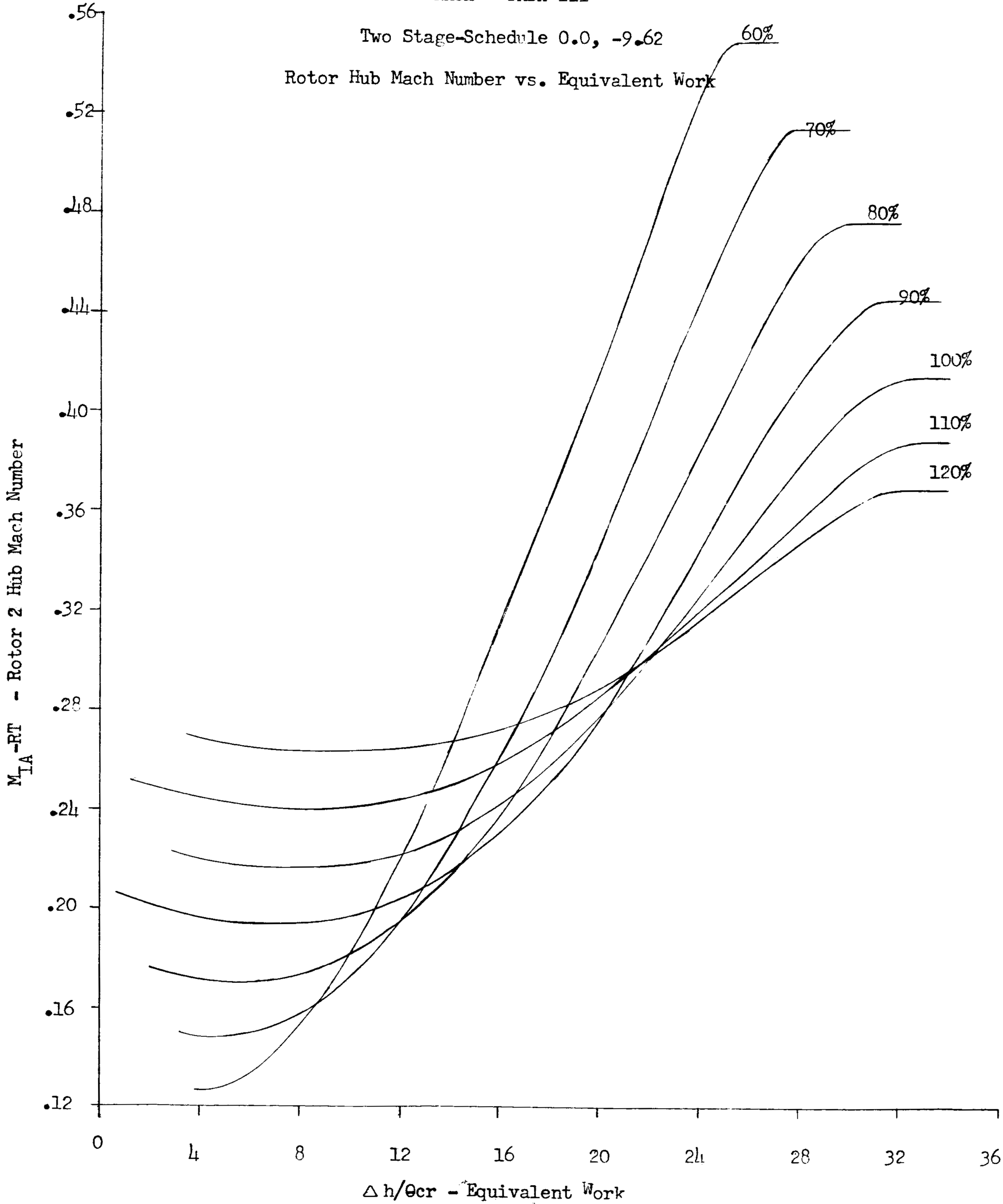

Figure 68

NASA - TASK III

Two Stage-Schedule 0.0, -9.62

Stage 1 Hub Reaction vs. Equivalent Work

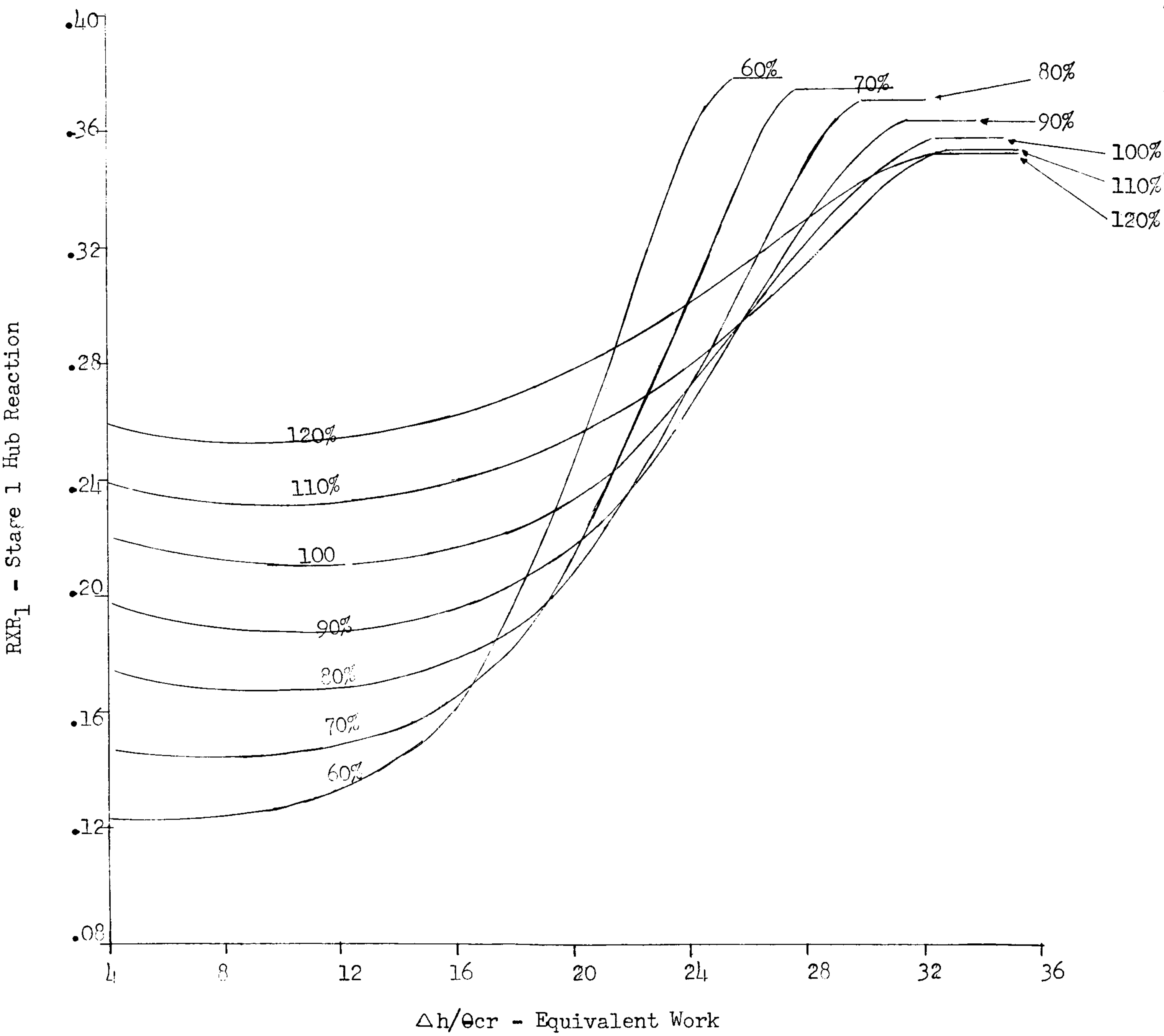

Figure 69

NASA - TASK III

Two Stage-Schedule 0.0, -9.62

Stage 2 Hub Reaction vs. Equivalent Work

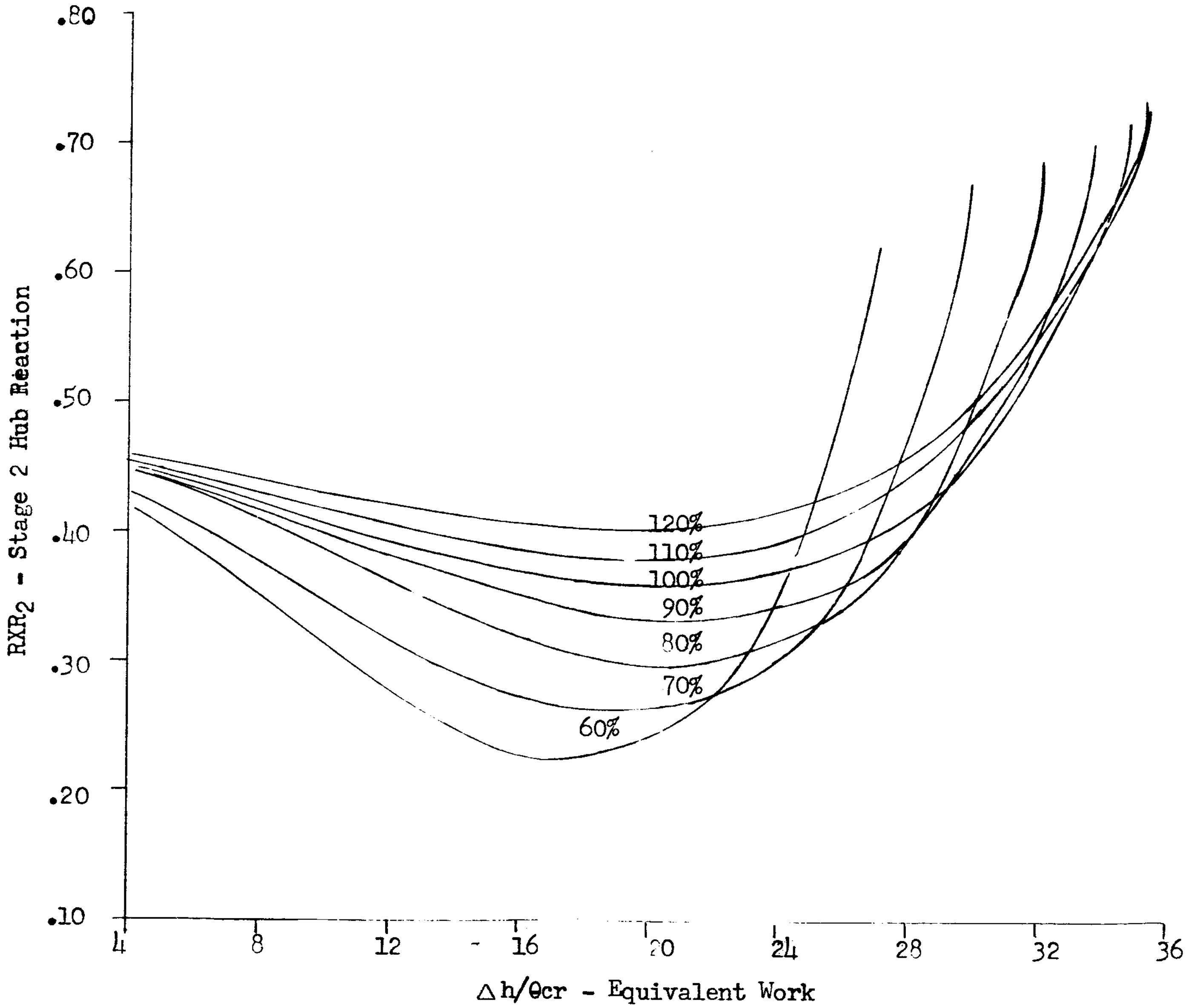

Figure 70

NASA - TASK III

Two Stage-Schedule -7.53, -9.62

Performance Map

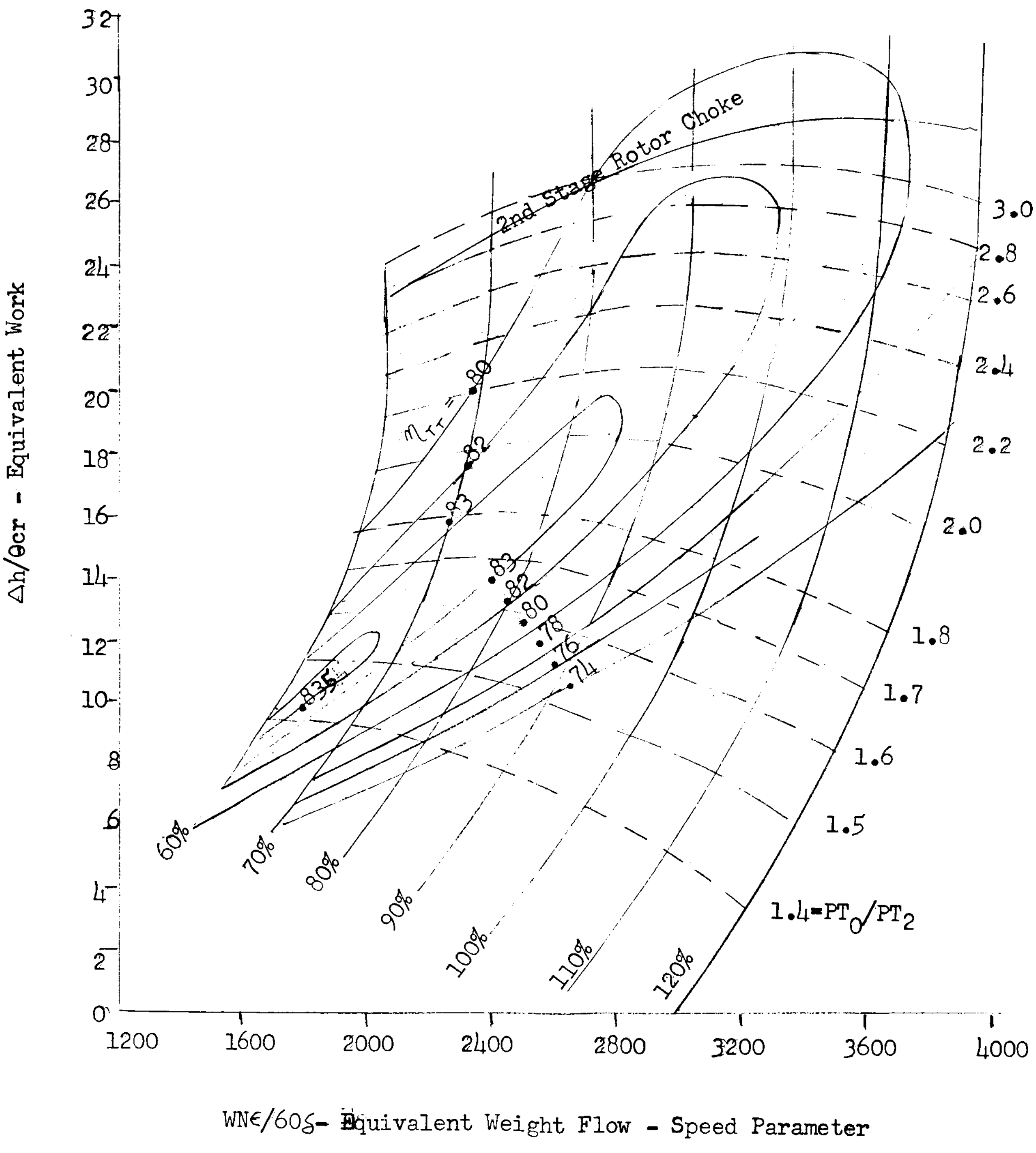

Figure 71

NASA - TASK III

Two Stage-Schedule -7.53, -9.62

Equivalent Flow vs. Pressure Ratio

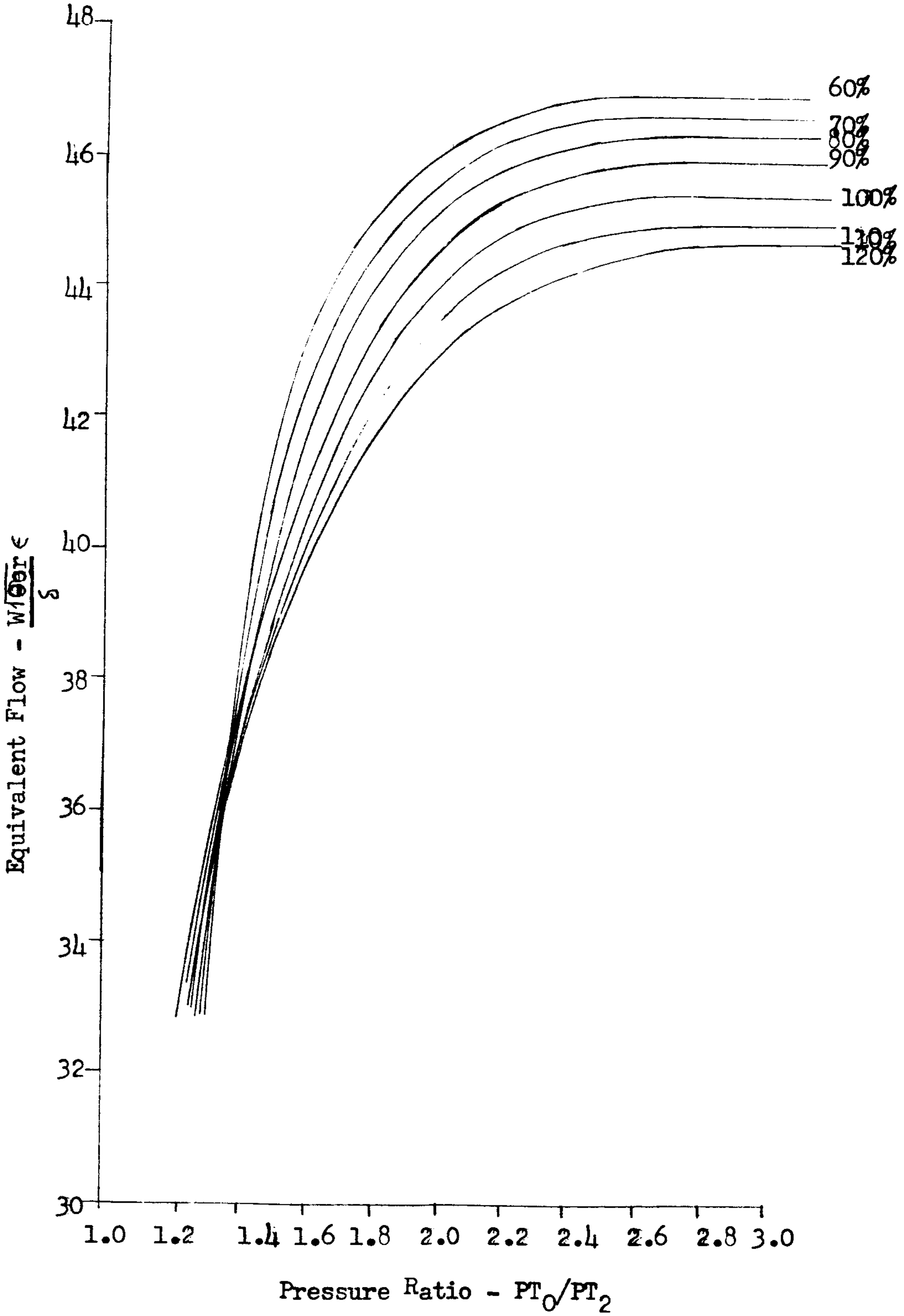

Figure 72

NASA - TASK III

Two Stage-Schedule -7.53, -9.62

Rotor 1 Incidence vs. Equivalent Work

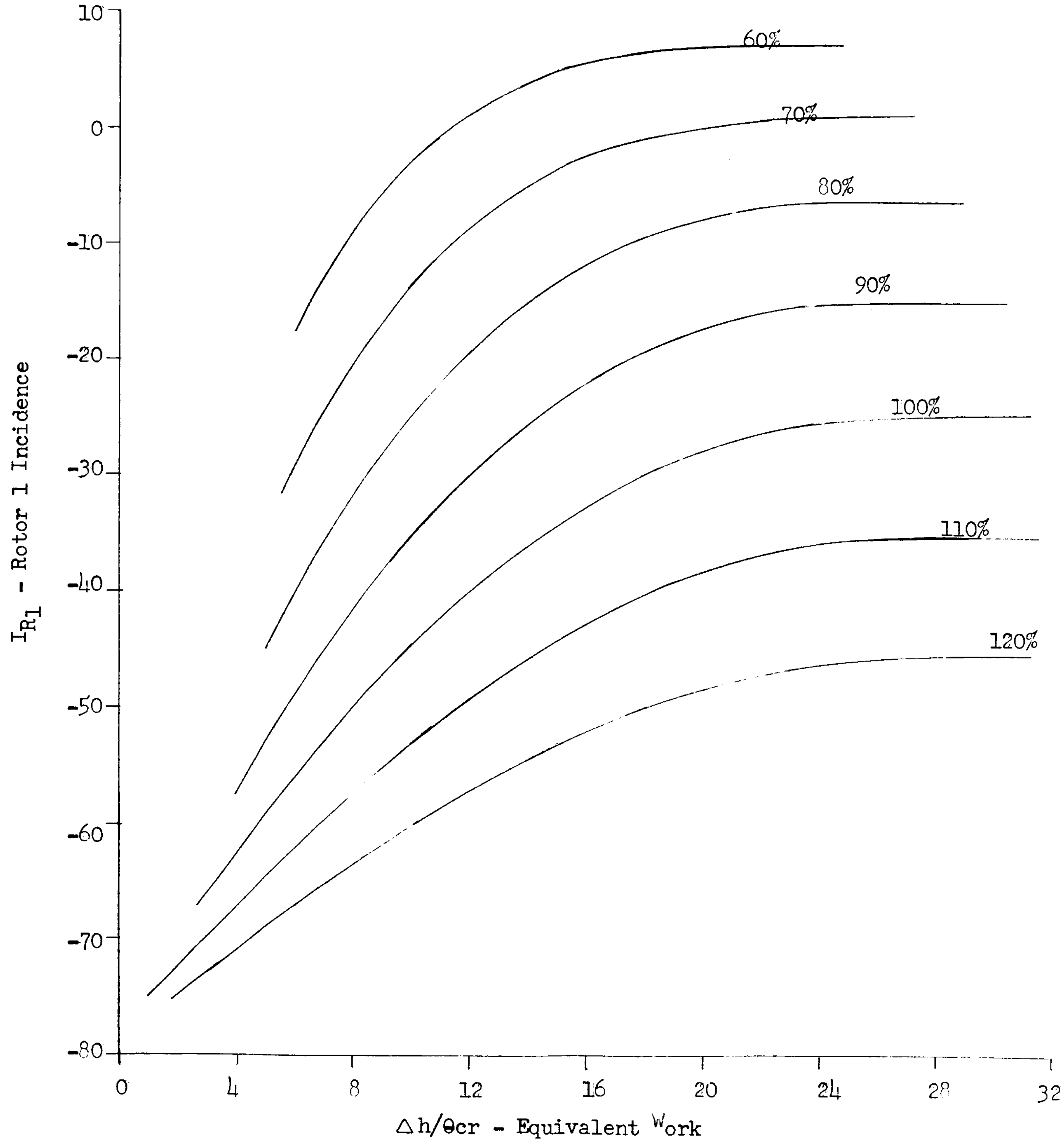

Figure 73

NASA - TASK III

Two Stage-Schedule -7.53, -9.62

Stator 2 Incidence vs. Equivalent Work

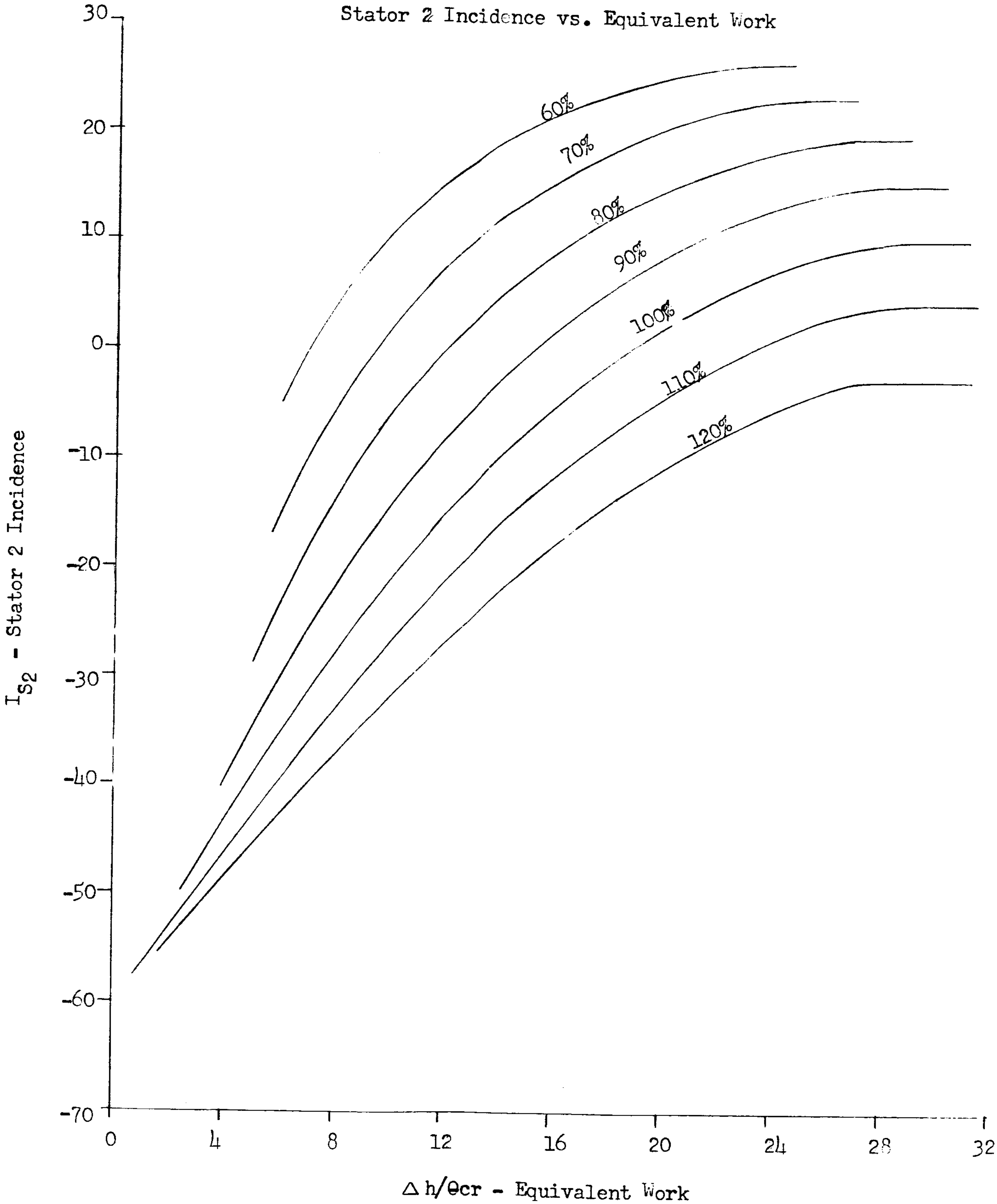

Figure 74

NASA - TASK III

Two Stage-Schedule -7.53, -9.62

Rotor 2 Incidence vs. Equivalent Work

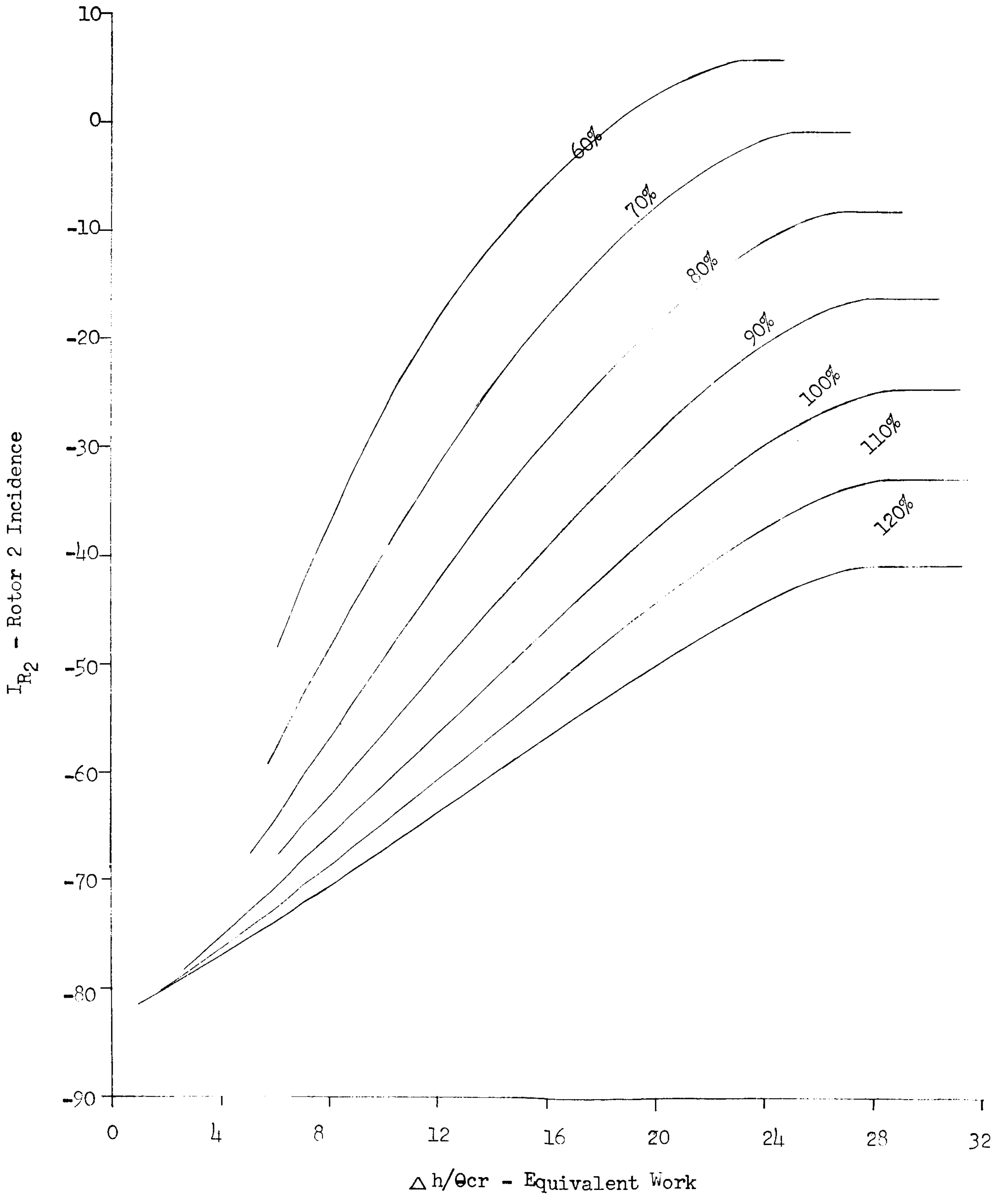

Figure 75

NASA - TASK III

Two Stage-Schedule -7.53, -9.62

Exit Angle
vs.
Equivalent Work

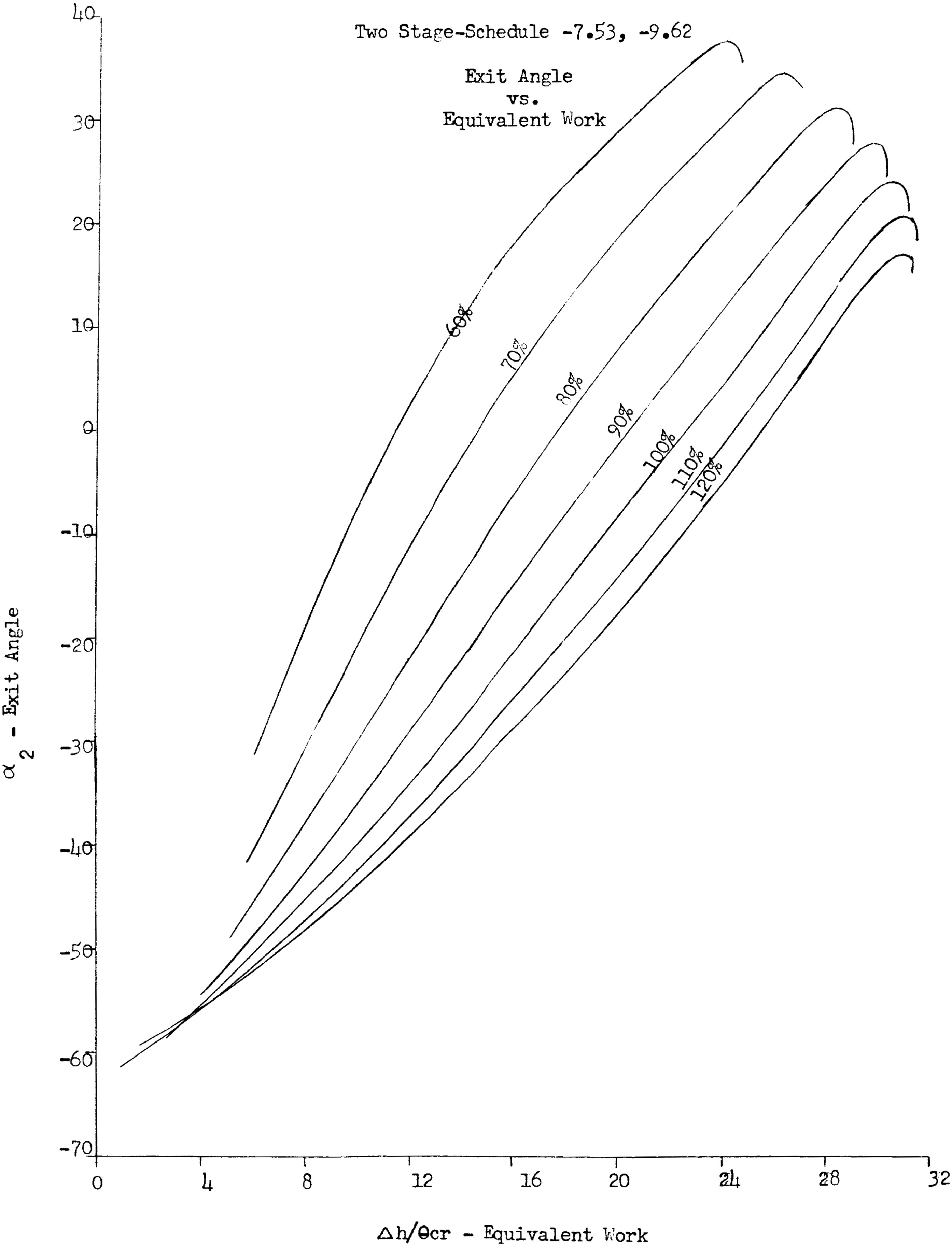

Figure 76

NASA - TASK III

Two Stage-Schedule -7.53, -9.62

Rotor 1 Hub Mach Number
vs.
Equivalent Work

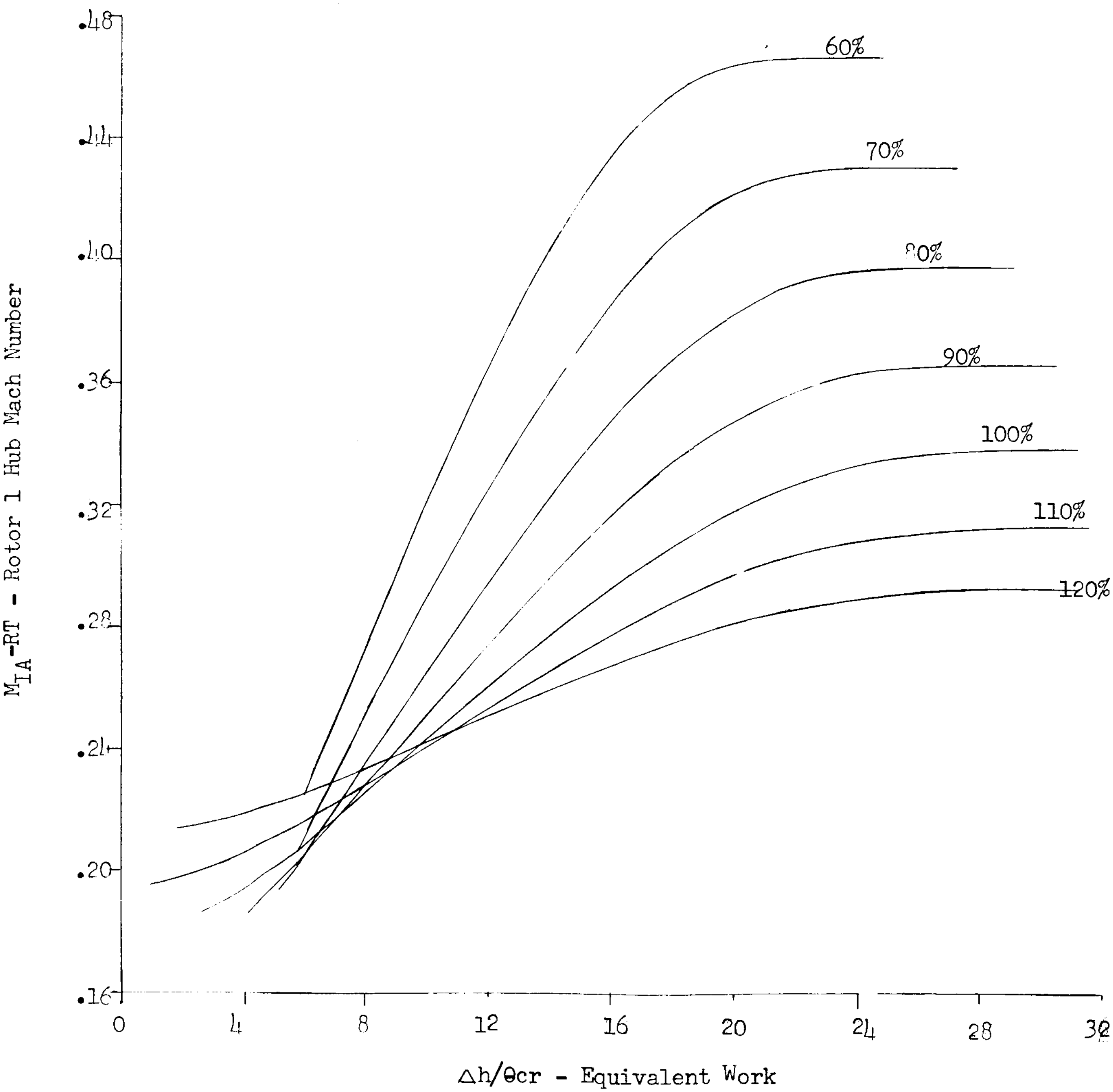

Figure 77

NASA - TASK III

Rotor 2 Hub Mach Number
vs.
Equivalent Work

Two Stage-Schedule -7.53, -9.62

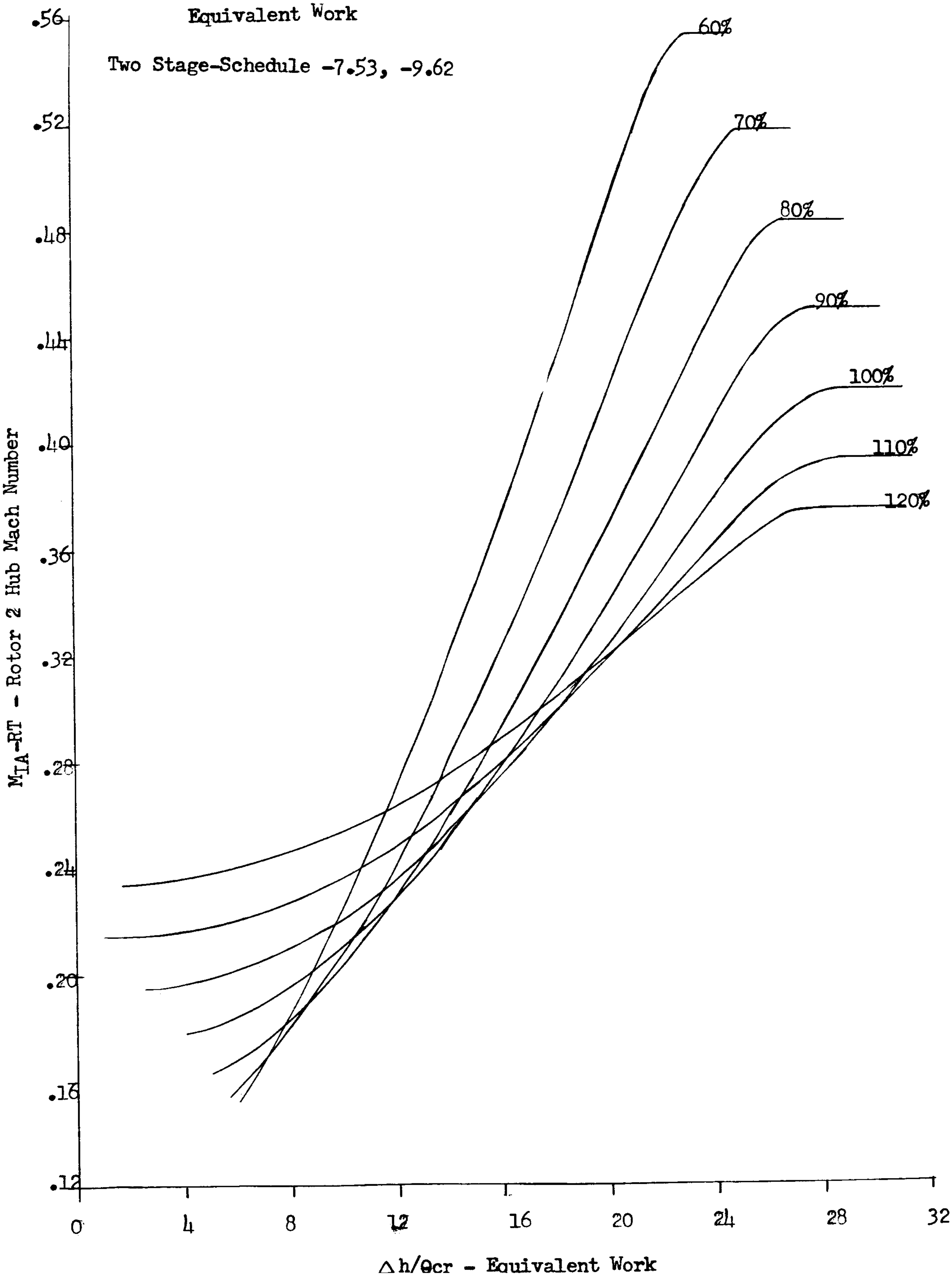

Figure 78

NASA - TASK III

Two Stage-Schedule -7.53, -9.62

Stage 1 Hub Reaction vs. Equivalent Work

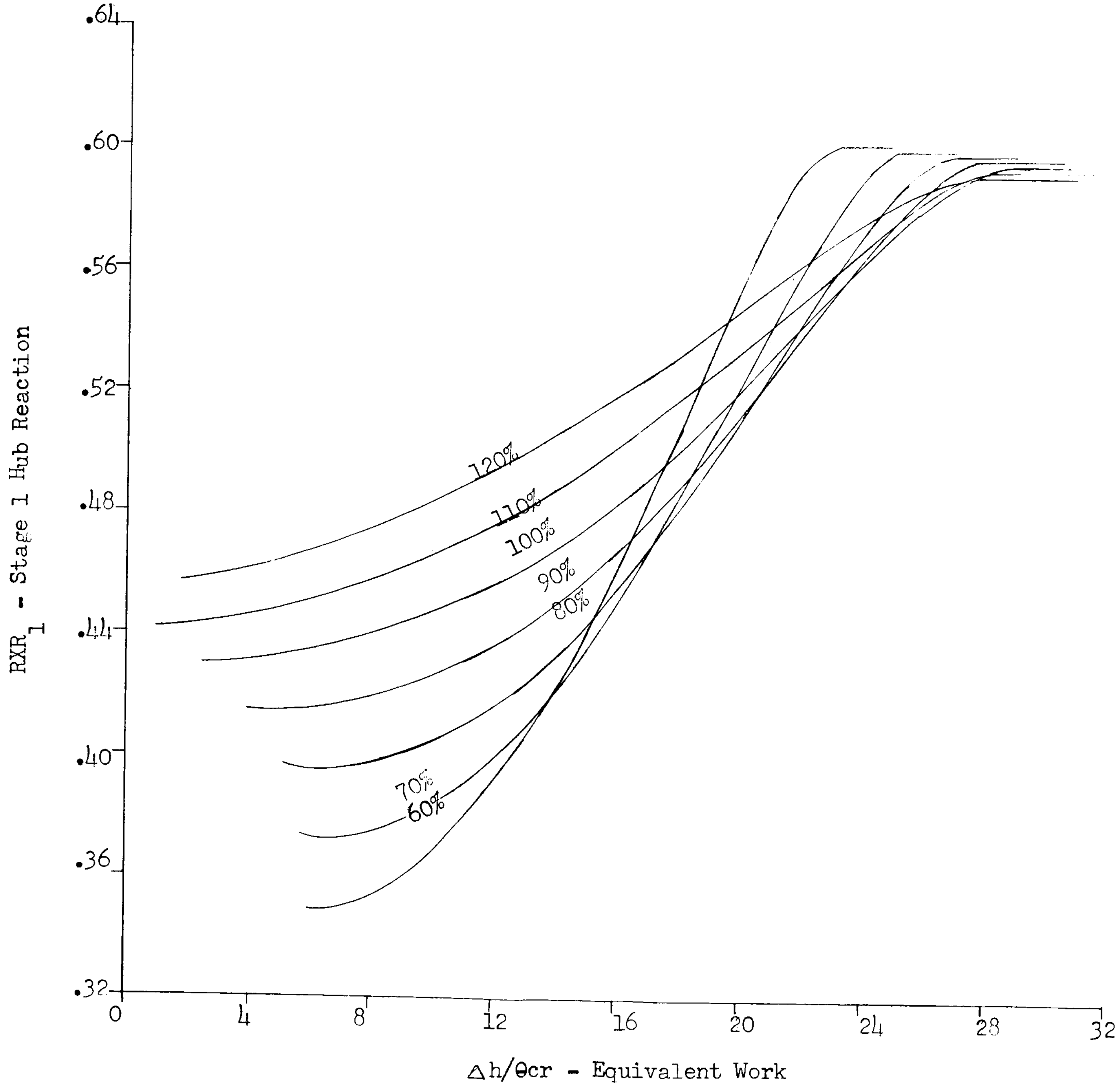

Figure 79

NASA - TASK III

Two Stage-Schedule -7.53, -9.62

Stage 2 Hub Reaction vs. Equivalent Work

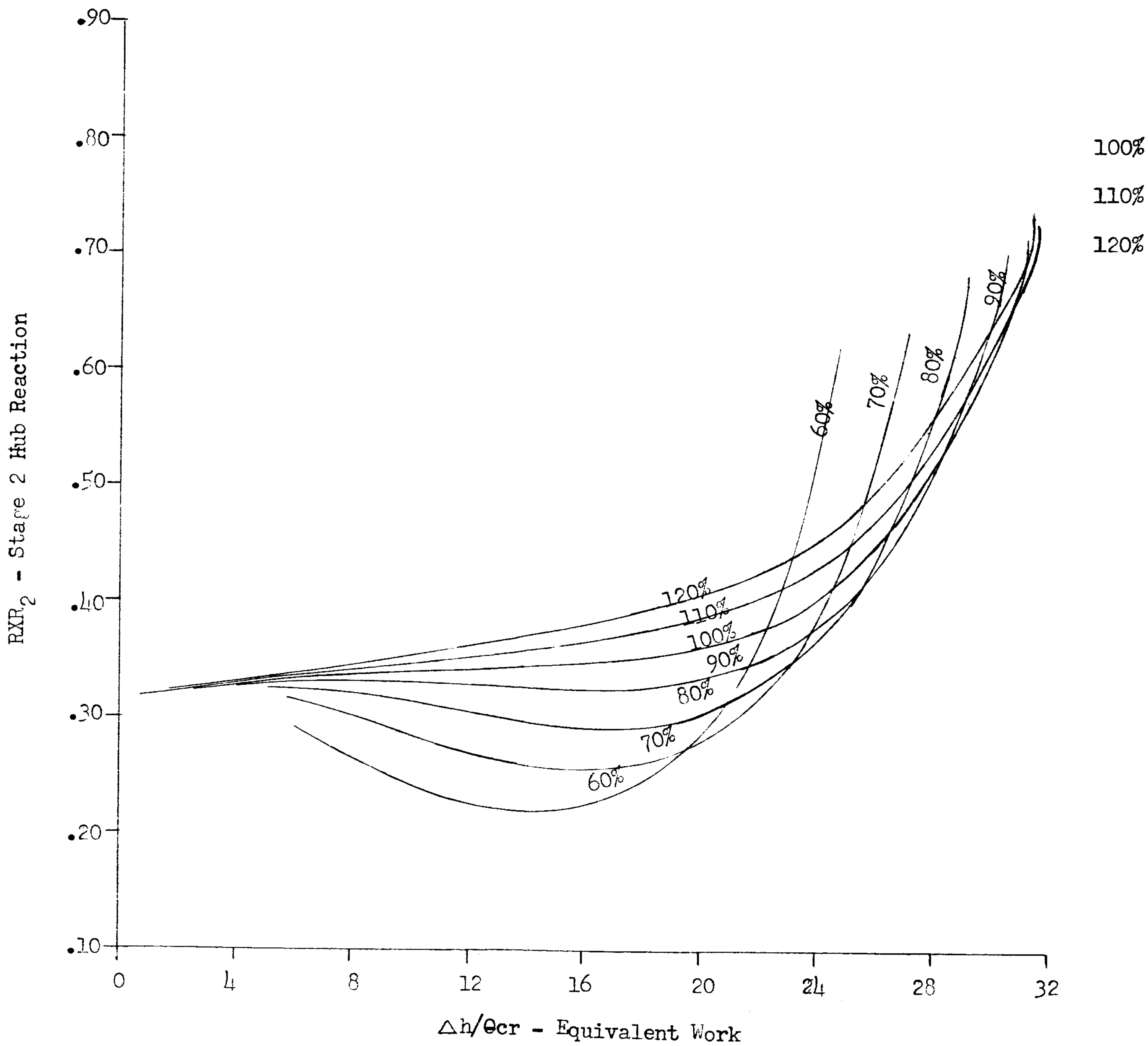

Figure 80

NASA - TASK III

Two Stage-Schedule 7.13, -9.62

Performance Map

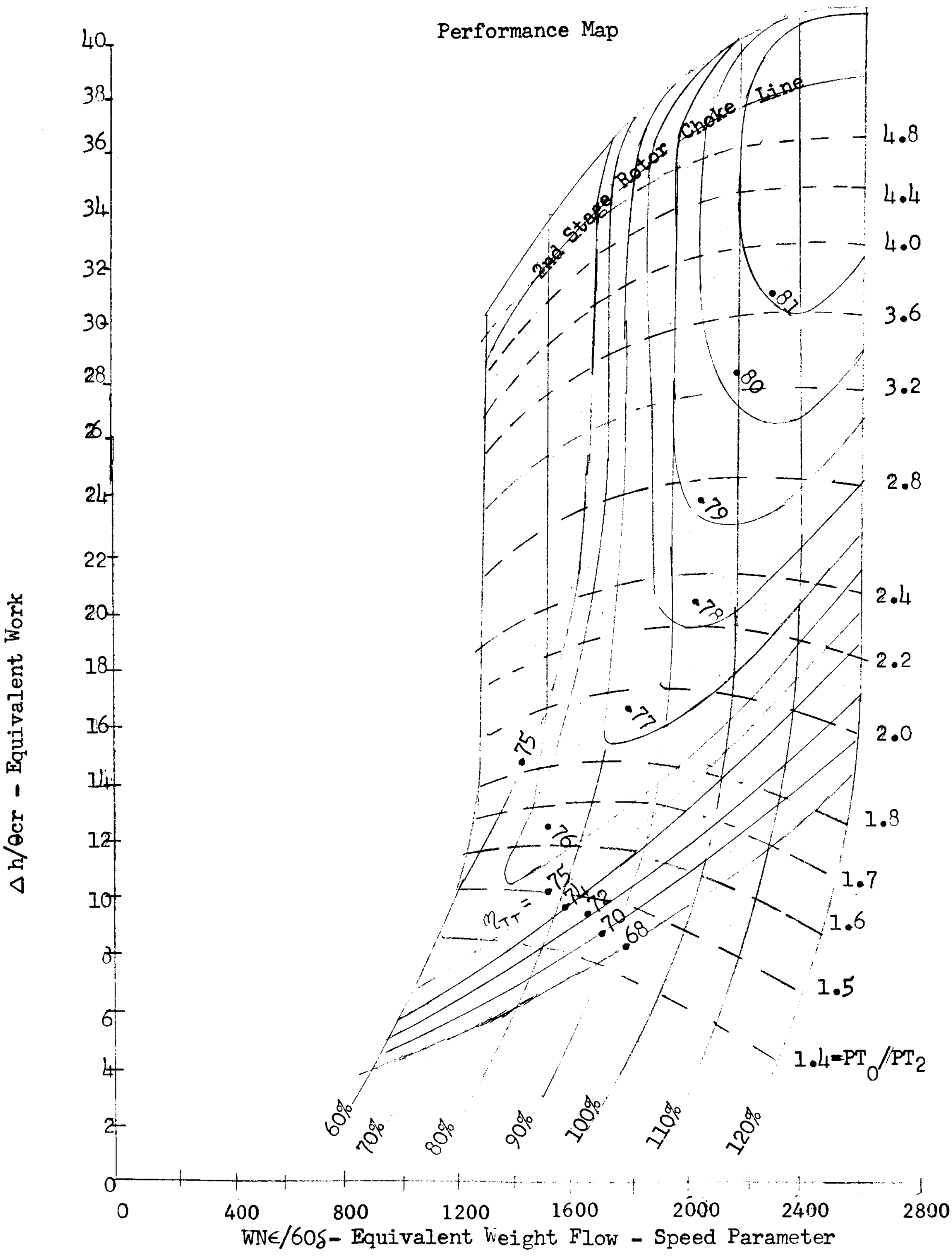

Figure 81

NASA - TASK III

Two Stage-Schedule 7.13, -9.62

Equivalent Flow vs. Pressure Ratio

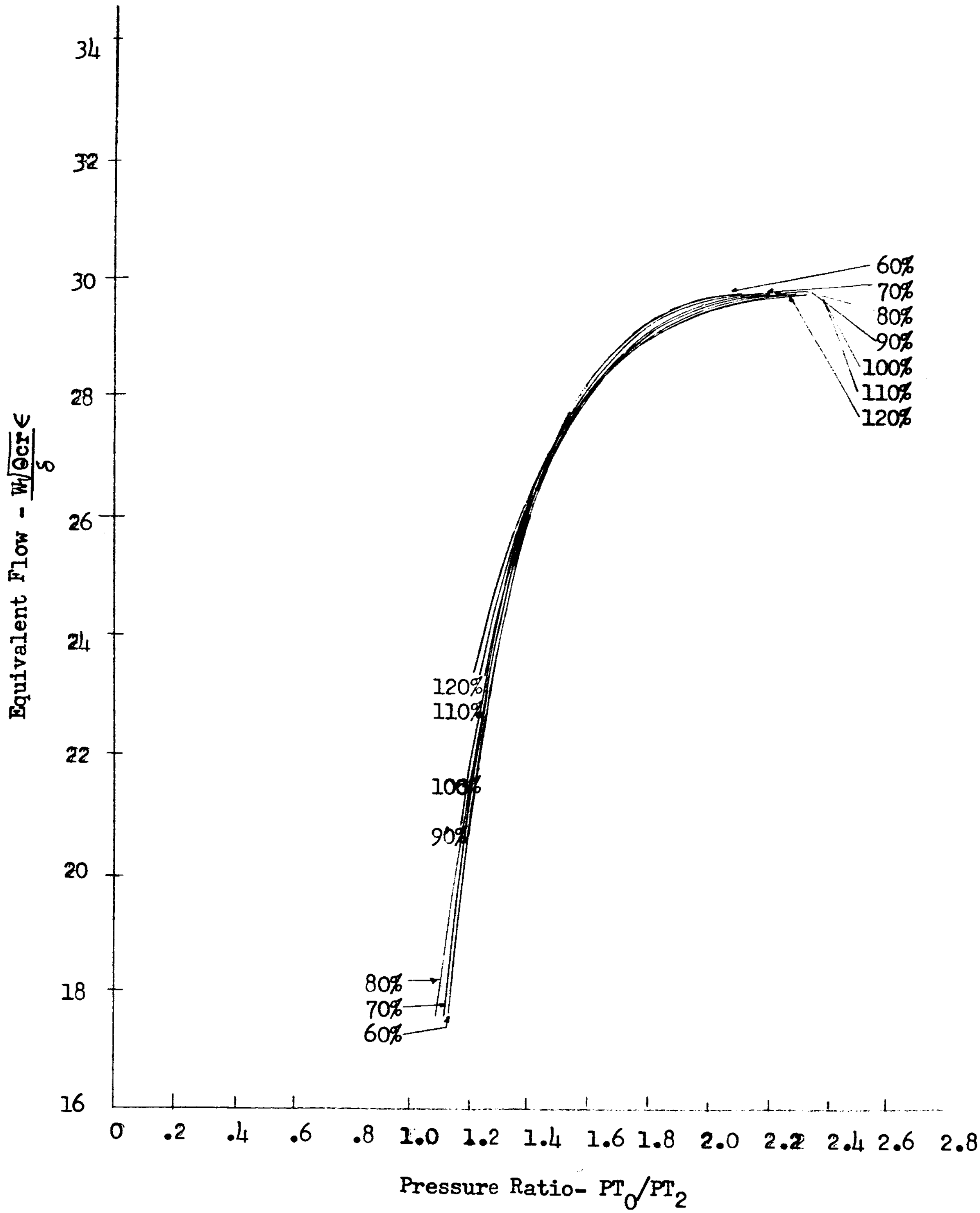

Figure 82
NASA - TASK III

Two Stage-Schedule 7.13, -9.62

Rotor 1 Incidence vs. Equivalent Work

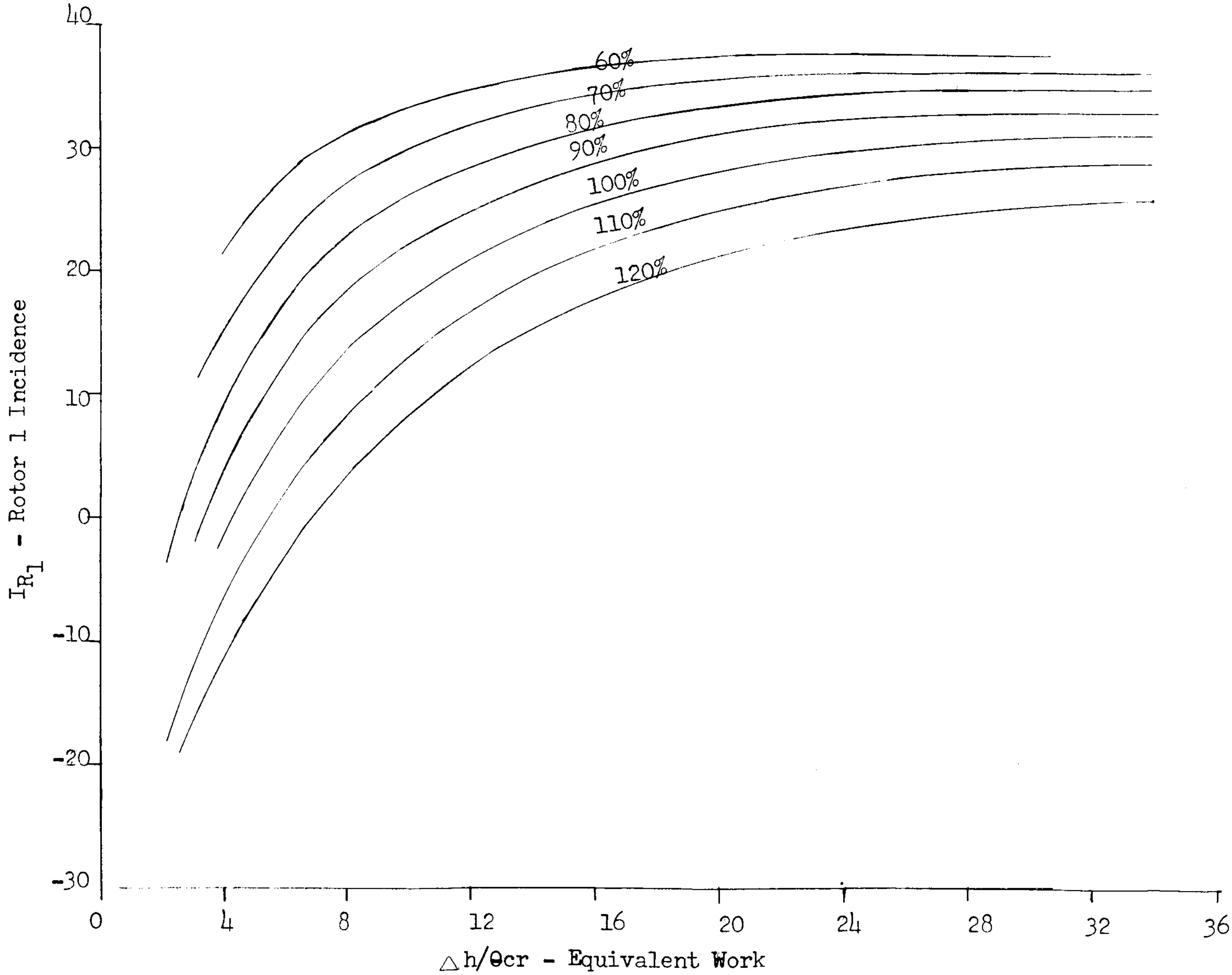

Figure 83

NASA-TASK III

Two Stage-Schedule 7.13, -9.62

Stator 2 Incidence vs. Equivalent Work

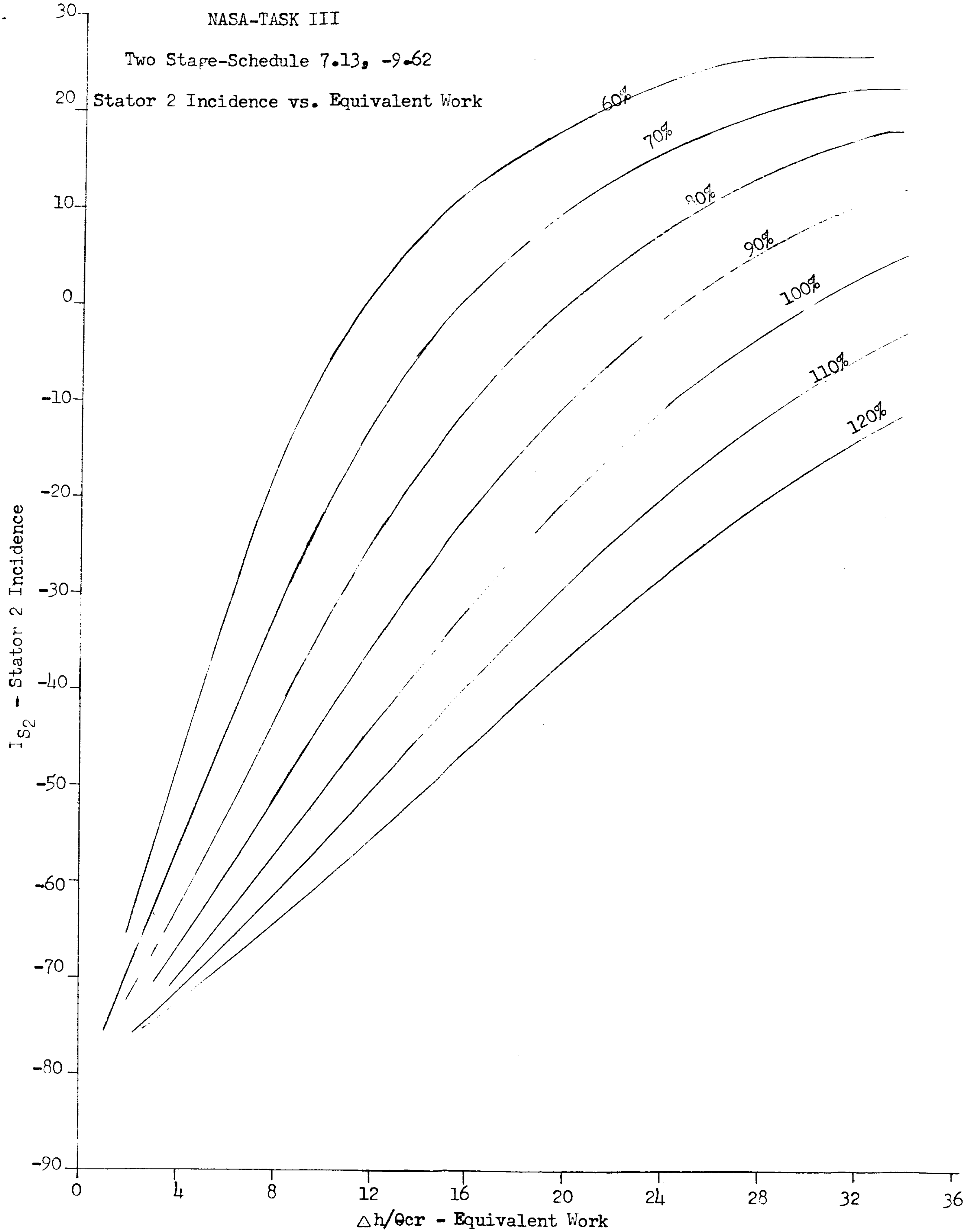

Figure 84

NASA - TASK III

Two Stage-Schedule 7.13, 9.62

Rotor 2 Incidence vs. Equivalent Work

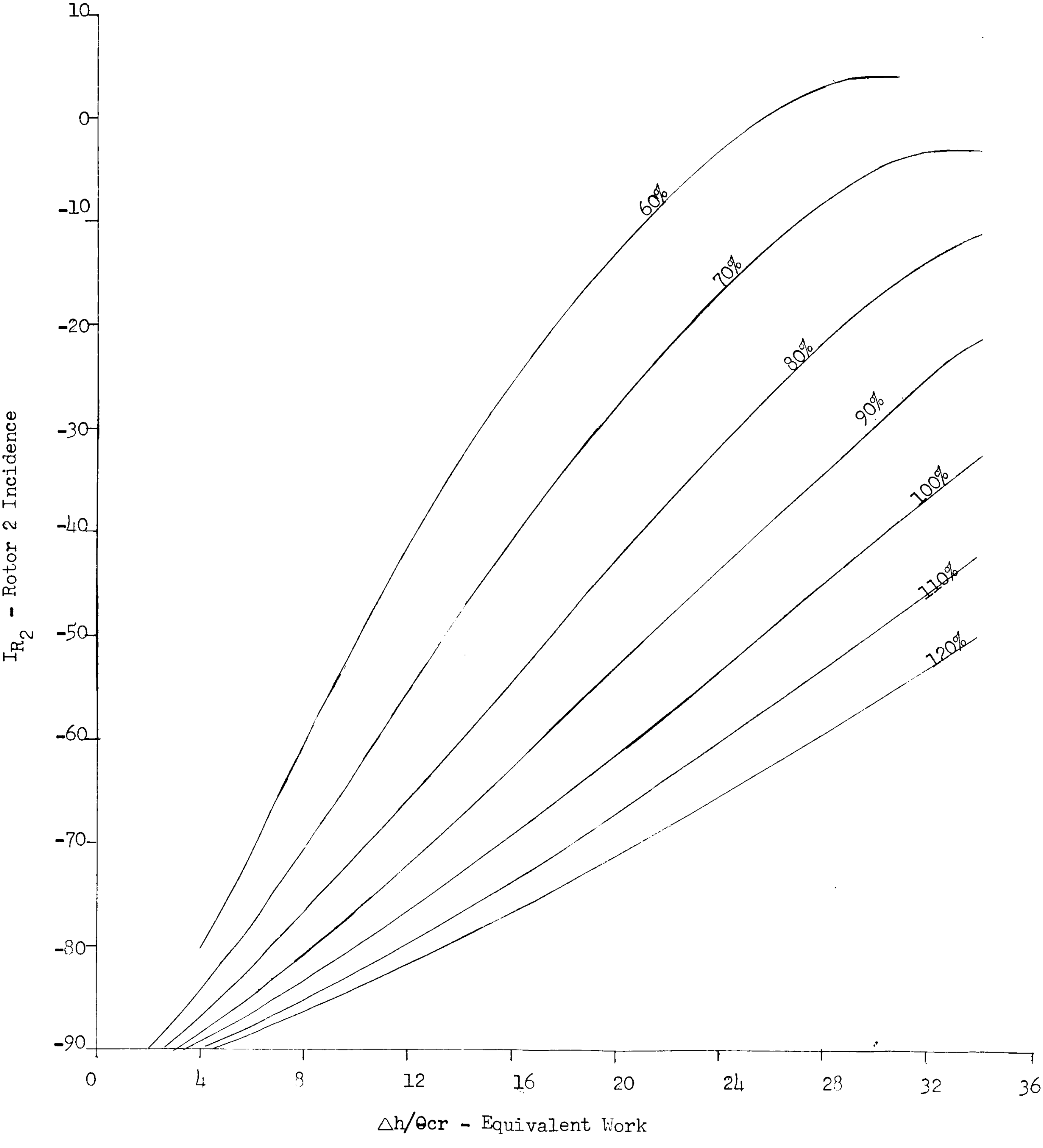

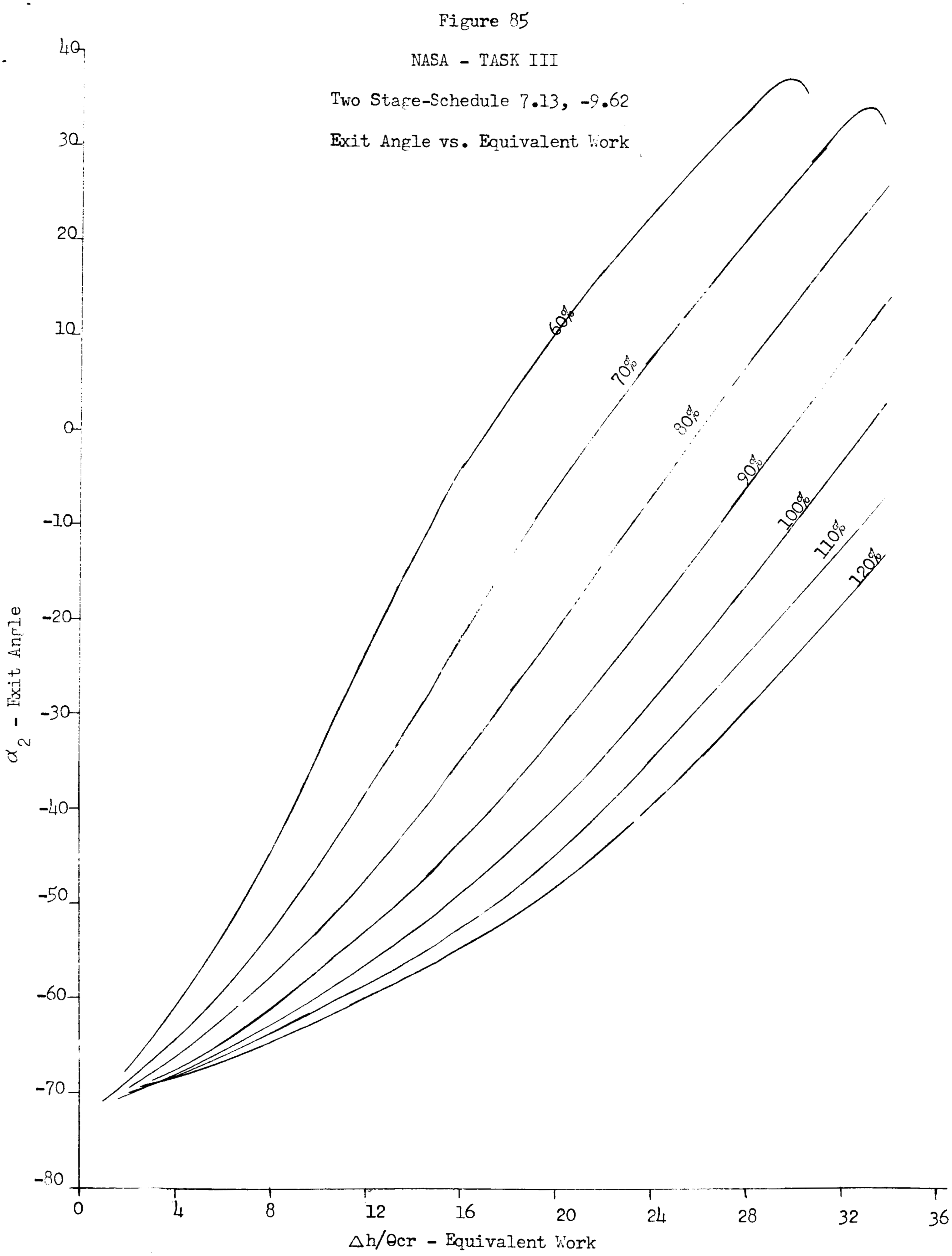
Figure 85
NASA - TASK III
Two Stage-Schedule 7.13, -9.62
Exit Angle vs. Equivalent Work
40
30
20
10
0
-10
-20
-30
-40
-50
-60
-70
-80
α_2 - Exit Angle
0
4
8
12
16
20
24
28
32
36
$\Delta h/\theta cr$ - Equivalent Work
60%
70%
80%
90%
100%
110%
120%

Figure 86

NASA - TASK III

Two Stage-Schedule 7.13, -9.62

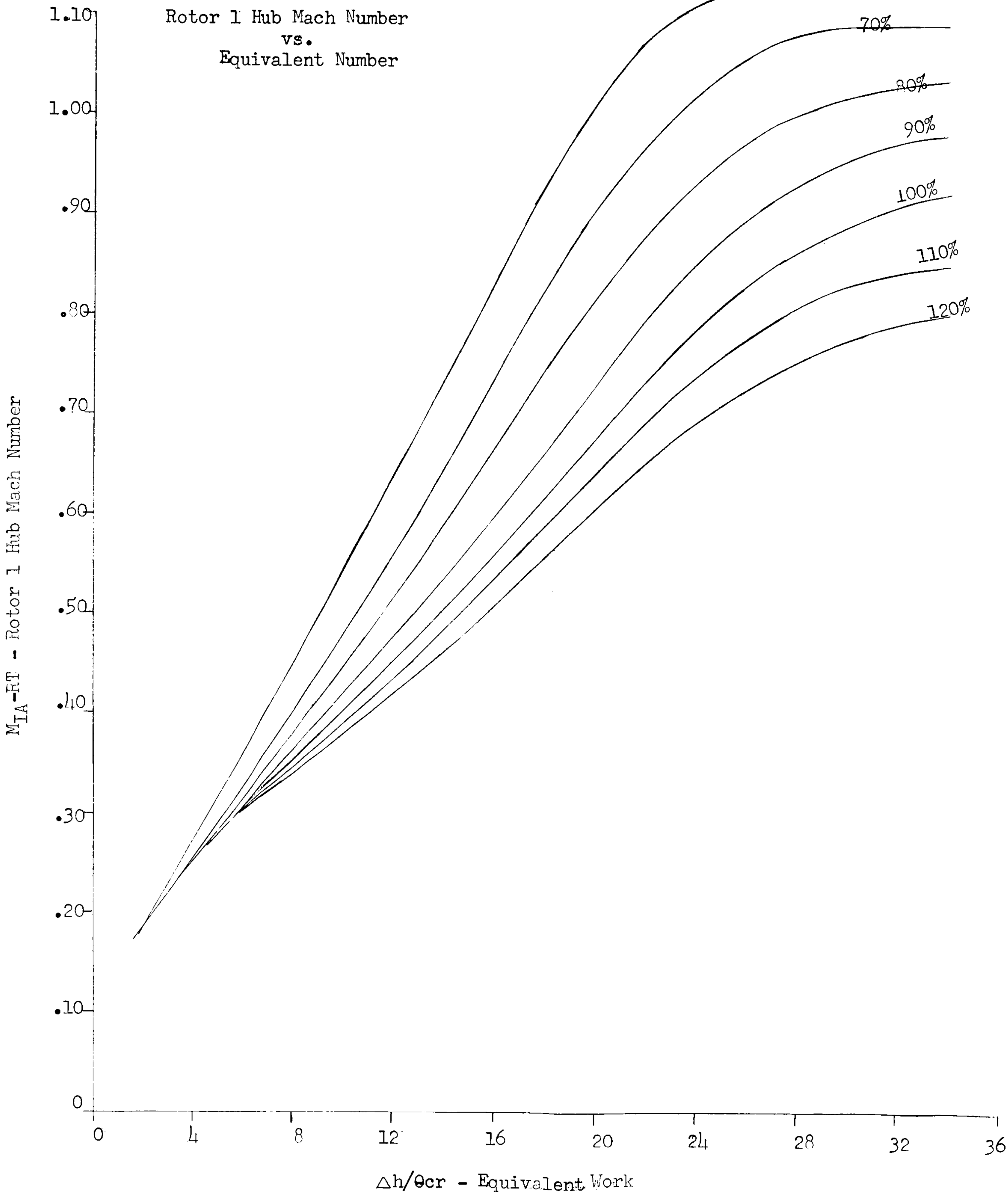

Figure 87

NASA - TASK III

Two Stage-Schedule 7.13, -9.62

Rotor 2 Hub Mach Number vs. Equivalent Work

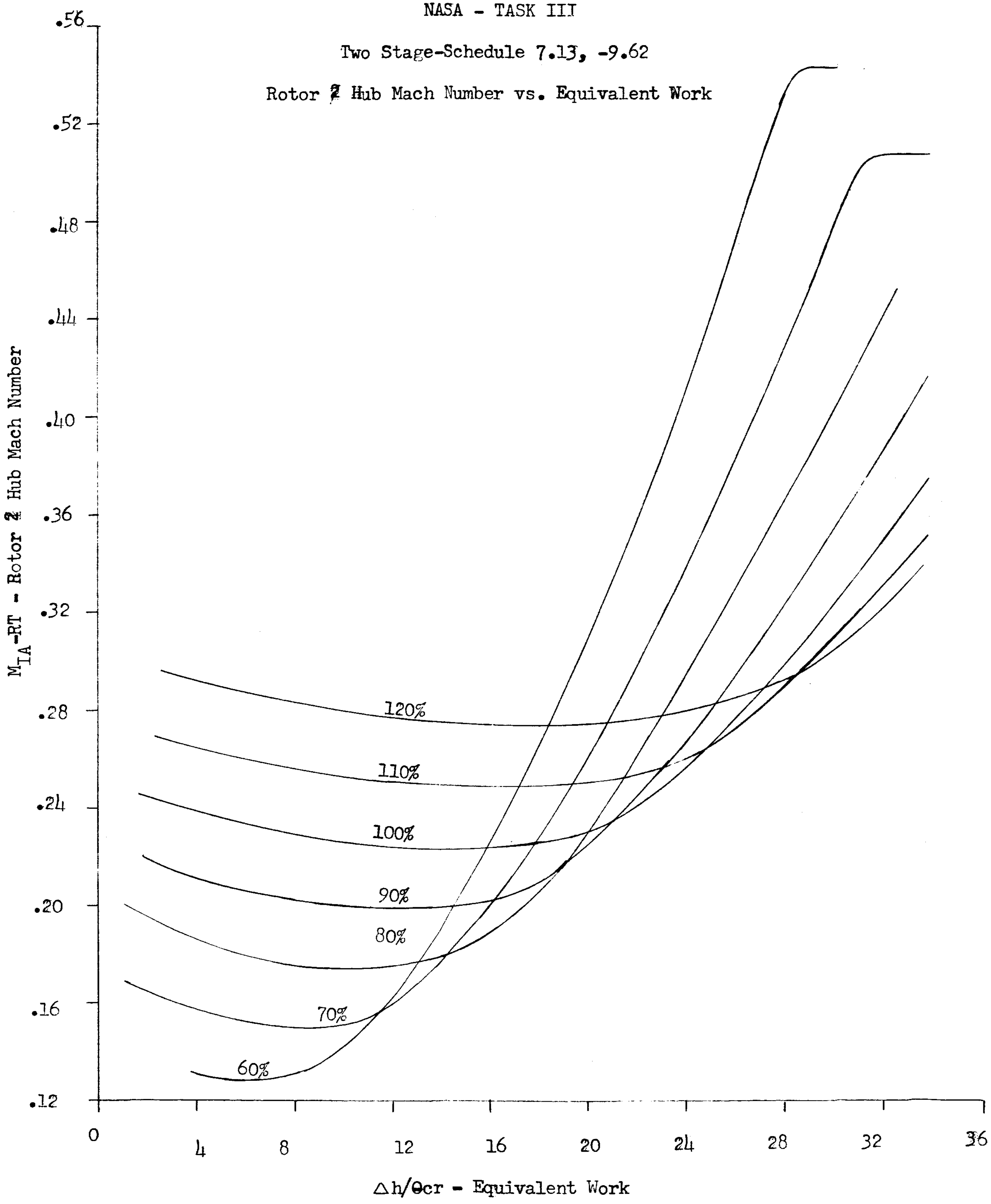

Figure 88

NASA - TASK III

Two Stage-Schedule 7.13, -9.62

Stage 1 Hub Reaction vs. Equivalent Work

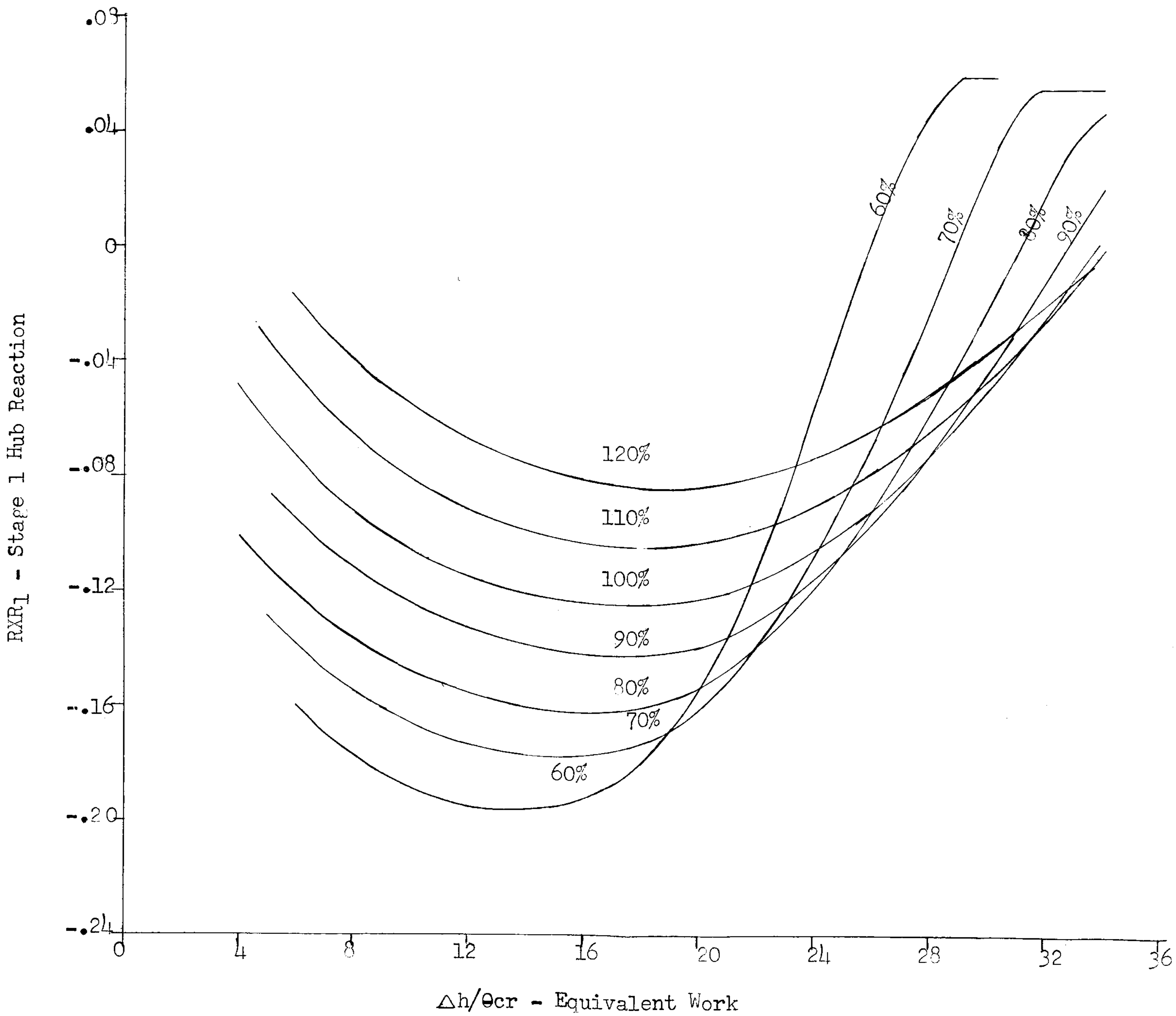

Figure 89

NASA - TASK III

Two Stage-Schedule 7113, -9,62

Stage 2 Hub Reaction vs. Equivalent Work

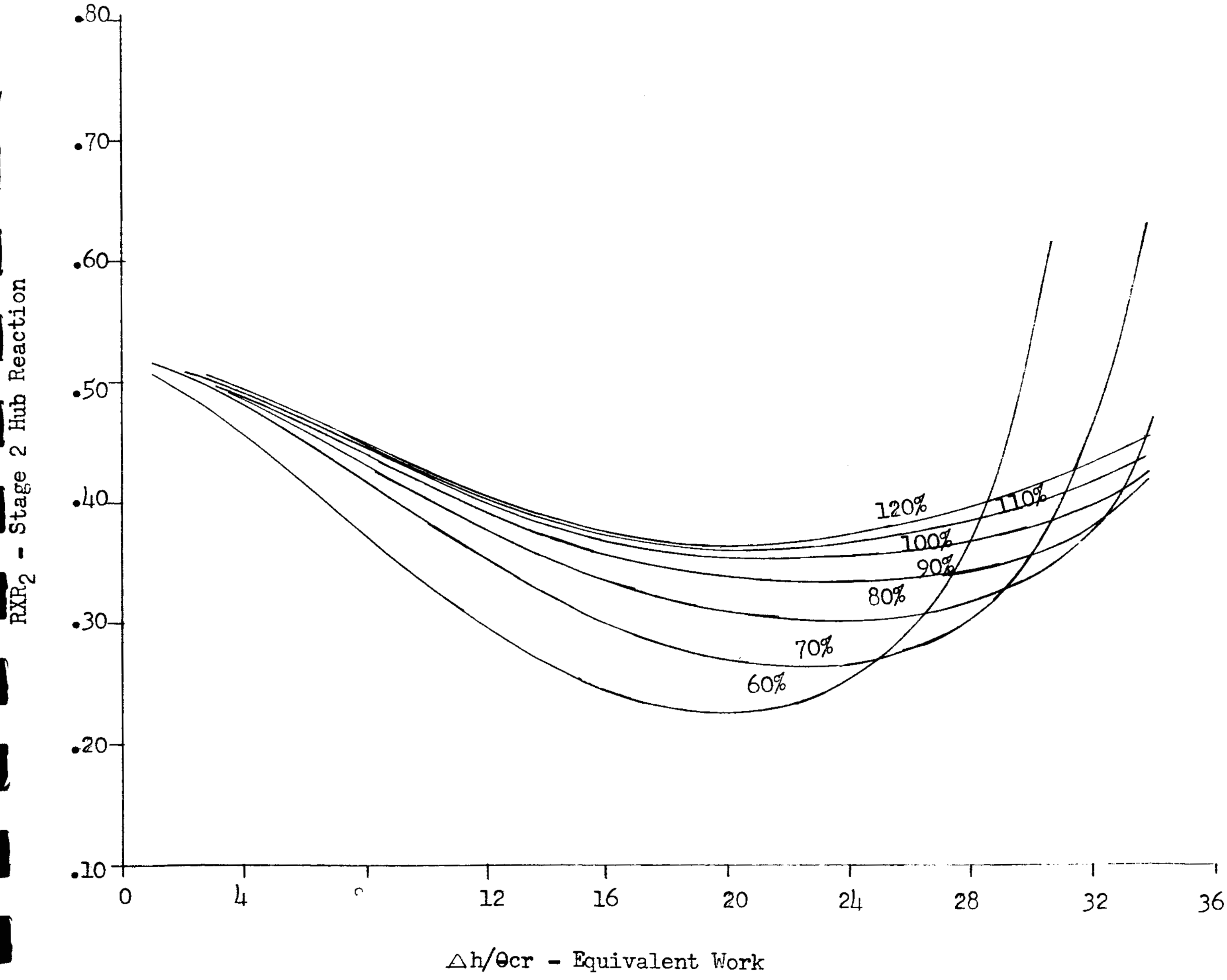

Figure 90

NASA - TASK III

Two Stage Schedule 0.0, 8.81

Performance Map

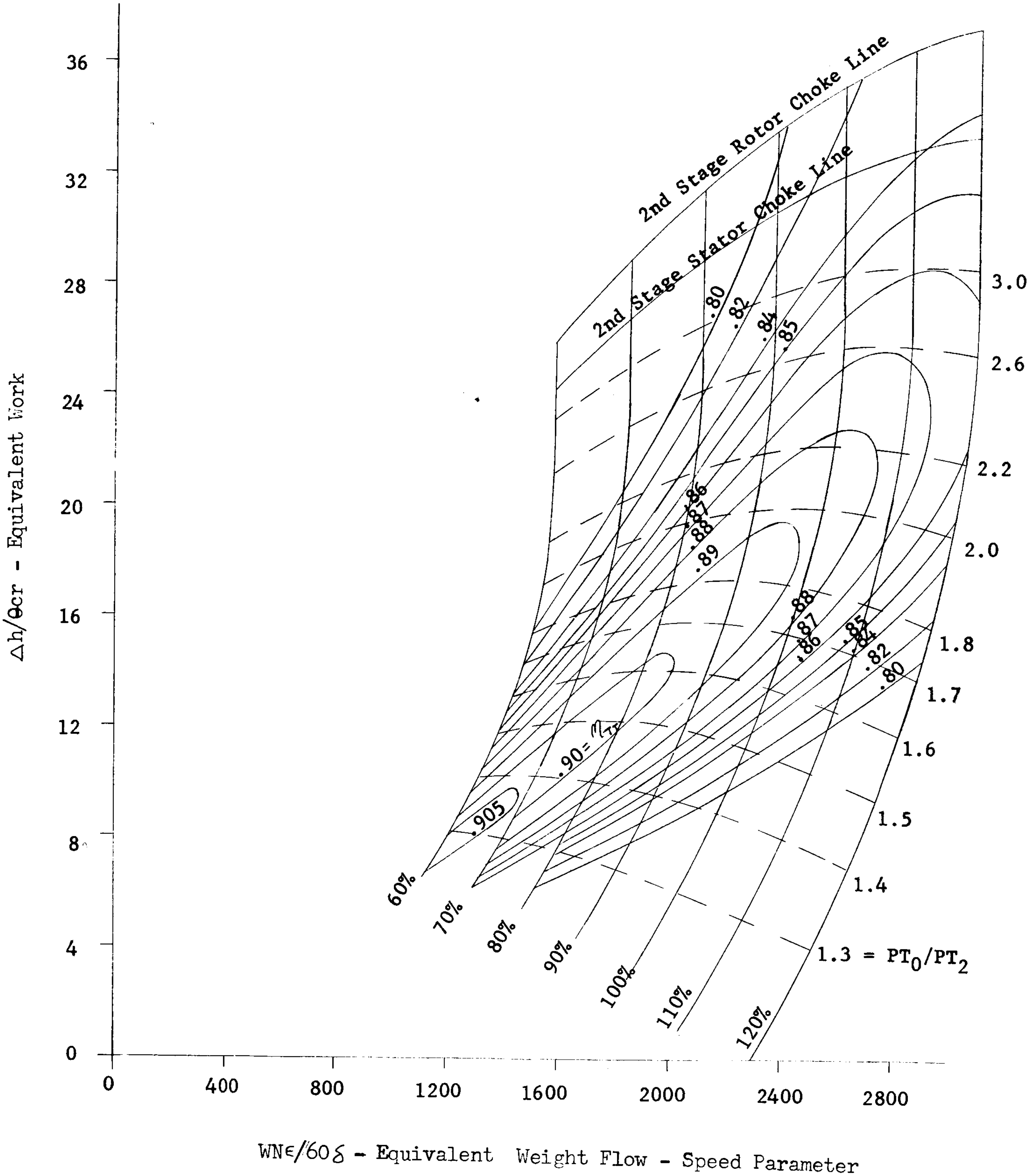

Figure 91

NASA - TASK III

Two Stage-Schedule 0.0, 8.81

Equivalent Flow vs. Pressure Ratio

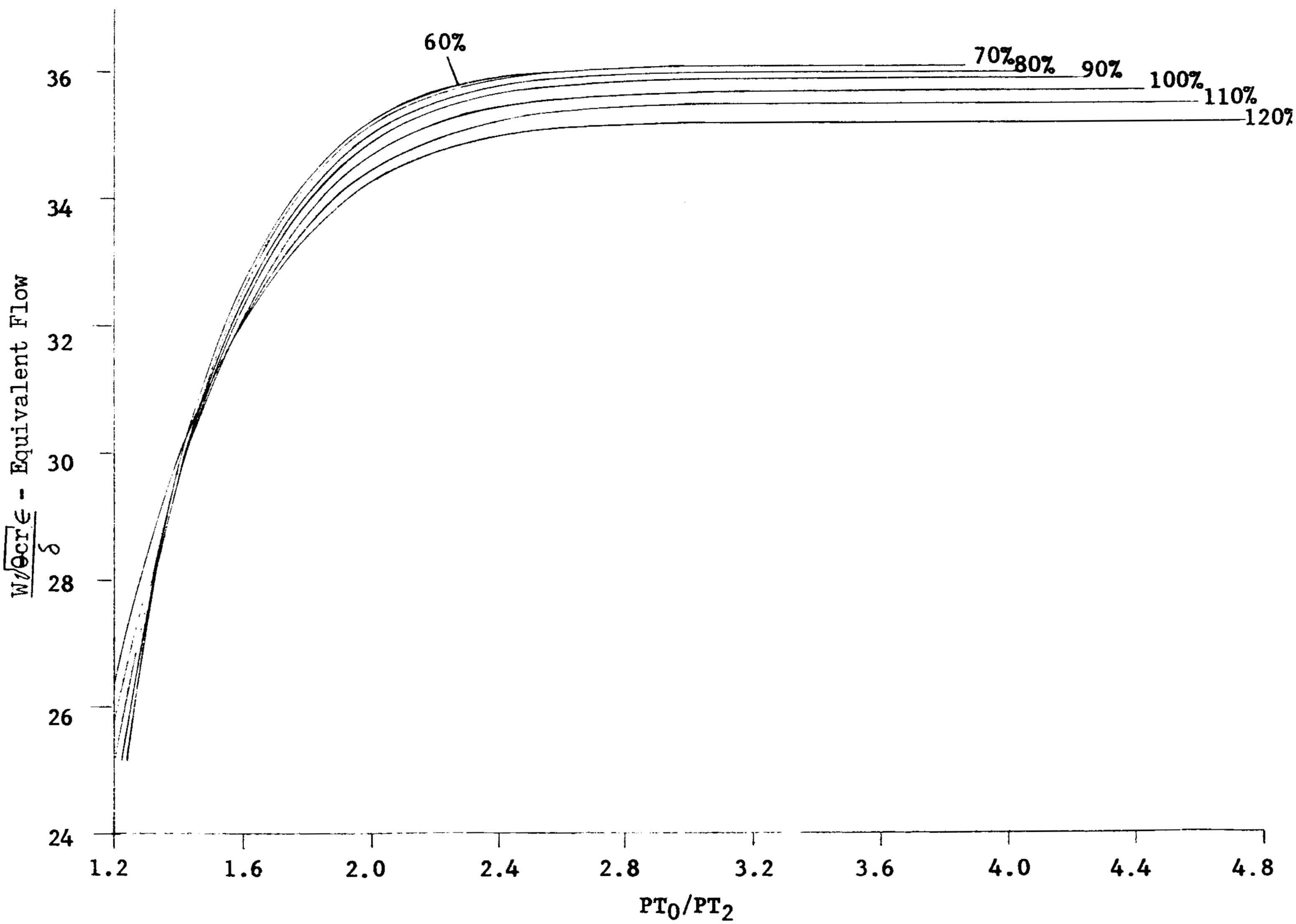

Figure 92

NASA - TASK III

Two Stage-Schedule 0.0, 8.81

Rotor 1 Incidence vs. Equivalent Work

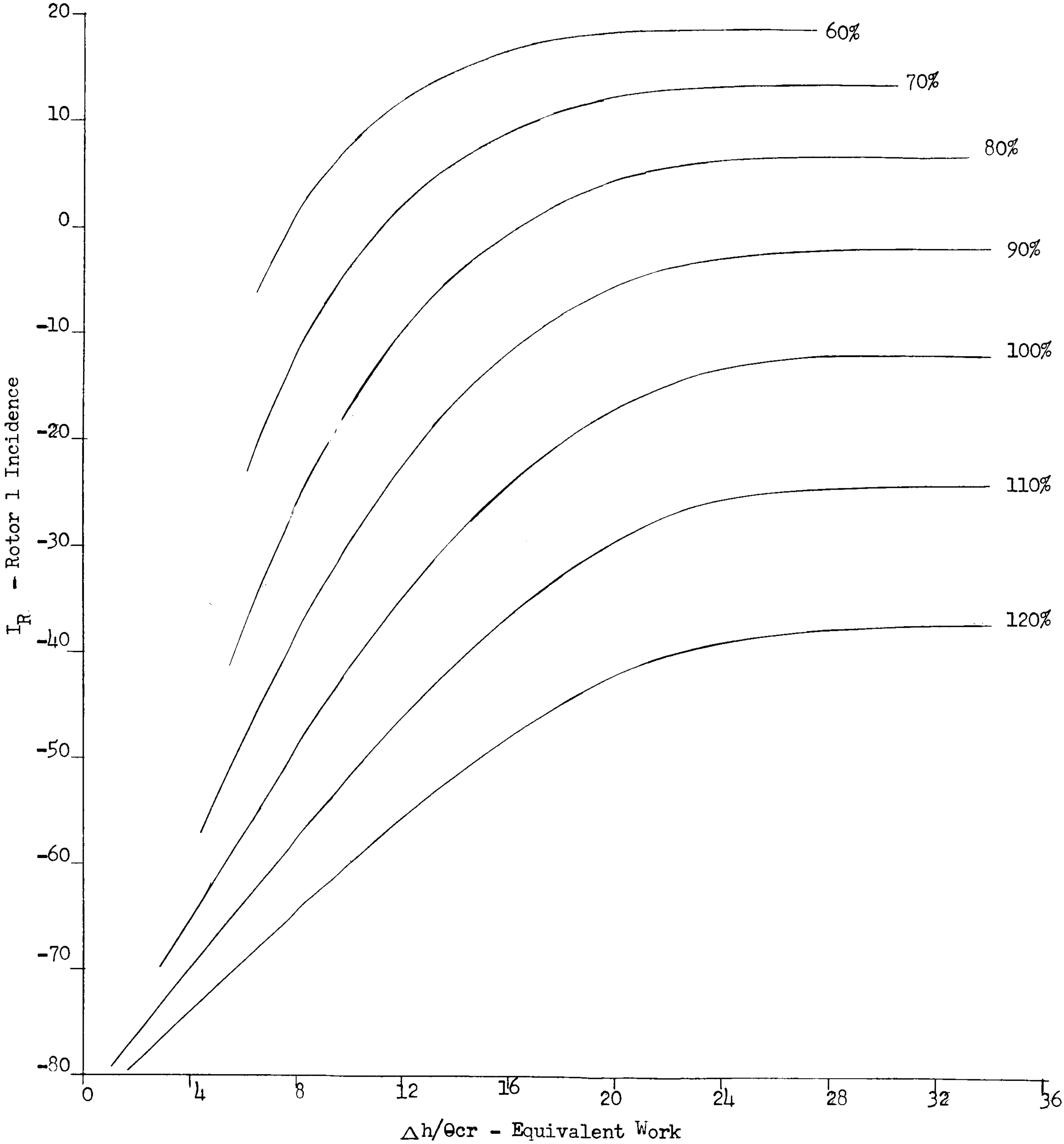

Figure 93

NASA - TASK III

Two Stage-Schedule 0.0, 8.81

Stator 2 Incidence vs. Equivalent Work

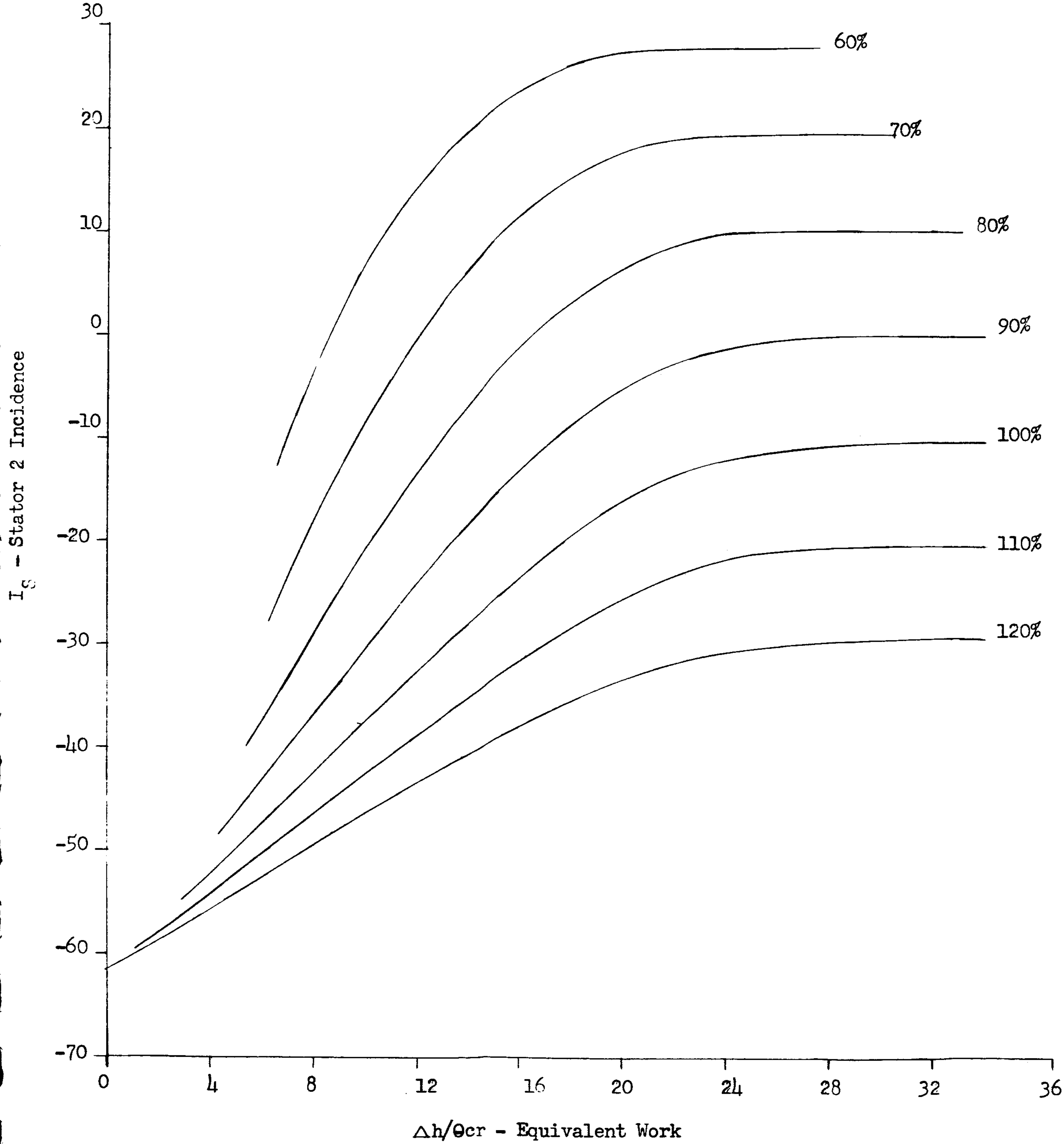

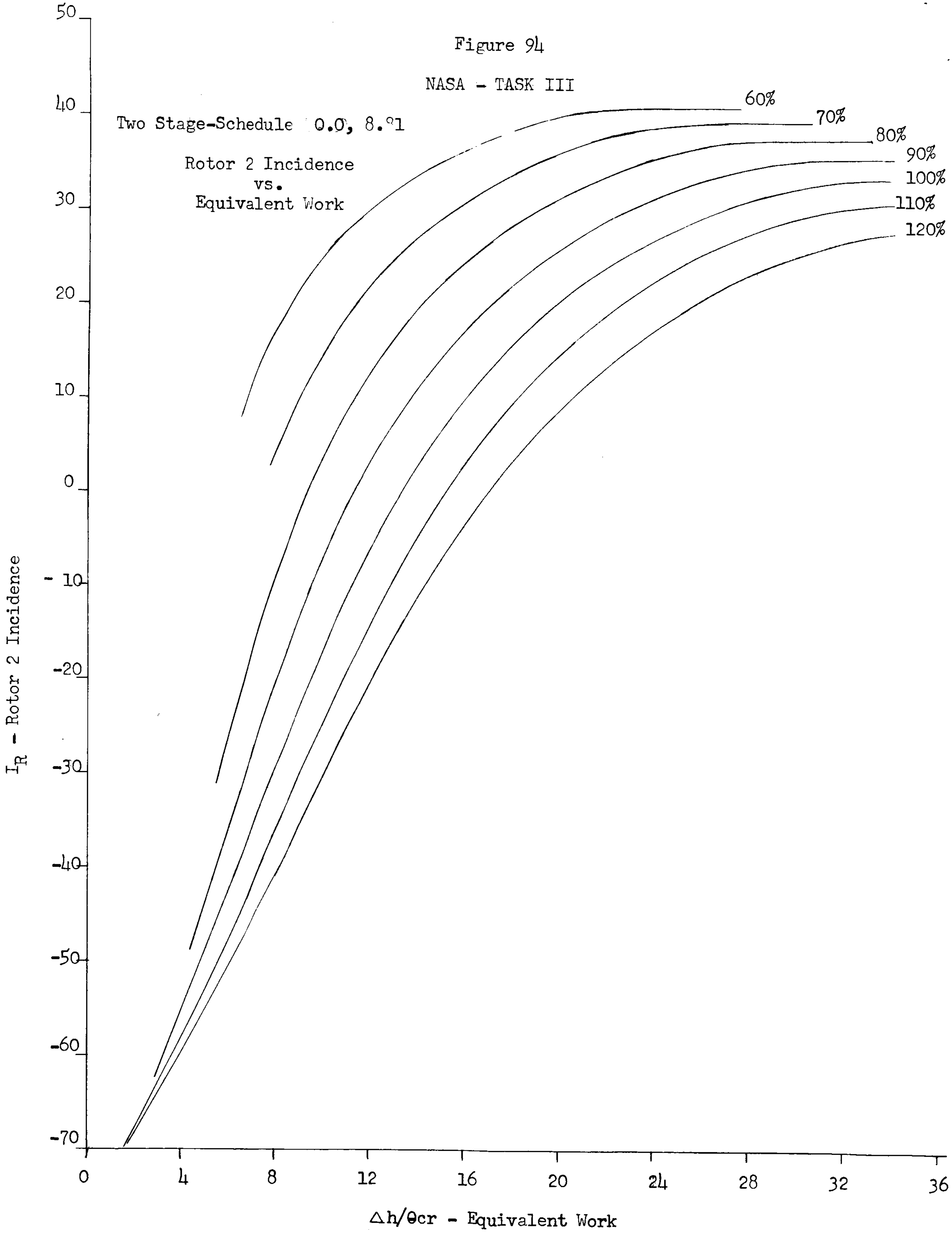

Figure 94
NASA - TASK III
Two Stage-Schedule 0.0, 8.91
Rotor 2 Incidence
vs.
Equivalent Work
60%
70%
80%
90%
100%
110%
120%
50
40
30
20
10
0
- 10
-20
-30
-40
-50
-60
-70
0
4
8
12
16
20
24
28
32
36
I_R - Rotor 2 Incidence
$\Delta h/\theta cr$ - Equivalent Work

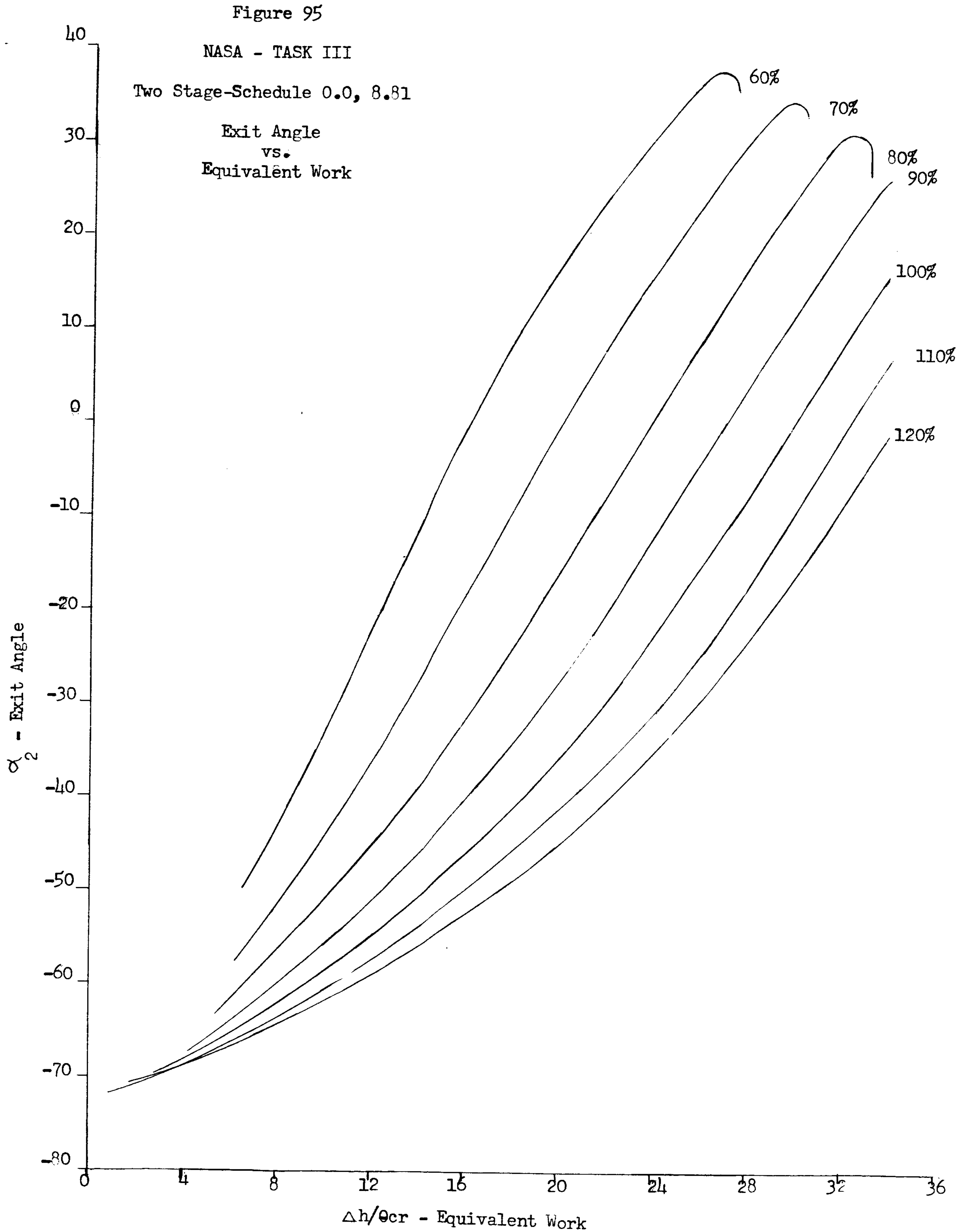
Figure 95
NASA - TASK III
Two Stage-Schedule 0.0, 8.81
Exit Angle
vs.
Equivalent Work
60%
70%
80%
90%
100%
110%
120%
40
30
20
10
0
-10
-20
-30
-40
-50
-60
-70
-80
0
4
8
12
16
20
24
28
32
36
α_2 - Exit Angle
$\Delta h/\theta cr$ - Equivalent Work

Figure 96

NASA - TASK III

Two Stage-Schedule 0.0, 8.81

Rotor 1 Hub Mach Number vs. Equilavent Work

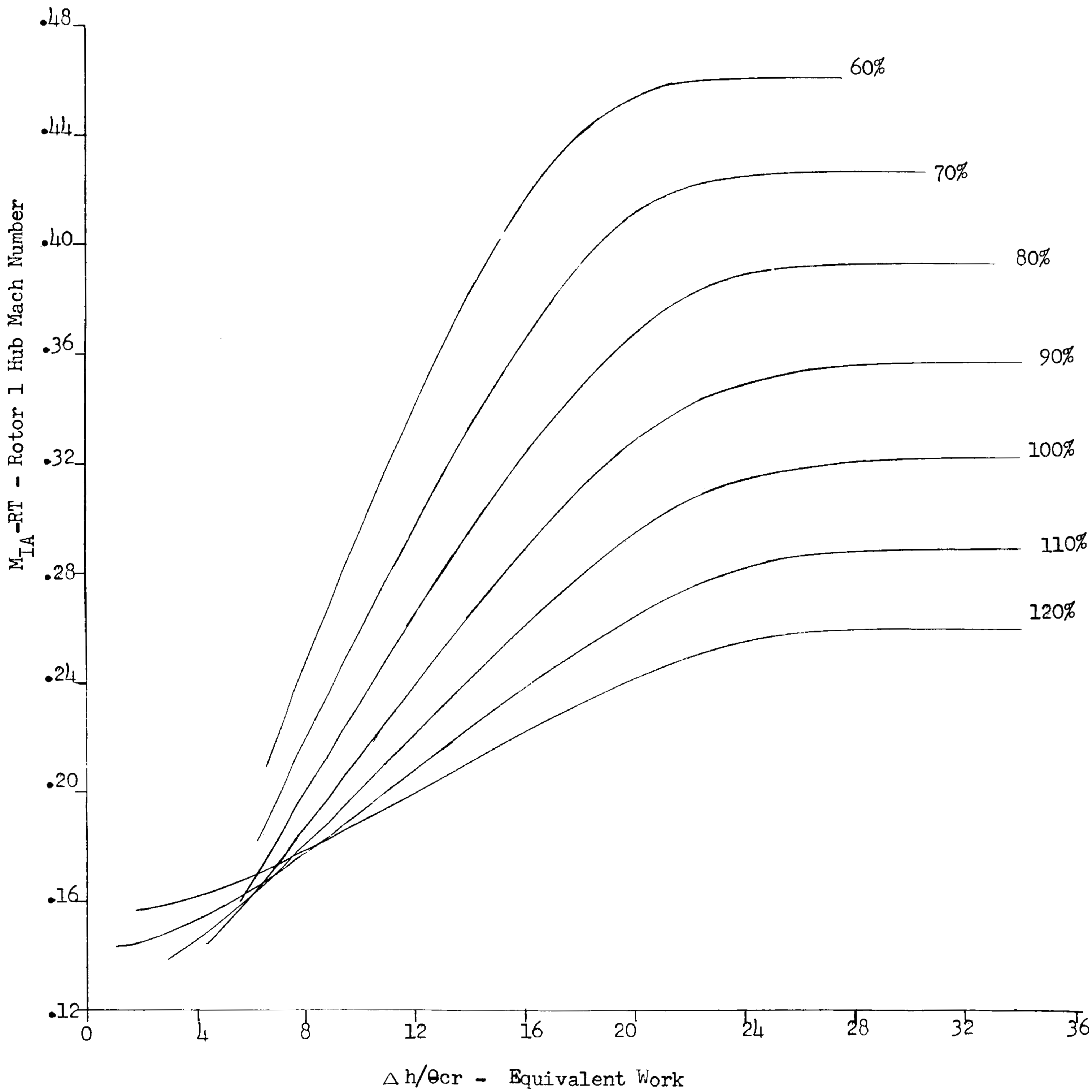

Figure 97

NASA - TASK III

Two Stage-Schedule 0.0, 8.81

Rotor 2 Hub Mach Number
vs.
Equivalent Work

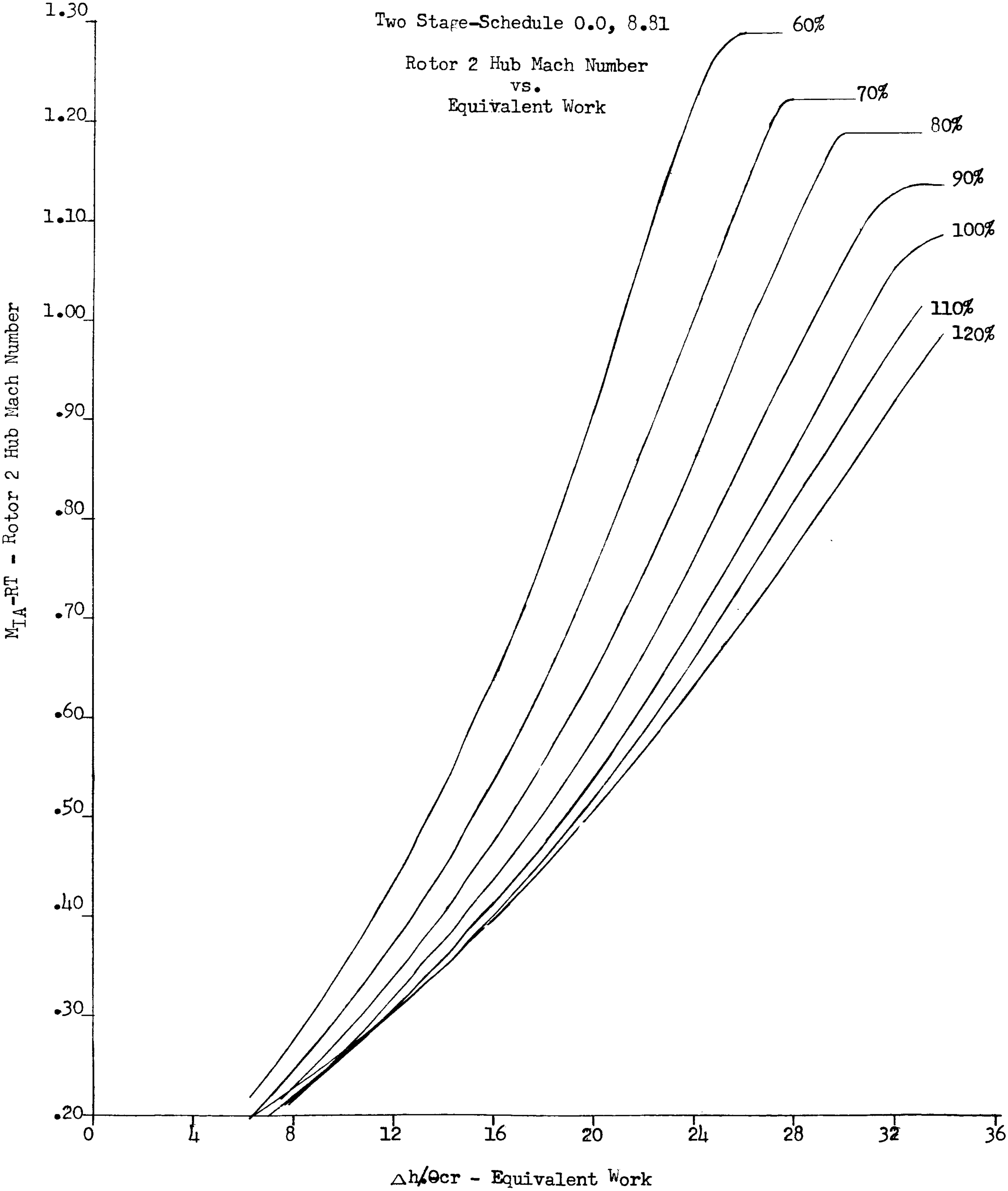

Figure 98

NASA - TASK III

Two Stage Schedule 0.0, 8.81

Stage 1 Hub Reaction vs. Equivalent Work

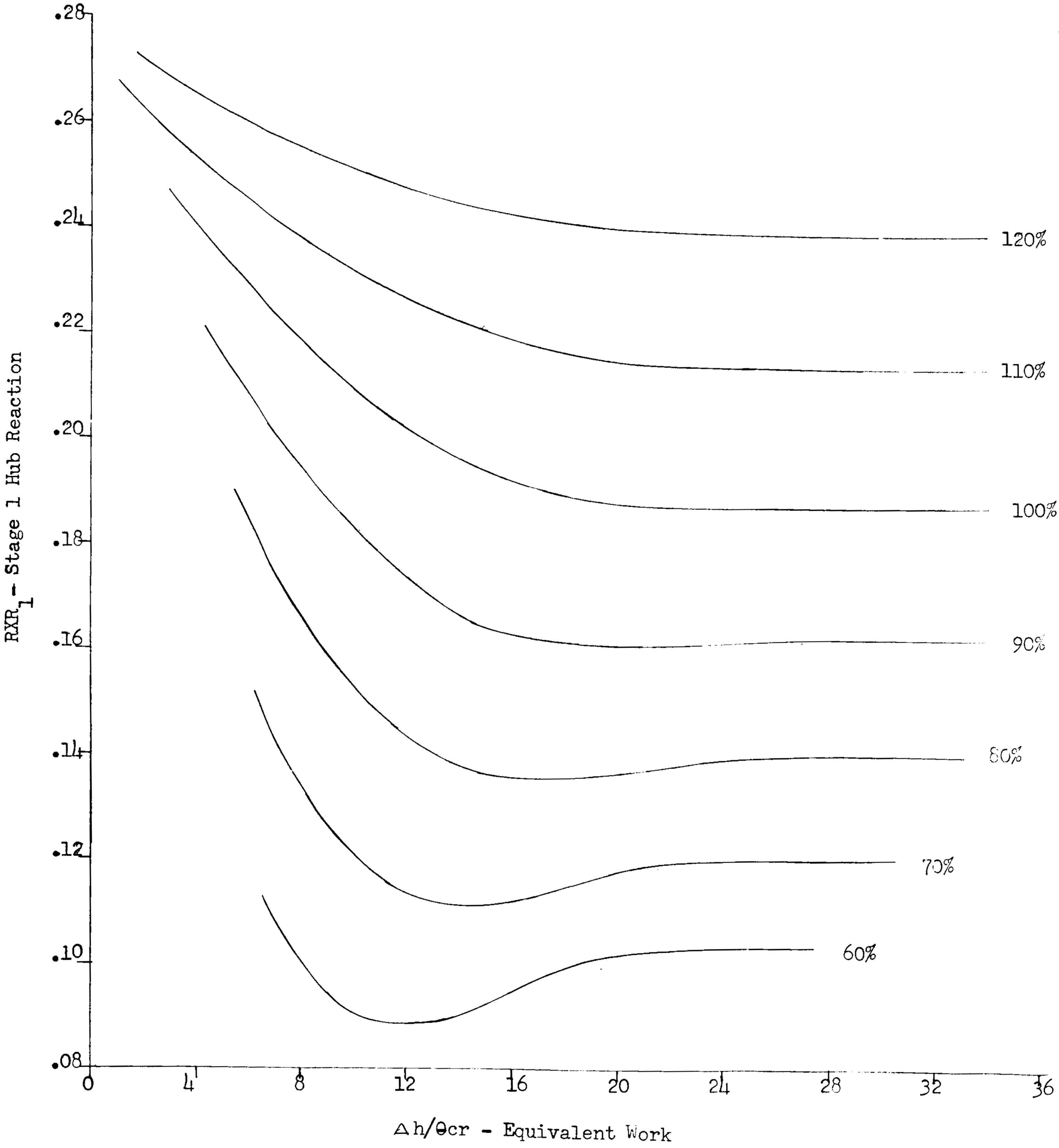

Figure 99

NASA - TASK III

Two Stage-Schedule 0.0, 8.81

Stage 2 Hub Reaction vs. Equivalent Work

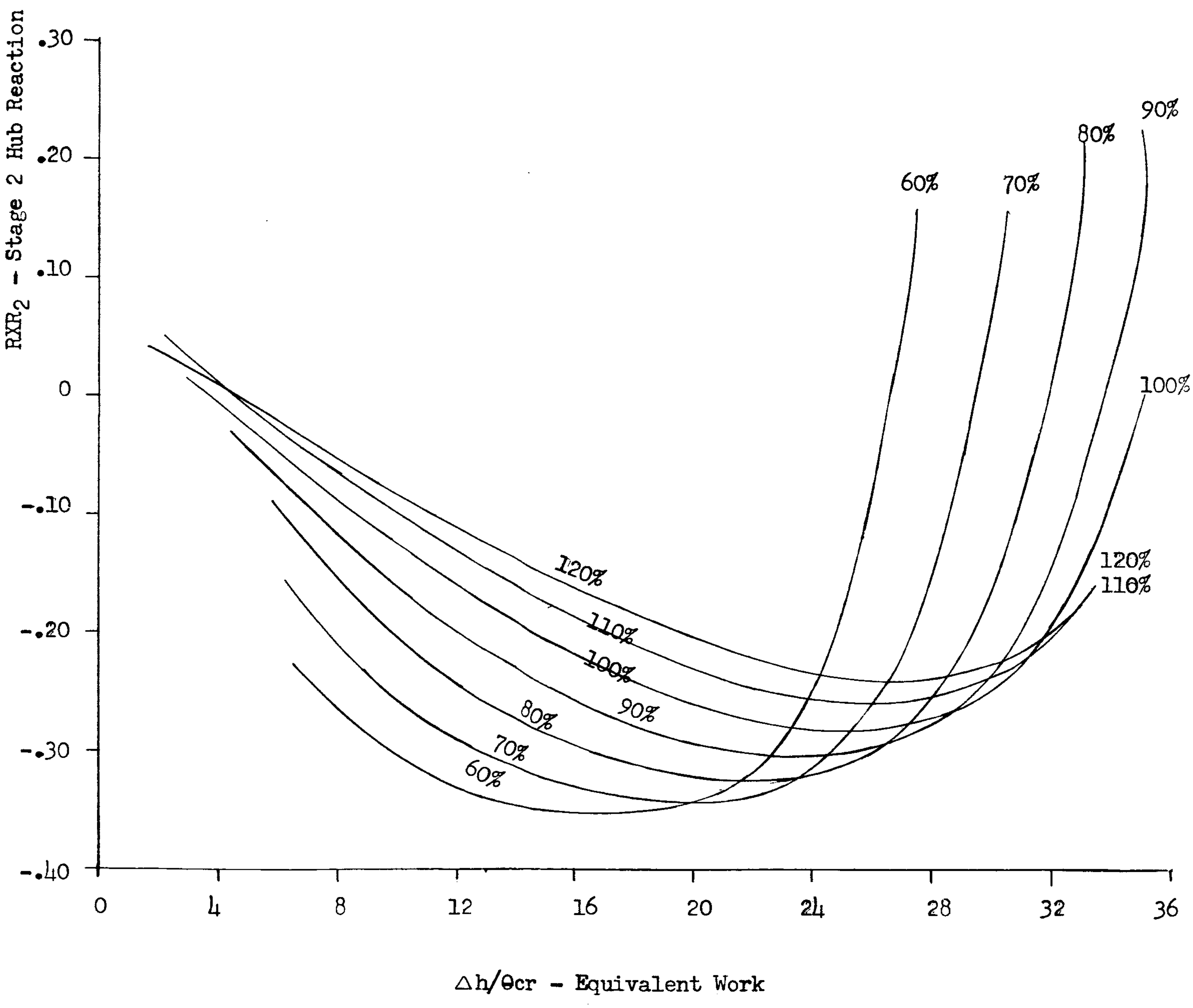

Figure 100

NASA - TASK III

Two Stage-Schedule -7.53, 8.81

Performance Map

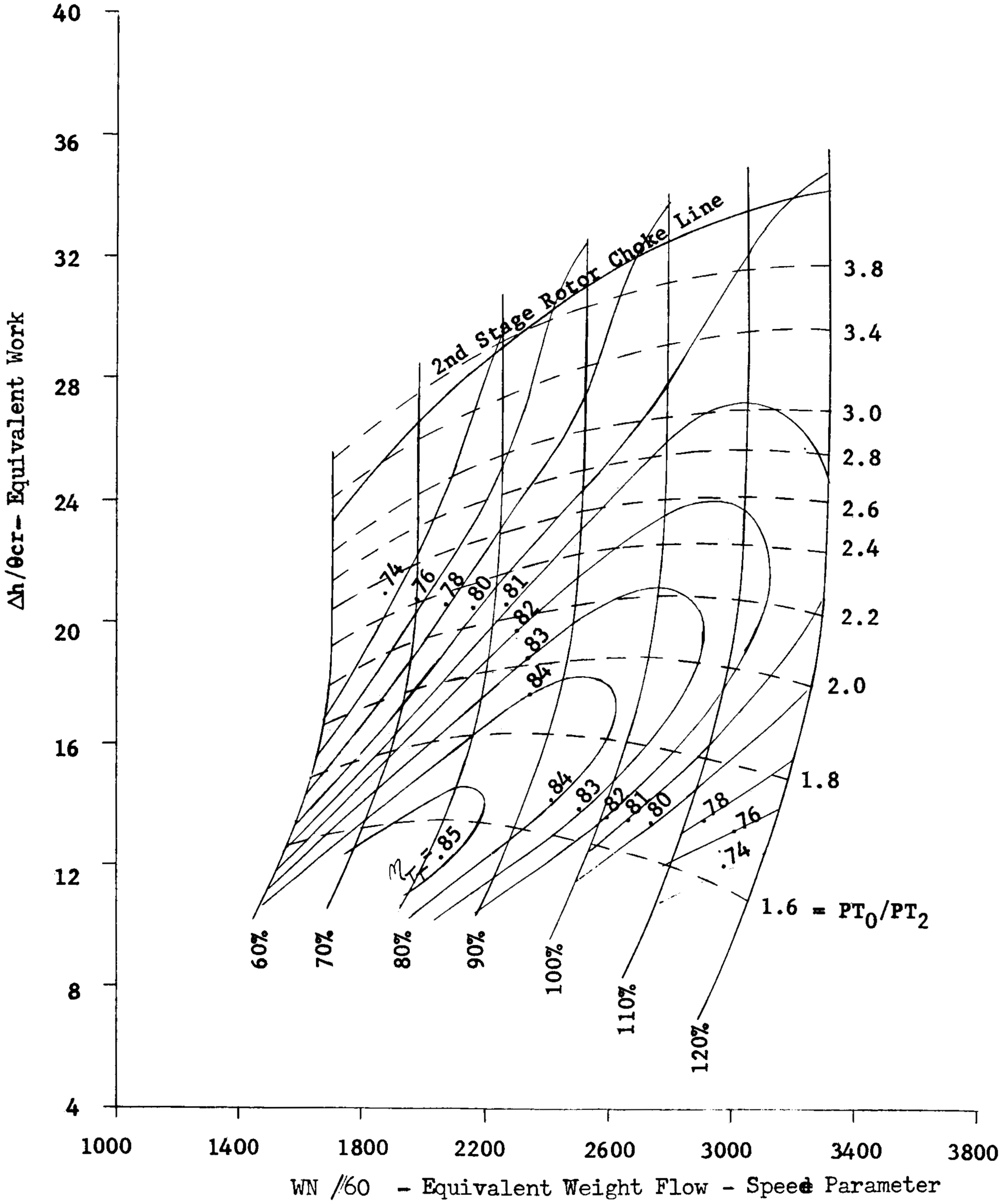

Figure 101

NASA - TASK III

Two Stage-Schedule -7.53, 8.81

Equivalent Flow vs. Pressure Ratio

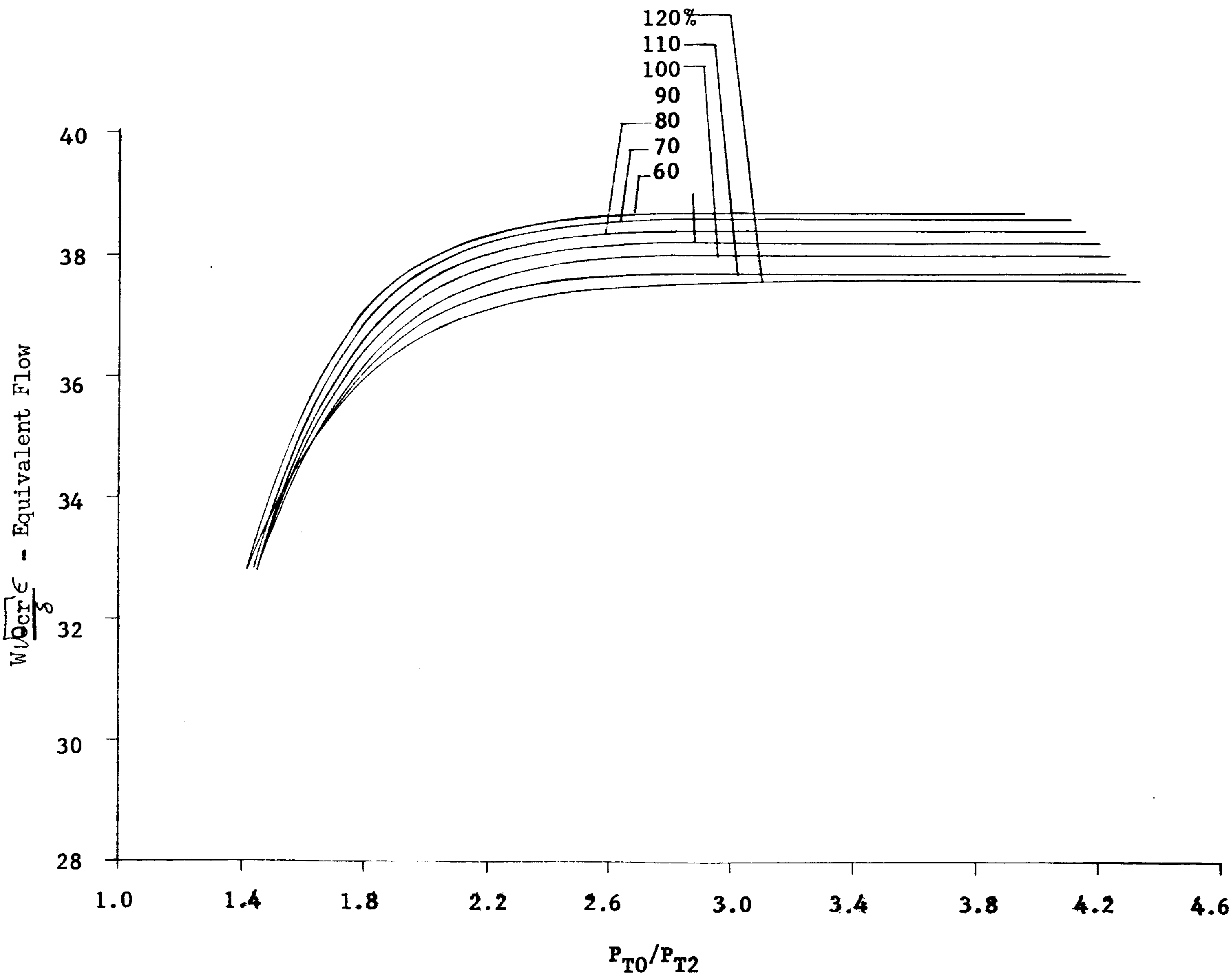

Figure 102

NASA - TASK III

Two Stage-Schedule -7.53, 8.81

Rotor 1 Incidence vs. Equivalent Work

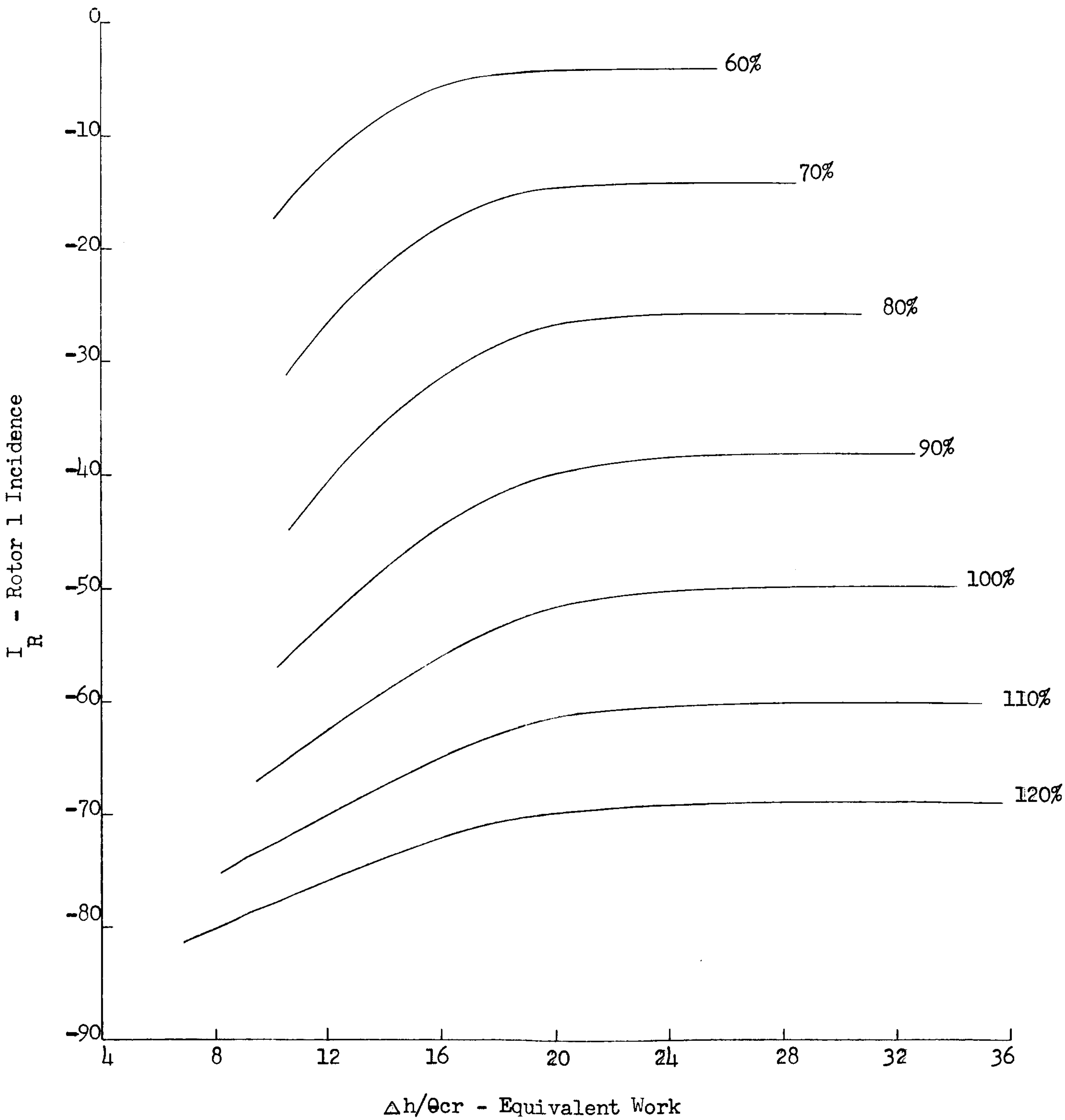

Figure 103

NASA - TASK III

Two Stage Schedule -7.53, 8.81

Stator 2 Incidence vs. Equivalent Work

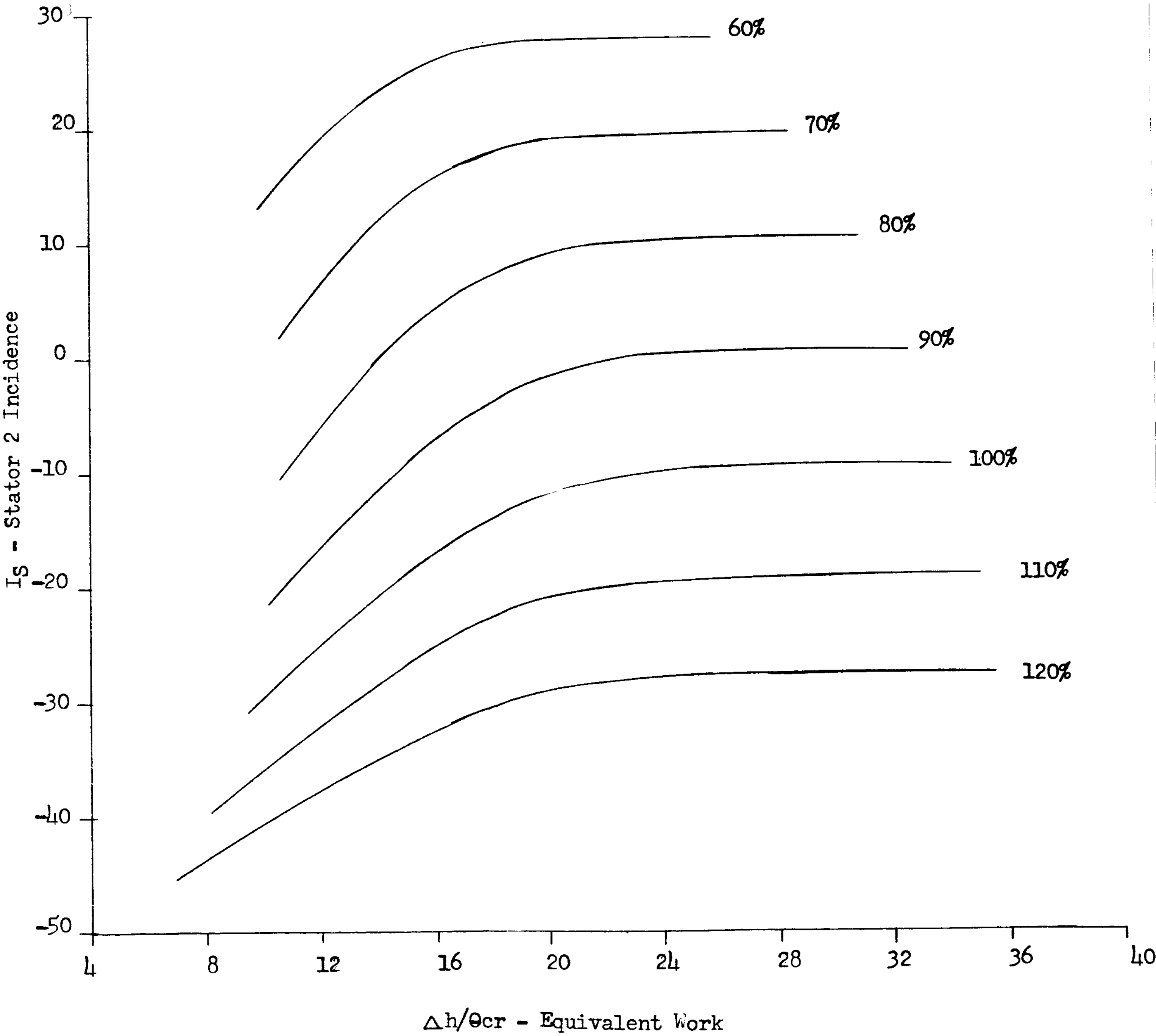

Figure 104

NASA - TASK III

Two Stage-Schedule -7.53, 8.81

Rotor 2 Incidence vs. Equivalent Work

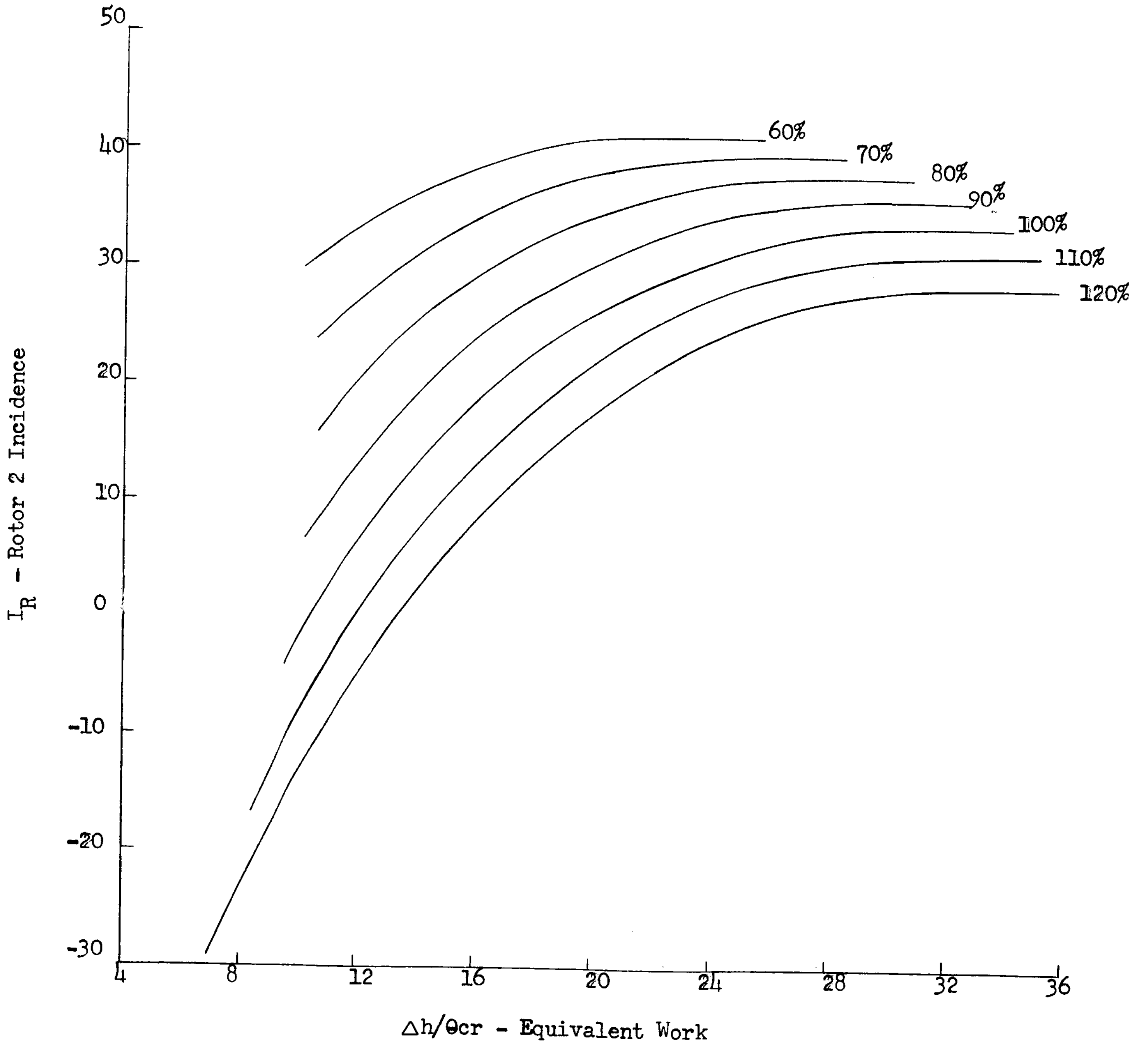

Figure 105

NASA - TASK III

Two Stage-Schedule -7.53, 8.81

Exit Angle vs. Equivalent Work

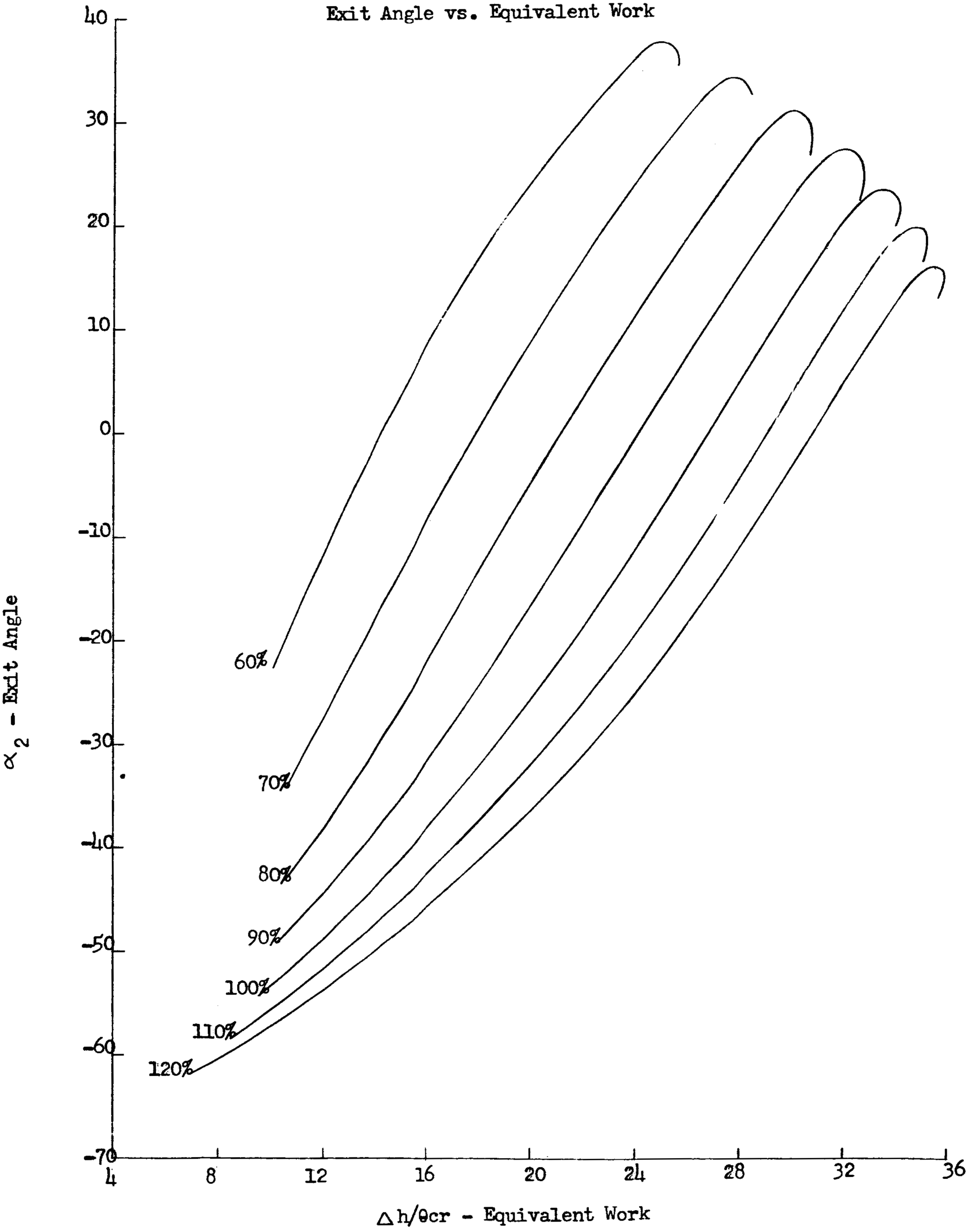

Figure 106

NASA - TASK III

Two Stage-Schedule -7.53, 8.81

Rotor 1 Hub Mach Number vs. Equivalent Work

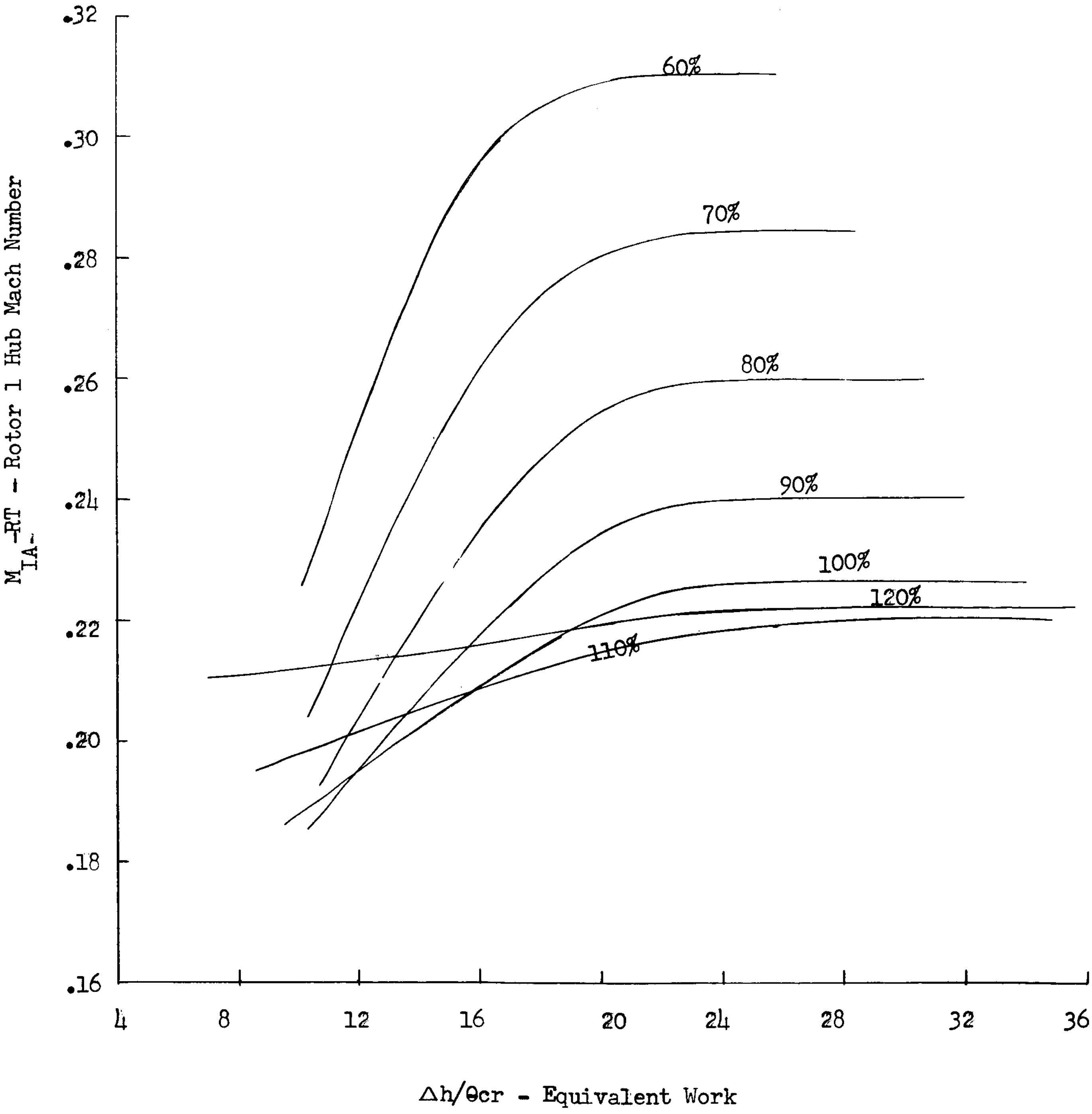

Figure 107

NASA - TASK III

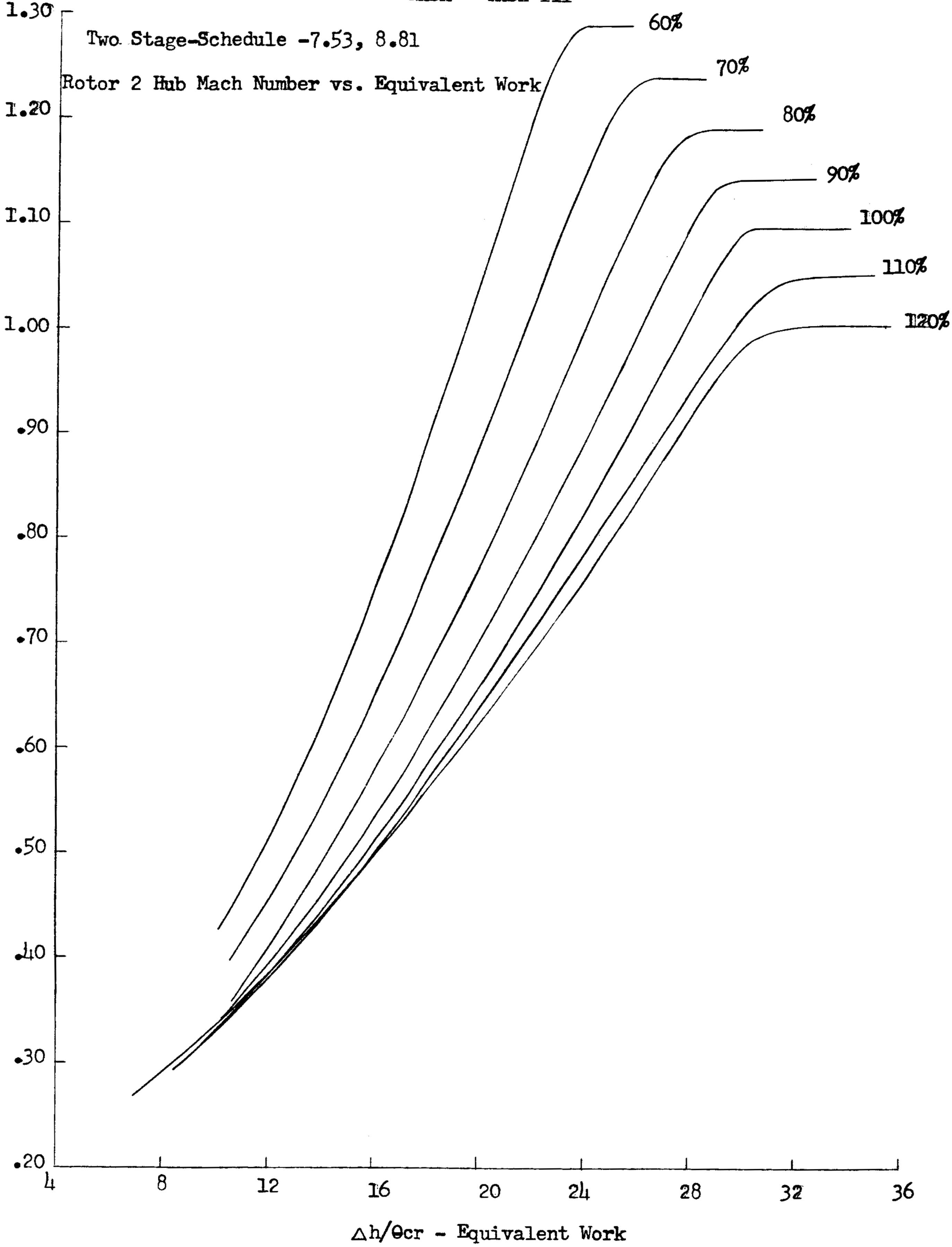

Figure 108

Two Stage-Schedule -7.53, 8.81

NASA - TASK III

Stage 1 Hub Reaction vs. Equivalent Work

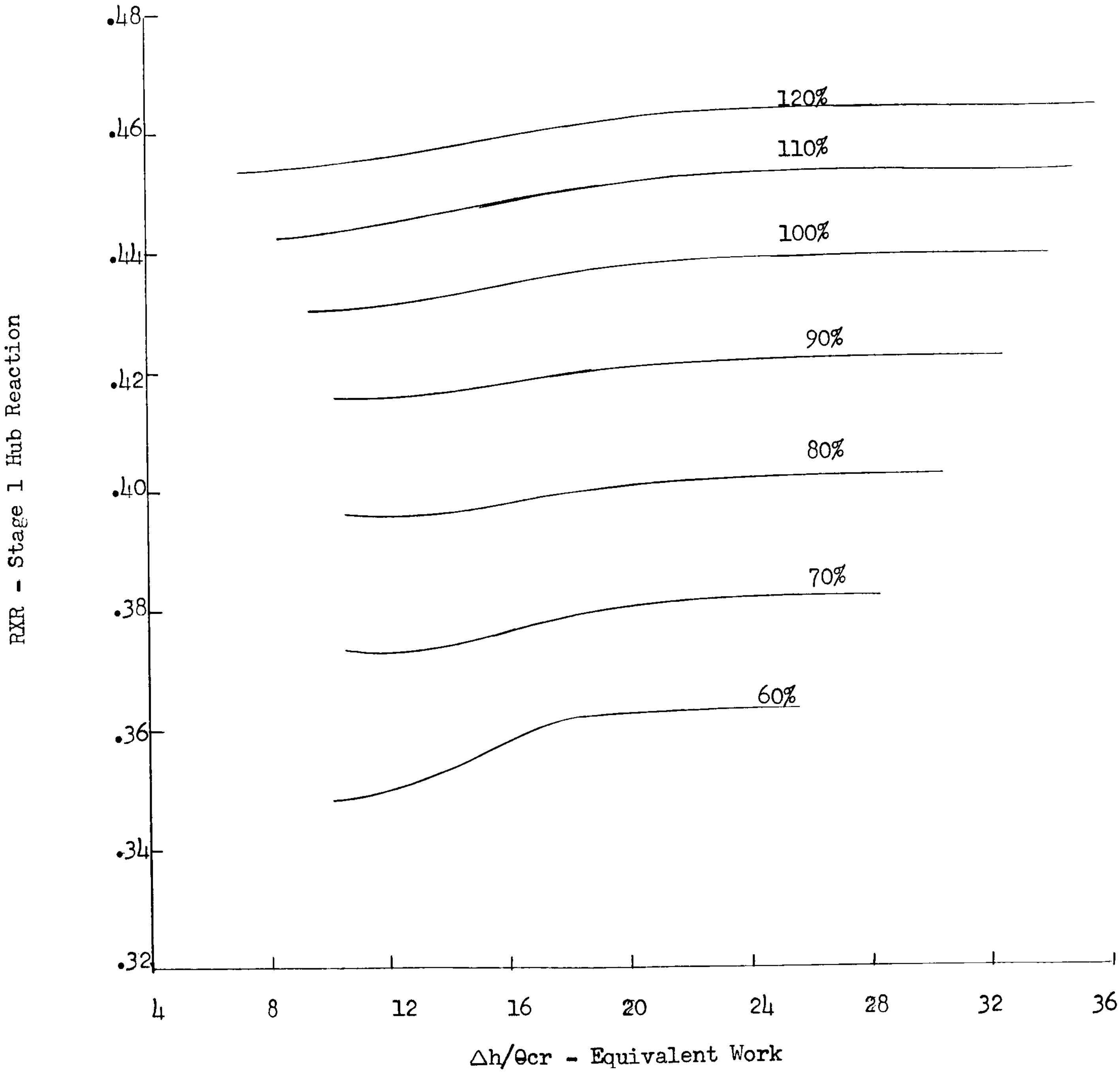

Figure 109

NASA - TASK III

Two Stage-Schedule -7.53, 8.81

Stage 2 Hub Reaction vs. Equivalent Work

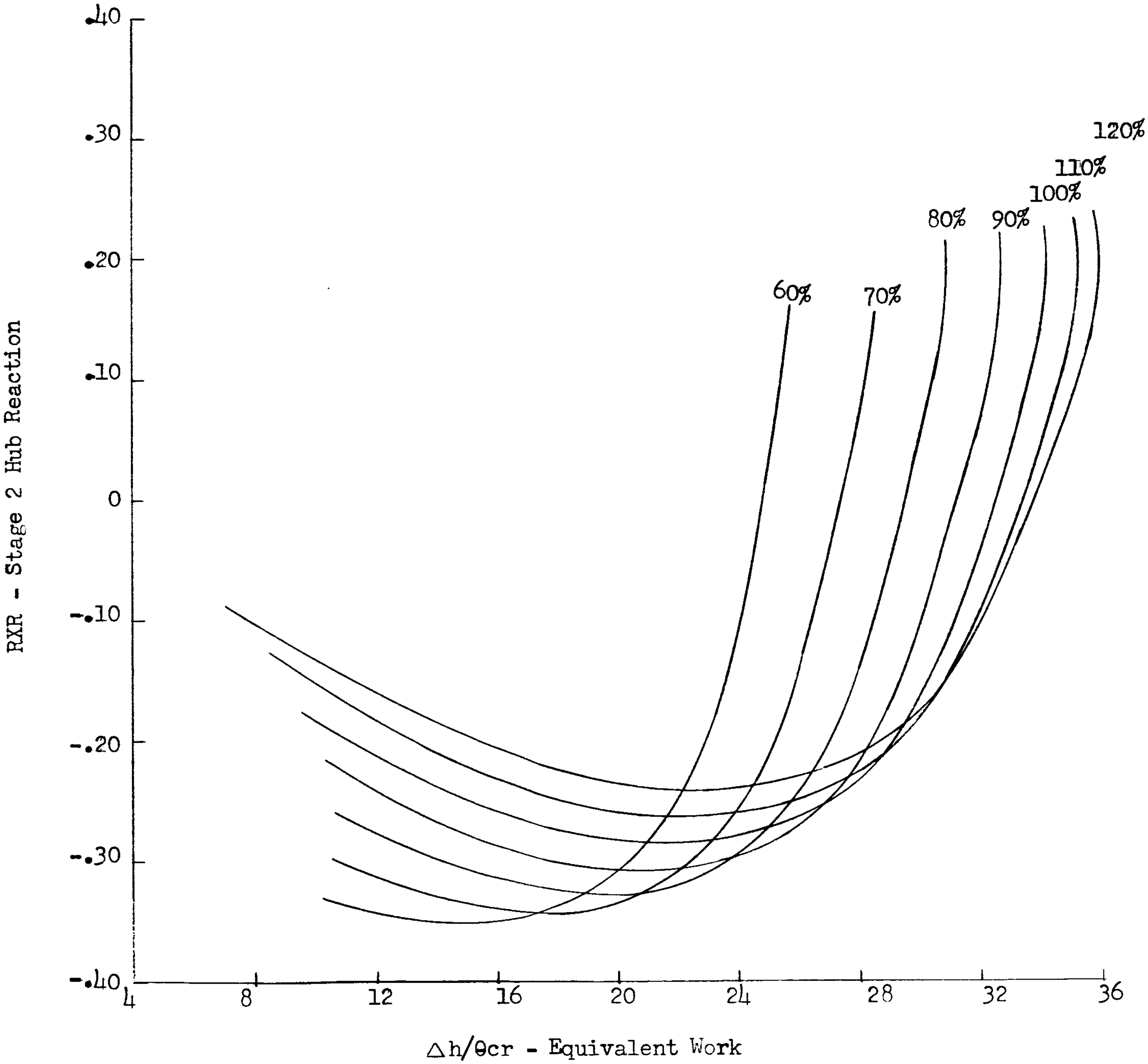

Figure 110

NASA - TASK III

Two Stage-Schedule 7.13, 8.81

Performance Map

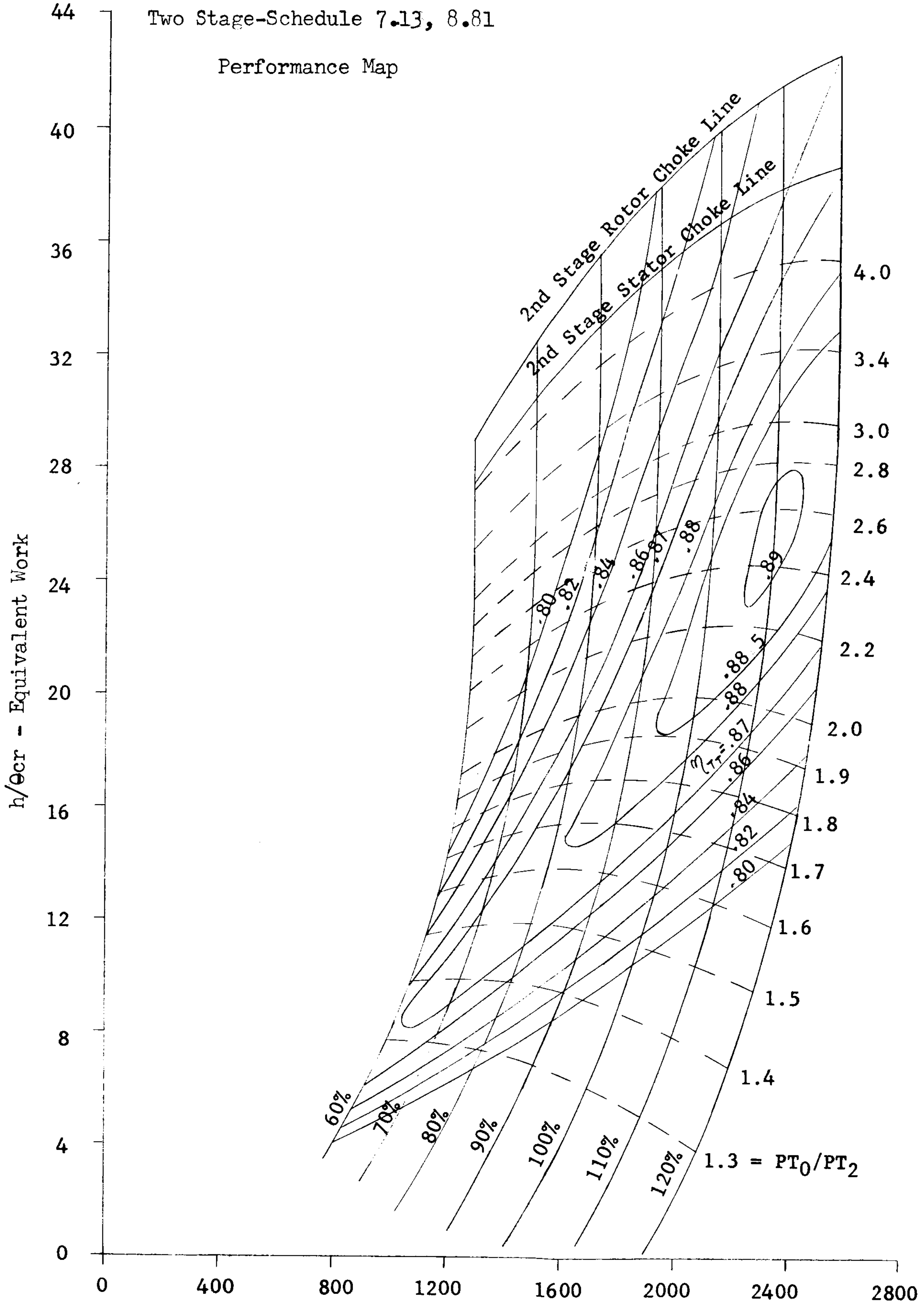

Figure 111

NASA - TASK III

Two Stage-Schedule 7.13, 8.81

Equivalent Flow vs. Pressure Ratio

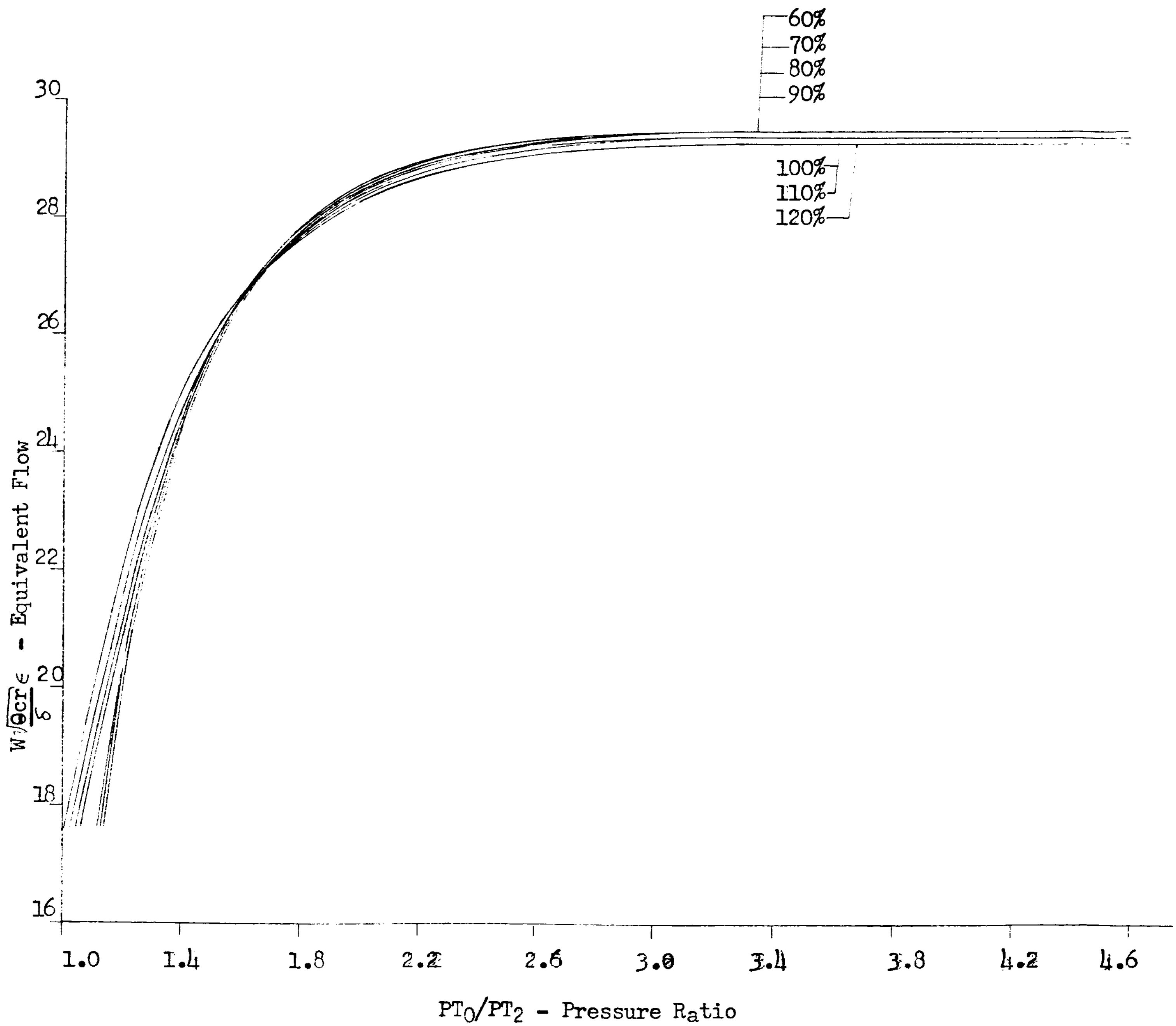

Figure 112

NASA - TASK III

Two Stage-Schedule 7.13, 8.81

Rotor 1 Incidence vs. Equivalent Work

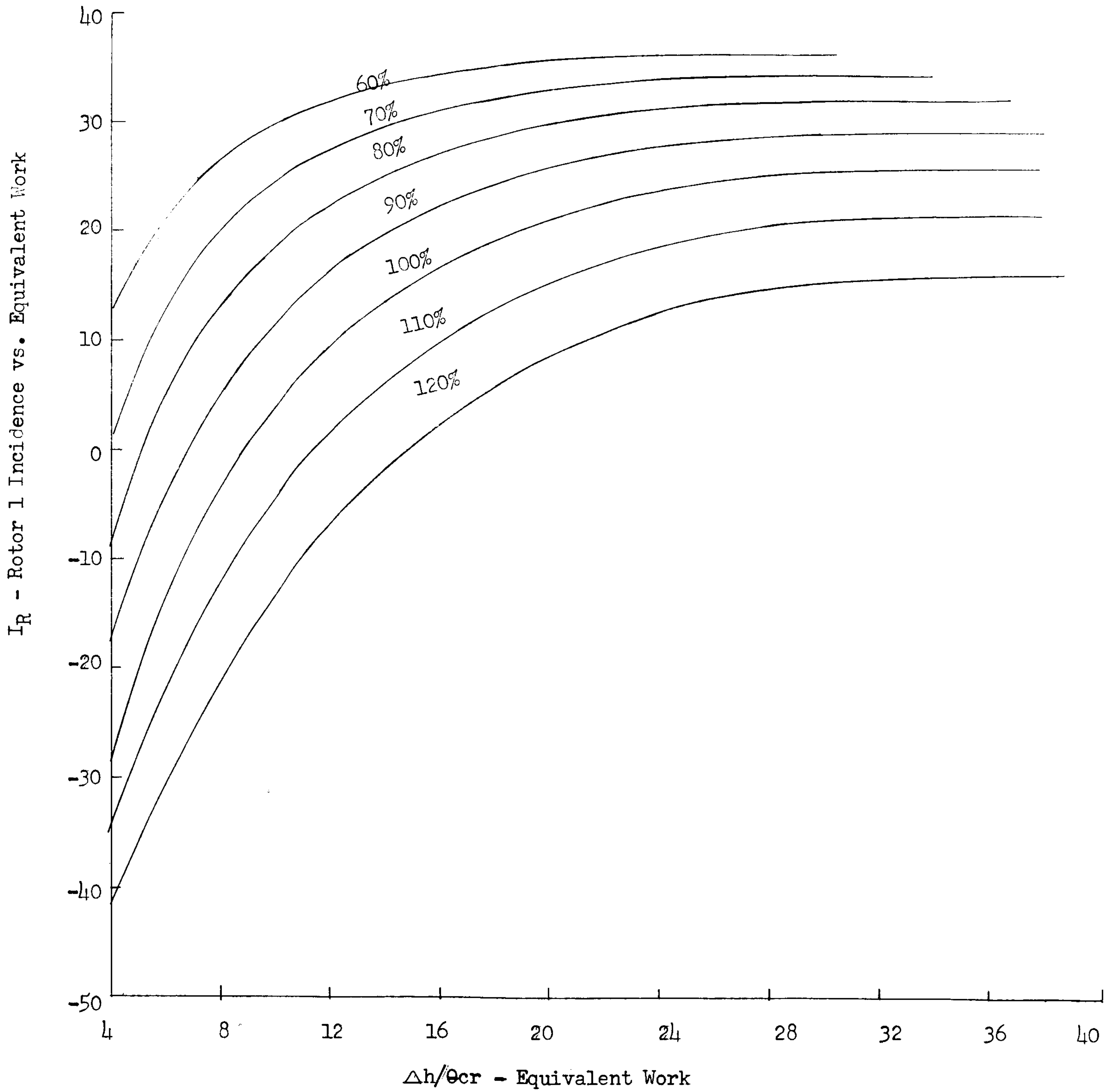

Figure 113

NASA - TASK III

Two Stage-Schedule 7.13, 8.81

Stator 2 Incidence vs. Equivalent Work

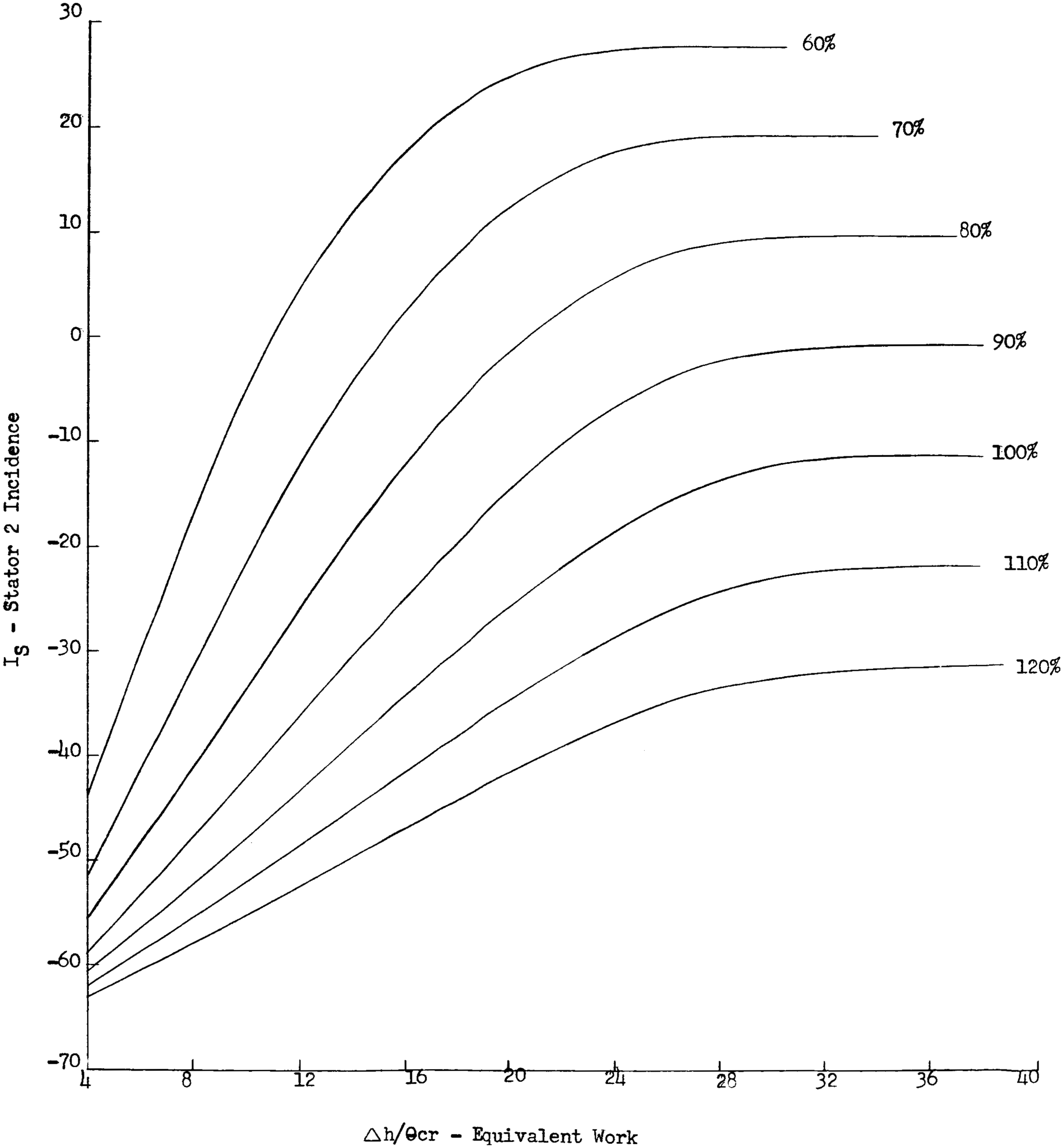

Figure 114

NASA - TASK III

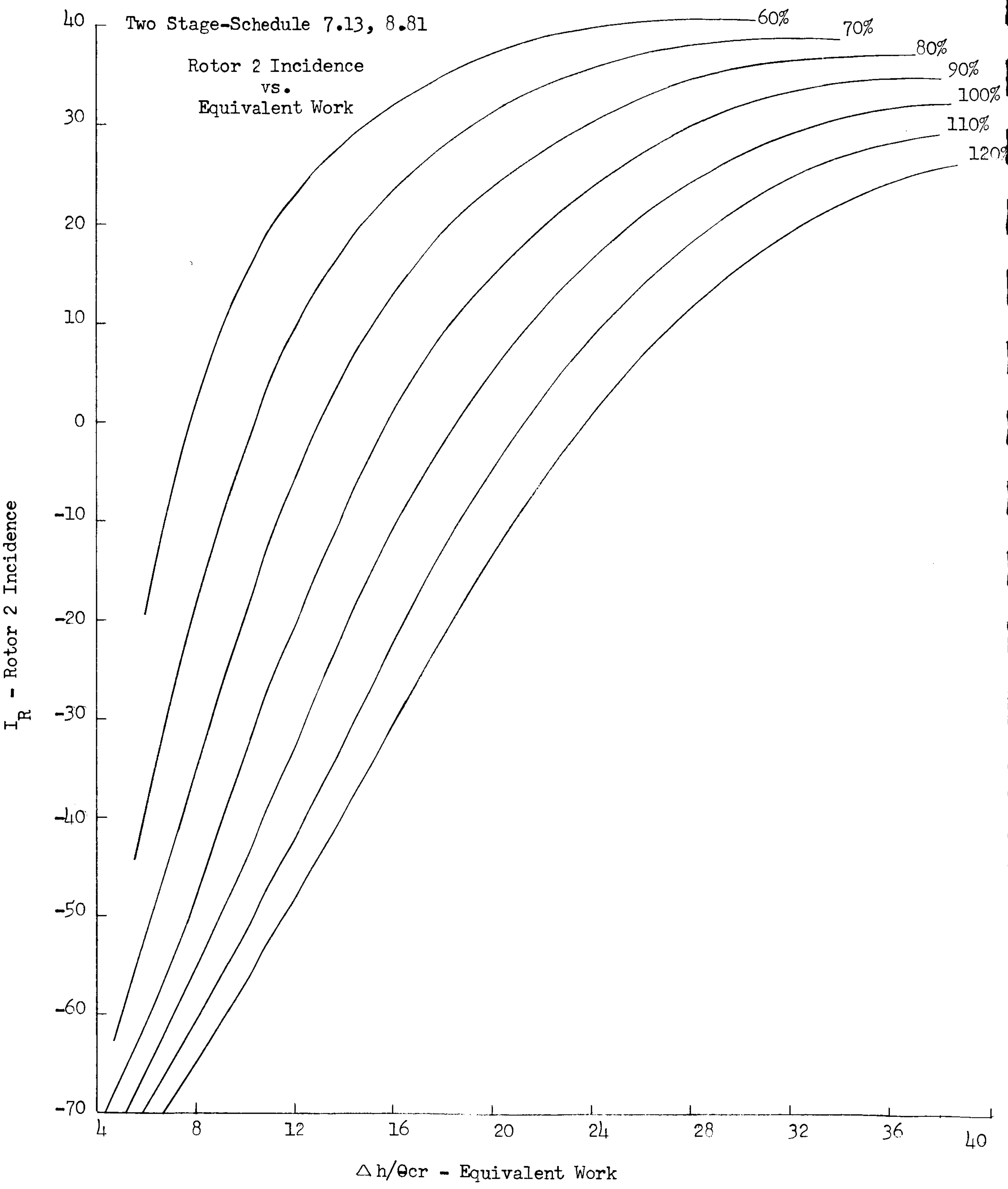

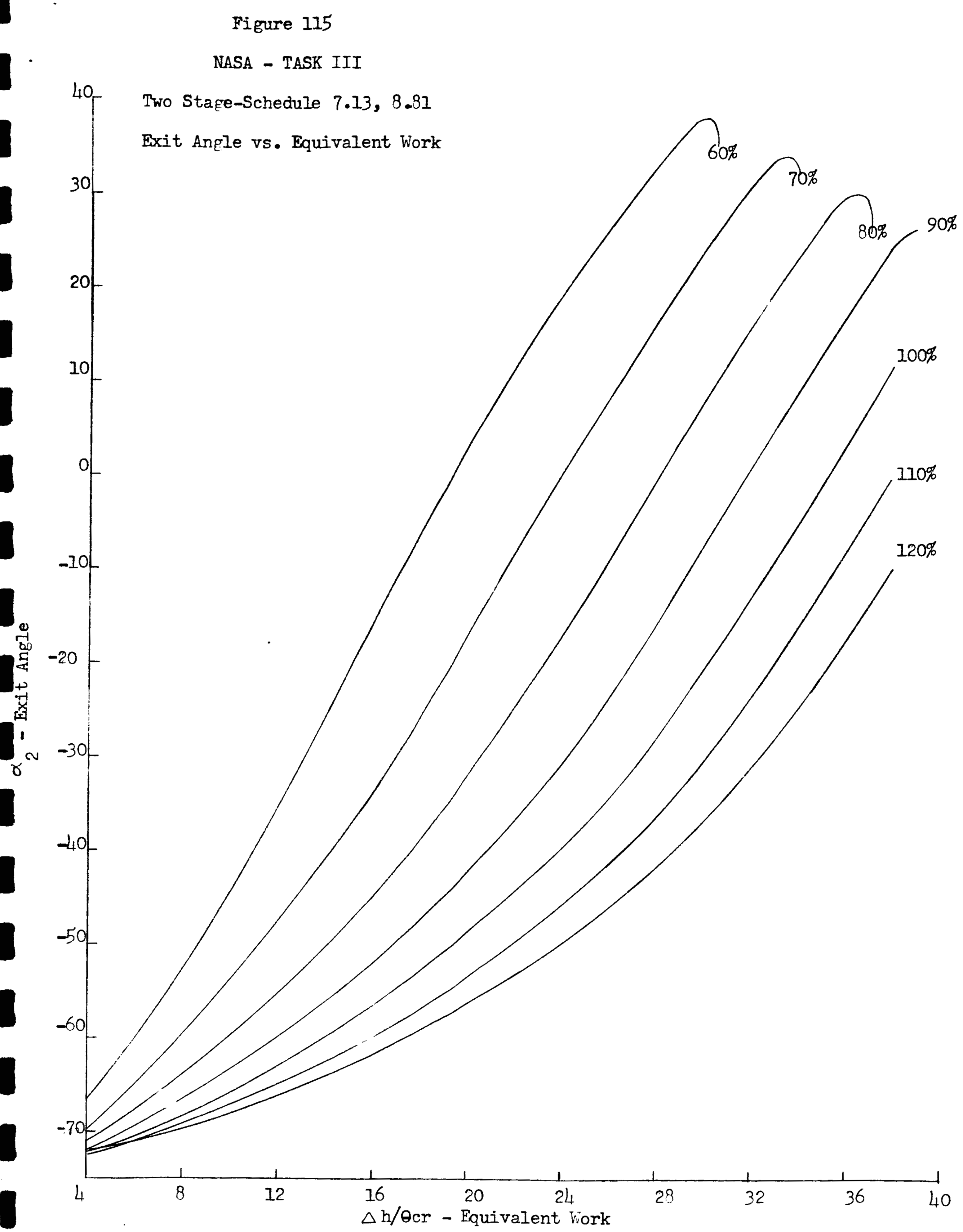

Figure 115
NASA - TASK III
Two Stage-Schedule 7.13, 8.81
Exit Angle vs. Equivalent Work
60%
70%
80%
90%
100%
110%
120%
40
30
20
10
0
-10
-20
-30
-40
-50
-60
-70
α2 - Exit Angle
4
8
12
16
20
24
28
32
36
40
△h/θcr - Equivalent Work

Figure 116

NASA - TASK III

Two Stage-Schedule 7.13, 8.81

Rotor 1 Hub Mach Number vs. Equivalent Work

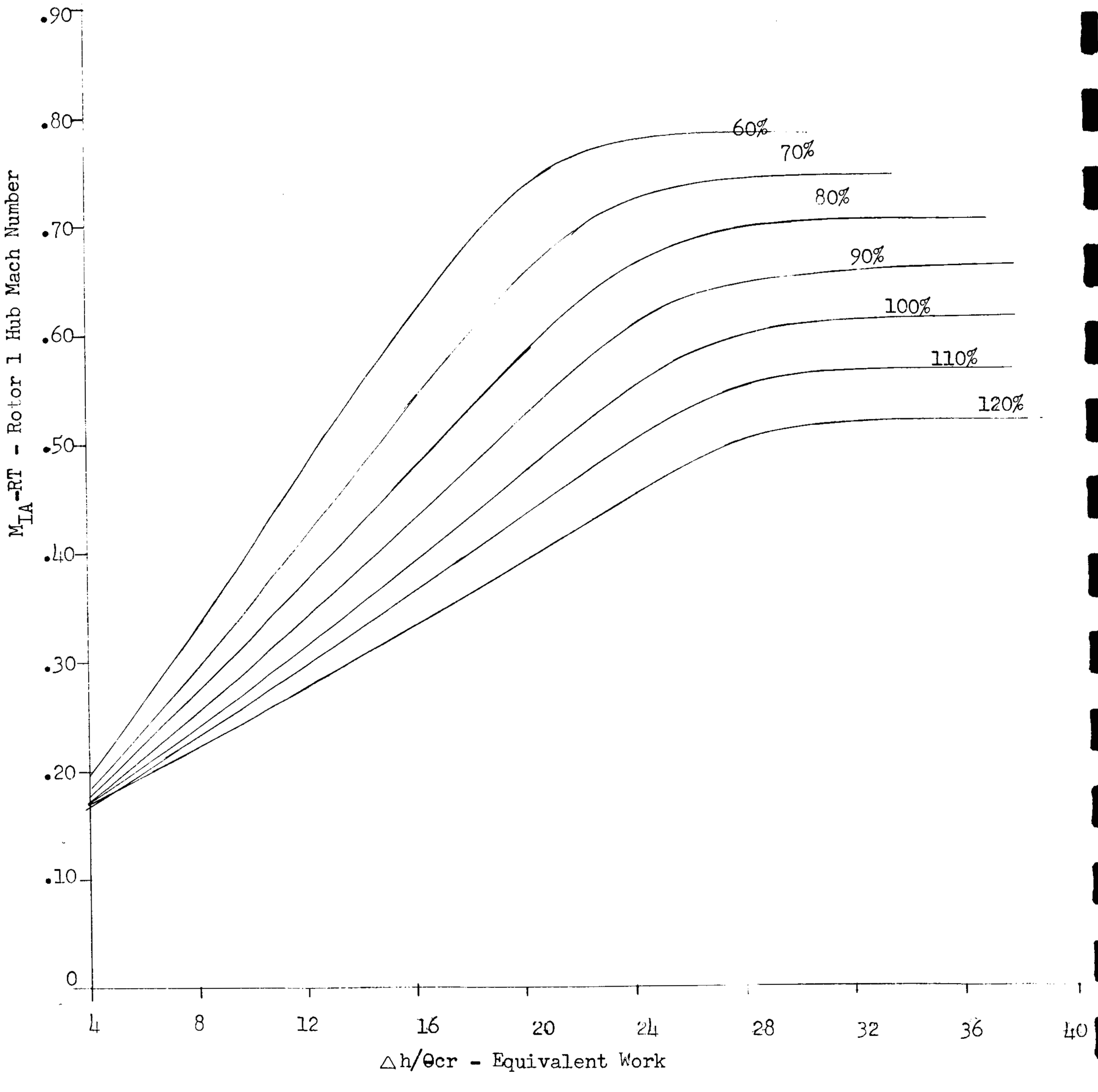

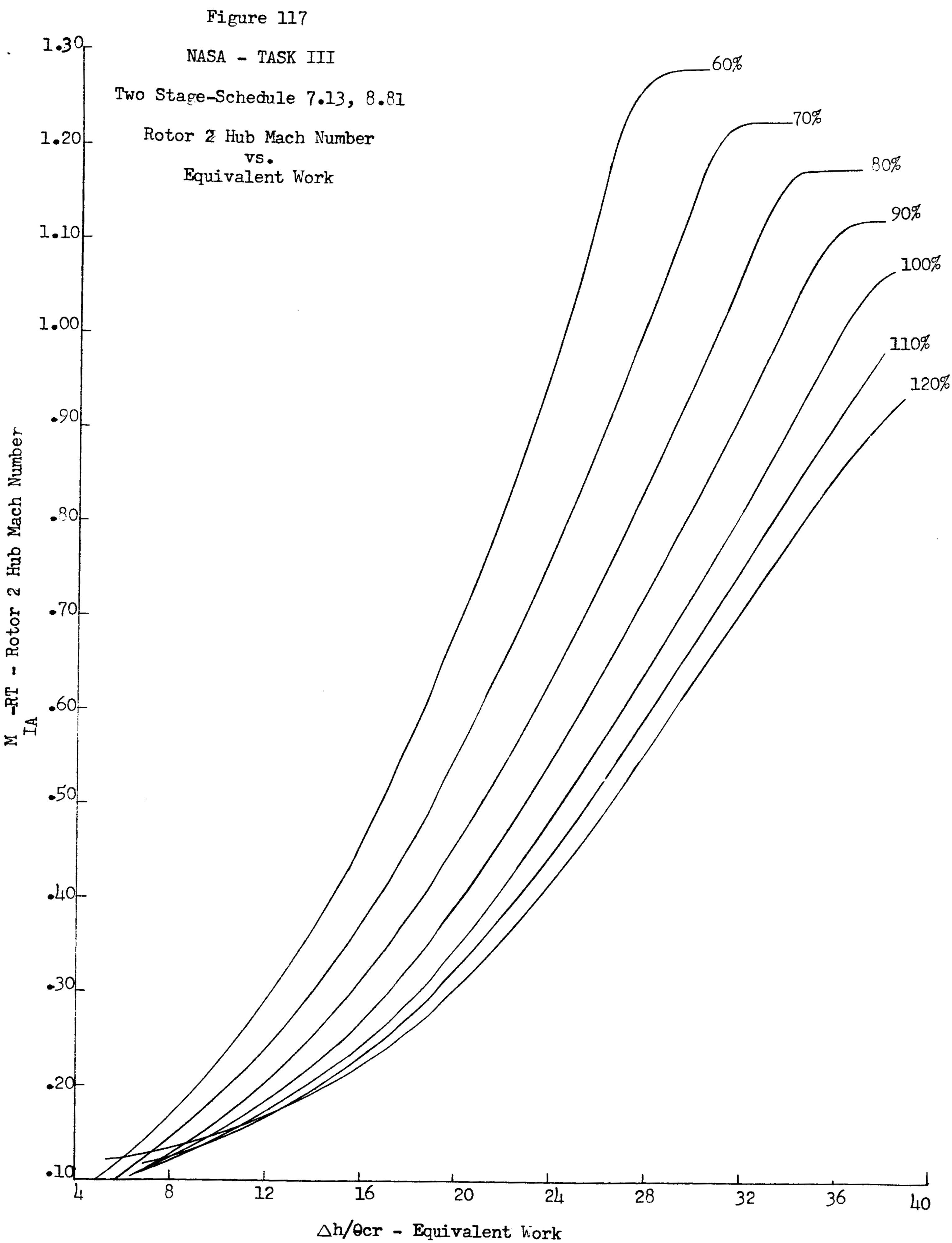
Figure 117
NASA - TASK III
Two Stage-Schedule 7.13, 8.81
Rotor 2 Hub Mach Number
vs.
Equivalent Work
60%
70%
80%
90%
100%
110%
120%
1.30
1.20
1.10
1.00
.90
.80
.70
.60
.50
.40
.30
.20
.10
4
8
12
16
20
24
28
32
36
40
M_IA -RT - Rotor 2 Hub Mach Number
Δh/θcr - Equivalent Work

Figure 118

NASA - TASK III

Two Stage-Schedule 7.13, 8.81

Stage 1 Hub Reaction vs. Equivalent Work

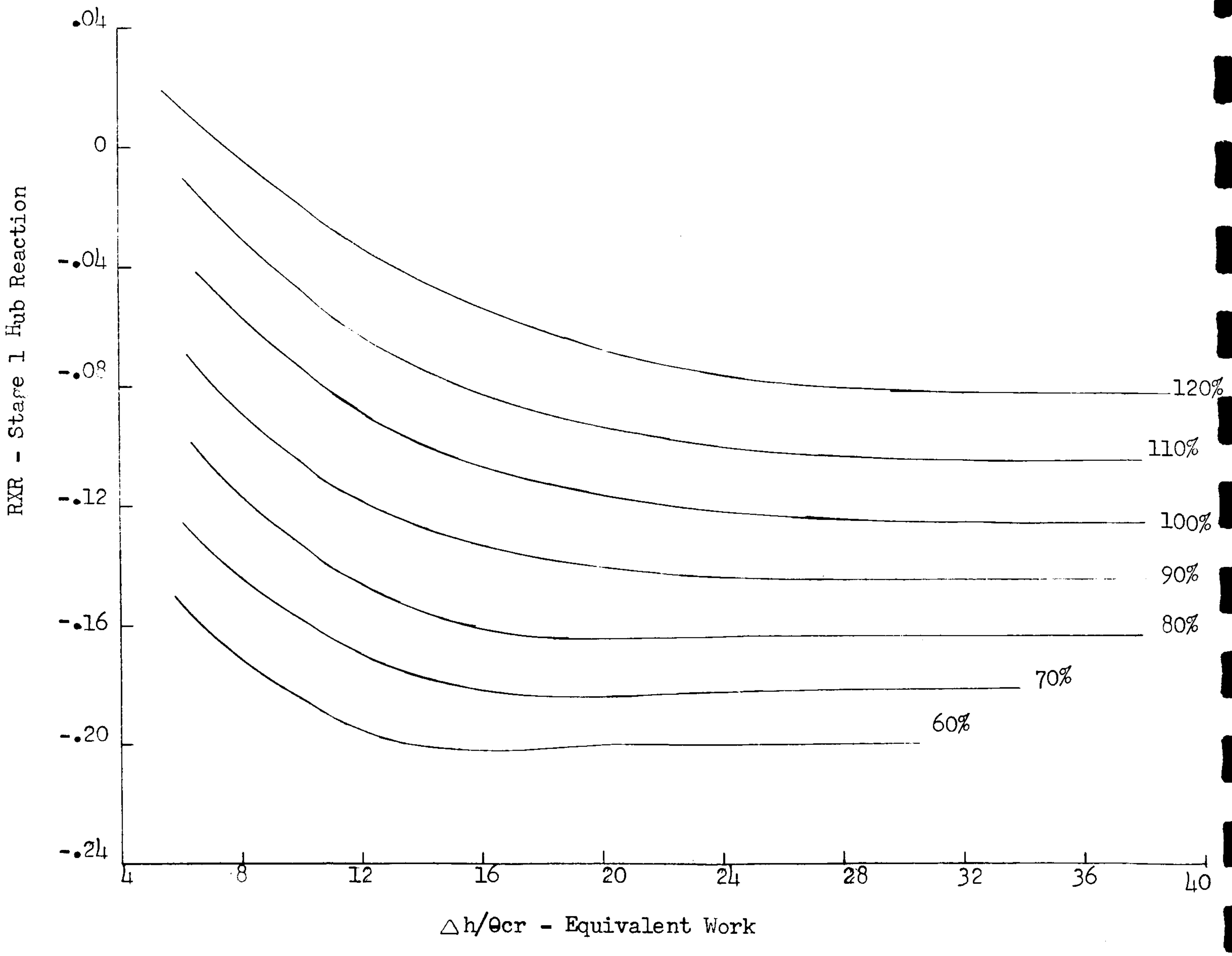

Figure 119

NASA - TASK III

Two Stage-Schedule 7.13, 8.81

Stage 2 Hub Reaction vs. Equivalent Work

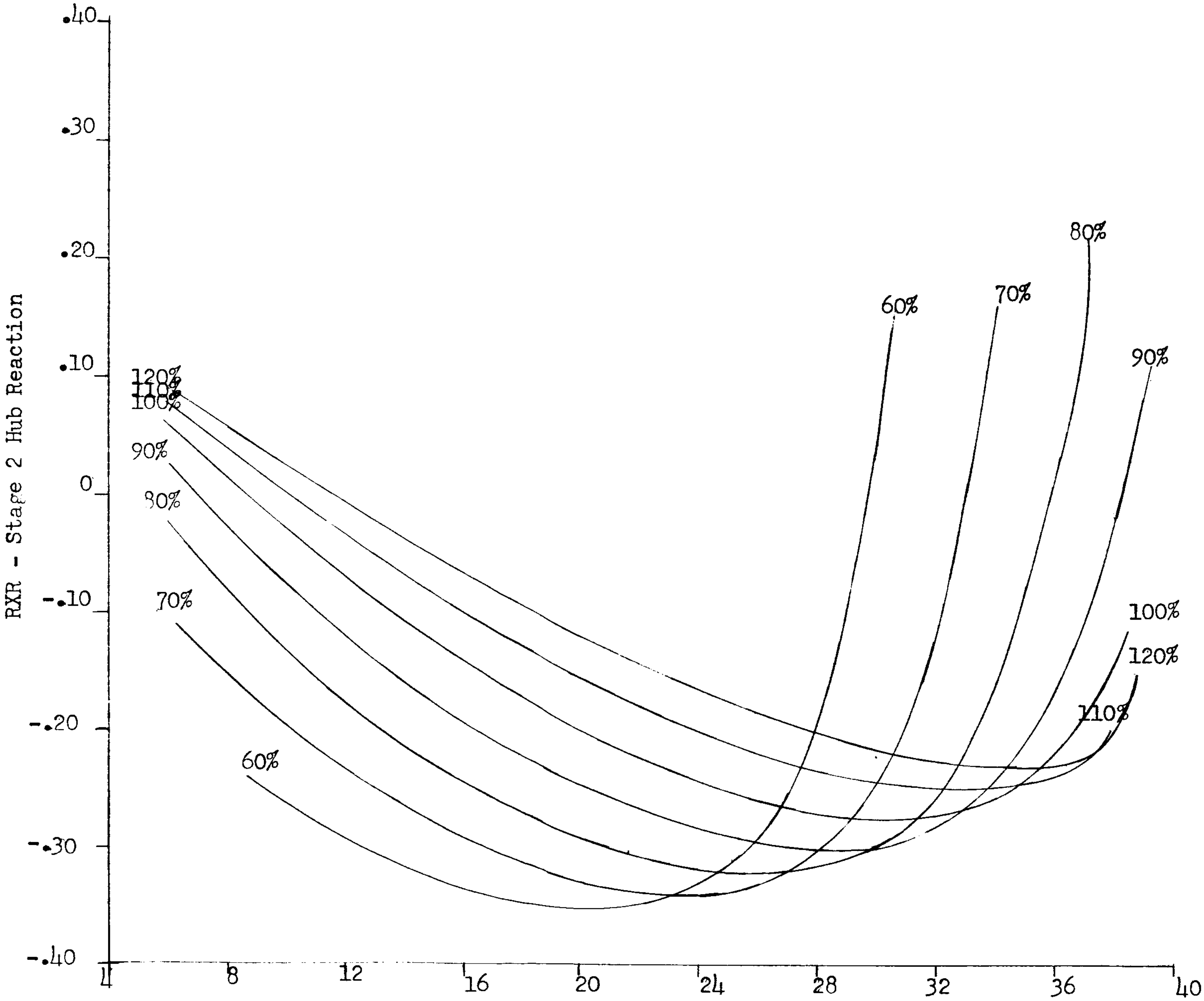

$\Delta h/\theta cr$ - Equivalent Work